

REPORT SERIES IN AEROSOL SCIENCE  
N:o 208 (2018)

**Proceedings of the NOSA-FAAR Symposium 2018**

Editors: Petri Clusius, Joonas Enroth and Antti Lauri

Helsinki 2018

ISSN 0784-3496  
ISBN 978-952-7091-98-2 (electronic publication)  
Aerosolitutkimusseura ry

–Finnish Association for Aerosol Research FAAR  
<http://www.atm.helsinki.fi/FAAR>

## CONTENTS

P. Aakko-Saksa, H. Vesala, T. Murtonen, H. Timonen, N. Kuittinen, P. Karjalainen, M. Bloss, K. Teinilä, P. Koponen, R. Pettinen, K. Lehtoranta, and T. Rönkkö METAL CONTENTS OF EXHAUST FROM FOUR MARINE ENGINES USING DIFFERENT FUELS .....	17
C. Andersen, A.M. Kraus, A.C. Eriksson, J. Jakobsson, C.H. Lindh, J. Löndahl, J. Pagels, J. Nielsen, A. Gudmundsson, and A. Wierzbicka A HUMAN EXPOSURE STUDY OF DERMAL AND INHALATION UPTAKE OF PARTICLE AND GAS PHASE PHTHALATES .....	18
M. Aurela, M. Bloss, N. Kuittinen, J. Alanen, P. Karjalainen, T. Rönkkö, J. Keskinen, L. Ntziachristos, K. Lehtoranta, S. Nyssönen, H. Vesala, and H. Timonen PRIMARY AND SECONDARY PARTICLE EMISSIONS FROM DUAL-FUEL MARINE ENGINE .....	19
T. J. Bannan, M. Le Breton, M. Priestley, S. Worrall, J. Hammes, M. Hallquist, R. Alfarra, U. K. Krieger, J. Reid, G. McFiggans, H. Coe, C. J. Percival, D. Topping A METHOD FOR EXTRACTING CALIBRATED VOLATILITY INFORMATION FROM THE FIGAERO ToF CIMS AND APPLICATION TO LABORATORY AND FIELD MEASUREMENTS .....	20
S.M. Blichner, M.K. Sporre, F. Stordal, H. Tang, and T.K. Berntsen BVOC-FEEDBACK SENSITIVITY TO NUCLEATION PARAMETERIZATION IN THE NORWEGIAN EARTH SYSTEM MODEL (NorESM) .....	21
M. Bloss, P. Karjalainen, N. Kuittinen, T. Murtonen, H. Vesala, T. Rönkkö, P. Aakko-Saksa, and H. Timonen CHEMICAL COMPOSITION OF EMISSIONS MEASURED IN REAL TIME FROM A MODERN SHIP ENGINE DURING A CRUISE .....	22
S. Bohlmann, M. Filioglou, E. Giannakaki, X. Shang, A. Saarto, S. Romakkaniemi, and M. Komppula CHARACTERIZATION OF ATMOSPHERIC POLLEN WITH MULTI-WAVELENGTH RAMAN LIDAR MEASUREMENTS .....	23
N. Borduas-Dedeking, Z.A. Kanji, and K. McNeill PHOTOCHEMISTRY OF FIELD COLLECTED COMPLEX ORGANIC MATTER AND ITS ABILITY TO ACT AS CLOUD CONDENSATION NUCLEI .....	24

A. Brostrøm, K. Mølhave, and K.I. Kling QUANTIFYING AEROSOL SIZE, SHAPE, AND COMPOSITION DISTRIBUTIONS BY ELECTRON MICROSCOPY OF MICRO INERTIAL IMPACTOR SAMPLES .....	26
A. Buchholz, A. Ylisirniö, C. Mohr, C. Faiola, E. Kari, A.T. Lambe, Z. Li, A. Pajunoja, S.A. Nizkorodov, S. Schobesberger, D.R. Worsnop, T. Yli-Juuti, and A. Virtanen CHEMICAL COMPOSITION CHANGES DURING SOA PARTICLE EVAPORATION .....	27
I. Bulatovic, A.M.L. Ekman, C. Leck, I. Riipinen AEROSOL INDIRECT EFFECT IN MARINE STRATOCUMULUS: DOES THE MODEL REPRESENTATION OF CLOUD DROPLET ACTIVATION MATTER? .....	28
M. A. Burgos, G. Titos, E. Andrews, P. Zieger A GLOBAL OVERVIEW OF THE EFFECT OF WATER UPTAKE ON AEROSOL PARTICLE LIGHT SCATTERING USING IN-SITU SURFACE MEASUREMENTS .....	30
D. Chen, P. Zhou, D. Taipale, and M. Boy DECADAL TRENDS OF ATMOSPHERIC OXIDANTS AT A BOREAL FOREST IN FINLAND .....	31
X. Chen, S. Barbosa, A. Mäkelä, J. Paatero, V.-M. Kerminen, T. Petäjä, and M. Kulmala CHARACTERISING THE FEATURES IN THE SURFACE ATMOSPHERIC ELECTRIC FIELD IN RELATION TO AEROSOL PROCESSES IN THE LOWER ATMOSPHERE .....	32
S. Christiansen, M. E. Salter, Q. Nguyen, and M. Bilde LABORATORY GENERATED SEA SPRAY AEROSOLS: VARYING FLOW RATE, ALGAE CONCENTRATION AND TEMPERATURE .....	33
L. Dada, M. Heinritzi, M. Simon, C. Yan, D. Stolzenburg, M. Kulmala, J. Kirkby, and the CLOUD Collaboration WHERE IN THE WORLD IS PURE BIOGENIC NUCLEATION? SIMULATION OF ATMOSPHERIC COMPLEXITY IN THE CLOUD CHAMBER .....	34
K. R. Daellenbach, I. El Haddad, I. Kourttchev, A. L. Vogel, G. Stefenelli, C. Bozzetti, A. Vlachou, P. Fermo, A. Piazzalunga, J. G. Slowik, S. M. Luedin, V. Pflueger, G. Vogel, J.-L. Jaffrezo, M. Kalberer, U. Baltensperger, A. S.H. Prévôt LONG-TERM SOURCE CONTRIBUTIONS TO ORGANIC AEROSOL AND SOA COMPOSITION IN CENTRAL EUROPE .....	35

T. N. Dallafior, S. Krishna, A. Lewinschall, I. Riipinen, A. M.L. Ekman, and H-C Hansson COMBINING CLIMATE MODELING AND OBSERVATIONS TO UNDERSTAND AEROSOL EFFECTS ON THE ARCTIC CLIMATE .....	36
E. L. D'Ambro, S. Schobesberger, F. D. Lopez-Hilfiker, J. E. Shilling, B. H. Lee, J. A. Thornton MOLECULAR CHARACTERIZATION AND VOLATILITY EVOLUTION OF $\alpha$ -PINENE OZONOLYSIS SOA DURING ISOTHERMAL EVAPORATIONS .....	37
J. Dou, B.P. Luo, T. Peter, M. Ammann, and U. Krieger PHOTOCHEMICAL AGING PROCESSES IN IRON CONTAINING AEROSOLS .....	38
E.-M. Duplissy, S. Hakala, V. Sinclair, R. Väänänen, V.-M. Kerminen, T. Petäjä, and M. Kulmala EFFECT OF ARCTIC SEA ICE ON AEROSOLS IN EASTERN LAPLAND .....	39
J. Duplissy, M. Sahyoun, E. Freney, R. Dupuy, A. Colomb, D. Picard, J. Brito, C. Denjean, T. Bourianne, M. Kulmala, M. Riva, H. Juninen, A. Schwarzenboeck, C. Planche, and K. Sellegri FLYING INSIDE VOLCANO'S PLUME WITH A MASS SPECTROMETER TO STUDY NEW PARTICLE FORMATION .....	40
M. Elmgren, M. Norman, S. Silvergren, and C. Johansson SUCCESSFULLY MITIGATING PM <sub>10</sub> IN STOCKHOLM CITY .....	41
M.B. Enghoff, H. Svensmark, N.J. Shaviv, and J. Svensmark HOW INCREASED IONIZATION CAN BOOST AEROSOL GROWTH TO CLOUD CONDENSATION NUCLEI .....	42
A.C. Eriksson, , C. Andersen, A.M. Kraus, J. Klenø Nøjgaard, P.-A., Clausen, A. Wierzbicka, and J. Pagels PHTHALATE UPTAKE FROM VINYL FLOORING BY AMBIENT AND LABORATORY GENERATED PARTICLES .....	43
E. Ezhova, V.-M. Kerminen, K.E.J. Lehtinen, and M. Kulmala ON THE STRUCTURE AND DYNAMICS OF THE CONDENSATION SINK IN THE ATMOSPHERE: A SIMPLE SEMI-ANALITICAL MODEL .....	44
J. Falk, T.B. Kristensen, R. Lindgren, C. Andersen, R. Carvalho, K. Korhonen, V. Berg Malmberg, A. C. Eriksson, C. Boman, J. H. Pagels, and B. Svenningsson CCN EMISSION FACTORS OF SOLID BIOMASS FUELS RELATED TO RESIDENTIAL COOKING .....	45

B. Foreback, M. Boy, A. Mahura, R. Kouznetsov INTEGRATION OF IMPROVED AEROSOL CHEMISTRY AND PHYSICS ALGORITHMS INTO THE SILAM MODEL .....	46
S. M. Gaita, M. Le Breton, J. Boman, R. K. Pathak, Å. M. Hallquist, Q. Liu, J. Zheng, Z. Du, S. Lou, S. Guo, C. K. Chan, M. Hu, and M. Hallquist SNAPSHOT OF PM <sub>2.5</sub> , PM <sub>1</sub> , BLACK CARBON AND ORGANIC COMPONENTS OF PARTICULATE MATTER IN BEIJING, SUMMER 2016 .....	47
O. Garmash, L. Yao, F. Bianchi, O. Peräkylä, Y. Zhang, C. Yan, T. Petäjä, D. Worsnop, M. Kulmala, L. Wang, and M. Ehn MEASUREMENTS OF ORGANIC AEROSOL PRECURSOR GASES IN SHANGHAI .....	48
P. Glantz, L. Merkulova, E. Freud, E. M. Mårtensson, and D. E. Nilsson EFFECT OF WIND SPEED ON MODIS AEROSOL OPTICAL DEPTH OVER NORTH PACIFIC .....	49
M. Glasius, L.S. Iversen, A.M.K. Hansen, K. Wang, T. Hoffmann, M. Bilde, and R.-J. Huang MOLECULAR TRACERS OF SECONDARY AEROSOLS IN XI'AN, CHINA DURING SUMMER AND WINTER .....	50
L. Gren, V.B. Malmberg, P. C. Shukla, S. Shamun, C. Isaxon, PA. Clausen, M. Tunér, U. Vogel, and J. Pagels GENERATING BIODIESEL AND FOSSIL DIESEL EXHAUST PARTICLES WITH VARIED PHYSICO-CHEMICAL PROPERTIES FOR TOXICOLOGICAL STUDIES .....	51
S. Hakala, P. Paasonen, V. Vakkari, H. Lihavainen, A. Hyvärinen, K. Neitola, J. Kontkanen, T. Hussein, M. Kulmala, M. A. Alghamdi NEW PARTICLE FORMATION, GROWTH AND SHRINKAGE AT A RURAL BACKGROUND SITE IN WESTERN SAUDI ARABIA .....	52
P. Heikkilä, J. Rossi, A. Järvinen, A. Rostedt, S. Saari, J. Toivonen, J. Keskinen ELEMENTAL ANALYSIS OF AIRBORNE SUPERMICRON PARTICLES .....	53
A. Helin, J.V. Niemi, A. Virkkula, L. Pirjola, K. Teinilä, J. Backman, M. Aurela, S. Saarikoski, T. Rönkkö, E. Asmi, and H. Timonen CHARACTERISTICS AND SOURCES OF BLACK CARBON IN THE HELSINKI METROPOLITAN AREA, FINLAND .....	54

H. Hellén, A.P. Praplan, T. Tykkä, S. Schallhart, and H. Hakola SESQUITERPENES ARE IMPORTANT SECONDARY ORGANIC AEROSOL PRECURSORS IN BOREAL FOREST .....	55
M. Hemmilä, H. Hellén, A. Virkkula, U. Makkonen, A. P. Praplan, J. Kontkanen, L. Ahonen, M. Kulmala, and H. Hakola AMINE MEASUREMENTS IN BOREAL FOREST AIR .....	56
Y. N. Husein, D. A. Pripachkin, A. K. Budyka ESTIMATION METHOD OF PARTICLE SIZE DISTRIBUTION (PSD) OF RADIOACTIVE AEROSOLS BY USING INERTIAL SEPARATORS .....	57
Y. N. Husein, D. A. Pripachkin, A. K. Budyka EVALUATION OF SPECTROMETRIC AND RADIOMETRIC CHARACTERISTICS OF PLUTONIUM ALPHA-EMITTING RADIONUCLIDES AND THEIR INFLUENCE ON THE VALUE OF AMAD .....	58
N. Hyttinen, R.V. Otkjær, S. Iyer, H.G. Kjaergaard, M.P. Rissanen, P.O. Wennberg, and T. Kurtén COMPUTATIONAL COMPARISON OF DIFFERENT REAGENT IONS IN THE CHEMICAL IONIZATION OF OXIDIZED MULTIFUNCTIONAL COMPOUNDS .....	59
S. Isokääntä, E. Kari, A. Buchholz, A. Virtanen, and S. Mikkonen STATISTICAL DIMENSION REDUCTION TECHNIQUES APPLIED TO MULTIVARIATE CAR EXHAUST EMISSION DATA .....	60
S. Iyer, H. Reiman, K.H. Møller, M.P. Rissanen, H. Kjaergaard, T. Kurtén COMPUTATIONAL INVESTIGATION OF RO <sub>2</sub> + HO <sub>x</sub> REACTIONS .....	61
J. Jakobsson, H. L. Aaltonen, P. Wollmer, and J. Löndahl WHAT CAN BE LEARNED ABOUT THE LUNG FROM INHALED NANOPARTICLES? .....	62
A.C.Ø. Jensen, N. Bertram, I.K. Koponen, A.J. Koivisto TOWARDS A SOURCE LIBRARY FOR MODELLING – COMPARING SMALL AND LARGE CHAMBER CONCENTRATIONS .....	63
J. Julin, B.N. Murphy, D. Patoulias, C. Fountoukis, T. Olenius, S.N. Pandis, and I. Riipinen IMPACTS OF FUTURE EUROPEAN EMISSION REDUCTIONS ON AEROSOL NUMBER CONCENTRATIONS WITH FOCUS ON ULTRAFINE PARTICLES .....	64

P. Juuti MOBILE APPLICATION BASED AEROSOL CALCULATOR FOR EASING THE LIFE OF STUDENTS AND RESEARCHERS .....	65
L. Järvi, L. Pirjola, M. Kurppa, H. Kuuluvainen, A. Malinen, A. Balling, S. Karttunen, T. Rönkkö, J.V. Niemi, and P. Rantala THE EFFECT OF METEOROLOGY ON POLLUTANT DISTRIBUTIONS WITHIN STREET CANYON NETWORK IN HELSINKI .....	66
J. Kalliokoski, H. Timonen, H. Kuuluvainen, R. Hietikko, M. Isotalo, N. Kuittinen, M. Aurela, J. Niemi, J. Keskinen, and T. Rönkkö THE VOLATILITY AND CHEMICAL COMPOSITION OF SUBMICRON PARTICLES IN A STREET CANYON IN HELSINKI .....	67
J. Kangasluoma, L. R. Ahonen, T. Laurila, R. Cai, J. Enroth, S. Buenrostro Mazon, F. Korhonen, P.P. Aalto, M. Kulmala, M. Attoui, T. Petäjä IMPROVING THE ACCURACY AND PRECISION OF SUB-10 NM ATMOSPHERIC NANOPARTICLE MEASUREMENTS WITH A NEW HIGH FLOW DMPS .....	68
J. Kesti, J. Backman, E. Asmi, E. J. O’Connor, Ö. Gustafsson, and K. Budhavant LONG-RANGE TRANSPORTED AEROSOLS AT THE MALDIVES AND THE IMPACT OF WET DEPOSITION ON PARTICLE NUMBER AND SIZE .....	69
M. Khansari, A. Nikandrova, P. Paasonen, V.-M Kerminen, and M. Kulmala STDUDYING AEROSOL RADIATION FEEDBACK LOOP BASED ON SATELITE DATA .....	70
N. Kivekäs and S. Sorvari ACTRIS – SHAPING THE FUTURE OF ATMOSPHERIC RESEARCH .....	71
A.J. Koivisto, A.S. Fonseca, I.K. Koponen, and A.C.Ø Jensen REGULATORY EXPOSURE MODELLING – CURRENT STATUS AND WORK NEEDED .....	72
J. Kontkanen, T. Olenius, M. Kulmala, and I. Riipinen MOLECULAR-RESOLUTION SIMULATIONS OF THE GROWTH OF ATMOSPHERIC CLUSTERS BY ORGANIC VAPORS .....	73
M. Kotorova, S. Gromov A COMPARISON OF LONG-TERM AIR CONCENTRATION TRENDS OF PAH AT THE BACKGROUND REGIONS OF THE RUSSIAN FEDERATION AND IN SOME EMEP COUNTRIES .....	74



J. Kubečka, T. Kurtén, and H. Vehkamäki CONFIGURATIONAL SAMPLING OF ATMOSPHERIC MOLECULAR CLUSTERS .....	75
M. Kurppa, A. Hellsten, M. Auvinen, S. Karttunen, P. Kumar, and L. Järvi NOVEL HIGH-RESOLUTION URBAN AIR QUALITY MODEL: DEVELOPMENT AND EVALUATION .....	76
T. Kurtén, N. Hyttinen, P. Roldin, M. P. Rissanen, G. Michailoudi, N. Prisle USING COSMOTHERM TO EVALUATE PROPERTIES OF TERPENE OXIDATION PRODUCTS: PROMISES AND PITFALLS .....	77
J. Kuula, T. Mäkelä, R. Hillamo, and H. Timonen RESPONSE CHARACTERIZATION OF AN INEXPENSIVE AEROSOL SENSOR .....	78
H. Kuuluvainen, R. Hietikko, P. Karjalainen, J. Keskinen, R. Hillamo, J. V. Niemi, L. Pirjola, H. J. Timonen, S. Saarikoski, E. Saukko, A. Järvinen, H. Silvennoinen, A. Rostedt, M. Olin, J. Yli-Ojanperä, P. Nousiainen, A. Kousa, M. Dal Maso, and T. Rönkkö TRAFFIC PRODUCES A SIGNIFICANT FRACTION OF ATMOSPHERIC NANOCLUSTER AEROSOL IN URBAN AREAS .....	79
J. Laakia, K. Teinilä, H. Timonen, S. Saarikoski, M. Bloss, P. Karjalainen, N. Kuittinen, H. Vesala, R. Pettinen, P. Aakko-Saksa, and J.-P. Jalkanen FIRST RESULTS FROM “ENVISUM” PROJECT: EMISSION MEASUREMENTS ONBOARD A RORO PASSENGER SHIP UNDER REAL OPERATING CONDITIONS .....	80
A. Laakso, D. Millet, S. Liess, A.-I. Partanen, H. Kokkola, and P. Snyder CLIMATE RESPONSES TO SOLAR RADIATION MANAGEMENT AND CARBON DIOXIDE REMOVAL IN TWO EARTH SYSTEM MODELS .....	81
J. Lampilahti, K. Leino, L. Beck, A. Manninen, P. Poutanen, H. Junninen, A. Nikandrova, M. Peltola, P. Hietala, L. Dada, L. Quéléver, I. Pullinen, S. Schobesberger, T. Petäjä, M. Kulmala FRESHLY FORMED PARTICLES IN THE CAPPING INVERSION .....	82
R. Lange, M. Dall’Osto, R. Harrison, D. C. S. Beddows, H. Skov, and A. Massling EXPANDING FIELD STUDY CCN MEASUREMENTS WITH CLUSTER ANALYSIS OF LONG TERM SMPS DATA .....	83
K. Lehtipalo, C. Yan, L. Dada, F. Bianchi, R. Wagner, J. Duplissy, J. Kirkby, U. Baltensperger, M. Kulmala, D. R. Worsnop, and The CLOUD collaboration NEW PARTICLE FORMATION FROM BIOGENIC PRECURSORS - EFFECT OF SO <sub>2</sub> , NO <sub>x</sub> AND NH <sub>3</sub> .....	84

A. Li SIZE DISTRIBUTIONS OF WATER-SOLUBLE IONS IN ATMOSPHERIC AEROSOLS IN THE EASTERN CHINA AND THE IMPLICATIONS FOR THE FORMATION MECHANISM OF HEAVILY POLLUTED DAYS .....	85
Z. Li, A. Buchholz, O.-P. Tikkanen, E. Kari, L. Hao, T. Yli-Juuti, and A. Virtanen EFFECT OF TEMPERATURE ON EVAPORATION OF A-PINENE SECONDARY ORGANIC AEROSOL .....	86
J.J. Lin, S.K. Purdue, H. Lin, J.C. Meredith, A. Nenes, and N.L. Prisle CCN ACTIVITY OF SIX POLLENKITTS AND THE INFLUENCE OF THEIR SURFACE ACTIVITY .....	87
K. Lovén, C. Isaxon, A. Wierzbicka, and A. Gudmundsson CLEANING SPRAY AEROSOLS: CHARACTERIZATION OF AIRBORNE PARTICLES .....	88
K. Luoma, A. Virkkula, P. Aalto, and T. Petäjä TRENDS OF AEROSOL OPTICAL PROPERTIES AT THE SMEAR II STATION .....	89
A. Mahura, R. Makkonen, M. Boy, T. Petäjä, M. Kulmala, S. Zilitinkevich, and “Enviro-PEEX on ECMWF” modelling team SEAMLESS MULTI-SCALE AND -PROCESSES MODELLING ACTIVITIES AT INAR .....	90
R. Makkonen and M. Kulmala IDENTIFYING GLOBAL AEROSOL-CLIMATE INTERACTIONS THROUGH GEOSPATIAL NETWORK ANALYSIS .....	91
J. Malila and N.L. Prisle A PHYSICALLY CONSISTENT PARTITIONING SCHEME FOR TREATMENT OF SURFACTANTS IN AQUEOUS AEROSOLS .....	92
E.J. Mallon, M. Chuamou, and P. Agbe CONSEQUENCES OF AEROSOL ABSORPTION BY BEKOKO MINES EMPLOYEES IN SOUTH WEST CAMEROON .....	93
V.B. Malmberg, A.C. Eriksson, C. Andersen, S. Török, C. Boman, R. Lindgren, K. Lovén, M. Tuner, P-E. Bengtsson, and J. Pagels RELATING AEROSOL MASS SPECTRA AND THERMAL OPTICAL ANALYSIS (OC/EC) FOR PRIMARY BROWN CARBON EMISSIONS .....	94

E. Miettinen, P. Salo, and J. Vanhanen FOCUS ON 1 NM PARTICLES – CHALLENGES AND POSSIBILITIES OF MEASUREMENTS	95
M. Miettinen, A. Leskinen, G. Abbaszade, J. Orasche, K. Kuuspalo, M. Sainio, H. Koponen, P. Jalava, L. Hao, J. Ruusunen, D. Fang, Q. Wang, C. Gu, Y. Zhao, J. Schnelle-Kreis, K.E.J. Lehtinen, R. Zimmermann, M. Komppula, J. Jokiniemi, M-R. Hirvonen, and O. Sippula PM <sub>2.5</sub> CONCENTRATION AND COMPOSITION BEFORE, DURING, AND AFTER THE 2014 YOUTH OLYMPIC GAMES IN NANJING, CHINA	96
N. Myllys, J. Elm, T. Olenius, and T. Kurtén OXIDIZED ORGANIC COMPOUNDS IN THE INITIAL STEPS OF PARTICLE FORMATION	97
N. Myllys, M. Panssananti, A. Shcherbacheva, and E. Zapadinsky MODELING THE IMPACT OF BACKGROUND GAS PRESSURE ON THE FRAGMENTATION OF MOLECULAR CLUSTERS INSIDE THE APi-TOF	98
T. Nieminen, J. Joutsensaari, V. Leinonen, S. Mikkonen, T. Yli-Juuti, P. Miettinen, A. Virtanen, K. E. J. Lehtinen, A. Laaksonen, S. Decesari, L. Tarozzi, and M. C. Facchini LONG-TERM TRENDS IN PARTICLE NUMBER SIZE-DISTRIBUTIONS AND NEW PARTICLE FORMATION OBSERVED AT SAN PIETRO CAPOFIUME, ITALY	99
A. Nikandrova, K. Tabakova, A. Manninen, R. Väänänen, T. Petäjä, M. Kulmala, V.-M. Kerminen, and E. O’Connor COMBINING AIRBORNE IN SITU AND GROUND-BASED LIDAR MEASUREMENTS FOR ATTRIBUTION OF AEROSOL LAYERS	100
M. Ozon, A. Seppänen, J.P. Kaipio, and K.E.J. Lehtinen ESTIMATION OF NUCLEATION AND CONDENSATION RATES FROM SIZE DISTRIBUTION MEASUREMENTS USING STATISTICAL INVERSE METHODOLOGY	101
P. Paasonen, M. Peltola, J. Kontkanen, H. Junninen, V.-M. Kerminen, and M. Kulmala PARTICLE GROWTH RATES FROM NUCLEATION MODE TO CLOUD CONDENSATION NUCLEI SIZES	102
O. H. Pakarinen, G. Roudsari, and H. Vehkamäki EFFECT OF SURFACE GEOMETRY ON HETEROGENEOUS ICE NUCLEATION	103
Y. Palamarchuk and M. Sofiev DISTRIBUTION OF ATMOSPHERIC AEROSOLS AND TRACE GASES OVER FINLAND MODELLED WITH HIGH RESOLUTION	104

A.-I. Partanen, N. Mengis, J. Jalbert, and H.D. Matthews CARBON BUDGET UNCERTAINTY DUE TO UNCERTAINTY IN AEROSOL FORCING AND TRANSIENT CLIMATE RESPONSE .....	105
M. Passananti, E. Zapadinsky, J. Kangasluoma, N. Myllys, B. Reischl, R. Halonen, M. Attoui, and H. Vehkamäki STUDY ON FRAGMENTATION OF ATMOSPHERIC CLUSTERS INSIDE A MASS SPECTROMETER .....	106
M. Peltola, P. Paasonen, F. Xausa, R. Makkonen, and M. Kulmala DETERMINING THE UNDERLYING REASONS FOR BIASES IN PARTICLE NUMBER CONCENTRATIONS IN AN AEROSOL-CLIMATE MODEL .....	107
A.S. Pipal, P.G. Satsangi, A. Taneja, and S. Tiwari SOURCES AND CHARACTERISTICS OF CARBONACEOUS AEROSOLS IN NORTHERN PART OF INDIA .....	108
N.L. Prisle, G. Michailoudi, M. Toivola, M. Patanen, H. Yuzawa, M. Nagasaka, N. Hyttinen, M. Huttula, N. Kosugi, and T. Kurten MOLECULAR LEVEL STUDIES OF AQUEOUS OXIDIZED ORGANICS AND THEIR SALTING INTERACTIONS USING SYNCHROTRON RADIATION X-RAY ABSORPTION SPECTROSCOPY AND QUANTUM-CHEMISTRY BASED COSMO-RS .....	109
I. Pullinen, A. Ylisirniö, O. Väisänen, L. Q. Hao, A. Buchholz, S. Schobesberger, Z. Li, E.Kari, P. Miettinen, P. Yli-Pirilä, and A. Virtanen SECONDARY ORGANIC AEROSOL FORMATION FROM $\alpha$ -PINENE VERSUS REAL PLANT EMISSIONS: CHEMICAL AND PHYSICAL PROPERTIES .....	110
I. Pullinen, J. Wildt, E. Kleist, M. Springer, C.Wu, S. Andres, S.H.Schmitt, A. Wahner, and T.F. Mentel THE EFFECT OF CHEMISTRY AND PARTICLE TOTAL SURFACE AREA ON LOSS RATE OF HIGHLY OXIDIZED MULTIFUNCTIONAL ORGANIC MOLECULES (HOM) .....	111
X. M. Qi, A. J. Ding, P. Roldin, and M. Boy MODELLING STUDY ON HOM CONCENTRATIONS AND THEIR CONTRIBUTIONS TO NEW PARTICLE FORMATION AT THE BOREAL FOREST AND POLLUTED URBAN .....	112
L. L. J. Quéléver, K. Kristensen, L. N. Jensen, B. Rosati, R. Teiwes, H. B. Pedersen, M. Bilde, and M. Ehn EFFECT OF TEMPERATURE ON THE FORMATION OF HIGHLY OXYGENATED MOLECULES (HOMS) FORMED FROM $\alpha$ -PINENE OZONOLYSIS .....	113

B. Reischl, M. Passananti, N. Myllys, R. Halonen, E. Zapadinsky, and H. Vehkamäki MOLECULAR DYNAMICS SIMULATIONS OF SULFURIC ACID CLUSTER COLLISIONS .....	114
B. Rosati, R. Lange, A. Massling, and M. Bilde THE EFFECT OF SEA SPRAY AEROSOL AGEING ON ITS HYGROSCOPIC AND CLOUD FORMING POTENTIAL .....	115
G. Roudsari, O. H. Pakarinen, and H. Vehkamäki HETEROGENEOUS ICE NUCLEATION BY MINERAL DUSTS IN MIXED PHASED CLOUDS: MOLECULAR DYNAMICS SIMULATIONS .....	116
A. Rusanen, P. Kolari, M. Kaukolehto, M. Kulmala, and H. Junninen DEVELOPMENT OF SMEARCORE .....	117
A. Ruuskanen, A. Leskinen, S. Romakkaniemi, M. Komppula RELATIONS OF CLOUD DROPLET PROPERTIES AND IN-CLOUD ICING .....	118
S. Saari, P. Karjalainen, H. Kuuluvainen, A. Taipale, and T. Rönkkö INDOOR FILTRATION AND TRAFFIC RELATED ULTRAFINE NANOPARTICLES .....	119
S. Saarikoski, J. Alanen, H. Vesala, T. Murtonen, M. Isotalo, S. Martikainen, M. Bloss, M. Aurela, T. Maunula, K. Kallinen, J. Torrkulla, H. Timonen, T. Rönkkö, and K. Lehtoranta CHARACTERIZATION OF SECONDARY PARTICULATE EMISSIONS FROM ENGINE OPERATED BY NATURAL GAS AND PROPANE .....	120
L. Salo, Z. Liu, Y. Xie, and T. Rönkkö ATMOSPHERIC EFILTER MEASUREMENTS IN BEIJING, CHINA .....	121
N. Sarnela, M. Sipilä, T. Petäjä, M. Kulmala, and T. Jokinen OBSERVATIONS OF AEROSOL PRECURSOR VAPOURS IN BOREAL FOREST .....	122
P. M. Shamjad, K. Wang, T. Hoffmann, R. J. Huang, M. Glasius, and M. Bilde THE EFFECT OF TEMPERATURE AND SEED AEROSOL ACIDITY ON THE FORMATION AND COMPOSITION OF SECONDARY ORGANIC AEROSOLS FROM ISOPRENE OXIDATION .....	123
D. J. Shang, M. Hu, K. D. Lu, P. Roldin, J. Größ, S. Kecorius, Y. S. Wu, T. Olenius, B. Birger, L. M. Zeng, Y. H. Zhang, A. Wiedensohler, M. Boy MODELING STUDY ON IMPORTANCE OF ANTHROPOGENIC AMONNIA AND ORGANICS ON NEW PARTICLE FORMATION IN NORTH CHINA PLAIN .....	124

Y. Shen, A. Virkkula, , A. Ding, J. Wang, X. Chi, W. Nie, X. Qi, X. Huang, Q. Liu, L. Zheng, Z. Xu, T. Petäjä, P. P. Aalto, C. Fu, and M. Kulmala LONG TERM MEASUREMENT OF AEROSOL OPTICAL PROPERTIES AT SORPES, NANJING	125
.....	
M. Sofiev, J. Winebrake, L. Johansson, E.Carr EFFECT OF SHIP SULPHUR EMISSION REDUCTION ON GLOBAL AEROSOL LOAD	126
.....	
K. Teinilä, H. Timonen, S. Saarikoski, R. Hooda, M. Bloss, M. Aurela, E. Asmi, A. Malinen, L. Pirjola, B. Lal, A. Datta, S. Subudhi, R. Suresh, Md. H. Rahman, D. Verma, L. Salo, P. Simonen, P. Karjalainen, H. Kuuluvainen, K. Kulmala, J. Nuottimäki, J. Keskinen, T. Rönkkö, and H. Lihavainen, UNDERSTANDING LINK BETWEEN TRAFFIC AND AIR QUALITY IN INDIA, FIRST RESULTS OF “TAQIITA” PROJECT: CHEMICAL CHARACTERIZATION OF EXHAUST PARTICLES FROM PASSENGER CARS	128
.....	
P. Tiitta, A. Hartikainen, M. Ihalainen, P. Yli-Pirilä, M. Kortelainen, J. Tissari, H. Lamberg, A. Leskinen, J. Jokiniemi, and O. Sippula TIME-RESOLVED ANALYSIS OF SOA FORMATION FROM LOGWOOD COMBUSTION UPON PHOTOCHEMICAL AGING IN PEAR FLOW TUBE REACTOR	129
.....	
O.-P. Tikkanen, V. Hämäläinen, A. Lipponen, A. Buchholz, Z. Li, A. Virtanen, K.E.J. Lehtinen, and T.Yli-Juuti QUANTIFYING THE PROPERTIES OF SECONDARY ORGANIC AEROSOL THROUGH OPTIMIZING PROCESS-BASED MODELS	130
.....	
H. Timonen, M. Bloss, J. Kuula, A. Arffman, J. Alanen, K. Teinilä, M. Aurela, L. Salo, R. Hillamo, S. Saari, P. Oyola, F. Reyes, Y. Vásquez, R. Salonen, J. Keskinen, T. Rönkkö, E. Asmi, and S. Saarikoski COMPOSITION AND PROPERTIES OF PARTICULATE EMISSIONS FROM MINING ACTIVITIES	131
.....	
J. Tonttila, H. Kokkola, I. Kudzotsa, T. Raatikainen, J. Ahola, A. Afzalifar, H. Korhonen, and S. Romakkaniemi CLOUD-SCALE MODELLING OF AEROSOL-CLOUD-PRECIPIATION INTERACTIONS WITH UCLALES-SALSA	132
.....	
E. Tsiligiannis, J. Hammes, M. Le Breton, T. Mentel, and M. Hallquist FORMATION OF HIGHLY OXYGENATED MOLECULES (HOMs) DURING THE OXIDATION OF 1,3,5 TRIMETHYLBENZENE (TMB)	133
.....	

A. Virkkula, V.-M. Kerminen, T. Petäjä, G. De Leeuw, E. Asmi, D. Brus, T. Laurila, H. Timonen, K. Teinilä, E. Rodriguez, J. Svensson, V. Aaltonen, J. Backman, R. Hillamo, M. Sipilä, T. Jokinen, E. Järvinen, T. Nieminen, R. Väänänen, H. Manninen, X. Chen, P.P. Aalto, H. Grythe, M. Busetto, C. Lanconelli, A. Lupi, V. Vitale, R. Weller, A.C. Saulo, and M. Kulmala FINAL RESULTS OF A PROJECT ON ANTARCTIC AEROSOLS IN 2013 - 2016	134
.....	
D. Wimmer, P. Winkler, L.R. Ahonen, K. Lehtipalo, J. Kangasluoma, M. Kulmala, and T. Petäjä EXPERIMENTAL INVESTIGATION OF AEROSOL PARTICLE COMPOSITION AND GROWTH RATES	135
.....	
C. Xavier , P. Roldin, R. Makkonen, and M. Boy AEROSOL YIELDS FOR SELECTED BVOC AS A FUNCTION OF DIFFERENT PARAMETERS	136
.....	
C. Yan, J. Kangasluoma, F. Bianchi, T. Chan, B. Chu, L. Dada, K. Dällenbach, C. Deng, Y. Fu, X. He, L. Heikkinen, H. Junninen, Y. Liu, Y. Lu, Q. Ma, X. Qiao, P. Rantala, A. Rusanen, W. Wang, Y. Wang, M. Xue, G. Yang, R. Yin, Y. Zhou, J. Kujansuu, T. Petäjä, Y. Liu, M. Ge, H. He, L. Wang, J. Jiang, M. Kulmala FIRST MEASUREMENTS FROM SMEAR BEIJING STATION: NEW PARTICLE FORMATION IN URBAN BEIJING	137
.....	
T. Yli-Juuti, C. Mohr, A. Heitto, F. D. Lopez-Hilfiger, J. Hong, E. L. D'Ambro, S. Schobesberger, U. Makkonen, M. Rissanen, R. L. Mauldin III, M. Sipilä, N. M. Donahue, M. Kulmala, T. Petäjä, I. Riipinen, and J. Thornton GROWTH AND VOLATILITY OF SECONDARY AEROSOL PARTICLES AT HYYTIÄLÄ IN SPRING 2014	138
.....	
A. Ylisirniö, A. Buchholz, C. Mohr, A. Lambe, C. Faiola, E. Kari, T. Yli-Juuti, S.A. Nizkorodov, D. R. Worsnop, S. Schobesberger, and A. Virtanen TRACKING SOA COMPOSITION AND THERMAL DESORPTION BEHAVIOR WITH OXIDATIVE AGING: $\alpha$ -PINENE VS. REAL PLANT EMISSIONS	139
.....	
I. Ylivinkka, M. Kulmala, J. Itämies, and D. Taipale THE EFFECT OF AUTUMNAL MOTH INDUCED VOLATILE ORGANIC COMPOUND EMISSIONS TO AEROSOL LOAD IN SUBARCTIC REGION	140
.....	
M.A. Zaidan, V. Haapasilta, R. Relan, P. Paasonen, V.-M. Kerminen, H. Junninen, M. Kulmala, and A.S. Foster MUTUAL INFORMATION BETWEEN NEW PARTICLE FORMATION AND ATMOSPHERIC VARIABLES	141
.....	

Y. Zhang, O. Peräkylä, C. Yan, L. Heikkinen, M. Äijälä, M. Riva, Q. Zha, L. Quéléver, K. Daellenbach, P. Paatero, M. Kulmala , W. Douglas, M. Ehn NOVEL FACTOR ANALYTICAL TECHNIQUES APPLIED TO HIGHLY OXYGENATED MOLECULES (HOMS)	142
P. Zhou, L. Ganzeveld, D. Taipale, Üllar Rannik, Pekka Rantala, M. P. Rissanen, D. Chen, and M. Boy BOREAL FOREST BVOC EXCHANGE: EMISSIONS VERSUS IN-CANOPY SINKS	143
P. Zieger, M.E. Salter, B. Rosati, E.D. Nilsson LINKING RECENT FINDINGS FROM THE STOCKHOLM SEA SPRAY CHAMBER TO GLOBAL CLIMATE MODELS	144



# METAL CONTENTS OF EXHAUST FROM FOUR MARINE ENGINES USING DIFFERENT FUELS

P. AAKKO-SAKSA<sup>1</sup>, H. VESALA<sup>1</sup>, T. MURTONEN<sup>1</sup>, H. TIMONEN<sup>2</sup>, N. KUITTINEN<sup>3</sup>, P. KARJALAINEN<sup>3</sup>, M. BLOSS<sup>2</sup>, K. TEINILÄ<sup>2</sup>, P. KOPONEN<sup>1</sup>, R. PETTINEN<sup>1</sup>, K. LEHTORANTA<sup>1</sup>, AND T. RÖNKKÖ<sup>3</sup>

<sup>1</sup> VTT Technical Research Centre of Finland, P.O. Box 1000, 02044 VTT Espoo, Finland

<sup>2</sup> Atmospheric Composition Research, Finnish Meteorological Institute, Helsinki, 00560, Finland

<sup>3</sup> Aerosol Physics, Faculty of Natural Sciences, Tampere University of Technology, Tampere, 33101, Finland

Keywords: ship, marine, metal, trace element, vanadium, nickel

Presenting author email: paivi.aakko-saksa@vtt.fi

Ships travel near densely inhabited coastal areas (Eyring, 2010), and emit large amounts of exhaust having many constituents harmful to health. For example, ultrafine particles and related chemical species have lately been linked with heart and pulmonary diseases and even with Alzheimers disease (Oudin et al. 2016). Engine exhaust particles consists of elemental and organic carbon, sulphur, nitrogen, oxygen and trace elements. Soluble metals from combustion sources may be biologically active and toxic (Laing et al. 2014). In this study, trace metals from marine engine exhaust were studied in laboratory (engine E1), on-board ship A (engines E2 and E3) and ship B (engine E4) using fuels with sulphur contents up to 2.5%. From several engine loads studied, the results presented here were achieved at 75% load for E1-E3, and at 65% load for E4. For E2, the results are after scrubber, and for E3 after scrubber and a selective catalyst reduction (SCR) system. For E4, engine-out results are shown, as metal concentrations after the emission control devices were below the detection limit. PM samples were collected from diluted (ISO 8178) exhaust using quartz filters. The extracts (EN 14385) were analysed by inductively coupled plasma mass spectrometry (ICP-MS). Trace elements analysed were Ag, Al, As, B, Ba, Be, Bi, Ca, Cd, Co, Cr, Cu, Fe, K, Li, Mg, Mn, Mo, Na, Ni, Pb, Rb, Sb, Se, Sr, Th, Tl, U, V ja Zn, Br, Cl, P, S, Si and Sn. For detailed E1-E3 results, see Aakko-Saksa et al. (2017) and Timonen et al. (2017).

The highest concentrations of trace elements in marine engine exhaust were observed for V, Ni, Ca, Na, Fe, Ca, and in some cases for Al. From priority heavy metals (As, Cd, Cr, Cu, Ni, Pb, Se, Zn), only Ni was present in exhaust at noticeable concentrations. Metals in the engine exhaust originate from fuel, engine oil and wear. HFO-type fuels at the highest sulphur contents (1.9 and 2.2%S) contained also high concentrations of V (110 and 430 mg/kg) and Ni (21 and 75 mg/kg), while concentrations of Ca, Na and Fe were lower (from 6 to 24 mg/kg). For these fuels, V and Ni in exhaust were apparently originating mainly from fuel, and Ca, Na and Fe at least partly. Modest concentrations of V, Ca, Na and Fe were present in the exhaust using fuels at sulphur contents below 0.7%S. These fuels contained less V than 20 mg/kg and concentrations of the other metals were low. For fuel containing 30% of biocomponent (Bio30), concentrations of the metals in both exhaust and fuel were particularly low. Engine oil contained high amount of Ca

(12-16 g/kg), and this is one source of Ca in exhaust. Substantial amount of Al was found on some exhaust samples, which may indicate engine wear.

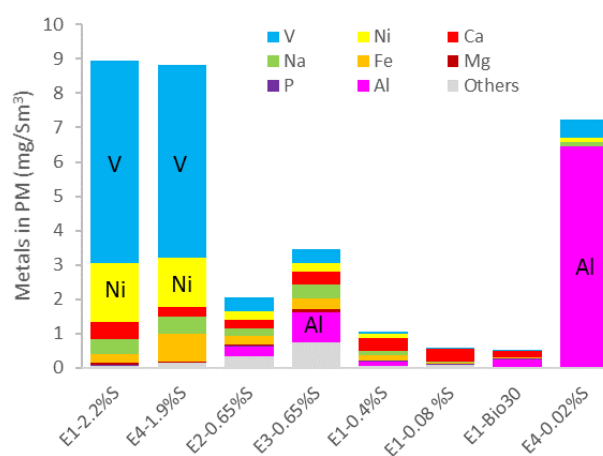


Figure 1: Metal concentrations in the exhaust from engines in laboratory (E1) and on-board two ships (E2-E4). Fuels with 2.2%, 1.9%, 0.65%, 0.4%, 0.08% and 0.02% sulphur contents were used, as well as a fuel containing 30% of biocomponent.

The financial support for the SEA-EFFECTS BC project from Tekes (40356/14), Trafi (172834/16) and from industrial partners, Wärtsilä, Pegasor, Spectral Engines, Gasmot, VG-Shipping, HaminaKotka Satama Oy, Oiltanking Finland Oy and Kine Robotics, is gratefully acknowledged, and for the EnviSuM project from Trafi (58942/17, VTT's measurements).

Aakko-Saksa, P. et al. (2017) Research Report: VTT-R-02075-17. [www.vtt.fi/sites/sea-effects](http://www.vtt.fi/sites/sea-effects)  
Eyring, V et al (2010), *Atmos. Environ.*, 44, 4735–4771.  
IMO (*International Maritime Organization*), 2016 available at: <https://business.un.org/en/entities/13>  
Laing, J. et al. (2014) *Atmospheric Environment* 88: 285–296.  
Oudin, A. et al. (2016) *Environmental Health Perspectives* 124(3): 306–312.  
Timonen, H. et al. (2017) Research Report: VTT-R-04493-17. [www.vtt.fi/sites/sea-effects](http://www.vtt.fi/sites/sea-effects)

## A human exposure study of dermal and inhalation uptake of particle and gas phase phthalates

C. ANDERSEN<sup>1</sup>, A.M. KRAIS<sup>2</sup>, A.C. ERIKSSON<sup>1</sup>, J. JAKOBSSON<sup>1</sup>, C.H. LINDH<sup>2</sup>, J. LÖNDAHL<sup>1</sup>, J. PAGELS<sup>1</sup>, J. NIELSEN<sup>2</sup>, A. GUDMUNDSSON<sup>1</sup> and A. WIERZBICKA<sup>1</sup>

<sup>1</sup>Ergonomics and Aerosol Technology, Lund University, Sweden

<sup>2</sup>Division of Occupational and Environmental Medicine, Lund University, Sweden

Keywords: human exposure, SVOCs, phthalates, dermal uptake, lung deposition

Phthalates are used in a large variety of consumer products, such as cosmetics, fragrances, food packaging, medical equipment and building materials. They belong to the group of semi-volatile organic compounds (SVOCs), and are not covalently bound in products. Thereby they can migrate or evaporate from consumer products and building materials, which makes up an exposure route to humans. Exposure to phthalates has been associated with endocrine disruption effects, including reduction of male reproductive hormones in humans, as well as allergies, and asthma (Joensen et al., 2012). While the oral uptake of phthalates have been studied, there are only few studies on the airborne exposure through dermal and inhalation routes in indoor environments.

The aim of this work was to elucidate the dermal and inhalational uptake of two deuterium labelled phthalates. This is the first human exposure study of the uptake of deuterium labelled DEHP aerosol particles by inhalation and dermal uptake, and on the comparison of the two routes in humans.

We have conducted a human exposure study of dermal and inhalational uptake of particle and gas phase phthalates. Sixteen participants were exposed during 3 hours to two deuterium labelled phthalates: particulate di(2-ethylhexyl) phthalate (DEHP) and gaseous diethyl phthalate (DEP). Urine samples were collected before exposure and for 24 hours after exposure. During dermal exposures, uptake by inhalation was eliminated by supplying clean air to the participants through a hood sealed around the neck.

DEHP particles were measured during the exposures with a scanning mobility particle sizer (SMPS, TSI Inc.) and a high resolution aerosol mass spectrometer (HR-AMS, Aerodyne Research Inc.). Further, particles were collected on Teflon filters. DEP was collected on sorbent Tenax tubes. Both filters and Tenax tubes were extracted and subsequently analyzed with gas chromatography tandem mass spectrometry (GC-MS/MS). Six metabolites were analyzed in urine samples with liquid chromatography tandem mass spectrometry (LC-MS/MS).

The deposited fraction of inhaled particles was calculated with the MPPD (multiple-path particle dosimetry) model version 3.04.

The results show a higher uptake of DEP compared to DEHP for both dermal and combined dermal and inhalation uptake (Figure 1). For both exposure to DEHP particles and gaseous DEP the primary uptake was through inhalation. The concentration of urinary metabolites after dermal exposure to DEHP was below the limit of detection.

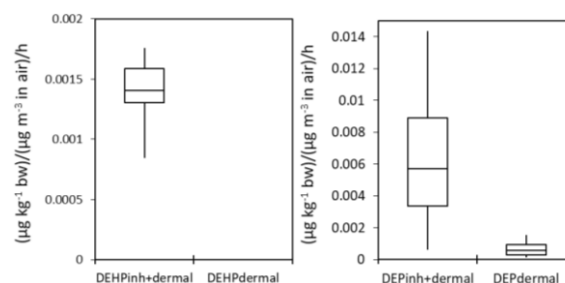


Figure 1. The median, 25 and 75 percentiles of the uptake in  $(\mu\text{g kg}^{-1} \text{bw})/(\mu\text{g m}^{-3} \text{in air})/\text{h}$  for the exposure scenarios  $\text{DEHP}_{\text{inh+dermal}}$ ,  $\text{DEHP}_{\text{dermal}}$  (below the detection limit),  $\text{DEP}_{\text{inh+dermal}}$ ,  $\text{DEP}_{\text{dermal}}$ .

We calculated an average deposited fraction of inhaled DEHP in the extrathoracic region, tracheobronchial region, and alveolar region to 3, 9, and 14 %, respectively.

The results also showed that 73 % of the deposited DEHP mass was detected in urine as metabolites. For DEP only 53 % of the inhaled mass was detected as metabolite in urine samples, when 100 % uptake of the inhaled DEP was assumed. These numbers differ from the previous reported number for oral ingestion (Anderson et al., 2011), and can in the future be applied in urine screening studies where back-calculations are needed to estimate the uptake.

In conclusion, this study shows that the primary route of uptake of airborne phthalates is through inhalation, while also highlighting the importance of including the deposited fraction in studies of uptake of inhaled particles.

The study was financed by the Swedish research council FORMAS (Project Dnr 216-2013-1478).

Joensen, U. N. et al. (2012). *Environ Health Perspect*, 120, (10), 1397-403.

Anderson, W. A. et al. (2011). *Food Chem Toxicol*, 49, (9), 2022-9.

# PRIMARY AND SECONDARY PARTICLE EMISSIONS FROM DUAL-FUEL MARINE ENGINE

M. AURELA<sup>1,2</sup>, M. BLOSS<sup>1</sup>, N. KUITTINEN<sup>2</sup>, J. ALANEN<sup>2</sup>, P. KARJALAINEN<sup>2</sup>, T. RÖNKKÖ<sup>2</sup>, J. KESKINEN<sup>2</sup>, L. NTZIACHRISTOS<sup>2</sup>, K. LEHTORANTA<sup>3</sup>, S. NYSSÖNEN<sup>3</sup>, H. VESALA<sup>3</sup>, and H. TIMONEN<sup>1</sup>

<sup>1</sup> Atmospheric Composition Research, Finnish Meteorological Institute, Helsinki, Finland

<sup>2</sup> Aerosol Physics, Faculty of Natural Science, Tampere University of Technology, Tampere, Finland

<sup>3</sup> VTT Technical Research Centre of Finland, Espoo, Finland

Keywords: emissions, marine engine, dual-fuel, secondary aerosol, primary aerosol

The International Maritime Organization has implemented regulations to reduce emissions from ships. Since January 2015 the allowed sulphur content in marine fuel oils was limited to 0.1 % in sulphur emission control areas (SECAs). Emissions will be further reduced in the remaining EU sea areas with the implementation in 2020 of the 0.5% regional limit.

The emission measurements of marine engine were conducted in a test-bed engine lab equipped with a four cylinder medium-speed diesel engine, which was modified to run with compressed natural gas (CNG) in dual fuel (DF) mode. In addition to natural gas, which was used as main fuel, a pilot liquid fuel was needed to operate the engine. The pilot (liquid) fuel was marine gas oil (MGO), which was of road diesel quality (EN 590:2009) with very low sulphur level. Two different contributions of pilot fuel (pilot normal and pilot high) were tested with two different engine loads (85% and 40%). The engine loads were selected to represent the conditions at open sea (85%) and at harbour areas (40%). For comparison, the engine was also operated using MGO and marine diesel oil (MDO) as main fuels.

Chemical composition and physical properties of both primary and secondary submicron particles were studied. An oxidative flow reactor called potential aerosol mass (PAM) chamber (Kang *et al.*, 2007) was used to simulate secondary aerosol formation potential of gaseous exhaust emissions in the atmosphere. Aerosol chemical composition (organic matter, sulphate, nitrate, ammonium, chloride and refractory black carbon) was measured with a Soot-Particle Aerosol Mass Spectrometer (SP-AMS, Onasch *et al.*, 2015). Optical absorption properties of soot particles were measured on line using an Aethalometer (ModelAE33-7, Drinovec *et al.*, 2015) measuring at seven wavelengths (370-950 nm). Physical properties of particles were measured with a scanning mobility particle sizer (SMPS). The volatility of the particles was studied both with and without a thermo denuder and catalytical stripper.

The flue gas was diluted using a porous tube diluter and double-ejector system for primary and secondary particles, respectively. Furthermore, an additional ejector for both system was needed to get enough high sample flow rate for the instruments. Dilution ratio was

calculated based on the ratio between trace gas concentrations mainly using CO<sub>2</sub> concentration at raw emissions and after the last ejector.

The mass concentrations of primary particles were significantly lower when using CNG as the main fuel compared to MGO or MDO fuels (Fig. 1). The engine load was also found to have a significant effect on primary particle formation. At lower engine load, the particle mass concentrations were found to be higher with all fuels than with high engine load (Fig. 1). The main component was organic particulate matter followed by black carbon. For aged aerosol, the main component was also particulate organic matter followed by either black carbon or sulfate (not shown).

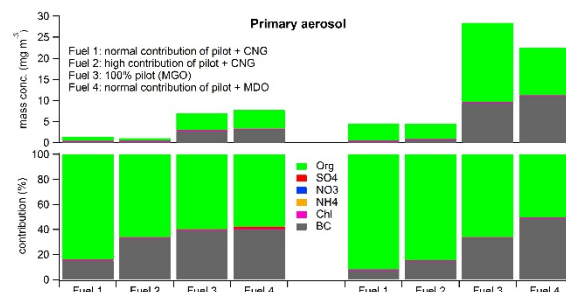


Figure 1: Chemical composition of PM<sub>1</sub> and contribution of primary particulate emissions from DF engine for two different engine loads and four different fuels.

This work was conducted in the framework of the HERE project funded by Tekes (the Finnish Funding Agency for Innovation), Agco Power Oy, Dinex Ecocat Oy, Dekati Oy, Neste Oyj, Pegasor Oy and Wärtsilä Finland Oy.

Drinovec, L., Močnik, G., Zotter, P., Prévôt, A.S.H., Ruckstuhl, C., Coz, E., Rupakheti, M., Sciare, J., Müller, T., Wiedensohler, A., and Hansen, A.D.A. (2015). *Atmos. Meas. Tech.*, 8:1965–1979.

Kang, E., Root, M., Toohey, D. and Brune W. (2007). *Atmos. Chem. Phys.*, 7: 5727–5744.

Onasch, T., Trimborn, A., Fortner, E., Jayne, J., Kok, G., Williams, L., Davidovits, P. and Worsnop, D. (2012). *Aerosol Sci. Technol.* 46:804-817.

## A method for extracting calibrated volatility information from the FIGAERO ToF CIMS and application to laboratory and field measurements

Thomas J. Bannan<sup>1</sup>, Michael Le Breton<sup>2</sup>, Michael Priestley<sup>1</sup>, Stephen Worrall<sup>1</sup>, Julia Hammes<sup>2</sup>, Mattias Hallquist<sup>2</sup>, Rami Alfarra<sup>1,3</sup>, Ulrich. K. Krieger<sup>4</sup>, Jonathan Reid<sup>5</sup>, Gordon McFiggans<sup>1</sup>, Hugh Coe<sup>1</sup>, Carl J. Percival<sup>†1</sup>, Dave Topping<sup>1</sup>

<sup>1</sup>Centre for Atmospheric Science, School of Earth, Atmospheric and Environmental Science, University of Manchester, Oxford Road, Manchester, M13 9PL, UK

<sup>2</sup>Department of Chemistry and Molecular Biology, University of Gothenburg, Gothenburg, Sweden

<sup>3</sup>National Centre for Atmosphere Science, UK

<sup>4</sup>Institute for Atmospheric and Climate Science, ETH Zürich, 8092 Zürich, Switzerland

<sup>5</sup>School of Chemistry, University of Bristol, Cantock's Close, Clifton, Bristol BS8 1TS

<sup>†</sup>Current address: Jet Propulsion Laboratory, 4800 Oak Grove Drive, Pasadena, CA 91109

The Filter Inlet for Gases and AEROsols Time of flight Chemical ionisation mass spectrometer (FIGAERO ToF CIMS) provides simultaneous molecular information relating to both the gas and particle phase and has been used to extract vapour pressures of the compounds desorbing from the filter, whilst giving quantitative concentrations in the particle phase. However, such extraction of vapour pressures of the measured particle phase components requires use of appropriate, well-defined, reference compounds. Most recently the homologous series of polyethylene glycols (PEG) ((H-(O-CH<sub>2</sub>-CH<sub>2</sub>)<sub>n</sub>-OH) for n=3 to n=8) has been shown to be reproduced well by a range of different techniques, including Knudsen Effusion Mass Spectrometry (KEMS), over a range of vapour pressures (VP) (10<sup>-1</sup> to 10<sup>-7</sup> Pa) that are atmospherically relevant. This is the first homologous series of compounds for which a number of vapour pressure measurement techniques have been found to be in agreement, indicating their utility as a calibration standard. The PEG series therefore provides an ideal set of benchmark compounds that allow accurate characterisation of the FIGAERO for extracting vapour pressure of measured compounds in chambers and the real atmosphere. To demonstrate this, single component and mixture vapour pressures measurements are made using two FIGAERO ToF CIMS instruments based on a new calibration line determined from the PEG series. This method is then applied to chamber and field measurements investigating oxidation and the vapour pressures of known products and the impacts on new particle formation.

# BVOC-FEEDBACK SENSITIVITY TO NUCLEATION PARAMETERIZATION IN THE NORWEGIAN EARTH SYSTEM MODEL (NorESM)

S.M. Blichner<sup>1</sup>, M.K. Sporre<sup>1</sup>, F. Stordal<sup>1</sup>, H. Tang<sup>1</sup> and T.K. Berntsen<sup>1</sup>

<sup>1</sup> Department of Geosciences, University of Oslo, Norway

Keywords: earth system modelling, nucleation, BVOC, organic aerosols, feedback

Vegetation feeds back to climate in several ways, one of which is through emissions of biogenic volatile organic compounds (BVOCs). Through oxidation in the atmosphere, various compounds of a range of volatility and hygroscopicity are produced (Ehn et al., 2014). The lowest volatility products are thought to contribute to the nucleation of new atmospheric particles, while products with higher (but still low) volatility can condense onto already existing particles.

The emission of BVOCs vary due to the type and density of the vegetation as well as environmental factors such as temperature, sunlight, CO<sub>2</sub> concentration, soil moisture ect. In sum BVOC emissions are thought to increase with increased temperatures and CO<sub>2</sub> levels, i.e. climate change. This introduces a possible negative feedback loop through increased temperatures → increased emissions of BVOC → increased aerosol number and mass concentration → direct and indirect negative aerosol forcing → reduced temperature increase.

The strength of this feedback loop depends among other factors, on how sensitive new particle formation is to the increase in BVOC emissions.

While it has been shown that oxidation products from BVOCs can participate in the formation of new particles from nano-sizes (alone or with e.g. sulphuric or ammonia) (Shrivastava et al., 2017), the process is poorly understood and the uncertainties with regards to parametrization are large. We investigate the sensitivity of the earlier mentioned BVOC feedback with different parameterizations of new particle formation in the Norwegian Earth System model (NorESM). The atmospheric component is the Community Atmospheric Model with the OsloAero aerosol scheme (CAM5.3-Oslo). The OsloAero scheme is a lifecycle scheme which tags the production mechanism for compounds in the aerosols. The current parameterization in NorESM based on Paasonen et al (2010), calculates the formation rate of new particles as linearly dependent on the concentrations of sulphuric acid and low volatility oxidation products of BVOCs (ORG\_LV) and is thus in accordance with activation theory for nucleation (nucleation rate  $J_{\text{nuc}} = k_1[\text{H}_2\text{SO}_4] + k_2[\text{ORG\_LV}]$ ).

We present preliminary results investigating the sensitivity of the feedback loop to changing the parameterization to either homo- and heteromolecular nucleation, also based on Paasonen et al. (2010)(eq. 19,  $J_{\text{nuc}} = k'_1[\text{H}_2\text{SO}_4]^2 + k'_2[\text{H}_2\text{SO}_4][\text{ORG\_LV}]$ , and eq. 20,  $J_{\text{nuc}} = k_1^*[\text{H}_2\text{SO}_4]^2 + k_2^*[\text{H}_2\text{SO}_4][\text{ORG\_LV}] +$

$k_3^*[\text{ORG\_LV}]^2$ ). We find that these alternative parameterizations give much weaker new particle formation rate and lower production of secondary aerosols, and that, contrary to expectation, they are less sensitive to increased BVOC emissions than the original parameterization.

Ehn, M., Thornton, J. A., Kleist, E., Sipilä, M., Junninen, H., Pullinen, I., Springer, M., Rubach, F., Tillmann, R., Lee, B., Lopez-Hilfiker, F., Andres, S., Acir, I.-H., Rissanen, M., Jokinen, T., Schobesberger, S., Kangasluoma, J., Kontkanen, J., Nieminen, T., Kurtén, T., Nielsen, L. B., Jørgensen, S., Kjaergaard, H. G., Canagaratna, M., Maso, M. D., Berndt, T., Petäjä, T., Wahner, A., Kerminen, V.-M., Kulmala, M., Worsnop, D. R., Wildt, J., and Mentel, T. F. (2014). A large source of low-volatility secondary organic aerosol. *Nature*, 506(7489):476–479.

Paasonen, P., Nieminen, T., Asmi, E., Manninen, H. E., Petäjä, T., Plass-Dülmer, C., Flentje, H., Birmili, W., Wiedensohler, A., Hörrak, U., Metzger, A., Hamed, A., Laaksonen, A., Facchini, M. C., Kerminen, V.-M., and Kulmala, M. (2010). On the roles of sulphuric acid and low-volatility organic vapours in the initial steps of atmospheric new particle formation. *Atmos. Chem. Phys.*, 10(22):11223–11242.

Shrivastava, M., Cappa, C. D., Fan, J., Goldstein, A. H., Guenther, A. B., Jimenez, J. L., Kuang, C., Laskin, A., Martin, S. T., Ng, N. L., Petaja, T., Pierce, J. R., Rasch, P. J., Roldin, P., Seinfeld, J. H., Shilling, J., Smith, J. N., Thornton, J. A., Volkamer, R., Wang, J., Worsnop, D. R., Zaveri, R. A., Zelenyuk, A., and Zhang, Q. (2017). Recent advances in understanding secondary organic aerosol: Implications for global climate forcing. *Reviews of Geophysics*, 55(2):2016RG000540.

# CHEMICAL COMPOSITION OF EMISSIONS MEASURED IN REAL TIME FROM A MODERN SHIP ENGINE DURING A CRUISE

M. BLOSS<sup>1</sup>, P. KARJALAINEN<sup>2</sup>, N. KUITTINEN<sup>2</sup>, T. MURTONEN<sup>3</sup>, H. VESALA<sup>3</sup>, T. RÖNKKÖ<sup>2</sup>, P. AAKKO-SAKSA<sup>3</sup>, AND H. TIMONEN<sup>1</sup>

<sup>1</sup> Atmospheric Composition Research, Finnish Meteorological Institute, Helsinki, 00560, Finland

<sup>2</sup> Aerosol Physics, Faculty of Natural Sciences, Tampere University of Technology, Tampere, 33101, Finland

<sup>3</sup> VTT Technical Research Centre of Finland, P.O. Box 1000, 02044 VTT Espoo, Finland

Keywords: SP-AMS, PAM, SOA

Presenting author email: matthew.bloss@fmi.fi

Shipping is the most cost effective form of transport for trading goods, with over 90% of trade worldwide being carried by sea (IMO, 2016). Approximately 70% of ship emissions are emitted within 400 km of land (Eyring, 2010). These exhaust emissions contain e.g. particulate organic matter (POM), refractive black carbon (rBC), carbon dioxide (CO<sub>2</sub>), nitrogen oxides (NO<sub>x</sub>), sulphur dioxide (SO<sub>2</sub>) and volatile organic compounds (VOC's) (Eyring, 2010). In the Baltic Sea region (Jonson et al, 2015) found that areas close to shipping lane emissions have a shortening of life expectancy by 0.1-0.2 years per person. To understand the effect shipping has on air quality it is important to determine ship emissions as accurately as possible.

Measurements were conducted during a real time voyage with a fully loaded ship. The particulate emissions of a main and auxiliary engine, operating at 40% and 75% load were measured. The ship after treatment system included a selective catalyst reduction (SCR) system and scrubber. The exhaust emissions from the two different fuel types, HFO (heavy fuel oil) and MGO (marine gas oil) were also measured. The emissions were diluted using a porous tube diluter combined with a residence time tube. The sample was further diluted using an ejector diluter (Dekati Ltd, Finland). The submicron particulate emissions were analysed using a Soot Particle - Aerosol Mass Spectrometer (SP-AMS) (Aerodyne Research Inc, US, Onasch et al, 2012) to gain information on the real time submicron particulate mass (PM) concentration, chemical composition, size distribution as well as concentrations of rBC and some metals. In addition, physical (e.g. size distribution, number concentration) and optical (light scattering coefficient) properties of submicron particles and trace gases were measured with a large variety of instruments. The secondary aerosol formation potential was studied using a PAM (Potential Aerosol Mass -chamber, Aerodyne Research Inc, US, Kang, 2007) chamber which allowed simulation of the atmospheric aging of the emissions.

The aim of this campaign was to compare primary and secondary particulate emissions originating from different fuels, engine loads and emission reduction technologies. The composition of primary particulate emissions was observed to be very different when compared to aged emissions after the PAM chamber. In the primary particulate exhaust emissions the contribution of organics (45.7%) and sulphate was observed to be

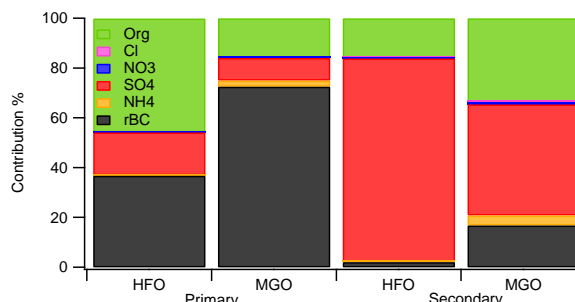


Figure 1: Contribution of inorganic species (sulphate, nitrate, ammonium, chloride), organics and rBC for when using HFO and MGO fuels types and with a SCR before the scrubber. During secondary PM measurements PAM was set to 2.4 volts corresponding to 2.8 days aging in the atmosphere.

highest for HFO (17.2%), whereas MGO had a higher rBC contribution (72.6%). For aged emissions, after PAM chamber, the contribution of submicron PM sulphates were high for both fuels (HFO; 81.6%, MGO 44.6%). In addition, organic contributions were higher for MGO fuel during secondary measurements. This shows the importance of fuel sulphur content, 0.7% for HFO and <0.1% for MGO.

The financial support from Tekes (40356/14, SEA-EFFECTS BC), Trafi (172834/2016) and from industrial partners, Wärtsilä, Pegasor, Spectral Engines, Gasmot, VG-Shipping, HaminaKotka Satama Oy, Oiltanking Finland Oy and Kine Robotics, are gratefully acknowledged.

Eyring, V et al (2010) Transport impacts on atmosphere and climate: shipping, *Atmos. Environ.*, 44, 4735–4771.

IMO: IMO profile, *IMO (International Maritime Organization)*, 2016 available at: <https://business.un.org/en/entities/13>

Jonson, J. E et al (2015) Model calculations of the effects of present and future emissions of air pollutants from shipping in the Baltic Sea and the North Sea, *Atmos. Chem. Phys.*, 15, 783–798.

Kang, E et al (2007) Introducing the concept of Potential Aerosol Mass (PAM), *Atmos. Chem. Phys.*, 7, 5727–5744

Onasch et al (2012) Soot Particle Aerosol Mass Spectrometer: Development, Validation, and Initial Application *Aerosol Sci. Tech.* 46 (7), 0278-6826

# CHARACTERIZATION OF ATMOSPHERIC POLLEN WITH MULTI-WAVELENGTH RAMAN LIDAR MEASUREMENTS

S. BOHLMANN<sup>1</sup>, M. FILIOGLOU<sup>1</sup>, E. GIANNAKAKI<sup>1,2</sup>, X. SHANG<sup>1</sup>, A. SAARTO<sup>3</sup>, S. ROMAANIEMI<sup>1</sup> and M. KOMPPULA<sup>1</sup>

<sup>1</sup>Finnish Meteorological Institute, P.O. Box 1627, 70211, Kuopio, Finland

<sup>2</sup>Department of Environmental Physics and Meteorology, University of Athens, Athens, Greece

<sup>3</sup>Aerobiology Unit, University of Turku, Finland

Keywords: atmospheric aerosols, pollen, remote sensing, lidar

Pollen is one type of primary biogenic atmospheric aerosol. In addition to the commonly known allergic impact, pollen has also various climatic, environmental and ecological/biological impacts. It can act as environmental pollutant by decreasing the visibility through scattering of sun light. Furthermore, pollen can act as ice nuclei (IN) and cloud condensation nuclei (CCN) and thus has impact on cloud formation and cloud optical properties as well (Steiner et. al., 2015).

Pollen is usually measured by Hirst-type pollen samplers which enable the microscopical identification of pollen types and their concentration with 2-hour time resolution. In Finland, a network of 9 stations collect pollen samples for further analysis. This method can only provide the pollen concentration at roof level (usually 10-15 m agl), yet very little is known on the vertical distribution and its optical properties. However, for modeling the dispersion of pollen and improving pollen forecasts, the vertical information is needed.

Aerosol lidars (light detection and ranging) provide vertical information of the atmosphere with good vertical and temporal resolution. Measuring backscattering, extinction and depolarization ratio of the detected particles, they can be characterized e.g. in terms of size and sphericity. It has been observed that the non-spherical pollen grains generate strong depolarization (Noh et. al., 2013). In the absence of other non-spherical particles, information about the shape of pollen can be retrieved using depolarization lidar measurements.

This study combines measurements with the multi-wavelength Raman polarization lidar Polly<sup>XT</sup> and the traditional Hirst-type sampler to investigate the optical properties of pollen and to enable a pollen classification with lidar measurements.

The measurement campaign took place in May-August 2016 in Kuopio, Finland and provided a dataset of particle optical properties for several different pollen types. These data revealed that certain pollen types show higher depolarization and thus the classification of different pollen types is possible. Meteorological data and backward trajectories were used to take the meteorological condition and possible long-range transported pollen into account.

On 8<sup>th</sup> May 2016 a pollination event was observed as presented in Figure 1. The Birch pollen concentration, measured by the Hirst-type sampler is provided in Fig 1(a). Profiles of the range corrected

signal at 1064 nm and volume depolarization at 532 nm are presented in Fig 1(b) and (c), respectively.

The roof level concentration shows peak values during the day time. The lidar signals show the features of the boundary layer top height increasing before 15:00 UTC and decreasing towards the night and also the dispersion of the depolarizing pollen particles throughout the whole boundary layer up to about 2.5 km altitude. The whole campaign dataset will be studied in detail and new information on the pollen type detection and their vertical distribution are provided.

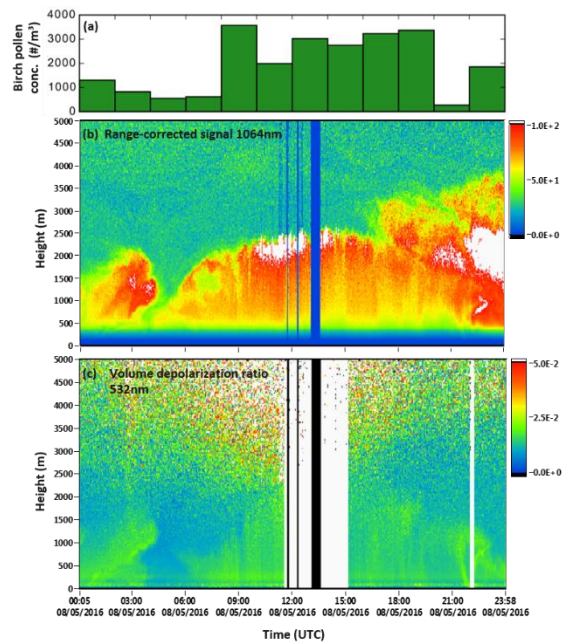


Figure 1: a) Birch Pollen concentration at roof level, b) range corrected lidar signal at 1064nm and c) volume depolarization ratio at 532nm on 8<sup>th</sup> May 2016.

Noh, M. Y., Müller, D., Lee, H., Choi, T. (2013).

*Influence of biogenic pollen on optical properties of atmospheric aerosols observed by lidar over Gwangju, South Korea*, Atmospheric Environment, 69, 139147.

Steiner, A. L., Brooks, S. D., Deng, C., Thornton, D. C. O., Pendleton, M. W., Bryant, V. (2015). *Pollen as atmospheric cloud condensation nuclei*. Geophysical Research Letters, 42, 3596-3602.

# PHOTOCHEMISTRY OF FIELD COLLECTED COMPLEX ORGANIC MATTER AND ITS ABILITY TO ACT AS CLOUD CONDENSATION NUCLEI

N. BORDUAS-DEDEKING<sup>1,2</sup>, Z.A. KANJI<sup>2</sup>, and K. MCNEILL<sup>1</sup>

<sup>1</sup> Institute for Biogeochemistry and Pollutant Dynamics, ETH Zurich, Switzerland

<sup>2</sup> Institute for Atmospheric and Climate Sciences, ETH Zurich, Switzerland

Keywords: organic aerosols, complex organic matter, cloud condensation nuclei, photochemistry

Organic aerosols account between 20 and 90% of the total mass of the submicron aerosol population and are thus important components of atmospheric aerosols (Jimenez et al., 2009; Zhang et al., 2007). Particularly in the free troposphere where aerosols have been atmospherically aged by photolysis, oxidation, gas-particle partitioning and cloud processing (activation / evaporation and deliquescence / efflorescence), the presence of particles between 50 and 1000 nm in diameter containing carbonaceous material is almost ubiquitous (Murphy et al., 2006). When organic carbon is present, a suite of chemical reactions can take place such as oxidation, substitution and acid-base reactions.

We focused our study on organic aerosol equivalents. Indeed, we argue that complex organic matter sampled from estuaries in the US can act as a proxy for organic aerosols as it is (1) a naturally occurring complex organic material, (2) directly relevant to lake spray aerosols (Axson et al., 2016; Slade et al., 2010) and (3) known to have both ions and organic material, and thus capable of acting as CCN. In this study, we identify through laboratory experiments field collected complex organic matter samples that are efficient cloud condensation nuclei (CCN). We subsequently further our study by asking which chemical compound within the organic matter is responsible for its hygroscopic growth? We show how the molecular subcomponents of organic matter individually contribute to a changing CCN ability with photochemical exposure (Figure 1). In particular, we used International Humic Substance Society isolates such as Suwannee River fulvic and humic acids and compounds such as lignin, proteins and carbohydrates to represent subcomponents of organic matter (Figure 1). We found that lignin is particularly good CCN with a kappa ranging from 0.1 to 0.3. To further compare our complex organic matter samples, we employ lab-generated  $\alpha$ -pinene and naphthalene SOA samples and show that a similar increase in kappa is observed for this reference material (Figure 1). We calculate that a 25 h UVB exposure time in our laboratory is equivalent to approximately 0.4 mE/cm<sup>2</sup> cumulative absorbed photon flux and to 3 days in the atmosphere.

Using chemical analyses, we also observed that the total organic content of organic matter and most of its subcomponents decreases during irradiation, with a concurrent production of CO and CO<sub>2</sub>. These observations further support a mineralization

mechanism, where direct and indirect photochemical processes lead to the oxidation of the organic material up to the highest form of oxidized carbon, CO<sub>2</sub>. We also speculate that the conversion of organic matter to CO<sub>2</sub>, the mineralization mechanism, is responsible for a change in the organic-to-inorganic compound ratio within the organic aerosol, contributing to the observed kappa increase with UVB exposure.

Our research contributes to the field of atmospheric science by highlighting the importance and complexity of the role of chemistry in aerosol-cloud interactions. As these interactions are currently the most uncertain parameter in understanding climate forcing, there is added motivation for furthering our understanding of the role of changing aerosol chemistry for particles acting as CCN.

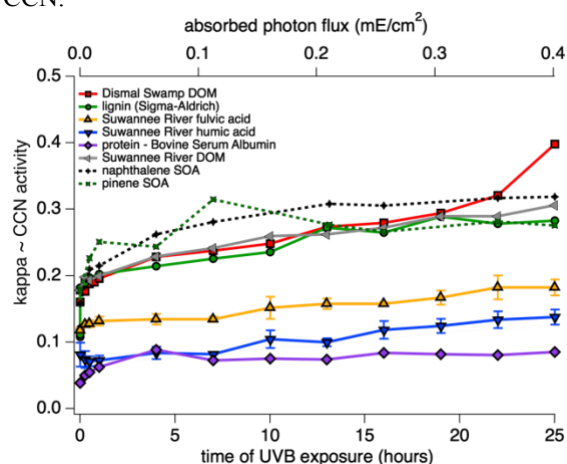


Figure 1: The evolution of kappa as a function of UVB exposure of different materials found in complex organic matter

Axson, J. L., May, N. W., Colón-Bernal, I. D., Pratt, K. A. and Ault, A. P.: Lake Spray Aerosol: A Chemical Signature from Individual Ambient Particles, *Environ. Sci. Technol.*, 50(18), 9835–9845, doi:10.1021/acs.est.6b01661, 2016.

Jimenez, J. L., Canagaratna, M. R., Donahue, N. M., Prevot, A. S. H., Zhang, Q., Kroll, J. H., DeCarlo, P. F., Allan, J. D., Coe, H., Ng, N. L., Aiken, A. C., Docherty, K. S., Ulbrich, I. M., Grieshop, A. P., Robinson, A. L., Duplissy, J., Smith, J. D., Wilson, K. R., Lanz, V. A., Hueglin, C., Sun, Y. L., Tian, J., Laaksonen, A., Raatikainen, T., Rautiainen, J., Vaattovaara, P., Ehn,



M., Kulmala, M., Tomlinson, J. M., Collins, D. R., Cubison, M. J., Dunlea, J., Huffman, J. A., Onasch, T. B., Alfarra, M. R., Williams, P. I., Bower, K., Kondo, Y., Schneider, J., Drewnick, F., Borrmann, S., Weimer, S., Demerjian, K., Salcedo, D., Cottrell, L., Griffin, R., Takami, A., Miyoshi, T., Hatakeyama, S., Shimojo, A., Sun, J. Y., Zhang, Y. M., Dzepina, K., Kimmel, J. R., Sueper, D., Jayne, J. T., Herndon, S. C., Trimborn, A. M., Williams, L. R., Wood, E. C., Middlebrook, A. M., Kolb, C. E., Baltensperger, U. and Worsnop, D. R.: Evolution of Organic Aerosols in the Atmosphere., *Sci. Wash. DC U. S.*, 326(Copyright (C) 2017 American Chemical Society (ACS). All Rights Reserved.), 1525–1529, doi:10.1126/science.1180353, 2009.

Murphy, D. M., Cziczo, D. J., Froyd, K. D., Hudson, P. K., Matthew, B. M., Middlebrook, A. M., Peltier, R. E., Sullivan, A., Thomson, D. S. and Weber, R. J.: Single-particle mass spectrometry of tropospheric aerosol particles, *J. Geophys. Res. Atmospheres*, 111(D23), D23S32, doi:10.1029/2006JD007340, 2006.

Slade, J. H., VanReken, T. M., Mwaniki, G. R., Bertman, S., Stirm, B. and Shepson, P. B.: Aerosol production from the surface of the Great Lakes, *Geophys. Res. Lett.*, 37(18), L18807, doi:10.1029/2010GL043852, 2010.

Zhang, Q., Jimenez, J. L., Canagaratna, M. R., Allan, J. D., Coe, H., Ulbrich, I., Alfarra, M. R., Takami, A., Middlebrook, A. M., Sun, Y. L., Dzepina, K., Dunlea, E., Docherty, K., DeCarlo, P. F., Salcedo, D., Onasch, T., Jayne, J. T., Miyoshi, T., Shimojo, A., Hatakeyama, S., Takegawa, N., Kondo, Y., Schneider, J., Drewnick, F., Borrmann, S., Weimer, S., Demerjian, K., Williams, P., Bower, K., Bahreini, R., Cottrell, L., Griffin, R. J., Rautiainen, J., Sun, J. Y., Zhang, Y. M. and Worsnop, D. R.: Ubiquity and dominance of oxygenated species in organic aerosols in anthropogenically-influenced Northern Hemisphere midlatitudes, *Geophys. Res. Lett.*, 34(13), L13801, doi:10.1029/2007GL029979, 2007.

# Quantifying Aerosol Size, Shape, and Composition Distributions by Electron Microscopy of Micro Inertial Impactor Samples

A. Brostrøm<sup>1,2</sup>, K. Mølhav<sup>1</sup>, and K.I. Kling<sup>2</sup>

<sup>1</sup> Department of Micro- and Nanotechnology, Technical University of Denmark, Denmark

<sup>2</sup> National Research Centre for the Working Environment, Denmark

Keywords: Electron Microscopy, Impactor, Particle Characterization

Air pollution is one of the major contributors to the global burden of disease, with particulate matter (PM) as one of its central concerns Landrigan et al. (2017). Thus, there is a great need for exposure and risk assessments associated with PM pollution. However, most of the current standard measurement techniques bring no knowledge of particle composition or shape, which has been identified as crucial parameters in toxicological studies. Additional measurement techniques are therefore needed to provide a more detailed description of aerosol populations, enabling more accurate risk assessments for regulating PM pollution.

Automated Scanning Electron Microscopy (SEM) coupled with Energy Dispersive X-ray Spectroscopy (EDS) is capable of providing single particle information of size, morphology, and elemental composition. The analysis has great potential as it can systematically map large areas of a collected sample in a repeatable manner without user intervention, providing sufficient data for statistical analysis. However, the technique lacks standard procedures for collecting and imaging particles, ensuring a reproducible and representative analysis.

Here we present the development of a standard operating procedure for sampling aerosol populations via impaction directly onto Transmission Electron Microscopy (TEM) grids, followed by automated SEM/EDS analysis. Recommendations are provided on choice of detector, where Scanning Transmission Electron Microscopy (STEM) detection was found most efficient for visualizing small light element based particles. We investigated different TEM grids and substrate thicknesses, where 400 mesh Ni-TEM grids coated with Formvar/carbon substrate of thickness 25-50/1 nm was found most efficient at withstanding the high speed impaction during sampling, while minimizing charging effects in the microscope.

The lowest stage of the impactor was further characterized experimentally, determining the collection efficiency curve using an atomized solution of 75 and 150 nm polystyrene latex beads (PSL). This was used in a comparison study between particle size distributions (PSD) obtained via scanning mobility particle sizer (SMPS) and via impaction followed by automated STEM analysis. The sampled aerosol was generated from an atomized solution of 100, 200, and 500 nm PSL. From the impacted sample it was found that the majority of particles above the impactor  $D_{50}$  at 103 nm

was collected directly underneath the orifice, with a distinctive deposition pattern governed by particle size. We investigated the deposition pattern in order to determine possible positions for obtaining a representative PSD. It was found that in order to represent all distances from the center of impaction, it was necessary to acquire a series of images from one edge of the impact area to the other going through its center. From the series of images a total of 2131 particles were recognized and the average PSD is shown in Figure 1 along with the PSD measured by SMPS after correcting for impactor collection efficiency.

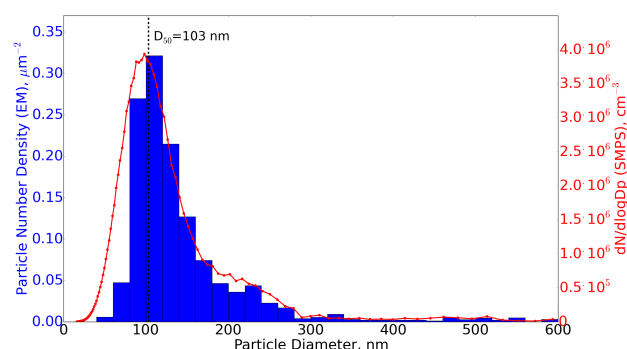


Figure 1: PSDs of an atomized solution of 100, 200, and 500 nm PSL measured by SMPS (red) and automated SEM analysis (blue).

It is seen that the STEM analysis underestimates the number of particles below approximately 100 nm, which can be attributed to uncertainties in the image analysis procedure, or to deposition occurring outside the impact area as is often observed for particles smaller than the impactor  $D_{50}$ . Above the impactor cut-off diameter the shape of the two PSDs are in good agreement showing that the automated STEM analysis can be used to obtain a representative PSD, thereby enabling a more detailed physical and elemental composition description.

Landrigan, P. J., Fuller, R., Acosta, N. J. R., Adeyi, O., Arnold, R., Basu, N., Zhong, M. (2017), *The Lancet Commission on pollution and health*, Lancet.

# CHEMICAL COMPOSITION CHANGES DURING SOA PARTICLE EVAPORATION

A. BUCHHOLZ<sup>1</sup>, A. YLISIRNIÖ<sup>1</sup>, C. MOHR<sup>2,3</sup>, C. FAIOLA<sup>1,5</sup>, E. KARI<sup>1</sup>, A.T. LAMBE<sup>4</sup>, Z. LI<sup>1</sup>, A. PAJUNOJA<sup>1</sup>, S.A. NIZKORODOV<sup>1,6</sup>, S. SCHOBESBERGER<sup>1</sup>, D.R. WORSNOP<sup>4</sup>, T. YLI-JUUTI<sup>1</sup>, and A. VIRTANEN<sup>1</sup>

<sup>1</sup>Department of Applied Physics, University of Eastern Finland, Kuopio, Finland.

<sup>2</sup>Institute of Meteorology and Climate Research, Karlsruhe Institute of Technology, Karlsruhe, Germany.

<sup>3</sup>Department of Environmental Science and Analytical Chemistry, Stockholm University, Stockholm, Sweden.

<sup>4</sup>Center for Aerosol and Cloud Chemistry, Aerodyne Research, Inc., Billerica, MA, USA.

<sup>5</sup>Department of Ecology and Evolutionary Biology, University of California Irvine, Irvine, CA, USA.

<sup>6</sup>Department of Chemistry, University of California Irvine, Irvine, CA, USA.

Keywords: secondary organic aerosol, volatility, evaporation, chemical composition, PMF.

Secondary Organic Aerosol (SOA) is a major constituent of atmospheric aerosol and consists of a multitude of organic compounds with a range of physical and chemical properties, such as viscosity and volatility (Hallquist et al., 2009). The volatility and concentration of a compound will determine its partitioning between particle and gas phase. This can be described with the Volatility Basis Set (VBS, Donahue et al., 2006) which groups compounds by their saturation vapour pressure. In previous studies, slower evaporation than expected from VBS distributions was observed for  $\alpha$ -pinene particles at dry conditions (Vaden et al., 2011, Yli-Juuti et al., 2017). This could be caused by physical limitations (e.g. mass transfer limitations in (semi)solid particles) or by chemical processes in the particle phase (e.g. oligomerization). It is therefore important to study the changes of the chemical composition of particles during evaporation to gain insights into the processes governing particle evaporation.

SOA with three different O:C ratios (0.55, 0.70, and 0.95) was generated from  $\alpha$ -pinene in a Potential Aerosol Mass reactor (PAM, Aerodyne Research Inc., Lambe et al., 2011) by varying the integrated oxidant exposure inside the reactor. A monodisperse size distribution was selected with a nano-Differential Mobility Analyser (DMA) operated with an open loop sheath flow system, thus also removing the majority of gas phase compounds. The sample was then either led directly to the measurement instruments or filled into a 100L stainless steel Residence Time Chamber (RTC) which was then closed off from all air flows. The RH in the size selection and measurement part, and the RTC was set to 0%, 40% or 80%. Samples were taken from the RTC in ~1h intervals to monitor changes in particle size. Chemical composition of the particles was studied with a High Resolution Time of Flight Aerosol Mass Spectrometer and a Filter Inlet for Gases and AEROSols coupled with a Chemical Ionization Time-of-Flight Mass Spectrometer (FIGAERO-CIMS, Lopez-Hilfiker et al., 2014) sampling the monodisperse aerosol directly after size selection or after ~3.5 h in the RTC.

Particle evaporation was enhanced at higher RH as observed in previous studies (Yli-Juuti et al., 2017). We observed a strong dependency of evaporation on the initial particle composition, with lower volatility for particles with higher O:C ratios. As shown in Fig 1, FIGAERO thermograms (total ion count vs desorption T) were shifted to higher desorption temperatures after

evaporation in the RTC. This indicates the shift towards lower volatility compounds in the residual particles.

Positive Matrix Factorisation (PMF, Paatero et al., 1994) was applied to the thermogram mass spectra data. The identified factors represent volatility classes which can be compared qualitatively to VBS distributions derived from other sources (Lopez-Hilfiker et al., 2016). Four to six PMF factors were needed to reproduce the measured thermograms. Larger contributions of the low volatility classes were observed with increasing average O:C ratios. The residual particles after RTC evaporation contained a higher contribution of low volatility classes but the average O:C ratio of the particles did not change.

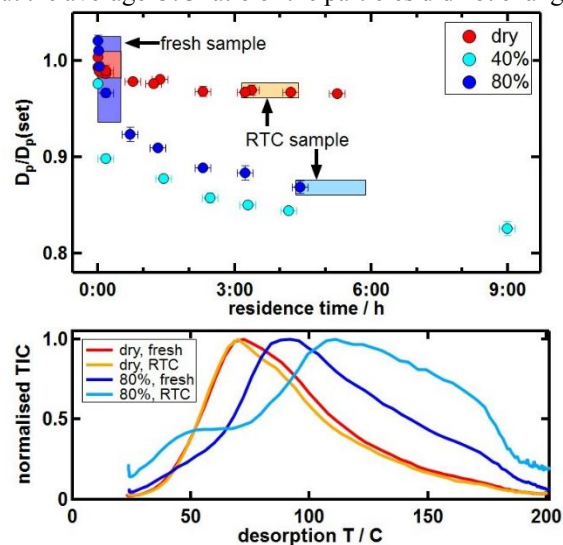


Figure 1: Observed evaporation (evapogram, top) and total ion count (thermogram, bottom) for high OC case. In evapogram, boxes in same colour as lines in thermograms indicate FIGAERO sampling intervals.

This work was supported by the Academy of Finland (no. 272041, 259005 and 299544), the European Research Council (ERC Starting Grant 335478) and strategic funding from the University of Eastern Finland.

Hallquist, M., et al. (2009). *ACP*, 9:5155-5236.

Donahue, N., et al. (2006). *EST*, 40:2635-2643.

Lambe, A. T., et al. (2011). *AMT*, 4:445-461.

Lopez-Hilfiker F. D., et al. (2014). *AMT*, 7:983-1001.

Lopez-Hilfiker F.D., et al. (2016). *EST*.

Paatero, P. and Tapper, U., (1994). *Environmetrics*, 5:111-126.

Vaden, T. D., et al. (2011). *PNAS*, 108:2190-2195.

Yli-Juuti, T., et al. (2017). *GRL*, 44:2562-2570.

# Aerosol indirect effect in marine stratocumulus: Does the model representation of cloud droplet activation matter?

I. Bulatovic<sup>1,2</sup>, A.M.L. Ekman<sup>1,2</sup>, C. Leck<sup>1,2</sup>, I. Riipinen<sup>2,3</sup>

<sup>1</sup>Department of Meteorology, Stockholm University, Sweden

<sup>2</sup>Bert Bolin Center for Climate Research, Stockholm University, Sweden

<sup>3</sup>Department of Environmental Science and Analytical Chemistry, Stockholm University, Sweden

Keywords: aerosol indirect effect (AIE), cloud droplet number concentration (CDNC), liquid water path (LWP)

## Introduction

An increased number of aerosol particles that can serve as cloud condensation nuclei (CCN) may change the microphysical structure of a cloud leading to smaller but more numerous cloud droplets provided that the liquid water path (LWP) in the cloud remains constant (first aerosol indirect effect, Twomey 1977). It may also result in less efficient precipitation and longer lifetime of the cloud, which will increase the liquid water path and further enhance cloud reflexivity (second aerosol indirect effects, Albrecht 1989).

General circulation models (GCMs) generally simulate a positive LWP response and higher cloud albedo with increasing aerosol concentration, in accordance with the theory described above. However, it seems that many GCMs overestimate the aerosol indirect effect (AIE) compared with satellite observations (e.g. Quaas et al. 2009; Wang et al. 2012). On the other hand, large-eddy simulations (LES), which have much higher spatial and temporal resolution compared to the GCMs, show that the LWP may both increase or decrease in more polluted clouds and that the response is related to the precipitation formation and cloud top entrainment (e.g. Ackerman et al. 2004; Lu and Seinfeld 2005; Wang and Feingold 2009b). These model results are also in a line with observations (Coakley and Walsh 2002; Matsui et al. 2006; Chen et al. 2014). In the study by Ackerman et al. (2004) it was found that LWP increases as a result of increased cloud droplet concentration only when the precipitation rates are higher than  $0.1 \text{ mm day}^{-1}$ .

When the precipitation generation is low, the moisture supply to the cloud from evaporating precipitation is weaker than the drying from increased entrainment of dry air at the cloud top which leads to a LWP reduction. In addition, previous studies only show a LWP reduction if sedimentation of the cloud droplets is allowed in the model.

The uncertainty in estimating the AIE by GCMs could be the result of an inability of these models to reproduce a LWP reduction for higher aerosol concentrations. If so, it is likely due to their coarse

grid resolution and the limitations of simplified parameterizations, such as the ones used for obtaining the cloud droplet number concentration (CDNC) which are present in some GCMs.

In the present study, we use the LES model MIMICA (Savre et al. 2014) to investigate the sensitivity of a stratocumulus cloud to various perturbations in the number concentration of cloud droplets, using two treatments with different complexity for obtaining CDNC. In other words, we explore if a simplified CDNC treatment plays a role in the AIE overestimation by GCMs.

## Methods

The simplified approach for obtaining CDNC in the model implies a prescribed initial cloud droplets number concentration, which remains constant in the whole model domain during the whole simulation. The second approach represents a modified power law for cloud droplet activation (Khvorostyanov and Curry, 2006). These two model versions are applied for both a nighttime period (between 1:00 and 07:00 LT) and a daytime period (between 08:00 and 14:00 LT) (Table 1).

Table 1: Simulation setup. The numbers indicate initial CDNC and CCN values used in the fixed CDNC versions and interactive CDNC versions, respectively.

Simulation setup	fixed CDNC	interactive CDNC
nighttime	10,30,55,150,500,1000	10,30,55,150,500,1000
daytime	10,30,55,150,500,1000	10,30,55,150,500,1000

Initialization of the model is done using observations from the second Dynamics and Chemistry of Marine Stratocumulus (DYCOMS II) field study (Stevens et al., 2003). For the baseline simulation (marked by red color in Table 1), the model setup follows Ackerman et al. (2009).

## Conclusions

For the nighttime simulations, our results show a similar LWP pattern with increasing cloud droplet number concentrations as previous LES studies: the response of the LWP is positive up to certain CDNC and precipitation thresholds, and above those thresholds the LWP starts to decrease. In the model version with interactive CDNC, the LWP decrease is postponed compared to the version with prescribed CDNC. The reason is a lower number of cloud droplets in all simulations where CDNC is calculated using CCN values and the supersaturation reached in the cloud (i.e. interactive CDNC). The fast disappearance of precipitation in the fixed CDNC simulations has a greater impact on entrainment rates at the top of the cloud compared to when interactive CDNC is used, which leads to a faster LWP reduction at lower CDNC. Indeed, for the nighttime cases, where an LWP reduction at high CDNC is present in both sets of simulations, the LWP decrease is smaller with interactive CDNC since the entrainment rates in general are lower in this set of simulations. Unlike previous studies, MIMICA reproduces a LWP reduction at high CDNC even if sedimentation of cloud water is not allowed, and regardless of the CDNC treatment in the model.

For the daytime simulations, LWP trends are in general smaller: there are no substantial changes in the response of LWP to increased cloud droplet number concentrations in both sets of simulations. However, the aerosol indirect effect is significantly larger in the set with prescribed CDNC. The cause of a greater cloud albedo in the set with fixed CDNC is a larger number of smaller cloud droplets at the top of the cloud, which more efficiently reflect solar radiation. These results indicate that the CDNC treatment in the model is important because, even though the LWP is similar between two daytime sets of simulations, the AIE is greater in the set with prescribed CDNC due to higher number concentration of cloud droplets and consequently their smaller sizes.

Ackerman, A.S., et al. (2004): The impact of humidity above stratiform clouds on indirect aerosol climate forcing, *Nature*, 432, 1014-1017

Ackerman, A.S., et al. (2009): Large-eddy simulations of a drizzling, *Mon. Weather Rev.*, 137, 1083-1110

Albrecht, B. A. (1989): Aerosols, cloud microphysics, and fractional cloudiness, *Science*, 245, 1227-1230

Chen, et al. (2012): Satellite-based estimate of global aerosol-cloud radiative forcing by marine warm clouds, *Nat. Geosci.*, 7, 643-646

Coakley, J. A. and Walsh, C. D. (2002): Limits to the aerosol indirect radiative effect derived from observations of ship tracks, *J. Atmos. Sci.*, 59,668-680

Khvorostyanov VI, Curry J.A. (2006): Aerosol size spectra and CCN activity spectra: Reconciling the lognormal, algebraic, and power laws, *J. Geophys. Res.*, 111, 2156-2202

Lu, M.L. and Seinfeld, J.H. (2005): Study of the aerosols indirect effect by large eddy simulations of marine stratocumulus, *J. Atmos. Sci.*, 62, 3909-3932

Matsui, et al. (2006): Satellite-based assessment of marine low cloud variability associated with aerosol, atmospheric stability, and the diurnal cycle, *J. Geophys. Res.-Atmos.*, 111, D17204

Quaas, et al. (2009): Aerosol indirect effects – general circulation model intercomparison and evaluation with satellite data, *Atmos. Chem. Phys.*, 9, 8697-8717

Savre, J., et al. (2014): Technical note: Introduction to Mimica, a large-eddy simulation solver for cloudy planetary boundary layers, *J. Adv. Model. Earth Syst.*, 6, 630-649

Stevens, B., et al. (2003): Dynamics and chemistry of marine stratocumulus: DYCOMS II, *Bull. Am. Meteorol. Soc.*, 84, 579-593

Twomey, S. (1977): Influence of pollution of short-wave albedo of clouds, *J. Atmos. Sci.*, 34, 1149-1152

Wang, H. L., et. al. (2012): Constraining cloud lifetime effects of aerosols using A-Train satellite observations, *Geophys. Res. Lett.*, 39, L15709

Wang, H. L. and Feinglod, G. (2009b): Modeling Mesoscale Cellular Structures and Drizzle in Marine Stratocumulus. Part II: The Microphysics and Dynamics of the Boundary Region between Open and Closed cells, *J. Atmos. Sci.*, 66, 3257-3275

# A GLOBAL OVERVIEW OF THE EFFECT OF WATER UPTAKE ON AEROSOL PARTICLE LIGHT SCATTERING USING IN-SITU SURFACE MEASUREMENTS

María A. BURGOS<sup>1,\*</sup>, Gloria TITOS<sup>2,3</sup>, Elisabeth ANDREWS<sup>4</sup>, Paul ZIEGER<sup>1</sup>

<sup>1</sup>Stockholm University, Stockholm, Sweden

<sup>2</sup>Institute of Environmental Assessment and Water Research, Barcelona, Spain

<sup>3</sup>Andalusian Institute for Earth System Research, University of Granada, Granada, Spain

<sup>4</sup>Cooperative Institute for Research in Environmental Studies (CIRES) University of Colorado, Boulder, USA

Ambient aerosol particles can take up water and thus change their optical properties depending on their hygroscopicity, their size, and the relative humidity (RH) of the surrounding air. Knowledge of the hygroscopicity effect is of importance for radiative forcing calculations but is also needed for the evaluation of remote sensing and model results with in-situ measurements. The dependence of particle light scattering on RH can be described by the scattering enhancement factor  $f(\text{RH})$ , which is defined as the particle light scattering coefficient at a given RH divided by the scattering coefficient at dry conditions (see Titos et al., 2016 for a recent review).

In this study,  $f(\text{RH})$  measurements performed at 25 sites (with a wide global coverage and representing a variety of aerosol types) have been compiled and harmonized to provide a benchmark data set. Most of the measurement stations which provided data are part of active measurement networks such as ACTRIS or NOAA. An identical data treatment process has been applied to all measurements in terms of instruments corrections, post-calibrations, fitting assumptions, etc. Data quality is assured by a thorough inspection of each dataset and quality checks. Instrument metadata has been reviewed, and flags indicating the quality of the measurements have been added. Due to instrumentation and experimental set-ups differences, some site-specific corrections were also needed.

In this study, we will show the results of the joint analysis of high frequency humidogram data. The climatology of worldwide  $f(\text{RH})$  values under different atmospheric conditions and predominant aerosol type will be presented. This study is part of a model-measurement exercise embedded within the AeroCom project, in which the ultimate goal is to assess how well global models simulate the aerosol/water interaction using in-situ measurements of aerosol hygroscopicity.

Titos, G. et al., (2016). Effect of hygroscopic growth on the aerosol light-scattering coefficient: A review of measurements, techniques and error sources, *Atmos. Environ.* doi: 10.1016/j.atmosenv.2016.07.021

# DECADAL TRENDS OF ATMOSPHERIC OXIDANTS AT A BOREAL FOREST IN FINLAND

D. CHEN<sup>1</sup>, P. ZHOU<sup>1</sup>, D. TAIPALE<sup>2</sup> AND M. Boy<sup>1</sup>

<sup>1</sup>Institute for Atmospheric and Earth System Research / Physics  
Faculty of Science, University of Helsinki, Finland

<sup>2</sup>Institute for Atmospheric and Earth System Research / Forest Science, Faculty of Agriculture and Forestry,  
University of Helsinki, Finland

Keywords: model, climate change, decadal trend, atmospheric oxidants, vertical distribution

12-years simulation with the 1-dimensional chemical-transport model SOSAA (Boy et al.,2011) were performed to investigate the atmospheric oxidants trends at SMEAR II, Hyytiälä, Finland. The atmospheric oxidation capacity is strongly influenced by the OH, ozone and NO<sub>3</sub> concentrations, however, real-time measurement data are only available at few sites for some campaigns. The SOSAA model was validated to simulate OH concentration with reasonable results in earlier publications (Boy et al., 2011, Mogensen et al., 2011).

The SOSAA version applied in this study is based on the version of Zhou et al. (2017). In this newest version, a new module to simulate the dry deposition of gases was added, besides the existing modules for meteorology, BVOCs emission, chemistry and aerosol. However, here we turned the aerosol module off to save computational time. For our simulations, we used SOSAA with 51 logarithmic layers from 0-3000 m. The model is semi-online, which means that it calculates meteorological and soil data from reanalysis data but also reads in some of them from station measurement directly. Trace gases including CO, NO, NO<sub>2</sub>, SO<sub>2</sub> and ozone are also provided as input. These gases come mainly from anthropogenic sources and are thus vulnerable. Although ozone mainly come from secondary sources, we don't use the calculated values since a certain fraction is related to downward transport from the free troposphere.

SOSAA is written in Fortran90 with the MPI parallel libraries. Chemistry and aerosol dynamics in each layer of the atmosphere can be calculated in parallel making it possible to increase the length of simulations and include more chemical reactions. Simulating one month with approximately 8000 chemical reactions and aerosol dynamics takes about 5 hours runtime, using 32 processor cores on a cluster computer.

Figure 1 shows the time series from year 2005 to 2016 for OH and NO<sub>3</sub>. Ozone is also in our focus, but it comes from measurements, thus not presented here. OH concentrations show a distinct seasonal cycle, which is driven by radiation. There is a evident decrease in OH concentration in the first two years, since then it keeps stable. NO<sub>3</sub> concentrations indicate a clear decreasing trend in the last decade. There is also a seasonal variation of NO<sub>3</sub>, mostly peaking in autumn

or spring, and always reaching the bottom in summer. Here OH comes from photolysis, and NO<sub>3</sub> are more efficiently produced during night-time. SMEARII is in high latitude, and the difference of incoming radiation makes the seasonal trend important.

With the model simulations for over one decade, we aim to understand how the atmospheric oxidants change through climatic patterns in northern Europe boreal forest. Next step will be to discuss the correlation of the oxidants and their sources with different climate parameters. We also plan to validate the results with observation campaigns carried out with OH and NO<sub>3</sub>, and to improve the weakness in modelling winter scenarios.

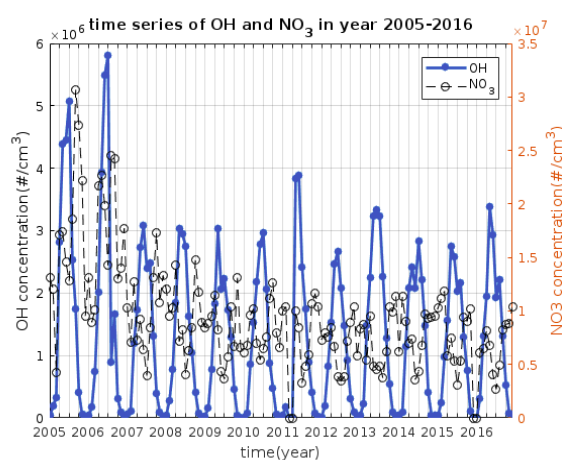


Fig. 1 Time series of OH and NO<sub>3</sub> in years 2005- 2016.

Boy, M.,Sogachiev, A.,Lauros, J. et al.Atmos. Chem.Phys., 11, 43a<sup>51</sup>,  
<https://doi.org/10.5194/acp-11-43-2011>,

Mogensen, D., Smolander, S., Sogachiev, A. et al.Atmos. Chem. Phys., 11, 9709a<sup>9719</sup>,  
<https://doi.org/10.5194/acp-11-9709-2011>, 2011

Zhou, P., Ganzeveld, L., Taipale, D. et al.Atmos. Chem. Phys., 17, 14309-14332,  
<https://doi.org/10.5194/acp-17-14309-2017>, 2017.

# Characterising the features in the surface atmospheric electric field in relation to aerosol processes in the lower atmosphere

X. Chen<sup>1</sup>, S. Barbosa<sup>2</sup>, A. Mäkelä<sup>3</sup>, J. Paatero<sup>3</sup>, V.-M. Kerminen<sup>1</sup>, T. Petäjä<sup>1</sup>, and M. Kulmala<sup>1</sup>

<sup>1</sup>Institute for Atmospheric and Earth System Research / Physics, Faculty of Science, University of Helsinki, Finland

<sup>2</sup>INESC TEC - INESC Technology and Science, Porto, Portugal

<sup>3</sup>Finnish Meteorological Institute, Helsinki, Finland

Keywords: nucleation, atmospheric aerosols, atmospheric electric field, ionising radiation

In the Earth's atmosphere, there is an electric field present under fair weather conditions of an order of 100–150 Vm<sup>-1</sup> (e.g. (Tinsley 2008)). The efforts in measuring this electric field in the beginning of the 20<sup>th</sup> century have shown an average diurnal variation regardless of measurement locations in the Earth's fair weather atmospheric electric field, which is known as the Carnegie curve (Harrison 2013). The diurnal pattern in the Carnegie curve has been attributed to the global distributions of thunderstorms (Whipple 1929), which supports the global circuit concept initially constituted by C. T. R. Wilson (Wilson 1921).

In the global circuit concept, the flow of air ions under fair weather conditions is a primary component that discharges the circuit composed of the Earth's surface and the ionosphere. Air ions in the atmosphere are produced mainly by ionising radiation. Chen et al. (2016) have demonstrated the connection between the variations in the air ion concentrations and ionising radiation levels. In the lower atmosphere, once formed, air ions participate in aerosol formation and dynamics. Atmospheric new particle formation is one of the natural aerosol processes that modifies significantly the aerosol loadings and the number size distributions of air ions (Kulmala and Kerminen 2008). Since atmospheric electric field is sensitive to the air ion concentration, it is worth investigating how atmospheric electric field varies with aerosol processes.

We measured atmospheric electric field, together with ionising radiation at Hyytiälä SMEAR II station (61°51' N, 24°17' E, 181 m above sea level) during June–November, 2017. The measurement station situates in a boreal forest in southern Finland (Hari and Kulmala 2005). As part of the routine measurement system at the station, the number size distribution data of air ions and aerosol particles are available to be used to study together with atmospheric electric field. Also, meteorological parameters are accessible to further assist our analysis.

During fair weather conditions (5–6 Sept.), the atmospheric electric field followed a similar variation to that in the 0.8–1 nm ion concentrations during daytime (Fig. 1). However, this variation represented a reduction in the 0.8–1 nm ion concentration but an increase in the magnitude of the electric field to the negative values, which is likely related to the consumption of the ions in aerosol processes. Precipitation was observed on the following four days. Correspondingly, increases in

gamma counts and electric field (to the positive values) were seen in relation to the precipitation episodes. The increase in the gamma counts came from the washout of radon progeny in the air along with the wet deposition of aerosol particles, which can temporarily increase the production of air ions and modify the atmospheric electric property. Moreover, the positive electric field is also modulated by the presentation of clouds during the rainy episodes. Further analysis is under progress.

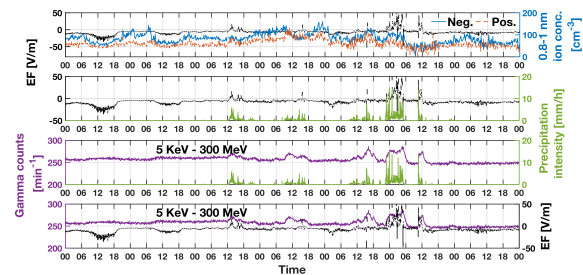


Figure 1: Electric field, 0.8–1 nm ion concentrations, precipitation intensity and gamma counts in the energy window of 5 KeV–300 MeV measured during 5–11 Sept., 2017.

- Chen, X., Kerminen, V.-M., Paatero, J., Paasonen, P., Manninen, H. E., Nieminen, T., Petäjä, T. and Kulmala, M. (2016). How do air ions reflect variations in ionising radiation in the lower atmosphere in a boreal forest? *Atmos. Chem. Phys.* 16:14297–14315.
- Hari, P. and Kulmala, M. (2005). Station for measuring ecosystem-atmosphere relations (SMEAR II). *Boreal Environ. Res.* 10:315–322.
- Harrison, R. G. (2013). The Carnegie Curve. *Surv Geophys* 34:209–232.
- Kulmala, M. and Kerminen, V.-M. (2008). On the formation and growth of atmospheric nanoparticles. *Atmos. Res.* 90:132–150.
- Tinsley, B. A. (2008). The global atmospheric electric circuit and its effects on cloud microphysics. *Rep. Prog. Phys.* 71:066801.
- Whipple, F. J. W. (1929). On the association of the diurnal variation of electric potential gradient in fine weather with the distribution of thunderstorms over the globe. *Q.J.R. Meteorol. Soc.* 55:1–18.
- Wilson, C. T. R. (1921). Investigations on lightning discharges and on the electric field of thunderstorms. *Philos. Trans. R. Soc. London A.* 221:73–115.



# LABORATORY GENERATED SEA SPRAY AEROSOLS: VARYING FLOW RATE, ALGAE CONCENTRATION AND TEMPERATURE

S. CHRISTIANSEN<sup>1</sup>, M. E. SALTER<sup>2</sup>, Q. NGUYEN<sup>1,†</sup> and M. BILDE<sup>1</sup>

<sup>1</sup> Department of Chemistry, Aarhus University, Denmark

<sup>2</sup> Department of Environmental Science and Analytical Chemistry, Stockholm University, Sweden

<sup>†</sup> Now at: Department of Engineering, Aarhus University, Denmark

Keywords: sea spray aerosols, ocean-atmosphere interactions, temperature-effects, sea spray flux, algae

## Introduction

Sea spray aerosols (SSA) are a major source of uncertainty in climate models. The physical processes governing SSA production play an important part in determining SSA size, emission, and chemical composition while our understanding remains limited (Lewis and Schwartz, 2004; de Leeuw et al., 2011). SSA is important as it acts as both a direct and indirect radiative forcing component (Boucher et al., 2013).

SSA are produced from entrained air bubbles in the ocean. When the bubbles reach the surface, the bubbles burst resulting in the release of many droplets. The best experimental approach to estimate SSA production has been a subject of scientific debate, because many environmental factors affect the production dynamics (Lewis and Schwartz, 2004; de Leeuw et al., 2011). To study and elaborate on the physico-chemical effects that govern SSA properties and production, a controlled environment is needed. One way of investigating this process in the laboratory is to generate a bubble plume using a plunging water jet or a diffuser/frit.

Here, we present our newly developed temperature-controlled sea spray chamber (AEGOR, Figure 1), that includes both a plunging jet and sintered glass diffuser configuration, along with a series of laboratory characterisation experiments. Firstly, the effect of the plunging water jet flow rate and the diffuser air flow rate on the particle size distribution are studied. Secondly, experiments designed to investigate the effect of different seawater temperatures on the SSA production flux and particle size will be shown. Finally, we present an experiment designed to test how phytoplankton blooms impact the SSA production flux.

## Methods

The setup is illustrated in Figure 1 and shows how the particle size distributions are measured using a scanning mobility particle sizer (SMPS) and an optical particle sizer (OPS). The seawater temperature in the chamber was varied between -1.7 and 35 °C, while the size and number of SSA were measured. The chamber consists of a stainless steel jacketed cylindrical container (34 L) equipped with an exchangeable poly-carbonate window for sampling ports and visual inspection of the bubble plume.

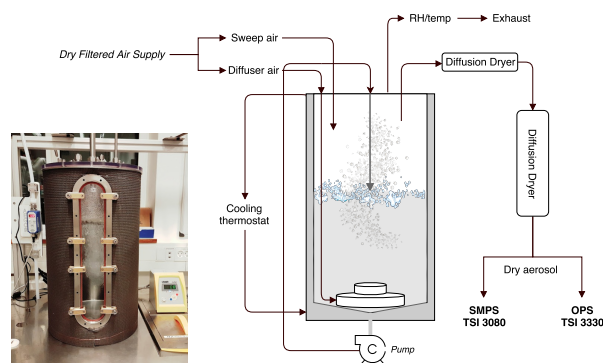


Figure 1: A schematic depicting the new sea spray chamber AEGOR.

## Conclusion

AEGOR is a new temperature-controlled sea spray chamber that allows us to study SSA generation at the process level. Preliminary analysis of a series of experiments highlight that:

- The size distribution of aerosols produced in the chamber varies as a function of the plunging jet flow rate and diffuser air flow rate.
- The relationship between seawater temperature and aerosol particle production differs depending on whether the plunging jet or diffuser was used to generate particles.
- The addition of a phytoplankton culture to the seawater affects aerosol particle production. However, no simple relationship between the amount of culture added and the particle production was apparent.

Lewis, E.R. and Schwartz, S.E. (2004). *Sea Salt Aerosol Production: Mechanisms, Methods, Measurements and Models - A Critical Review* American Geophysical Union

de Leeuw, G., E. L. Andreas, M. D. Anguelova, C. W. Fairall, E. R. Lewis, C. O'Dowd, M. Schulz, and S. E. Schwartz (2011). *Rev. Geophys.*, 49, RG2001.

Boucher, O., D. Randall, P. Artaxo, C. Bretherton, G. Feingold, P. Forster, V.-M. Kerminen, Y. Kondo, H. Liao, U. Lohmann, P. Rasch, S.K. Satheesh, S. Sherwood, B. Stevens and X.Y. Zhang (2013) *Clouds and Aerosols. In: Climate Change 2013: The Physical Science Basis. IPCC. Cambridge University Press*

# Where in the world is pure biogenic nucleation? Simulation of atmospheric complexity in the CLOUD chamber

Lubna Dada<sup>1</sup>, M. Heinritzi<sup>2</sup>, M. Simon<sup>2</sup>, C. Yan<sup>1</sup>, D. Stolzenburg<sup>3</sup>, M. Kulmala<sup>1</sup>, J. Kirkby<sup>2,4</sup> and the CLOUD Collaboration

<sup>1</sup>Institute for Atmospheric and Earth System Research, University of Helsinki, Helsinki, Finland

<sup>2</sup>Institute for Atmospheric and Environmental Sciences, Goethe-University of Frankfurt, Frankfurt, Germany

<sup>3</sup>Faculty of Physics, University of Vienna, Vienna, Austria

<sup>4</sup>CERN, CH-1211 Geneva 23, Switzerland

Keywords: new particle formation, cloud experiment, ozonolysis

Presenting author email: Lubna.Dada@helsinki.fi

Atmospheric aerosols affect Earth's radiative balance (IPCC, 2013). New particle formation (NPF) via gas-to-particle conversion is estimated to contribute to a substantial fraction of the global cloud condensation nuclei (Merikanto et al., 2009). Originally, it was thought that NPF can only occur in the presence of sulfuric acid vapour and that ions do not play a major role in particle formation. However, chamber and laboratory experiments have shown that particles can form from organic precursors in the absence of sulfuric acid. Such phenomenon, known as pure biogenic NPF, was first reported by Kirkby *et al.* (2016) within the CLOUD experiment (Cosmics Leaving OUtdoor Droplets) and have had resulted from ozonolysis of a single monoterpene ( $\alpha$ -pinene) at 5 °C. Additionally, several recent studies have encountered biogenic NPF in the real atmosphere, making the phenomenon important for further investigation. Accordingly, we report the influence of several environmental stressors on pure biogenic nucleation measured in the CLOUD chamber in 2015 and 2016.

Our measurements serve to understand the interactions between different precursor volatile organic compounds by introducing a pure monoterpene, a sesquiterpene and isoprene individually and all together to form what we call a pure biogenic “soup”. Using different concentrations of the aforementioned precursor vapors at various temperatures (-25, 5, 25 °C), we studied their effect on NPF by measuring the formation and growth rates. Besides, we studied the effect of urban pollutants such as NO and NO<sub>2</sub> on the distributions of biogenic highly oxidized molecules resulting from the changed oxidation pathway of the biogenic soup and the subsequent effect on NPF. Trying to mimic the complexity of the real atmosphere, we also describe the effect of various ionization levels on NPF which demonstrates the different layers of the atmosphere among other variables. Shown in Figure 1, upon increasing the concentrations of the individual components of the mixture, an increase in nucleation and growth rates is evident. The size distribution was measured with three instruments, a scanning PSM (Vanhanen et al. 2011), a DMA-train (Stolzenburg et al. 2016) and a TSI nano-SMPS (Wang and Flagan 1990).

Studying pure biogenic nucleation helps understand night-time NPF which occurs in the absence of sulfuric acid, and also NPF in very clean environments such as rain forests or at high altitudes as well as in the pristine pre-industrial climate. Our aim is to study the influence of realistic atmospheric conditions on pure biogenic nucleation.

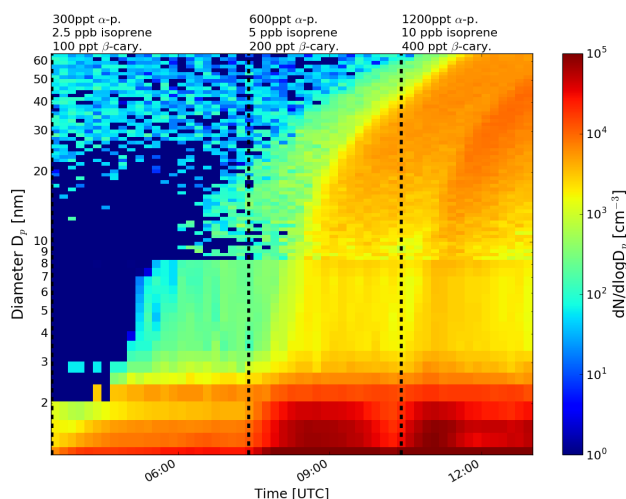


Figure 1. The time evolution of the number size distribution during a typical pure biogenic NPF experiment in the CERN CLOUD chamber.

IPCC: (2013). *Cambridge University Press*, **1**, 535-531.

Kirkby, J et al (2016). *Nature*, **533**, 521-526.

Merikanto, J.,(2009). *Atmos Chem Phys*, **9**, 8601-8616.

Stolzenburg, D. et al (2016) *Atmos. Meas. Tech. Discuss.*, doi:10.5194/amt-2016-346.

Vanhanen, J et al. (2011). *Aerosol Sci. Tech.*, **45**:533–542

Wang, S. C., and Flagan, R. C. (1990): *Aerosol Sci Tech*, **13**, 230-240.

We thank the European Organization for Nuclear Research (CERN) for supporting CLOUD with important technical and financial resources and for providing a particle beam from the CERN Proton Synchrotron as well as all the research academics and institutes for providing the financial support for the CLOUD experiment.

# Long-term source contributions to organic aerosol and SOA composition in central Europe

K. R. Daellenbach<sup>1,2</sup>, I. El Haddad<sup>1</sup>, I. Kourtchev<sup>3</sup>, A. L. Vogel<sup>1</sup>, G. Stefenelli<sup>1</sup>, C. Bozzetti<sup>1</sup>, A. Vlachou<sup>1</sup>, P. Fermo<sup>5</sup>, A. Piazzalunga<sup>6,\*</sup>, J. G. Slowik<sup>1</sup>, S. M. Luedin<sup>7,\*\*</sup>, V. Pflueger<sup>7</sup>, G. Vogel<sup>7</sup>, J.-L. Jaffrezo<sup>4</sup>, M. Kalberer<sup>3</sup>, U. Baltensperger<sup>1</sup>, A. S.H. Prévôt<sup>1</sup>

<sup>1</sup>Laboratory of Atmospheric Chemistry, Paul Scherrer Institute, Villigen, Switzerland

<sup>2</sup>Institute for Atmospheric and Earth System Research / Physics, Faculty of Science, University of Helsinki, Helsinki, Finland

<sup>3</sup>Department of Chemistry, University of Cambridge, Cambridge, U. K.

<sup>4</sup>Université Grenoble Alpes, CNRS, IGE, Grenoble, France

<sup>5</sup>University of Milan, Department of Chemistry, Milan, Italy

<sup>6</sup>University of Milano Bicocca, Department of Environmental Science, Milan, Italy

<sup>7</sup>MABRITEC AG, Riehen, Switzerland

\*now at: Water and Soil Lab, Entratico, Italy

\*\*now at: University of Geneva, Geneva, Switzerland

Keywords: Aerosol mass spectrometer, FT-UHR MS, Source apportionment

Field deployments of the aerosol mass spectrometer (AMS) combined with the application of positive matrix factorization have advanced the measurement of organic aerosol (OA) and the quantification of its most important sources. However, the investigation of regional and seasonal differences by long-term deployments of the AMS is impractical because of instrument cost and maintenance. To overcome these limitations and in order to assess the detailed chemical composition of OA, we have adapted the AMS for the measurement of offline filter samples (oAMS, Daellenbach et al., 2015), in combination with a unique suite of analytical techniques, including laser-desorption/ionization-ToF MS (LDI, Daellenbach et al., 2018), ultrahigh-resolution mass spectrometer (Orbitrap), and organic marker analyses.

In this study, we assess the spatio-temporal variability of OA sources/components contributing to the particulate matter < 10  $\mu\text{m}$  (PM<sub>10</sub>) and study the chemical composition and origin of secondary organic aerosol (SOA) at locations with different exposure characteristics in central Europe for the entire year of 2013 (Daellenbach et al., 2017). We demonstrate that the dominant factors governing air quality can be region-specific (source apportionment using positive matrix factorization), e.g. primary organic aerosol concentrations from wood burning (BBOA) are strongly enhanced in alpine valleys relative to urban centers (oAMS, Fig. 1a). Based on comparison to laboratory wood burning experiments, LDI results suggest that the elevated BBOA concentrations in alpine valleys are mainly caused by more prominent inefficient burning conditions. While the winter-time OA pollution in alpine valleys is driven by BBOA, at the other sites a SOA factor correlating with anthropogenic secondary inorganic species is dominant during winter (oAMS, Fig. 1a). Samples collected during winter in alpine valleys have a similar molecular composition as fresh laboratory wood burning emission, at the same time in an urban center the wood burning emissions are more aged and also other SOA

precursors/formation pathways are important in winter (Orbitrap, Fig. 1b). We observe the production of largely non-fossil SOA in summer (SOOA), following the increase in biogenic emissions with temperature. The prominent contribution of compounds with an H/C of 1.5 observed for samples from Zurich collected during summer is consistent with SOA formation from biogenic precursors and the molecular composition is similar to biogenic SOA observed in Hyytiälä (Orbitrap, Fig. 1b).

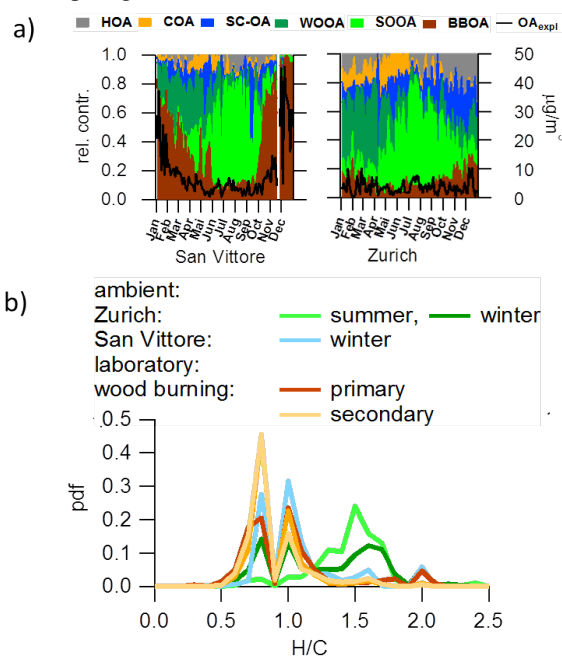


Figure 1: a) source apportionment results for 2 sites in central Europe (oAMS), b) H/C of OA from laboratory wood burning experiments and ambient OA in Zurich and San Vittore (Orbitrap).

Daellenbach, K. R., et al (2015), *Atmos. Meas. Tech.*, 9:23-39.

Daellenbach, K. R., et al. (2017), *Atoms. Chem. Phys.*, 17:13265-13282.

Daellenbach, K. R., et al. (2018), *Atmos. Chem. Phys.*, in press.

# COMBINING CLIMATE MODELING AND OBSERVATIONS TO UNDERSTAND AEROSOL EFFECTS ON THE ARCTIC CLIMATE

T. N. DALLAFIOR<sup>1,2</sup>, S. KRISHNA<sup>2,3</sup>, A. LEWINSCHALL<sup>3</sup>, I. RIIPINEN<sup>1,2</sup>,  
A. M.L. EKMAN<sup>2,3</sup> and H-C HANSSON<sup>1,2</sup>

<sup>1</sup>Department of Environmental Science and Analytical Chemistry, Stockholm University, Sweden

<sup>2</sup>Bolin Center for Climate Research, Stockholm University, Stockholm, Sweden

<sup>3</sup>Department of Meteorology, Stockholm University, Stockholm, Sweden

Keywords: aerosols, climate, Arctic, air quality

Previous studies using the Earth System model NorESM1 show that changing SO<sub>2</sub> emissions in various regions in the northern hemisphere mid-latitudes result in significant temperature responses in the Arctic (Acosta Navarro, 2016a). Evidence so far suggests that in NorESM1, the amplified Arctic surface temperature response is obtained despite a weak sea-ice albedo feedback and without significant aerosol-induced changes in cloud properties in the Arctic.

This presentation aims at gaining a process understanding of how the Arctic temperature response to mid-latitude emission changes happen. To this end, we evaluate aerosol size distributions, cloud properties, and other entities in the general circulation model NorESM1 against remote and in-situ observations at high latitudes and a newer version with - among others - improved representation of sea ice and convective transport of aerosols. Results will serve to identify critical microphysical processes in

the modelling set-up used for further sensitivity studies.

A preliminary comparison between the NorESM1 output and in-situ measurements of aerosol size-distributions show that the model underestimates particle sizes, which could be of direct importance to cloud condensation nuclei activation. Furthermore, a comparison with aerosol optical depths obtained from the CALIOP satellite instrument suggests that more aerosol is transported to the Arctic through the free troposphere in the model compared to observations. This would imply that the modelled aerosol impacts on high-latitude low-level clouds might be underestimated in NorESM1.

Acosta Navarro, J. C., Varma V., Riipinen I., Seland Ø., Kirkevåg A., Struthers H., Iversen T., Hansson, H.-C. and Ekman A. M. L., (2016), *Nature Geoscience*, DOI: 10.1038/NGEO2673

# MOLECULAR CHARACTERIZATION AND VOLATILITY EVOLUTION OF $\alpha$ -PINENE OZONOLYSIS SOA DURING ISOTHERMAL EVAPORATIONS

E. L. D'AMBRO<sup>1,2</sup>, S. SCHOBESBERGER<sup>3</sup>, F. D. LOPEZ-HILFIKER<sup>4</sup>, J. E. SHILLING<sup>5</sup>, B. H. LEE<sup>2</sup>, J. A. THORNTON<sup>1,2</sup>

<sup>1</sup>University of Washington, Department of Chemistry, USA

<sup>2</sup>University of Washington, Department of Atmospheric Sciences, USA

<sup>3</sup>University of Eastern Finland, Department of Applied Physics, Finland

<sup>4</sup>Paul Scherrer Institute, Laboratory of Atmospheric Chemistry, Switzerland

<sup>5</sup>Pacific Northwest National Laboratory, Atmospheric Sciences and Global Change Division, USA

Keywords:  $\alpha$ -pinene ozonolysis, isothermal evaporation, FIGAERO, volatility, oligomeric content

$\alpha$ -Pinene ( $C_{10}H_{16}$ ) is a large contributor to global biogenic secondary organic aerosol (SOA) budgets due to its high SOA yields upon oxidation [Shilling *et al.*, 2008]. We probe the volatility and evaporation behavior upon dilution of  $\alpha$ -pinene SOA to further our understanding of the nascent volatility distribution, viscosity, and how these evolve in time absent photochemical oxidation. We present molecular composition measurements of the gas and particle phases of  $\alpha$ -pinene ozonolysis SOA formed at 0% and 50% relative humidity (RH), followed by room-temperature evaporation in ultra-high purity  $N_2$  humidified to 20-90% RH. Experiments were performed in the Pacific Northwest National Laboratory 10.6 m<sup>3</sup> and the University of Washington 0.7 m<sup>3</sup> environmental chambers utilizing a Filter Inlet for Gases and AEROSOLS (FIGAERO) coupled to a high-resolution time of flight chemical ionization mass spectrometer utilizing iodide adduct ionization. We present novel insights into the total mass that evaporates as a function of time from 10 min to 24 hours without heating (Fig. 1), the molecular speciation of the evaporate, as well as the effective volatility and composition of the SOA mass remaining.

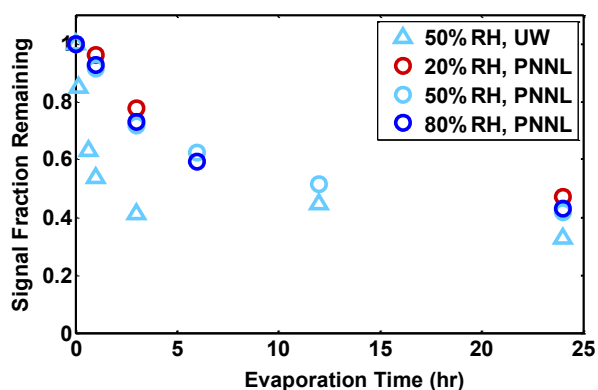


Figure 1: Total signal fraction remaining. Total signal is the sum of all compounds with formula  $C_xH_yO_zI-$ , normalized by  $x$  (the number of carbons).

Consistent with previous work [Vaden *et al.*, 2011], we find two stages of evaporation: a rapid loss of a large portion of the total signal over the course of  $\leq 3$  hours, followed by a stage of much slower

evaporation over the proceeding 21 hours. Varying the RH of formation effects evaporation rate on timescales  $\leq 3$  hours, however the mass fraction remaining after 24 hours converges to  $\sim 30$ -50% under all formation and evaporation RHs. We simulate the evaporation behavior and remaining fractions desorbed via temperature programmed thermal desorption to derive effective saturation vapor concentrations, mass accommodation coefficients, and rates of chemical evolution producing both higher and lower volatility components during the evaporation time period. For the bulk SOA, we arrive at a  $c^*$  of  $1.2 \mu\text{g m}^{-3}$  and an oligomer decomposition time scale of  $\sim 9$  hours at evaporation at 80% RH.

Shilling, J. E., Q. Chen, S. M. King, T. Rosenoern, J. H. Kroll, D. R. Worsnop, K. A. McKinney, and S. T. Martin (2008), Particle mass yield in secondary organic aerosol formed by the dark ozonolysis of alpha-pinene, *Atmos. Chem. Phys.*, 8(7), 2073-2088, doi: 10.5194/acp-8-2073-2008.

Vaden, T. D., D. Imre, J. Beranek, M. Shrivastava, and A. Zelenyuk (2011), Evaporation kinetics and phase of laboratory and ambient secondary organic aerosol, *Proc. Natl. Acad. Sci. U. S. A.*, 108(6), 2190-2195, doi: 10.1073/pnas.1013391108.

# Photochemical Aging Processes in Iron Containing Aerosols

J. DOU<sup>1</sup>, B.P. LUO<sup>1</sup>, T. Peter<sup>1</sup>, M. Ammann<sup>2</sup> and U. KRIEGER<sup>1</sup>

<sup>1</sup> Institute for Atmospheric and Climate Science, ETH Zurich, Switzerland

<sup>2</sup> Laboratory of Environmental Chemistry, Paul Scherrer Institute, Switzerland

Keywords: dust aerosols, photochemical aging, iron containing complexes

Fe(III)-citrate (Fe<sup>III</sup>Cit) complex photochemistry plays an important role in aerosol aging, especially in the lower troposphere (Abida et al., 2012; Pozdnyakov et al., 2012). It can easily get excited by light below 500 nm, inducing the reduction of Fe<sup>III</sup> and oxidation of carboxylate ligands (Weller et al., 2014). When O<sub>2</sub> is present, ensuing peroxy radical chemistry will likely lead to more decarboxylation, peroxides and oxygenated volatile organic compounds (OVOC) production. The peroxides (e.g., OH•, HO<sub>2</sub>•) in turn allow re-oxidation of Fe<sup>II</sup> to Fe<sup>III</sup>, closing this so-called photocatalytic cycle, where Fe<sup>III</sup>Cit complex acts as a photocatalyst.

In atmospheric aerosol particles, containing both carboxylic acids and iron oxides, especially in mineral dust, they may combine to form iron carboxylate complexes, making the photochemical degradation of these carboxylate ligands possible, much easier, and continuous, while iron amount stays constant.

In this research, mass and size changes of a single particle levitated in an electrodynamic balance (EDB) are tracked during photochemical processing. The particle can contain pure citric acid (CA), or a mixture of CA/Fe<sup>III</sup>Cit, or a CA/Fe<sub>2</sub>O<sub>3</sub> nanoparticles mixture, or a CA/ATD (Arizona Test Dust, 0-3 μm in size, with 2-5% weight percent of Fe<sub>2</sub>O<sub>3</sub>) mixture. As Figure 1 shows, pure CA particles cannot be photolysed by 473 nm light. However, if Fe<sup>III</sup> containing complexes are added, obvious size decrease is observed due to the evaporation of CO<sub>2</sub> and OVOC. The particle containing Fe<sup>III</sup>Cit shows the fastest loss rate, followed by the one with Fe<sub>2</sub>O<sub>3</sub> nanoparticles, and then the one with ATD. We suggest that Fe<sup>III</sup>Cit can be photochemically active as soon as the particle is illuminated; while for the particle containing Fe<sub>2</sub>O<sub>3</sub> nanoparticles, Fe<sup>III</sup> needs to dissolve and to form photoactive Fe<sup>III</sup>Cit with CA. Furthermore, since the ATD particles inside the aerosol droplet are larger than the nanoparticles, and have a low content of Fe<sub>2</sub>O<sub>3</sub>, an even longer time is needed to start processing and the rate may be limited by the available iron. These are preliminary data and we will test the photochemistry occurring in these Fe<sup>III</sup> containing particles on a longer time scale.

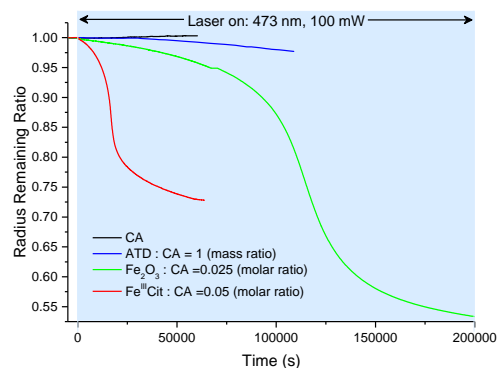


Figure 1: Radius decrease rate of a single particle levitated in EDB during photochemical reactions.

Meanwhile, a numerical model, which includes the equilibria of each component, main chemical reactions, and the transport of volatile and semi-volatile products, was developed to simulate photochemical aging processes in particles containing iron complexes. Comparing model output with experimental data will enable us to determine some of the crucial parameters like equilibrium constants, reaction rates and liquid phase diffusion coefficients.

- Abida, O., Kolar, M., Jirkovsky, J., and Mailhot, G. (2012). *Photochem. Photobiol. Sci.*, 11:794-802.
- Pozdnyakov, I. P., Kolomeets, A. V., Plyusnin, V. F., Melnikov, A. A., Kompanets, V. O., Chekalin, S. V., Tkachenko, N., and Lemmetyinen, H. (2012). *Chem. Phys. Lett.*, 530:45-48.
- Weller, C., Tilgner, A., Bräuer, P., and Herrmann, H. (2014). *Environ. Sci. Technol.*, 48 :5652-5659.

# EFFECT OF ARCTIC SEA ICE ON AEROSOLS IN EASTERN LAPLAND

E.-M. DUPLISSY<sup>1</sup>, S. HAKALA<sup>1</sup>, V. SINCLAIR<sup>1</sup>, R. VÄÄNÄNEN<sup>1</sup>, V.-M. KERMINEN<sup>1</sup>, T. PETÄJÄ<sup>1</sup> and M. KULMALA<sup>1</sup>

<sup>1</sup> Institute for Atmospheric and Earth System Research (INAR) / Physics, Faculty of Science, University of Helsinki, Finland

Keywords: Aerosol concentration, aerosol size distribution, Arctic sea ice, Arctic Oscillation.

Decreasing sea ice is expected to change largely the sources and sinks of aerosols in the Arctic. On the other hand, the changes in sea ice can have an effect on large-scale atmospheric circulation and vice versa. Here we show, i) how the aerosol concentrations and size distributions change in the continental Arctic with respect to the time that air masses spend over sea ice or open ocean before entering our site in Eastern Lapland, Finland, ii) how the atmospheric large-scale variability, namely Arctic Oscillation (AO) changes the situation. We also speculate about the changes in aerosol-cloud interactions in the future based on the results.

We calculated linear regressions to median aerosol concentrations and mode peak diameters at SMEAR I station in Värriö, Eastern Lapland, as a function of time over sea ice (TOSI), time over open sea (TOOS) and time over land (TOL). The data was divided into summer (Jun-Sep) and winter (Oct-May) as well as AO positive and negative phases. In the analysis we used aerosol size distribution data from DMPS (Differential Mobility Particle Sizer), SO<sub>2</sub> concentration data, HYSPLIT 96 hour back-trajectories, sea ice concentration data from NSIDC (National Snow and Ice Data Center) and daily AO indices. TOL and SO<sub>2</sub> were used in order to reduce the effect of land and sulphur emissions from Kola and we repeated the calculations for four different datasets: 1) TOL<sub>2</sub> 40h and SO<sub>2</sub><75<sup>th</sup> percentile; 2) TOL<sub>2</sub> 40h; 3) SO<sub>2</sub><75<sup>th</sup> percentile and 4) no limitations. In our trajectory calculations for all datasets, we took into account only those trajectories that had spent >90% of their travel time North of Värriö.

In general, the aerosol concentrations during winter (median 363 cm<sup>-3</sup>) were about 1/3<sup>rd</sup> of the summer values (median 928 cm<sup>-3</sup>). Nucleation mode concentrations were higher in more pristine air masses (AM), and including AMs with high SO<sub>2</sub> increases the concentration of all modes whereas including AMs with high TOL decreases the nucleation mode and increases the concentration of Aitken and accumulation modes. The phase of AO affects the concentrations: during summer the total concentration is higher during positive AO, but the accumulation mode concentration is higher during AO- phases. In winter, the total concentration is higher during AO- but the nucleation and Aitken modes have higher concentrations during AO+.

During summer, the total aerosol number, Aitken mode and accumulation mode concentrations

were decreasing with increasing time the air mass spent over the sea ice by -8.9, -5.3 and -1.6 cm<sup>-3</sup>h<sup>-1</sup>, respectively. The Aitken mode diameter was decreasing -0.3 nm/h and the accumulation mode diameter -0.5 nm/h. Accumulation mode concentration and diameter increased by +0.8 cm<sup>-3</sup>h<sup>-1</sup> and +0.3 nm/h, respectively, as a function of TOOS. During winter there was a decrease in total, nucleation mode and Aitken mode concentrations (-1.3, -0.3, -0.6 cm<sup>3</sup>/h, respectively) as a function of TOSI. Accumulation mode concentration and diameter were decreasing by -0.4 cm<sup>-3</sup>h<sup>-1</sup> and -0.2 nm/h as a function of TOOS.

Thus, the decrease of Arctic sea ice seems to have an opposite effect to the concentrations of potential CCN (=accumulation mode) during summer and winter. The increased amount of potential CCN due to less sea ice will probably pose a cooling effect on climate through aerosol-cloud interactions in summer. In winter, however, the clouds have much more complex effects on the radiative balance in the Arctic due to surface snow cover and longwave radiative cooling (Quinn, 2008). Thus, the increase in potential CCN might still lead to cooling effect on climate through aerosol-cloud interactions.

AO phase affected the relationships between TOSI and aerosol concentrations: during negative AO aerosol concentrations were increasing with increasing TOSI while during positive AO the trend was opposite. Since the decreasing sea ice is likely favoring negative AO (Vihma, 2014), the abovementioned possible cooling effect on climate might be diminished.

Finally, we conclude, that Arctic sea ice has a strong impact on aerosol concentrations in Eastern Lapland and that the decreasing sea ice most likely will change the aerosol population in the continental Arctic. Thus, the changes in the sea ice extent and the time that the air parcel spends over sea ice can have an influence on the aerosol-cloud interactions in the continental Arctic. The overall strength and sign of the radiative forcing is unknown and cannot be assessed based on our results, but our data suggests that at least during summer the decreasing sea ice seems to have a cooling effect through the changes in the aerosol-cloud interactions.

Quinn, P.K. et al. (2008). *Atmos. Chem. Phys.*, 8:1723-1735.

Vihma, T. (2014). *Surv. Geophys.*, 35:1175-1214.

# FLYING INSIDE VOLCANO'S PLUME WITH A MASS SPECTROMETER TO STUDY NEW PARTICLE FORMATION

J. Duplissy<sup>1</sup>, M. Sahyoun<sup>2</sup>, E. Freney<sup>2</sup>, R. Dupuy<sup>2</sup>, A. Colomb<sup>2</sup>, D. Picard<sup>2</sup>, J. Brito<sup>2</sup>, C. Denjean<sup>3</sup>, T. Bourianne<sup>3</sup>, M. Kulmala<sup>1</sup>, M. Riva<sup>1</sup>, H. Juninen<sup>1</sup>, A. Schwarzenboeck<sup>2</sup>, C. Planche<sup>2</sup> and K. Sellegri<sup>2</sup>

<sup>1</sup>Institute for Atmospheric and Earth System Research / Physics, Faculty of Science, University of Helsinki, Finland

<sup>2</sup>Université Clermont Auvergne, Laboratoire de Météorologie Physique, UMR-CNRS, Clermont-Ferrand, France

<sup>3</sup>LISA, UMR-CNRS 7583, UPEC-UPD, Institut Pierre Simon Laplace (IPSL), Créteil, France

Keywords: new particle formation, aerosol nucleation, volcanic particles

Presenting author email: m.sahyoun@opgc.univ-bpclermont.fr

Keywords: Sulfuric acid, new particle formation, STRAP, API-TOF, Volcano's plume, Flight measurement.

Volcanic emissions are one of the major natural sources of particles in the atmosphere. Volcanic particles injected in the atmosphere can act as cloud condensation nuclei (CCN) (Hobbs et al., 1982) or ice nuclei (IN) (Hoyle et al., 2011) affecting the cloud physical and microphysical properties and, consequently, the Earth's radiation budget causing significant impact on weather and climate. Different measurement techniques have been adopted to study tropospheric volcanic aerosols including in situ sampling techniques and remote sensing either from ground, from airborne measurements or from satellite. To date only few in-situ measurements of volcanic emissions have been carried out, largely due to difficulties associated with coordinating the measurements in space and time with volcanic eruptions, as well as due to the relatively harsh environment in the vicinity of volcanic plumes.

Previous in-situ measurement studies have reported: a) the occurrence of nucleation and new secondary particle formation (NPF) events within the volcanic plume (Boulon et al., 2011) and b) the presence of larger particles in the range of 2-3  $\mu\text{m}$  in locations far from the respective volcano. The phenomenon is attributed to particle growth and transport processes (Hervo et al., 2012)

In June 2016, as part of the CLERVOLC/STRAP project, a series of ground based and airborne based (French research aircraft, ATR-42) measurements were performed around Etna and Stromboli volcanos in Italy. The ATR-42 was equipped with a number of instruments, including: Scanning Mobility Particle Sizer (SMPS) and two Condensation Particle Counters (CPCs) to measure aerosol physical properties. This combination of instruments covered a wide particle size range (3 nm up to 450 nm) allowing the direct detection of freshly nucleated particles and their growth process within the plume. Ozone, NO<sub>x</sub>, SO<sub>2</sub>, were also measured. In addition a newly develop Xray-API-tof was measuring sulfuric acid concentration. But most importantly, this mass spectrometer allows to monitor new particle formation from a cluster point of view. This is the first time that such instrument is used in an aircraft.

In this work, we present an overview of the aerosol and gas phase measurements made aboard the ATR-42.

Evidence of NPF was observed within the volcanic plume for both Etna and Stromboli. The NPF events coincided with increases in SO<sub>2</sub> concentrations. Most importantly, the composition of the molecular clusters involve in the new particle formation will be presented.

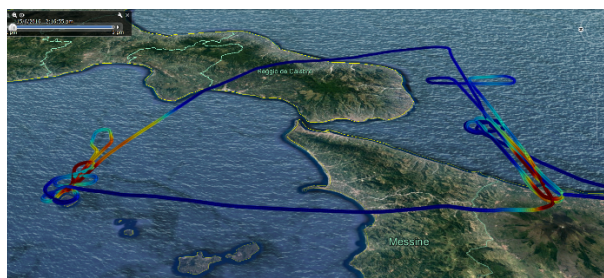


Figure 1: Preliminary data for SO<sub>2</sub> concentration during flight 14. Both plumes from Etna and Stromboli were investigate during this flight.

This work was supported by Labex ClerVolc (programme 1), ANR STRAP projects, and by the Academy of Finland Center of Excellence programme (grant no. 307331).

- Boulon, J., Sellegri, K., Hervo, M., Laj, P., 2011. Observations of nucleation of new particles in a volcanic plume. *Proc. Natl. Acad. Sci. U. S. A.* 108, 12223–6. doi:10.1073/pnas.1104923108
- Hervo, M., Quennehen, B., et al., 2012. Physical and optical properties of 2010 Eyjafjallajökull volcanic eruption aerosol: ground-based, Lidar and airborne measurements in France. *Atmos. Chem. Phys.* 12, 1721–1736. doi:10.5194/acp-12-1721-2012
- Hobbs, P. V., Tuell, J.P., et al., 1982. Particles and gases in the emissions from the 1980–1981 volcanic eruptions of Mt. St. Helens. *J. Geophys. Res.* 87, 11062. doi:10.1029/JC087iC13p11062
- Hoyle, C.R., Pinti, V., et al., 2011. Ice nucleation properties of volcanic ash from Eyjafjallajökull. *Atmos. Chem. Phys.* 11, 9911–9926. doi:10.5194/acp-11-9911-2011



## Successfully mitigating PM<sub>10</sub> in Stockholm city

M. Elmgren<sup>1</sup>, M. Norman<sup>1</sup>, S. Silvergren<sup>1</sup> and C. Johansson<sup>1,2</sup>

<sup>1</sup> Stockholm Environment and Health Administration, SLB-analys, SE 104 20, Stockholm, Sweden

<sup>2</sup> Department Environmental Science and Analytical Chemistry, ACES, Stockholm University, SE 106 91, Stockholm, Sweden

Keywords: PM<sub>10</sub>-mitigation, road dust, dust binding, CMA, studded tyre ban, Hornsgatan

Measurements of high PM<sub>10</sub>-concentrations in Stockholm are strongly anti-correlated with road wetness, this implies that PM<sub>10</sub> in Stockholm mainly is road dust, which is inhibited from re-suspending when roads are wet. Most of the road dust in Stockholm is generated by the wear and tear of studded winter tyres which are in use from late fall to early spring (Gustafsson et al., 2012, 2014, 2015, 2016). Starting in 2010 studded winter tyres were banned on some streets in Stockholm, studded tyre percentage decreased and PM<sub>10</sub>-concentrations followed. The decrease was substantial but not enough to meet regulations. In 2011 Stockholm city started applying a hygroscopic salt consisting of calcium magnesium acetate (CMA) to two inner city streets in order to keep them wet for longer periods, thus inhibiting road dust re-suspension, in 2013 dust binding with CMA was extended to 35 inner city streets which are treated roughly 40 times every season. The most polluted street in Stockholm city, Hornsgatan, went from 58 days exceeding the daily average limit value of 50 µg m<sup>-3</sup> for PM<sub>10</sub> in 2011 to only 17 days in 2017, hence meeting regulations, see Figure 1. Similar results were seen on all monitored streets in Stockholm city. Dust binding with CMA was established to having a decreasing effect of 20-40% on daily average PM<sub>10</sub>-concentrations during days with treatment (Gustafsson et al., 2010)

Stockholm aims to meet Sweden's environmental goals for air quality by 2030, which are stricter than the EU-regulations. This means that PM<sub>10</sub>-concentrations need to decrease even further. In March 2017 daytime dust binding was tested in addition to regular dust binding applied night time. It was applied around midday only when PM<sub>10</sub>-concentrations were high. A test site (Sveavägen 59) and a reference site (Sveavägen 83) are situated on the same street separated by a few city blocks. Dust binding night time was conducted on both sites throughout the test period, while daytime dust binding only was applied at the test site. The results show an additional decrease on PM<sub>10</sub>-concentrations with 3-4% on daily averages, for days with daytime dust binding. Daytime dust binding is not likely to continue due to difficulties applying in heavy traffic.

All streets in inner city Stockholm has met the air quality regulations for PM<sub>10</sub> for four straight years. PM<sub>10</sub> in Stockholm city is mitigated.

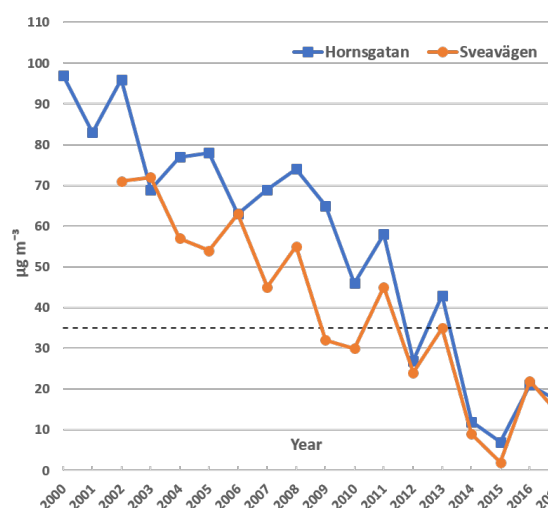


Figure 1: Amount of days per year exceeding the daily average limit value of 50 µg m<sup>-3</sup> for PM<sub>10</sub> for two inner city streets in Stockholm, Hornsgatan (blue) and Sveavägen (orange) since 2000

- Gustafsson, M., Blomqvist, G., Janhäll, S., Johansson, C., & Norman, M. (2016). *Driftåtgärder mot PM<sub>10</sub> i Stockholm: utvärdering av vintersäsongen 2014-2015*, VTI Rapport 897, in press 2016.
- Gustafsson, M., Blomqvist, G., Janhäll, S., Johansson, C., & Norman, M. (2015). *Driftåtgärder mot PM<sub>10</sub> i Stockholm: utvärdering av vintersäsongen 2013-2014*, VTI Rapport 847, in press 2015.
- Gustafsson, M., Blomqvist, G., Janhäll, S., Johansson, C., & Norman, M. (2014). *Driftåtgärder mot PM<sub>10</sub> i Stockholm: utvärdering av vintersäsongen 2012-2013*, VTI Rapport 802, in press 2014.
- Gustafsson, M., Blomqvist, G., Johansson, C., & Norman, M. (2012). *Driftåtgärder mot PM<sub>10</sub> på Hornsgatan och Sveavägen i Stockholm: utvärdering av vintersäsongen 2011-2012*, VTI Rapport 767, in press 2012.
- Gustafsson, M., Blomqvist, G., Jonsson, P., & Ferm, M. (2010). *Effekter av dammbindning av belagda vägar*, VTI Rapport 666, in press 2010.

# How increased ionization can boost aerosol growth to cloud condensation nuclei

M.B. Enghoff<sup>1</sup>, H. Svensmark<sup>1</sup>, N.J. Shaviv<sup>2</sup> and J. Svensmark<sup>1,3</sup>

<sup>1</sup>National Space Institute, Technical University of Denmark, Denmark

<sup>2</sup>Racah Institute of Physics, Hebrew University of Jerusalem, Israel

<sup>3</sup>Dark Cosmology Center, Niels Bohr Institute, University of Copenhagen, Denmark

Keywords: atmospheric aerosols, ionization, growth, cloud condensation nuclei

In this study (Svensmark et al, 2017) the effect of ionization on the growth of aerosols into cloud condensation nuclei is investigated theoretically and experimentally. We show that the mass-flux of small ions can constitute an important addition to the growth caused by condensation of neutral molecules.

Under atmospheric conditions the growth from ions can constitute several percent of the neutral growth. We performed experimental studies which quantify the effect of ions on the growth of aerosols between nucleation and sizes up to 20 nm and find good agreement with theory. Ion-induced condensation could be of importance not just in Earth's present day atmosphere for the growth of aerosols into cloud condensation nuclei under pristine marine conditions, but also under elevated atmospheric ionization caused by increased supernova activity.

We propose an addition to the condensation equation based on the additional mass-flux of ions to aerosols of the form:

$$\Gamma = 4 \left( \frac{n_{ion}}{n_0} \right) \left( \frac{\beta^{\pm 0}}{\beta^{00}} \right) \left( \frac{m_{ion}}{m_0} \right) \left( \frac{N^0(r, t)}{N^{tot}(r, t)} \right), \quad (1)$$

In Equation 1 the first term is the ratio of the number concentration of ions to the number concentration of neutrals, the second term is the ratio of the interaction coefficient between ions and neutral aerosols to the interaction coefficient between neutral molecules and aerosols, the third term is the ratio of the ion mass to the neutral mass and the final term is the ration of the amount of neutral aerosols to the total amount of aerosols. While the second and fourth terms are (nearly) constant under most conditions the ion/neutral number concentrations and mass vary depending on atmospheric conditions. In a pristine environment at high ionization levels the effect can account for almost 20% of the growth rate of small aerosols and a significant enhancement up to 20-30 nm.

The theory was tested experimentally in 7 m<sup>3</sup> atmospheric reaction chamber, measuring the aerosol size distribution and (for some of the experiments) the sulphuric acid concentration. A total of 3100 hours of data with varying gas and ion concentrations were analyzed.

In Figure 1 an example of an experimental run can be seen. Panel a) shows a series of experiments where ionizing gamma sources were opened and closed with 2 hour intervals. Panel b) shows all the individual experiments from panel a) superposed onto each other,

clearly revealing the growth profile. Analyzing these superposed growth profiles allowed us to compare growth rates with and without ionization to the theory and we found a good agreement between the two.

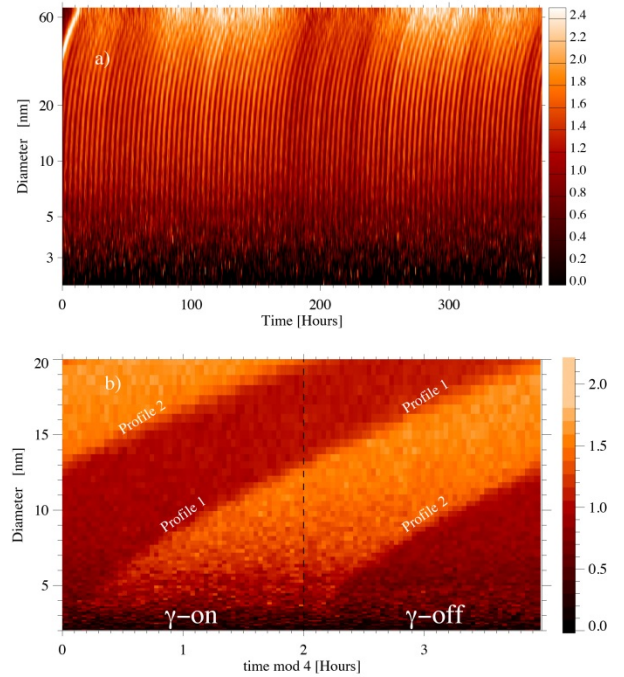


Figure 1: Example of a series of experiments (a) and superposed data (b)

The mechanism is favoured by high ionization, low gas concentrations, and low aerosol concentrations. This points to pristine settings, such as over oceans away from continental and polluted areas. Potentially the mechanism can contribute significantly to the production of cloud condensation nuclei, but to fully assess the impact the mechanism should be included in global climate simulations.

Svensmark, H., Enghoff, M. B., Shaviv, N. J., and Svensmark, J. (2017). *Nat. Commun.*, 8:2199.

# PHTHALATE UPTAKE FROM VINYL FLOORING BY AMBIENT AND LABORATORY GENERATED PARTICLES

A.C. ERIKSSON<sup>1,2</sup>, C. ANDERSEN<sup>1</sup>, A.M. KRAIS<sup>3</sup>, J. KLENØ NØJGAARD<sup>4</sup>, P.-A., CLAUSEN<sup>5</sup>,  
A. WIERZBICKA<sup>1</sup> and J. PAGELS<sup>1</sup>

<sup>1</sup>Ergonomics and Aerosol Technology, Lund University, Sweden

<sup>2</sup>Nuclear Physics, Lund University, Sweden

<sup>3</sup>Occupational and Environmental Medicine, Lund University, Sweden

<sup>4</sup>Department of Environmental Science, Aarhus University, Roskilde, Denmark

<sup>5</sup>The National Research Centre for the Working Environment, Copenhagen, Denmark

Keywords: phthalates, DEHP, SVOC, organic aerosol, indoor air

Phthalate esters are known endocrine disruptors, which are used in a wide range of products including vinyl flooring. Phthalates are ubiquitous in indoor environments, and their metabolites are ubiquitous in humans. Hence understanding the exposure routes of phthalates is important. Furthermore, there is a robust link between ambient (outdoor) air pollution and adverse health effects, while exposure predominantly occurs indoors. Thus, understanding the interplay between indoor and outdoor pollutants is imperative. Therefore we have studied the uptake of bis(2-ethylhexyl) phthalate (DEHP), a semi volatile organic compound (SVOC, equilibrium concentration  $\sim 1 \mu\text{g}/\text{m}^3$ ), by laboratory generated ammonium sulfate particles as well as ambient aerosols.

We used a 1.2-l aluminum chamber with two  $\text{dm}^2$  of vinyl flooring, containing  $176 \text{ mg DEHP}/\text{cm}^3$ . Particle residence times varied between 1 and 12 minutes. We investigated the uptake by particles passing through the chamber using an aerosol mass spectrometer (AMS) calibrated with pure DEHP particles. We generated ammonium sulfate (AS) particles through nebulization and drying, followed by denuding at  $250^\circ\text{C}$  to reduce organic impurities. We also sampled ambient aerosol through the chamber. We used the ambient aerosol infiltrating the Lund aerosol laboratory. Comparison with aerosol chemical speciation monitor data from the ACTRIS station Hyltemossa, located 50 km north of Lund, show that long-range transport dominated sampled PM.

We observed DEHP uptake by the AS particles, in agreement with the findings of Benning *et al.* who performed similar experiments. The equilibration time was around 6 minutes, in contrast to the results of Benning *et al.*, (2013) who reported shorter equilibrium times based on offline measurements. Thermal denuding of the AS particles resulted in reduced DEHP uptake, which suggests absorption by organic aerosol (OA) enhance DEHP uptake.

Our experiment with ambient aerosol further corroborated the role of OA in DEHP uptake. After the ambient PM had passed through the chamber, it contained on average  $5 (\pm 1, 1\sigma) \%$  DEHP. The laboratory-generated AS particles were less efficient vectors and contained about 1% DEHP after passing through the chamber.

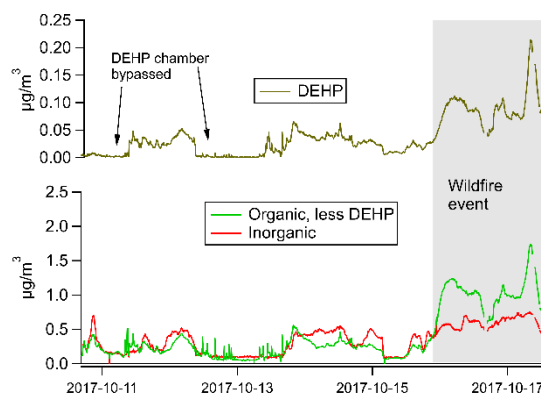


Figure 1: Concentration of DEHP, organic and inorganic  $\text{PM}_{10}$  during the ambient aerosol experiment.

Massive wildfires on the Iberian peninsula caused increased loadings of OA during the last two days of sampling (see Figure 1). Size resolved data from the wildfire event, shown in Figure 2, reveals that the sorbed DEHP was unevenly distributed in the ambient OA, with higher DEHP to OA ratio for smaller particles.

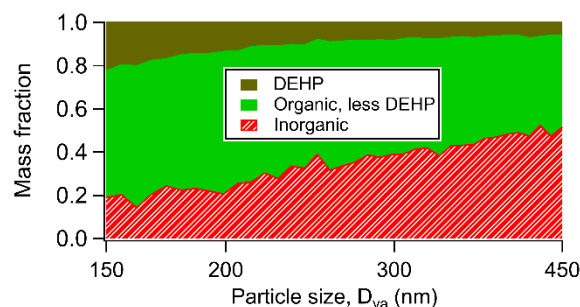


Figure 2: Average size resolved composition of ambient particles from Iberian wildfires after passing through the DEHP chamber in Lund.

Furthermore, the total DEHP fraction of OA was rather variable (5-11%) over the duration of the event, despite relatively constant environmental conditions in the laboratory and similar infiltrated PM. Further experiments are needed to explore which parameters govern indoor SVOC uptake by infiltrating PM.

Benning, J.L., *et al.* (2013). *Env. Sci. Tech.* 47: 2696–2703.

# ON THE STRUCTURE AND DYNAMICS OF THE CONDENSATION SINK IN THE ATMOSPHERE: A SIMPLE SEMI-ANALYTICAL MODEL

E. EZHOVA<sup>1</sup>, V.-M. KERMINEN<sup>1</sup>, K.E.J. LEHTINEN<sup>2</sup> and M. KULMALA<sup>3</sup>

<sup>1</sup> Institute for atmospheric and Earth system research/Physics, University of Helsinki, Finland

<sup>2</sup> Department of Applied Physics, University of Eastern Finland, Finland

Keywords: condensation sink, atmospheric aerosols, Fuchs-Sutugin coefficient

Condensation sink (CS) is an important parameter for aerosol dynamics quantifying the rate of the vapour condensation on the existing aerosol population. A time scale  $\tau = 1/CS$  has a clear physical meaning of a characteristic time for vapours to be condensed onto the surface of existing aerosol. Due to the similarity between the processes of vapour condensation on aerosol particles and coagulation of the smallest particles (monomers, dimers, clusters) with the larger particles from Aitken and accommodation modes, CS proves useful for the quantification of a coagulation sink. Then a competition between the process of small clusters coagulation with the larger aerosol particles, represented by CS, and the process of the clusters growth by condensation, represented by the particle growth rate, defines the probability of clusters survival and a new particle formation event (Kulmala et al., 2017).

A simple model allowing to describe the dynamics of a condensation sink in the atmosphere thus could be helpful for understanding of new particle burst and cut-off processes. We developed a model for the coupled dynamics of condensing vapours and aerosol using mainly analytical formulas.

Transformation of the mass flux towards the particle from the kinetic regime to the continuum regime is often described by the Fuchs-Sutugin coefficient (Fuchs and Sutugin, 1971). Kinetic regime can be obtained as a limiting case when only one term of the expansion of the Fuchs-Sutugin (FS) coefficient at large Knudsen numbers  $Kn$  is considered. We took into account the two first terms, and got the mass flux which agrees well with the full mass flux up to  $Kn \approx 0.5$ . This procedure allows to obtain an analytical solution of the condensation equation valid for the range of intermediate Knudsen numbers. We compared solutions in the kinetic regime and for intermediate Knudsen numbers. In the kinetic regime the number particle distribution does not change its shape, just the characteristic diameter grows. For intermediate Knudsen numbers the particle growth rate becomes diameter dependent and larger particles grow slower than smaller particles. This leads to narrowing of the number particle distribution. The analytical solution for the intermediate Knudsen numbers is in good agreement with the full numerical solution of the condensation equation.

The expansion was further applied to calculate analytically the condensation sink for the initial lognormal number particle distribution. We found the difference between the CS calculated using a kinetic regime formula and the CS calculated using our approach, i.e. defined the limits of applicability of the kinetic regime formula for the CS calculations.

The formula for CS was tested against field observations in boreal forests. Our approach results in up to a 5.5% overestimate of the CS below 500 nm as compared to the calculations from the definition using the full Fuchs-Sutugin coefficient. This is due to the fact that our approximation of the FS coefficient tends to slightly overestimate the full FS formula.

We investigated the contributions of different modes to the condensation sink depending on their parameters: Knudsen number corresponding to the geometric mean diameter of each mode and number concentration. The nucleation mode with a small characteristic diameter 2-3 nm does not contribute significantly to the atmospheric CS even for very high number concentrations (up to 10000 1/cm<sup>3</sup>), while the accumulation mode with a characteristic diameter 100 nm and larger contributes even if the number concentrations are as low as 100 1/cm<sup>3</sup>.

By adding an equation for a vapour concentration to the formulas for CS, we developed a simple coupled model for the dynamics of the condensation sink and condensing vapours. The model in its present form can be used for the characteristic mode diameters larger than 20 nm. As many modes as needed can be included into the model. The only external parameter is the initial growth rate of the mode. The model describes adequately dynamics of the condensation sink in the atmosphere during the periods of the aerosol modes growth by condensation.

Kulmala, M., V.-M. Kerminen, T. Petäjä, A.J. Ding and L. Wang (2017). *Faraday Discuss.*, 200: 271-288.  
Fuchs, N.A. and A.G. Sutugin (1971). In *Topics in current aerosol research*, pages 1-32, Pergamon, New York.

# CCN emission factors of solid biomass fuels related to residential cooking

J. Falk<sup>1</sup>, T.B. Kristensen<sup>1</sup>, R. Lindgren<sup>2</sup>, C. Andersen<sup>3</sup>, R. Carvalho<sup>2</sup>, K. Korhonen<sup>4</sup>, V. Berg Malmberg<sup>3</sup>, A. C. Eriksson<sup>3</sup>, C. Boman<sup>2</sup>, J. H. Pagels<sup>3</sup> and B. Svenningsson<sup>1</sup>

<sup>1</sup>Department of Physics, Lund University, SE-22100, Lund, Sweden

<sup>2</sup>Thermochemical Energy Conversion Laboratory, Umeå University, SE-90187, Umeå, Sweden

<sup>3</sup>Ergonomics and Aerosol Technology, Lund University, SE-22100, Lund, Sweden

<sup>4</sup>Department of Applied Physics, University of Eastern Finland, FI-70211, Kuopio, Finland

Keywords: CCN, biomass burning, emission factors, aerosol-cloud interactions

## Introduction

A sizeable portion of the world's population rely on biomass fuels for their everyday residential cooking and heating, resulting in globally significant emissions of primary and secondary aerosol particles. These particles influence human health, and may also act as cloud condensation nuclei (CCN) affecting cloud dynamics and climate. Recent model studies indicate that the aerosol indirect effect of CCN emissions from solid fuel cook stove burning results in a global radiative forcing of  $\sim -0.2 \text{ W/m}^2$  (Huang et al., 2017) However, CCN emission factors (EF) have previously not been studied in detail, which is the focus of the current study. The study was performed at Umeå University and carried out as part of the Salutary Umeå Study of Aerosols in Biomass Cook Stove Emissions (SUSTAINED).

## Methods

Four types of stove technologies were tested; three-stone fire (3S), rocket stove (RS), natural draft stove (NDS) and forced draft stove (FDS). The fuels tested, alone and in combinations were wood logs; sesbania, casuarina, birch, and pellets; softwood, sesbania, rice husk, water hyacinth and coffee husk. The latter three types were produced from agricultural residue related to Sub-Saharan Africa to investigate sustainable options.

The experiments were carried out by performing water boiling tests, and measurements were conducted on the flue gas or from injection into a  $15 \text{ m}^2$  stainless steel chamber held at room temperature ( $\sim 25^\circ\text{C}$ ) and low relative humidity ( $\sim 25\%$ ). A CCN counter (CCNC-100, DMT Inc.) was used to measure size-selected particles (mobility diameters of 60, 100, 200 and 350 nm) from the chamber after a Differential Mobility Analyzer (DMA) in order to obtain hygroscopicity  $\kappa$  values for each size. A Fast Aerosol Mobility Sizer (DMS500, Cambustion Inc.) was used to gather particle number size distribution directly from the flue gas.

A continuous size dependent  $\kappa$  value for the full range of relevance was obtained from inter- and extrapolation of measurements. The CCN EFs were then obtained by integrating the measured particle number size distributions normalized with respect to the fuel mass consumption. An oxidation flow

reactor (OFR) was also used to investigate the impact of atmospheric aging and secondary particle formation.

## Conclusions

The CCN EF for primary emissions show a large variability both within different stove technologies burning the same fuel (depicted in Fig. 1), as well as the same stove technology burning different fuels. For supersaturation levels of around 0.2%, large differences in CCN EFs can be observed. Furthermore, for supersaturations approaching 1% the CCN EFs may vary up to more than an order of magnitude. Our results indicate that changes/advances in technology and/or fuel may substantially influence the CCN population on both regional and global scales.

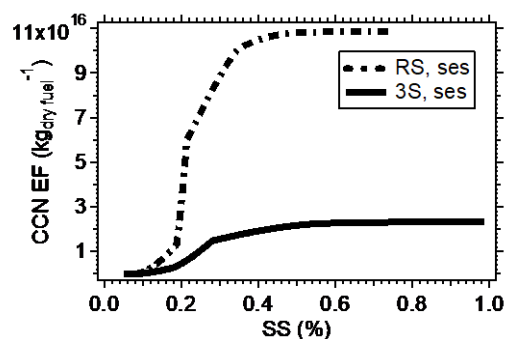


Figure 1. CCN per unit of dry fuel (CCN EF) as a function of supersaturation (SS) for combustion of sesbania (ses) wood logs in a rocket stove (RS) and a three-stone fire (3S).

*This work was supported by the Swedish research councils VR and Formas.*

Huang, Y., Unger, N., Storelvmo, T., Harper, K., Zheng, Y. & Heyes, C. (2017). *Atmos. Chem. Phys. Discuss.* 1–40.

# INTEGRATION OF IMPROVED AEROSOL CHEMISTRY AND PHYSICS ALGORITHMS INTO THE SILAM MODEL

B. FOREBACK<sup>1</sup>, M. BOY<sup>1</sup>, A. MAHURA<sup>1</sup>, R. KOUZNETSOV<sup>2</sup>

<sup>1</sup>Institute of Atmospheric and Earth Science Research / Physics,  
Faculty of Science, University of Helsinki, Finland

<sup>2</sup>Finnish Meteorological Institute, Helsinki, Finland

Keywords: Chemical Transport Modelling, Aerosol Modelling, SILAM, ADCHAM, Enviro-HIRLAM

Improving aerosol chemistry and physics for atmospheric chemical, transport, dispersion, and deposition models will help improve forecasting of air quality risks and hazards. New algorithms that have been developed from recent aerosol and atmospheric chemistry research at the University of Helsinki will be integrated into the System for Integrated Modelling of Atmospheric Composition (SILAM) model (Sofiev et al., 2015). The modifications will be based on Aerosol Dynamics, gas- and particle-phase chemistry model for laboratory CHAMber studies (ADCHAM; Roldin et al., 2014). This analysis will use meteorological output from the Environment-High Resolution Limited Area Model (Enviro-HIRLAM).

Enviro-HIRLAM is an online, integrated numerical weather prediction and atmospheric chemical transport model, used for forecasting meteorological, chemical and biological conditions (Baklanov et al., 2017). In this study, the 3-dimensional meteorological fields from Enviro-HIRLAM will be used as the input boundary conditions for experimental SILAM model runs. When combined, both models can work synergistically for better forecasts.

Enviro-HIRLAM output is available with four different modes: control (no aerosol effects), direct aerosol effect, indirect aerosol effect, and combined direct and indirect aerosol effect. The latter three modes include the influence of aerosols in numerical weather forecasting. A series of SILAM model simulations, including the updated version, in combination with Enviro-HIRLAM output from each of these four modes will be performed in order to determine the best results.

To begin, we will optimize the spatiotemporal resolutions of the SILAM model to ensure the results model a real-world scenario as accurately as possible. Accuracy, however, needs to be balanced with computational efficiency. This project will include a series of sensitivity tests using various permutations of grid sizes and time steps to determine the most suitable spatiotemporal resolution.

For validation, we will perform an analysis of the SILAM model results compared against in-situ measurements from observational stations in the model domain. Focus will be on the SMEAR-II station in Hyytiälä, Finland. By comparing model runs before and after adding the improvements to SILAM, we can determine the extent of the improvements made with the new atmospheric aerosol and chemical developments.

Figure 1 illustrates the approach for running both models and validating the changes to the SILAM model.

Preliminary results will be presented at the 2018 NOSA conference in March. If the model shows better performance and the results prove to be successful, then the updates will be integrated into a future version of the SILAM model.

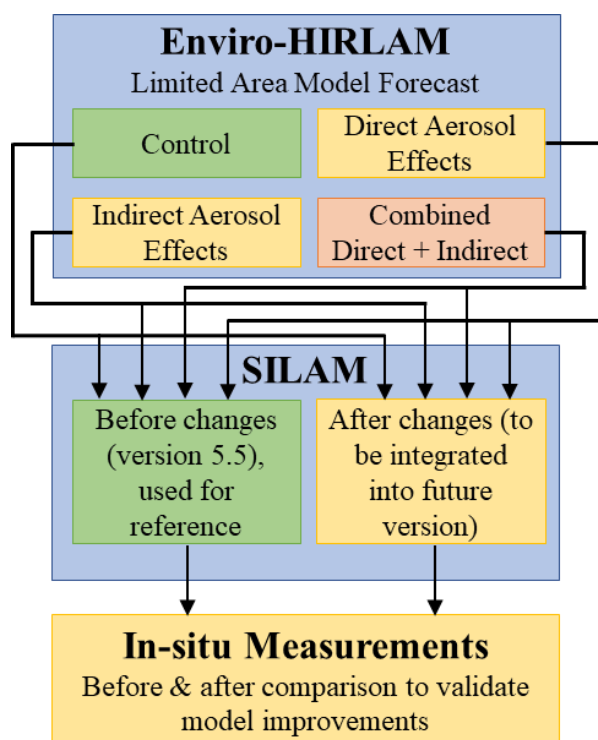


Figure 1: The approach of using Enviro-HIRLAM forecast data as the boundary conditions for the SILAM model runs and comparing results before and after improvements from Roldin et al., 2014, using in-situ observations for validation.

Baklanov, A., et al., (2017), *Enviro-HIRLAM online integrated meteorology-chemistry modelling system: strategy, methodology, developments and applications (v7.2)*. *Geosci. Model Dev.*, 10, 2971-2999.

Roldin, P., et al., (2014), *Modelling non-equilibrium secondary organic aerosol formation and evaporation with the aerosol dynamics, gas- and particle-phase chemistry kinetic multilayer model ADCHAM*. *Atmos. Chem. Phys.*, 14, 7953-7993.

Sofiev, M., et al., (2015), *Construction of the SILAM Eulerian atmospheric dispersion model based on the advection algorithm of Michael Galperin*, *Geosci. Model Dev.*, 8, 3497-3522

# SNAPSHOT OF PM<sub>2.5</sub>, PM<sub>1</sub>, BLACK CARBON AND ORGANIC COMPONENTS OF PARTICULATE MATTER IN BEIJING, SUMMER 2016

S. M. GAITA<sup>1</sup>, M. LE BRETON<sup>1</sup>, J. BOMAN<sup>1</sup>, R. K. PATHAK<sup>1</sup>, Å. M. HALLQUIST<sup>2</sup>, Q. LIU<sup>3</sup>, J. ZHENG<sup>4</sup>, Z. DU<sup>4</sup>, S. LOU<sup>5</sup>, S. GUO<sup>4</sup>, C. K. CHAN<sup>6</sup>, M. HU<sup>4</sup> and M. HALLQUIST<sup>1</sup>

<sup>1</sup>Department of Chemistry and Molecular biology, University of Gothenburg, Sweden

<sup>2</sup>IVL Swedish Environmental Research Institute, Sweden

<sup>3</sup>Division of Environment and Sustainability, Hong Kong University of Science and Technology, Hong Kong

<sup>4</sup>College of Environmental Sciences and Engineering, Peking University, China

<sup>5</sup>Shanghai Academy of Environmental Sciences, China

<sup>6</sup>School of Energy and Environment, City University of Hong Kong, Hong Kong

Keywords: black carbon, photochemical smog, PM<sub>2.5</sub>

Air pollution in China has attracted global attention as the country takes its place in the economic forefront (Hallquist et al., 2016). Sources and chemical composition of both gaseous and particulate pollutants are yet to be fully understood. This is critical since the extremity of the air pollution adds to social, political, and economical complexity of any country. In view of this, a collaborative research project titled "Photochemical Smog in China" was designed by Swedish and Chinese scientists with the aim of improving scientific knowledge on the photochemical smog pollution situation in China by measuring and modelling atmospheric gas- and particle-phase reactions. Samples in this study were collected at the measurement site on Changping University Campus, Peking University, situated at a semi-rural location 40 km northwest of Beijing. Le Breton et al. (2017) gives a detailed description of the site setup. Data on PM<sub>1</sub> and organic components as well as PM<sub>2.5</sub> samples were collected from 14<sup>th</sup> May 2016 to 20<sup>th</sup> June 2016.

PM<sub>2.5</sub> samples were collected on Teflon (polytetrafluoroethylene) filters on a 24 h interval using a cyclone sampler. The samples were analysed for black carbon and mass concentration at the University of Gothenburg. PM<sub>1</sub> data were collected using a time of flight aerosol mass spectrometer (ToF-AMS). In addition, a High-Resolution Time of Flight Chemical Ionization Mass Spectrometer (ToF-CIMS) was utilised to measure gas and particle-phase species in the ambient environment.

Table 1 shows the concentration of selected species from the field campaign. The concentration of PM<sub>2.5</sub> was above the WHO 24 h guideline limits 50% of the measurement days. 40% of the days were above the Chinese Grade I limit (35 µg m<sup>-3</sup>) and 29% above the Grade II (75 µg m<sup>-3</sup>). PM<sub>1</sub>, which has higher propensity of deposition into the deeper zones of the human respiratory system, was above WHO guideline limits 40% of the measurement days.

The average black carbon (BC) concentration was significantly higher (a factor of 7) than values from the Scandinavian city of Gothenburg (Boman et al., 2010). Of the PM<sub>1</sub> concentration, the organic component was approximately 50%, highlighting the importance of

primary and secondary organic aerosols in the particulate pollution in China.

**Table 1:** Statistics of measured atmospheric species in Changping during summer 2016.

Species	Max	Min	Mean	Sdev
PM <sub>1</sub> (µg m <sup>-3</sup> )	43	2.1	21	13
PM <sub>2.5</sub> (µg m <sup>-3</sup> )	270	3.1	51	56
BC (µg m <sup>-3</sup> )	11	0.6	3.1	2.4
Organics (µg m <sup>-3</sup> )	19	1.0	9.8	5.1

The presented results give a minute picture of the air pollution situation in this part of China. A detailed statistical analysis using tools such as positive matrix factorization (PMF) would provide an in-depth view of the possible source signatures. Adding the data from ToF-AMS and ToF-CIMS to the analysis will provide deeper understanding of the chemical transformation of organic components of the ambient aerosols.

This study is part of the framework program "Photochemical smog in China" financed by Swedish Research Council (639-2013-6917). The National Natural Science Foundation of China (21677002) and the National Key Research and Development Program of China (2016YFC0202003) also assisted in funding this work.

Hallquist, M., Munthe, J., Hu, M., Mellqvist, J., Wang, T., Chan, C. K., Gao, J., Boman, J., Guo, S., Hallquist, Å. M., Moldanova, J., Pathak, R. K., Pettersson, J. B. C., Pleijel, H., Simpson, D., and Thynell, M. (2016). *Nat. Sci. Rev.*, 3, 401-403, 2016.

Le Breton, M., Wang, Y., Hallquist, Å. M., Pathak, R. K., Zheng, J., Yang, Y., Shang, D., Glasius, M., Bannan, T. J., Liu, Q., Chan, C. K., Percival, C. J., Zhu, W., Lou, S., Topping, D., Wang, Y., Yu, J., Lu, K., Guo, S., Hu, M., and Hallquist, M. (2017). *Atmos. Chem. Phys. Discuss.* <https://doi.org/10.5194/acp-2017-814>, in review.

Boman, J., Wagner, A. and Gatari, M. J. (2010). *Spectrochimica Acta Part B: Atomic Spectroscopy* 65(6): 478-482. DOI: <http://dx.doi.org/10.1016/j.sab.2010.03.014>

# MEASUREMENTS OF ORGANIC AEROSOL PRECURSOR GASES IN SHANGHAI

O. GARMASH<sup>1</sup>, L. YAO<sup>2</sup>, F. BIANCHI<sup>1</sup>, O. PERÄKYLÄ<sup>1</sup>, Y. ZHANG<sup>1</sup>, C. YAN<sup>1</sup>, T. PETÄJÄ<sup>1</sup>, D. WORSNOP<sup>1,3</sup>  
M. KULMALA<sup>1</sup>, L. WANG<sup>2,4</sup> and M. EHN<sup>1</sup>

<sup>1</sup>Institute for Atmospheric and Earth System Research/Physics, University of Helsinki, Finland

<sup>2</sup>Shanghai Key Laboratory of Atmospheric Particle Pollution and Prevention (LAP3), Department of Environmental Science & Engineering, Fudan University, Shanghai, China

<sup>3</sup>Aerodyne Research, Inc., Billerica, MA, USA

<sup>4</sup>Collaborative Innovation Center of Climate Change, Nanjing, China

Keywords: OVOC, secondary organic aerosol, mass spectrometry

Secondary organic aerosol (SOA) comprise a large fraction of atmospheric aerosol budget (Jimenez *et al.* 2009). SOA forms in the atmosphere from oxidation products of volatile organic compounds (VOC), which can come from both anthropogenic and biogenic sources. The understanding of the composition and sources of the oxidized VOC (or OVOC) are pivotal for estimating the relative contribution of anthropogenic and biogenic vapours to global aerosol population as well as essential for tackling secondary aerosol pollution in urban areas.

During winter 2015-2016, we conducted an intensive campaign at Fudan University (Shanghai) during which we investigated the composition and diurnal variation of gas-phase compounds. We have deployed a high-resolution chemical ionisation mass spectrometry (CI-APi-TOF) that uses a selective NO<sub>3</sub><sup>-</sup> ionisation method to detect low-volatility organic compounds. This method was shown previously to detect Highly Oxygenated Molecules (HOM) in the boreal forest as well as in the laboratory oxidation experiments using a wide range of precursor gases (Ehn *et al.* 2014, Jokinen *et al.* 2015).

CI-APi-TOF is known to be selective for low-volatility compounds that have at least two H-bond donors (-OH or -OOH groups) (Hyytinen *et al.* 2015) and usually shows well-separated molecules in the mass spectrum. However, the results from Shanghai have demonstrated that NO<sub>3</sub><sup>-</sup> chemical ionization mass spectrometry in a Chinese megacity detect a wide range of compounds shifted to lower masses as compared to the results collected e.g. in Hyytiälä, Finland (boreal forest environment). The observed mass spectrum has shown no distinct HOM dimers that have been observed in other locations. On the other hand, the spectrum contained a high contribution of organic nitrogen-containing species both during the day and night, likely due to large contribution of NO<sub>x</sub> (NO+NO<sub>2</sub>) to atmospheric chemistry in Shanghai.

In such a complex environment as Shanghai, it proved challenging to identify the chemical composition of most of the observed organic compounds with high certainty. We have concluded

that many of the observed peaks in the mass spectrum contained more than one chemical compound or had multiple sources, which can be expected in an urban area. As a result, in order to investigate the sources for the observed compounds as well as identify their possible molecular composition we have applied a Positive Matrix Factorization (PMF) method to the mass spectrometry data (Paatero and Tapper 1994). In my presentation, I will present the results from this analysis suggesting possible sources and precursors for the observed organic species.

Acknowledgements: This study was supported by the National Natural Science Foundation of China (No. 21190053, 21222703, 21561130150, & 91644213), the Ministry of Science and Technology of China (2017YFC0209505), the Cyrus Tang Foundation (No. CTF-FD2014001), the Academy of Finland Centre of Excellence program (project no 272041, 307331), European Research Council (COALA grant 638703, ATM-GTP grant 742206), and Swiss National Science Foundation (grant P2EZP2\_168787).

Ehn, M., J. A. Thornton, *et al.* (2014). *Nature*, 506:476-479.

Hyytinen, N., O. Kupiainen-Maatta, *et al.* (2015). *Journal of Physical Chemistry A*, 119:6339-6345.

Jimenez, J. L., M. R. Canagaratna, *et al.* (2009). *Science*, 326:1525-1529.

Jokinen, T., T. Berndt, *et al.* (2015). *Proc Natl Acad Sci USA*, 112:7123-7128.

Paatero, P. and U. Tapper (1994). *Environmetrics*, 5:111-126.



# EFFECT OF WIND SPEED ON MODIS AEROSOL OPTICAL DEPTH OVER NORTH PACIFIC

P. Glantz<sup>1</sup>, L. Merkulova<sup>1</sup>, E. Freud<sup>1</sup>, E. M. Mårtensson<sup>2</sup>, and D. E. Nilsson<sup>1</sup>

<sup>1</sup>Department of Environmental Science and Analytical Chemistry, Stockholm University, Sweden

<sup>2</sup>Department of Earth Sciences, Uppsala University, Uppsala, Sweden

Keywords: AOD, surface wind speed, satellite retrievals, sea salt, ammonium sulfate, white caps

Oceans cover approximately two-thirds of the Earth's surface and are the major source of natural aerosol mass. In terms of mass, sea spray produced at the ocean surface dominates global aerosol flux with an annual sea salt production of 0.3 Pg to 30 Pg (Lewis and Schwartz, 2004) and organic matter of 8-50 Tg C year<sup>-1</sup> (Kieber et al, 2016). Due to high hygroscopicity of sea salt and regional abundance the aerosol provides a major contribution to scattering of solar radiation, resulting in a cooling effect (e.g Haywood et al, 1999).

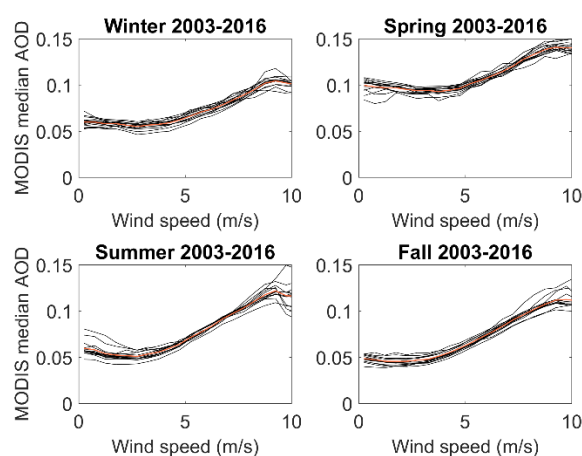
Here we have investigated the surface wind speed influences on aerosol optical depth (AOD), derived from the Moderate Resolution Imaging Spectroradiometer (MODIS) Aqua daily observations over the central North Pacific during the period 2003-2016. The 2m wind speed on satellite pixel basis has been interpolated from National Centers for Environmental Prediction (NCEP) reanalysis. In addition, daily averaged AOD derived from Aerosol Robotic Network (AERONET) measurements in the free-troposphere at the Mauna Loa Observatory (3397 asl), Hawaii, was subtracted from the MODIS column AOD values. The latter to reduce the contribution of aerosols above the planetary boundary layer.

Figure 1 presents adjusted median AOD (555 nm) on a seasonal basis, for all years investigated. In summer, fall and winter the median AOD increases roughly by a factor of 2 within the wind speed range about 3.5 - 9 m/s. In spring the increase in AOD is similar in absolute terms, however, the background AOD is substantially higher than in other seasons. This is likely due to the influence of continental aerosols from Asia.

Based on the results shown in Figure 1 the derived power law relationship  $AOD = 0.001 * U^{1.86} + 0.05$ , for summer, fall and winter, indicate a relatively strong wind dependency. The constant zero offset term ( $AOD \sim 0.05$ ) reflects a marine background situation, where we assume the presence mainly of secondary aerosols such as ammonium sulfate that are formed independently of the wind speed.

The present relationship estimated between AOD and surface wind speed has been compared to results obtained in several previous studies. In addition, we have also examined how surface wind speed are

influencing the contribution of coarse and fine mode aerosols to the AOD.



**Figure 1.** MODIS adjusted median AOD (555 nm) versus surface wind speed, subdivided with respect to season, for each year of the period 2003-2016. The orange solid line in each figure denote MODIS mean AOD, averaged over the investigation period.

To summarize, the current study shows a distinct increase in MODIS AOD for higher wind speeds. To our knowledge, the established parameterization is derived for the longest period of MODIS Aqua observations over the ocean. It can serve as a promising reference for future investigations of the AOD – wind speed relationship. Thus, the results presented in this study make the basis for subsequent investigations to estimate direct radiative effects over the North Pacific. Furthermore, the results of a relationship between AOT and wind speed is very promising in the sense that the latter quantity is associated with relatively small uncertainties in climate model calculations.

Lewis, E.R.; Schwartz, S.E. (2004). A Critical Review. American Geophysical Union, Washington, D. C., 2004.

Kieber, D.J.; et al., (2016). *Geophys. Res. Lett.*, 43, 2765–2772, doi:10.1002/2016GL068273.

Haywood, J.; Ramaswamy, V.; Soden, B. (1999), *Science*, 283, 1299–1303.

# MOLECULAR TRACERS OF SECONDARY AEROSOLS IN XI'AN, CHINA DURING SUMMER AND WINTER

M. GLASIUS<sup>1</sup>, L.S. IVERSEN<sup>1</sup>, A.M.K. HANSEN<sup>1</sup>, K. WANG<sup>2</sup>,  
T. HOFFMANN<sup>2</sup>, M. BILDE<sup>1</sup> AND R.-J. HUANG<sup>3</sup>

<sup>1</sup>Department of Chemistry, Aarhus University, 8000 Aarhus C, Denmark

<sup>2</sup>Institute of Inorganic and Analytical Chemistry, Johannes Gutenberg-Universität Mainz, Germany

<sup>3</sup>Key Lab of Aerosol Chemistry & Physics, Institute of Earth Environment, Chinese Academy of Sciences, China

Keywords: organosulfates, secondary organic aerosols, molecular tracers.

Studies in China show that severe pollution events can be dominated by secondary aerosols (Huang et al., 2014). Organosulfates (OS) are a group of secondary compounds formed via heterogeneous reactions of their organic precursors with newly formed, acidic sulphate aerosols (Surratt et al., 2008; Riva et al., 2016). The presentation will provide an overview of current knowledge of sources and occurrence of organosulfates in the atmosphere and present specific results from a study in Xi'an, China. Xi'an has about 8.6 million inhabitants, and is situated in the central part of the country (34.23°N, 108.88°E).

Particles (PM<sub>2.5</sub>) were collected on quartz fibre filters using a high volume sampler. Particle filter samples were extracted and analyzed using an Ultra-High Performance Liquid Chromatograph coupled through an electrospray inlet to a quadrupole time-of-flight mass spectrometer (Hansen et al., 2014). Organosulfates were identified using their characteristic MS fragments and quantified using a set of commercial and synthesized standards.

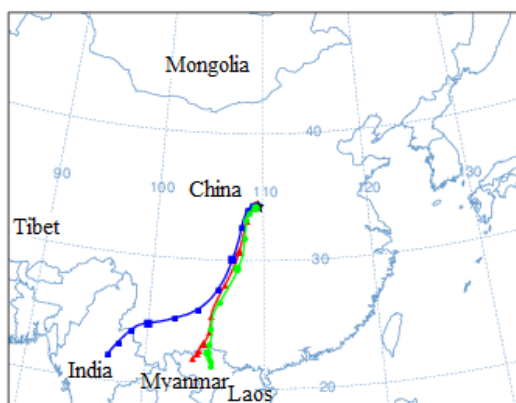


Figure 1. Typical air mass transport to Xi'an in summer campaign period (72h, calculated using HYSPLIT).

During summer, air masses were typically transported to Xi'an from forested, sub-/tropical regions south of the city (Fig. 1), while in winter air masses typically originated from arid, colder regions to the north. This change in transport patterns is clearly observed in the composition and levels of molecular tracers.

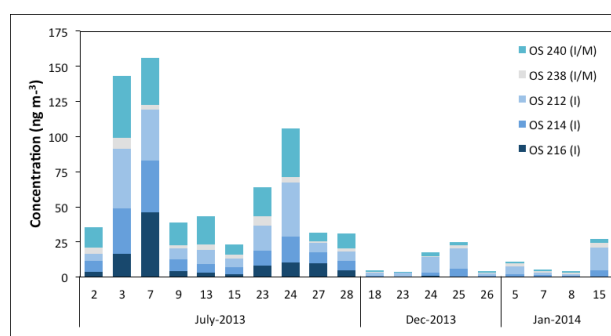


Figure 2. Estimated concentrations of biogenic organosulfates in Xi'an, China from either isoprene (I) or monoterpenes (M).

Levels of OS derived from isoprene and monoterpenes were much higher in summer than in winter samples (Fig. 2). Molecular tracers of biogenic secondary organic aerosols (BSOA) showed the same pattern, probably due to long-range transport of aerosols.

A large number of previously unidentified OS were observed at high levels during both summer and winter. In contrast, the concentration of organic carbon (OC) was much higher during winter ( $37 \pm 17 \mu\text{g m}^{-3}$ ) than in summer ( $6.1 \pm 2.5 \mu\text{g m}^{-3}$ ), implying that other components than organosulfates dominate OC during winter in Xi'an.

This work was supported by the Danish Agency for Science, Technology and Innovation. The authors gratefully acknowledge the NOAA Air Resources Laboratory for the provision of the HYSPLIT transport model (<http://www.ready.noaa.gov>).

Hansen, A.M.K. et al. (2014) *Atmos. Chem. Phys.* 14:7807–7823.

Huang, R.-J. et al. (2014) *Nature*, 514:218–222.

Riva, M. et al. (2016) *Environ. Sci. Technol.* 50:5580–5588

Surratt, J.D. et al. (2008) *J Phys. Chem. A* 112:8345–8378.

# GENERATING BIODIESEL AND FOSSIL DIESEL EXHAUST PARTICLES WITH VARIED PHYSICO-CHEMICAL PROPERTIES FOR TOXICOLOGICAL STUDIES

L. Gren<sup>1</sup>, V.B. Malmberg<sup>1</sup>, P. C. Shukla<sup>2</sup>, S. Shamun<sup>2</sup>, C. Isaxon<sup>1</sup>, PA. Clausen<sup>3</sup>, M. Tunér<sup>2</sup>, U. Vogel<sup>3</sup>, and J. Pagels<sup>1</sup>

<sup>1</sup> Division of Ergonomics and Aerosol Technology, Lund University, Box 118, SE-22100, Lund, Sweden

<sup>2</sup> Division of Combustion Engines, Lund University, Box 118, SE-22100, Lund, Sweden

<sup>3</sup> National Research Center for the Working Environment, Lersø Parkallé 105, DK-2100 Copenhagen, Denmark

Keywords: Diesel, Rapeseed methyl ester (RME), Hydrotreated vegetable oil (HVO), Exhaust gas recirculation (EGR), *in-vivo* toxicology

## Introduction

Diesel exhaust (DE) is classified as carcinogenic and is suspected to play an important role in the adverse effects of ambient PM in urban areas. Candidates for toxicologically relevant particle properties include the specific surface area and surface reactivity of the solid black carbon core, the liquid organic fraction including polycyclic aromatic hydrocarbons (PAHs), and transition metals.

The use of renewable fuels such as rapeseed methyl ester biodiesel (RME) and hydrotreated vegetable oil renewable diesel (HVO) in the commercial and private transport sectors is increasing. The fuels reduce net greenhouse gas and alter health relevant emissions compared to fossil diesel (Murtonen et al., 2009). The largest reduction of emitted PM is attributed to RME, however its oxygenated organic fraction has been linked to increased oxidative potential and higher *in-vitro* toxicity (Hedayat et al., 2016). The chemical composition of HVO fuel is more similar to fossil diesel, so far the knowledge of its exhaust emissions is limited.

We here describe an approach where the particle composition and properties can be varied over a wider range and in a more systematic way compared to previous studies while maintaining realistic engine operation conditions. Exhaust, from a modern heavy-duty diesel engine fueled by fossil diesel, 100% RME and 100% HVO biodiesel, was characterized and collected to be used in an *in-vivo* toxicological study.

## Method

A six cylinder heavy-duty diesel engine modified for a single cylinder operation was used for the experiment. The engine was run at a fixed engine operating load with varying exhaust gas circulation (EGR). The exhaust gas was sampled after a partial flow dilution tunnel. Exhaust particles were characterized using real-time aerosol mass spectrometry (AMS), a fast mobility particle analyzer (model DMS 500), aethalometer (model AE33), thermal optical analyser (OC/EC) and Transmission Electron Microscopy (TEM). Toxicological studies require large amount of PM (~30 mg). A High Volume Cascade Impactor (HVCI 900, BGI Inc.) followed by methanol extraction and a Versatile Aerosol Concentration Enrichment System (VACES) was used to collect the particles.

## Conclusion

EGR reduced the amount of O<sub>2</sub> and the temperature in the combustion cylinder (a common NO<sub>x</sub> reduction strategy). EGR also strongly affected PM emission levels and properties. PM with particle mass fractions ranged from: elemental carbon: 30-80%, organic carbon 20-70% and the PAH/org\* fraction: 0.002-0.080. The particle size varied with fuel type from 79 (RME) – 102 (diesel) nm. Low EGR affected the nucleation mode and CMD.

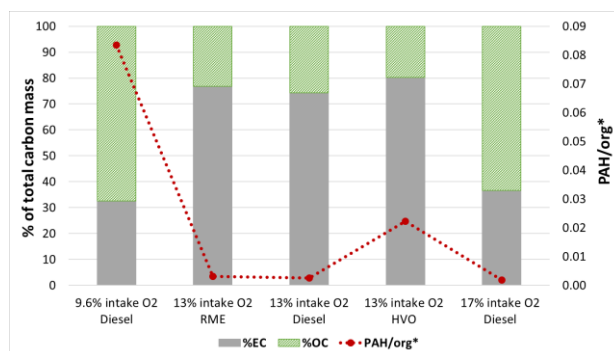


Figure 1. Results of OC/EC analysis (bars) and PAH/org\* fraction acquired with AMS of the diesel and renewable diesel exhaust particles.

The collected particles were successfully extracted from the HVCI filters with an extraction efficiency of 85-105%. Currently, a pulmonary exposure study of these particles in mice is in preparation, together with detailed characterization of collected nanomaterial including BET surface area analysis, Reactive Oxygen Species assays and a thorough TEM analysis of the soot micro- and nanostructure. The aim of the *in-vivo* study is to identify relationships between particle physico-chemical properties and biomarkers of genotoxicity, inflammation and cardiovascular effects.

This work has been supported by AFA Insurance and The Swedish Research Councils FORMAS and VR.

Hedayat, F., Stevanovic, S., Milic, A., Miljevic, B., Nabi, M. N., Zare, A. ... & Ristovski, Z. D. (2016). *Science of the Total Environment*, 545, 381-388.

Murtonen, T., Aakko-Saksa, P., Kuronen, M., Mikkonen, S., & Lehtoranta, K. (2009). *SAE International Journal of Fuels and Lubricants*, 2(2009-01-2693), 147-166

\*PAH mass is included in the total organic mass (org)

# NEW PARTICLE FORMATION, GROWTH AND SHRINKAGE AT A RURAL BACKGROUND SITE IN WESTERN SAUDI ARABIA

S. HAKALA<sup>1</sup>, P. PAASONEN<sup>1</sup>, V. VAKKARI<sup>2</sup>, H. LIHAVAINEN<sup>2</sup>, A. HYVÄRINEN<sup>2</sup>, K. NEITOLA<sup>2</sup>, J. KONTKANEN<sup>1</sup>, T. HUSSEIN<sup>1</sup>, M. KULMALA<sup>1</sup>, M. A. ALGHAMDI<sup>3</sup>

<sup>1</sup>University of Helsinki, INAR, Department of Physics, Finland

<sup>2</sup>Finnish Meteorological Institute, Finland

<sup>3</sup>Department of Environmental Sciences, Faculty of Meteorology, Environment and Arid Land Agriculture, King Abdulaziz University, Jeddah, Saudi Arabia

Keywords: aerosol particles, new particle formation, size distribution, aerosol shrinkage

We analyzed aerosol size distribution data measured at Hada Al Sham (21.802° North, 39.729° East, 254 m a.s.l.) to determine the general characteristics of new particle formation (NPF) at this rural background site in Western Saudi Arabia. The size distribution data was measured using a twin Differential Mobility Particle Sizer (DMPS). NPF event classification was done following the methods described by Dal Maso et al. (2005) and extended to separate the days that showed a clear shrinking mode during the later stages of the event. Particle growth and formation rates were determined for the NPF days as described by Kulmala et al. (2012) and air mass history was studied using a Lagrangian particle dispersion model FLEXPART version 9.02 (Stohl et al., 2005). European Centre for Medium-Range Weather Forecasts (ECMWF) operational forecast was used as input data to FLEXPART.

The NPF event classification (Figure 1) shows that NPF events are observed very frequently (73 % of all classified days) throughout the year, and that clear non-event days are extremely rare. Furthermore, approximately three quarters of the NPF days show shrinking, with a generally higher fraction of shrinking events occurring during the summer months.

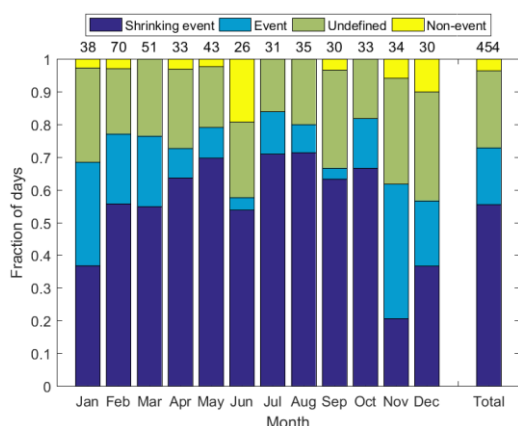


Figure 1: Breakdown of the NPF event classification separately for each month and all of the 454 classified days combined. The numbers above the bars indicate the number of analyzed days.

The high frequency of NPF days is likely connected to the typically prevailing clear-sky conditions and high global radiation, in combination with sufficient amounts of precursor vapors for particle

nucleation and growth. NPF events seem to be related to anthropogenic emissions from the coastal urban and industrial areas, located to the west, as no NPF-events are observed in easterly air masses. The median formation and growth rates for the event days were 8.7 #/cm<sup>3</sup> and 7.4 nm/h, respectively, both showing slightly higher values during the summer.

To the author's knowledge, the observed frequency of shrinkage events in Hada Al Sham is far greater than at other measurement sites reported in the literature, which indicates highly favorable circumstances for such events. The shrinkage might, therefore, be caused by evaporation of semivolatile species under high ambient temperature and wind induced mixing, which are both very frequent phenomena at the site. This is further supported by the higher fraction of shrinkage events observed during the warmer and windier summer months, as well as by the typical onset time of shrinkage around the temperature and wind maxima.

However, no clear differences are found in the temperatures and atmospheric mixing states when comparing the shrinking and non-shrinking NPF days. This leads us to discuss the possibility of an apparent shrinkage process, where the decreasing mode mean diameter would be caused by continuous observations of particles that have grown less during their lifetime. Air mass back trajectories show that the particles observed during the shrinkage are likely formed outside the region of strong anthropogenic emissions, which could possibly explain their slower growth.

This study was funded by the Deanship of Scientific Research (DSR), King Abdulaziz University (KAU), Jeddah, under Grant no. (I-122-430), and the Academy of Finland Centre of Excellence program (grant no 307331). The authors acknowledge with thanks DSR and KAU for technical and financial support.

Dal Maso, M. et al. (2005). *Bor. Environ. Res.*, 10:323-336.

Kulmala, M. et al. (2012). *Nature Protocols*, 7:1651-1667.

Stohl, A. et al. (2005). *Atmos. Chem. Phys.*, 5:2461-2474

# ELEMENTAL ANALYSIS OF AIRBORNE SUPERMICRON PARTICLES

P. HEIKKILÄ<sup>1</sup>, J. ROSSI<sup>2</sup>, A. JÄRVINEN<sup>1</sup>, A. ROSTEDT<sup>1</sup>, S. SAARI<sup>1</sup>, J. TOIVONEN<sup>2</sup>, J. KESKINEN<sup>1</sup>

<sup>1</sup> Laboratory of Physics, Tampere University of Technology, Finland

<sup>2</sup> Laboratory of Photonics, Tampere University of Technology, Finland

Keywords: elemental analysis, electrodynamic balance, LIBS

Supermicron airborne particles play a role in many atmospheric and human health-related processes. In the atmosphere they can act as ice nuclei, which can have an important effect on rain formation (Huffman et al., 2013). As it comes to human health, supermicron bacteria, fungal spores and e.g. emission particulate containing transition metals can be harmful to human health. On-site study of the elemental content of these particles can open new opportunities for the better understanding of the origin of the particles, especially in the ongoing field of ice nucleation study. It can also be useful to have on-site monitoring of potential hazardous components particles may be carrying.

We demonstrate a way of charging and capturing the particle electrodynamically into such a small volume that a high-energetic laser beam (i.e. a LIBS = *laser induced breakdown spectroscopy* pulse) can be focused on the particle, ionizing its atoms, thus forming plasma from the particle. When the electrons from the ionized atoms of the particle return to their atomic orbits and to the lower energy states, an emission spectrum is emitted and collected, from which an elemental analysis can be accomplished. This has been done before to charged water droplet residual particles by e.g. Järvinen et al. (2014). However, it is beneficial to trap the particles straight from the ambient air, to analyze e.g. atmospheric particles online, and to avoid unwanted water-related contaminants.

An electrodynamic balance chamber with a similar design as reported in Heinisch et al. (2009) was used as the levitation chamber, and a lens-focused 355 nm LIBS pulse with an energy of 5 mJ was used to ionize the particle. The aerosol was introduced to the chamber from an inlet from the side of the chamber wall, and directed out from the middle of the upper electrode, therefore creating a path of aerosol that enables the presence of a charged particle in the range of the electrodynamic trap after turning off the aerosol flow. The spatial location of the particle was monitored by CMOS camera and the pulse laser was triggered manually, when the particle had been driven to the focus spot.

A new aerosol charger was designed and built to maximise the charging state of the particles, as it affects the force acting on the particle in the electric field, due to Lorentz force

$$\mathbf{F} = q\mathbf{E} + q\mathbf{v} \times \mathbf{B} = q\mathbf{E}, \quad (1)$$

where  $\mathbf{F}$  is the force experienced by the particle,  $\mathbf{E}$  is the electric field produced by the electrodes,  $q$  is the charge

of the particle and  $\mathbf{B}(= 0)$  is the magnetic field in the presence of the particle.

Results showed that the particle can be effectively trapped and analyzed using a combination of electrodynamic balance and laser-induced breakdown spectroscopy straight from the aerosol phase. A variation of mineral dusts and inkjet-generated salt and mineral particles were analyzed. The spectrum from the measured mineral dusts showed that when no water was involved in the generation of the aerosol, the presence of calcium-related emission peaks vanished or significantly decreased in intensity, as presented in figure 1.

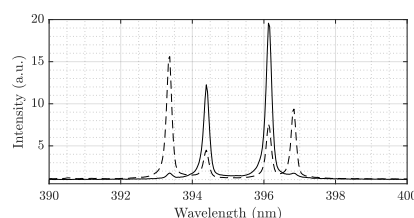


Figure 1: A difference in the emission spectrum between analyzing airborne dust particles (solid line) and the same particles generated from water (dashed line). The inner peaks at 394.4 nm and 396.2 nm represent aluminium, as the outer ones represent calcium.

The next steps for the online elemental analysis of aerosol particles will be developing a way to go sub-micron scale in the particle size, and to add more automation and mobility to the measurement. This way the equipment could be used effectively to analyze the elemental composition of aerosols in several in situ destinations, such as traffic, urban aerosol, mining sites, combustion or natural sources, and therefore add to the understanding of the formation, origin or the potential health effects of different aerosol types.

Järvinen, S. T., Saari, S., Keskinen, J., and Toivonen, J. (2014). *Spectrochim. Acta B*, 116:218–228.

Huffman, J. A., Prenni, A. J., DeMott, P. J., Pöhlker, C., Mason, R. H., Robinson, N. H., ... and Gochis, D. J. (2013). *Atmospheric Chem. Phys.*, 13(13):6151–6164.

Heinisch, C., Wills, J. B., Reid, J. P., Tschudi, T. and Tropea, C. (2009). *Phys. Chem. Chem. Phys.*, 11(42), 9720–9728.

# CHARACTERISTICS AND SOURCES OF BLACK CARBON IN THE HELSINKI METROPOLITAN AREA, FINLAND

A. HELIN<sup>1</sup>, J.V. NIEMI<sup>2</sup>, A. VIRKKULA<sup>1</sup>, L. PIRJOLA<sup>3</sup>, K. TEINILÄ<sup>1</sup>, J. BACKMAN<sup>1</sup>, M. AURELA<sup>1</sup>, S. SAARIKOSKI<sup>1</sup>, T. RÖNKKÖ<sup>4</sup>, E. ASMI<sup>1</sup> and H. TIMONEN<sup>1</sup>

<sup>1</sup> Atmospheric Composition Research, Finnish Meteorological Institute, Helsinki, Finland

<sup>2</sup> Helsinki Region Environmental Services Authority, Helsinki, Finland

<sup>3</sup> Department of Technology, Metropolia University of Applied Sciences, Helsinki, Finland

<sup>4</sup> Aerosol Physics, Faculty of Natural Sciences, Tampere University of Technology, Tampere, Finland

Keywords: aethalometer, black carbon, fossil fuel, biomass burning

Black carbon is emitted from the incomplete combustion processes of carbonaceous material and it possess various air quality, climate and health impacts. Optical measurement techniques can be used to quantify the concentrations of equivalent BC (eBC) in the ambient air. A source apportionment method known as the Aethalometer model (Sandradewi *et al.*, 2008) can be used to further distinguish eBC from fossil fuel (BC<sub>FF</sub>) and wood burning (BC<sub>WB</sub>) sources. This model is based on assumption that the emissions from fossil fuel and wood burning sources follow spectral light absorption dependency of  $\lambda^{-1}$  and  $\lambda^{-2}$ , respectively. However, the Aethalometer model still requires careful assessment of the site specific absorption Ångström exponent ( $\alpha$ ) values to be used for fossil fuel ( $\alpha_{FF}$ ) and wood burning ( $\alpha_{WB}$ ).

In this study, eBC, BC<sub>FF</sub> and BC<sub>WB</sub> concentrations were measured during a long-term campaign at three sites in the Helsinki metropolitan area, Finland. One sampling site was located in an urban street canyon (SC) and two of the sites were located in suburban detached house areas (DH1 and DH2)

A dual-spot aethalometer (AE33, Magee Scientific) was used to measure aerosol light absorption at seven different wavelengths (370-950 nm). The Aethalometer model was used to estimate the biomass burning percentage (BB%) based on the wavelengths 470 nm and 950 nm. The eBC, BC<sub>FF</sub> and BC<sub>WB</sub> mass concentrations were reported based on the absorption measurements at wavelength 880 nm. The  $\alpha_{FF}$  and  $\alpha_{WB}$  values used in the eBC source apportionment were determined by utilizing concurrent levoglucosan measurements. The optimized  $\alpha$  values for different sites were as follows:  $\alpha_{FF}$ =1.10 and  $\alpha_{WB}$ =1.6 at SC, and  $\alpha_{FF}$ =0.95 and  $\alpha_{WB}$ =1.6 at both DH sites.

The sampling period at SC was from October 2015 to May 2017, at DH1 from December 2015 to December 2016 and at DH2 from January 2017 to May 2017.

The average mass concentrations measured at each site are summarized in Table 1. Overall, the highest eBC levels were observed at the urban SC. Only during cold periods, the contribution of BC<sub>WB</sub> increased at the suburban DH sites, and the total eBC concentrations

were similar to those observed at the SC site. The eBC concentration levels at the SC were dominated by BC<sub>FF</sub> from the nearby vehicular traffic emissions. The contribution of wood burning (BB%) was larger at the DH sites than at the SC site (Table 1).

Table 1. Average ( $\pm$  standard deviation) concentrations ( $\mu\text{g}/\text{m}^3$ ) measured at the different sites.

Parameter	Urban	Suburban	Suburban
	SC	DH1	DH2
eBC	1.7 $\pm$ 1.5	0.9 $\pm$ 1.5	1.0 $\pm$ 2.1
BC <sub>FF</sub>	1.6 $\pm$ 1.5	0.5 $\pm$ 0.8	0.5 $\pm$ 0.9
BC <sub>WB</sub>	0.1 $\pm$ 0.2	0.4 $\pm$ 0.8	0.5 $\pm$ 1.3
BB (%)	15 $\pm$ 14	41 $\pm$ 14	46 $\pm$ 15

Distinct diurnal cycles of eBC were observed between the different sites (Fig. 1). At the SC, the eBC diurnal cycle showed the characteristic morning and afternoon traffic rush hour peaks. At the DH1, the eBC levels increased towards the evening due to residential wood combustion. This increase towards the evening was especially pronounced during the winter season.

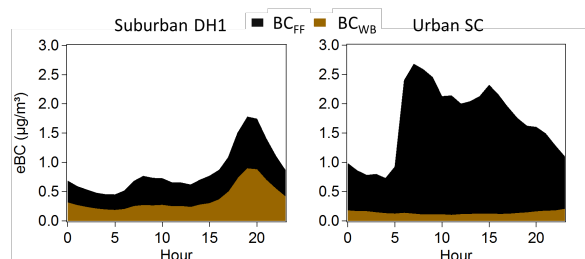


Figure 1. Diurnal cycles of BC<sub>FF</sub> and BC<sub>WB</sub> at the DH1 and SC sites during 2016.

As a summary, eBC was observed to be closely tied to the characteristics of the measurement site, meteorological conditions and the time of the day.

This study has been funded by TEKES funded INKA-ILMA/EAKR project (project no. 4588/31/2015) and project HAQT (AIKO014).

Sandradewi, J. *et al.*, (2008). *Environ. Sci. Technol.*, 42, 3316-3323.

# SESQUITERPENES ARE IMPORTANT SECONDARY ORGANIC AEROSOL PRECURSORS IN BOREAL FOREST

H. HELLÉN, A.P. PRAPLAN, T. TYKKÄ, S. SCHALLHART and H. HAKOLA

Finnish Meteorological Institute, Helsinki, Finland

Keywords: Monoterpenes, sesquiterpenes, VOCs, reactivity, SOA

Isoprene, monoterpenes (MTs) and sesquiterpenes (SQTs) are the major biogenic volatile organic compounds (BVOCs) emitted from the boreal forest. They are known to influence particle formation and growth, chemical communication by plants and insects, and the oxidation capacity of air. Other VOCs emitted from the vegetation include e.g. aldehydes, alcohols and volatile organic acids (VOAs), but their emissions are less studied and they are also produced in the air from the reactions of other VOCs.

In this study ambient air measurements of individual BVOCs and oxygenated VOCs (OVOCs) were conducted in Apr–Nov 2016 in a boreal forest at SMEAR II site in Hyytiälä using in situ gas chromatograph – mass spectrometers (GC-MSs). Ambient mixing ratios were used to estimate the importance of different compounds and compound groups regarding local atmospheric chemistry and secondary organic aerosol (SOA) production. Thus the reactivity with main oxidants (OH, NO<sub>3</sub> and O<sub>3</sub>) and production rates of oxidation products (OxPR) were calculated.

Of the studied VOCs, VOAs were found to have the highest mixing ratios mainly due to their low reactivity (Table 1). Of the terpenoids, MTs had highest mixing ratios at the site, but also 7 different SQTs were detected. Monthly and daily mean mixing ratios of most terpenoids, aldehydes and VOAs were found to be highly dependent on the temperature. Highest exponential temperature dependence ( $\beta=0.37$  (C<sup>-1</sup>)) and correlation ( $R^2=0.96$ ) of daily means was found for a SQT ( $\beta$ -caryophyllene) in summer.

pptv	Apr	May	Jun	Jul	Aug	Sep
Isop	0.4	11	13	50	15	6
MT	20	220	270	690	320	150
SQT	0.1	3	4	30	6	4
ALD	16	40	30	50	40	10
ALC	1	1	16	12	0.2	6
VOA	1280	1000	2220	1650	680	1620
AHC	80	50	40	50	60	50

ALD=C<sub>5</sub>-C<sub>10</sub> unbranched aldehydes, ALC=C<sub>5</sub>-C<sub>8</sub> unbranched alcohols, VOA=C<sub>2</sub>-C<sub>7</sub> unbranched volatile organic acid, AHC=aromatic hydrocarbons

Table 1: Ambient air mixing ratios (pptv) of different VOC groups at SMEAR II in 2016.

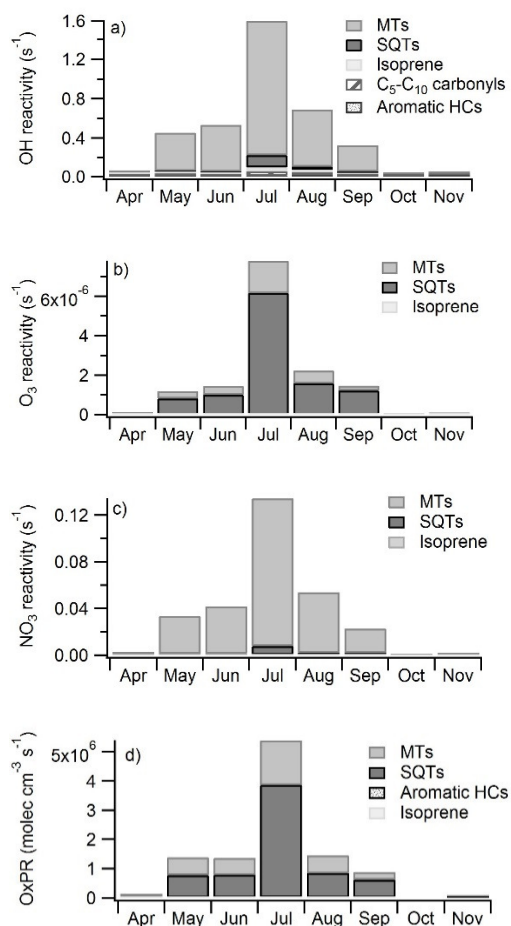


Figure 1: a) OH reactivity, b) O<sub>3</sub> reactivity and c) NO<sub>3</sub> reactivity and d) production rates of oxidation products (OxPR) of different VOC groups at SMEAR II during different months in 2016.

MTs dominated OH and NO<sub>3</sub> radical chemistry of VOCs (Figure 1), but SQTs had a major impact on ozone chemistry, even though mixing ratios of SQT were 30 times lower than MT mixing ratios (Table 1). Both MT and SQT oxidation was dominated by the ozone especially during summer and therefore SQTs were the key compounds for the formation of oxidation products at the site (Figure 1d). Other VOC groups had very minor contribution. Since products of SQTs are less volatile and SQTs have higher SOA yields than MTs or other studied VOCs, results clearly indicate the crucial role of SQTs for the local SOA production.

# AMINE MEASUREMENTS IN BOREAL FOREST AIR

M. HEMMILÄ<sup>1</sup>, H. HELLÉN<sup>1</sup>, A. VIRKKULA<sup>1,2</sup>, U. MAKKONEN<sup>1</sup>, A. P. PRAPLAN<sup>1</sup>, J. KONTKANEN<sup>2</sup>, L. AHONEN<sup>2</sup>, M. KULMALA<sup>2</sup> and H. HAKOLA<sup>1</sup>

<sup>1</sup>Finnish Meteorological Institute, Helsinki, Finland

<sup>2</sup>Institute for Atmospheric and Earth System Research/Physics, Faculty of Science, University of Helsinki, Helsinki, Finland

Keywords: Amines, Ammonia, Ammonium, MARGA-MS

## Introduction

Amines are gaseous bases, whose general formula is  $\text{RNH}_2$ ,  $\text{R}_2\text{NH}$  or  $\text{R}_3\text{N}$ . Models have shown that they could affect aerosol particle formation with sulfuric acid (Kurtén et al. 2008). Amines also affect hydroxyl radical (OH) reactivity and via that to the atmospheric chemistry (Hellén et al. 2014, Kieloaho et al. 2013).

## Method

Measurements were made at SMEAR II station (Hari and Kulmala, 2005) at Hyytiälä, Southern Finland (61°510'N, 24°170'E, 180 m a.s.l.) The measurements cover seven months, from March to May, July to August and November to December 2015. For sampling and measuring we developed a new method, MARGA-MS. MARGA (instrument for Measuring AeRosols and Gases in Ambient air, ten Brink et al., 2007) is an on-line ion chromatograph (IC) connected to a sampling system (sampling flow 1 m<sup>3</sup>/h). MARGA was coupled to an electrospray ionization quadrupole mass spectrometer (MS) to improve sensitivity of amine measurements. This new set-up enabled amine concentration measurements in ambient air both in aerosol- and gas-phases with a time resolution of only 1 hour. With MARGA-MS we analysed 7 different amines: monomethylamine (MMA), dimethylamine (DMA), trimethylamine (TMA), ethylamine (EA), diethylamine (DEA), propylamine (PA) and butylamine (BA). We also measured ammonia ( $\text{NH}_3$ , gas-phase) and ammonium ( $\text{NH}_4^+$ , aerosol-phase) concentrations at the same time with MARGA.

## Results

In spring we measured high concentrations of aerosol-phase MMA but when the days got warmer the concentrations decreased. In March and April the highest concentrations of MMA were measured during the warmest nights (max. 48 ng/m<sup>3</sup>). This indicates that melting snow or ground could be a source of MMA. In spring most of the MMA was in aerosol-phase, only less than 20 % was in gas-phase. The partitioning became more even as summer proceeded.  $\text{NH}_4^+$ -concentrations also had their maxima (1.5 μg/m<sup>3</sup>) in March and concentrations were decreasing in summer. Then also the gas- and aerosol-phase portions were leveling off.

DMA and TMA had summer maxima indicating biogenic sources. The highest concentrations of these compounds were measured in July. For DMA a diurnal variation was observed in August with a daytime maximum. Also isoprene, which has a light dependent source, has daytime maximum. That could indicate that also DMA have a light dependent source.

EA concentrations were low throughout the measurements, but showed a clear diurnal variation in July with a maximum at night. Monoterpene concentrations were measured simultaneously at the same site and they correlated well with EA concentrations. This could indicate that EA has a biogenic source.

Other amines than MMA, DMA, TMA and EA were most of the time under the detection limit. Ammonium had a clearer diurnal cycle in the spring and ammonia in the summer.

## Conclusions

A new measuring method, MARGA-MS, was developed. With it, we measured concentration of 7 different amines and ammonia in aerosol- and gas-phase with 1-hour time resolution. The amines turned out not to be a homogeneous group of compounds; different amines are likely to have different sources. MMA concentrations were highest in the spring and DMA, TMA and EA concentrations in the summer. EA concentrations correlated with monoterpene concentrations indicating biogenic source. Other measured amines were under the detection limit most of the time. Measured ammonium concentrations were higher in the spring and ammonia concentrations in the summer.

- Hari, P. & Kulmala, M. (2005). *Boreal Environ. Res.*, 10, 315-322
- Hellén, H, Kieloaho, A.-J. & Hakola, H. (2014). *Atmos. Environ.*, 94, 192-197
- Kieloaho, A.-J., Hellén, H., Hakola, H., Manninen, H.E., Nieminen, T., Kulmala, M. and Pihlatie, M. (2013). *Atmos. Environ.*, 80, 369-377
- Kurtén, T., Loukonen, V., Vehkamäki, H. & Kulmala, M. (2008) *Atmos. Chem. Phys.*, 8, 4095-4103.
- ten Brink, H. M., Otjes, R., Jongejan, P. & Slanina, J. (2007). *Atmos. Environ.*, 41, 2768-2779



# ESTIMATION METHOD OF PARTICLE SIZE DISTRIBUTION (PSD) OF RADIOACTIVE AEROSOLS BY USING INERTIAL SEPARATORS

Y. N. Husein <sup>1</sup>, D. A. Pripachkin <sup>1</sup>, A. K. Budyka <sup>1</sup>.

<sup>1</sup>Nat. Res. Nucl. University MEPHI, Moscow, 115522, Russia

Keywords: radioactive aerosol, inertial separator, deposition efficiency, aerodynamic diameter.

This paper introduces a method for estimating the particle size distribution (PSD) of radioactive aerosols by minimizing the error function, using single-cascade inertial separator by separating the spectrum of aerosol particles into fractions, and the experiment established efficiency dependency of particle deposition with the aerodynamic diameter.

An impactor was used as a single-cascade inertial separator, developed in State Research Center – Burnazyan Federal Medical Biophysical Center.

Estimation method of AMAD and geometric standard deviation (GSD) for dispersed composition of radioactive aerosols – using single-cascade has the following steps: first step is sampling aerosols on filter and measuring the activity of the particles deposited on the filter; the second one is pumping aerosol at a fixed linear velocity through a single-cascade filter for the same period of time, and also measured the activity of the particles deposited on the filter. The last step is repeating the second again, but with a different linear velocity.

A method of evaluating particle size distribution through partitioning the original spectrum of aerosol particles into fractions was proposed in the review of Fuchs (1978).

$$\eta_i^T(\mu, \sigma) = \int_0^{\infty} E_i(x) \cdot f(x, \mu, \sigma) dx, \quad i = 1..N$$

Where:  $E_i(x)$  – deposition efficiency of particles with an aerodynamic diameter of  $x$  at a fixed linear speed;  $f(x, \mu, \sigma)$  is the density distribution of aerosol particles from original spectrum. By dividing the spectrum into three parts  $\eta_i$  and comparing the calculated values  $\eta_i$  and theoretical  $\eta_i^T$  we can find the residual function  $Q(\mu, \sigma)$ , Cheng and Yeh (1980).

$$Q(\mu, \sigma) = \sqrt{(\eta_1 - \eta_1^T)^2 + (\eta_2 - \eta_2^T)^2} \quad (1)$$

The values of  $\mu$ – (AMAD) and  $\sigma$ – (GSD), for which the function (1) has a minimum value are AMAD and GSD of original spectrum. This approach has been implemented in the method of multilayer filters, which is widely used in Russia, Budyka *et al* (1993). In our case, the considered approach may be applied for assessing the AMAD and GSD.

In order to determine  $E_i(x)$  – deposition efficiency of particles studied have been carried out to spectrum of known aerosol particles which obtained by simulator source of aerosols in working area, typical of the nuclear industry. The study was performed on non-radioactive aerosols NaCl.

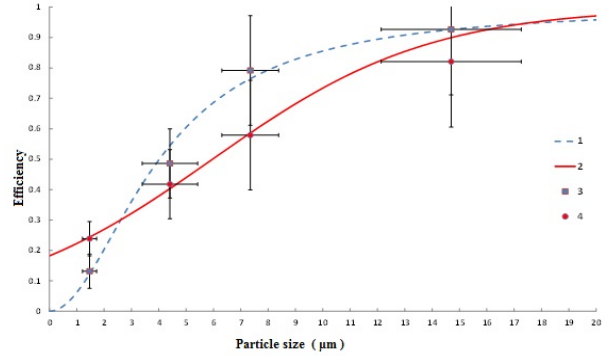


Fig. 1 dependence of deposition efficiency  $E(x)$  from the particle size (aerodynamic diameter). 1, 2 – approximation 3, 4 experimental data at a flow rate 50 and 20 l / min, respectively.

By knowing the dependence of  $E(x)$  with aerodynamic particle diameter, we can find  $\eta_i^T(\mu, \sigma)$ . Then, the obtained expression  $\eta_i^T(\mu, \sigma)$  puts in (1) and defines both of  $\mu$  and  $\sigma$  corresponding to the minimum of the function  $Q(\mu, \sigma)$ . Determining the minimum of the function  $Q(\mu, \sigma)$  analytically is impossible; therefore, to find it, we have to use numerical methods.

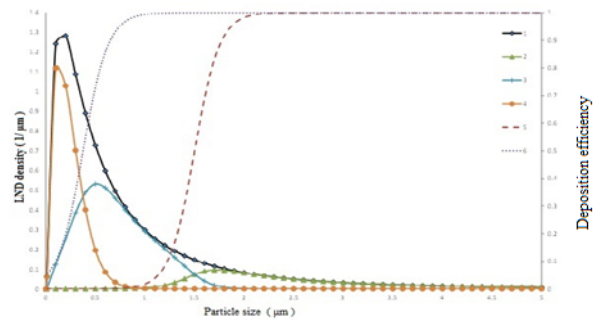


Fig.2 splitting the original spectrum LND in parts through efficiency curves. 1 - Original spectrum; 2, 3, 4 – spectra of the particles after application of the separator; 5, 6 - separation efficiency.

Fuchs, N.A. (1978). *Aerosol Impactors: A Review in Fundamentals of Aerosol Science*, ed. Wiley & Sons, New York.

Cheng, Y.S. and Yeh, H.C. (1980) *Theory of a screen-type diffusion battery*, J. Aerosol Sci.

Budyka, A.K., Ogorodnikov B.I. and Skitovich V.I. (1993) *Filter pack technique for determination of aerosol particle sizes*, J. Aerosol Sci.

# EVALUATION OF SPECTROMETRIC AND RADIOMETRIC CHARACTERISTICS OF PLUTONIUM ALPHA-EMITTING RADIONUCLIDES AND THEIR INFLUENCE ON THE VALUE OF AMAD

Y. N. HUSEIN<sup>1</sup>, D. A. PRIPACHKIN<sup>1</sup>, A. K. BUDYKA<sup>1</sup>

<sup>1</sup>Nat. Res. Nucl. University MEPhI, Moscow, Russia

Keywords: radioactive aerosol, inertial separator, aerodynamic diameter.

This article is proposed to consider using a new experimental stand for determining the volumetric activity and AMAD of  $\alpha$ -particles. It is proposed to evaluate the spectrometric and radiometric characteristics of the  $\alpha$ -emitting radionuclides plutonium and to determine their influence on the value of AMAD.

To compare the calculated values of the activity of plutonium isotopes in a special aerosol sources, obtained using the experimental stand and devices such as MKC-01A, UMF-2000. To estimate the relative error in the determination of AMAD using experimental stand.

In this study, an experimental stand was used consisting of: separation part, detection chamber, filter, rotameter and pump connected by a piping system. Alpha activity was determined by a spectrometer MKC-01A «MULITIRAD-AS» and radiometer UMF-2000.

The experimental stand was used to study the spectrum of  $\alpha$ -particles, determine the efficiency of registration, and calculate the activity for a source (1П9-type) based on  $^{239}\text{Pu}$  with an activity of 80.7 Bq and special aerosol sources for  $\alpha$ -radiation (CAИ) based on  $^{239}\text{Pu}$  with activity of 119 and 112 Bq.

By the efficiency of registration  $\alpha$ -particle, the results of the studies were compared with measurements of the same sources on the MKC-01A  $\alpha$ -spectrometer at the A.I. Burnazyan (Federal Medical and Biophysical Center-Russia) and the radiometer UMF-2000 in national research nuclear University MEPhI. According to the study, the spectrums of  $\alpha$ -radiation were compared only with them, which have been got by MKS-01A.

It is shown that the use of an experimental stand for sampling radioactive aerosols and subsequently evaluate the spectrometric and radiometric characteristics of samples using a silicon detector makes it possible to estimate the total activity of the  $\alpha$ -emitting radionuclides  $^{239}\text{Pu}$  and  $^{238}\text{Pu}$  in a source (1П9-type) and (CAИ) sources with a relative error about 5%.

For the considered combination of radionuclides, the relative error of the activity did not exceed 20%. In this case, the relative error in estimating the AMAD value of aerosols containing  $^{239}\text{Pu}$  by means of the method for determining the dispersed composition of radioactive aerosols based on

inertial separators [1] did not exceed 25%, which, in accordance with regulatory requirements [2], is acceptable.

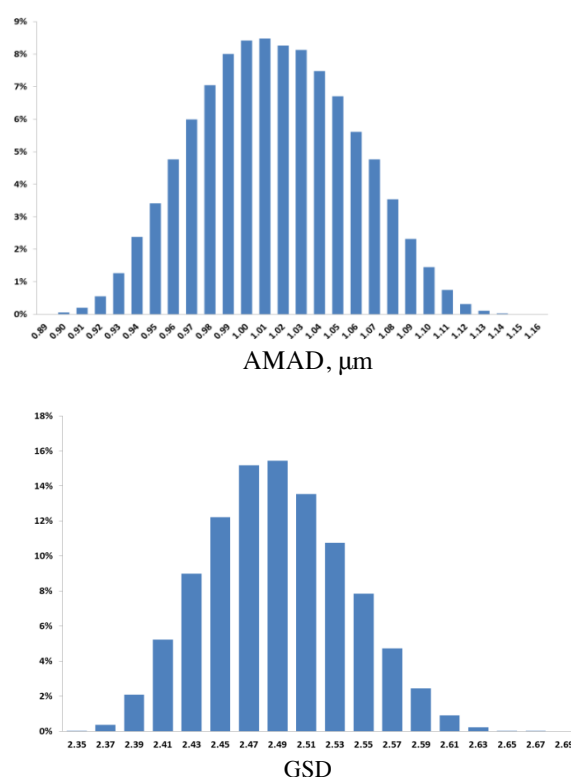


Figure 1 Distribution of AMAD and GSD with a random change in the activity of  $^{239}\text{Pu}$  by 20%.

Husein Y. N., Pripachkin D. A., Budyka A. K. (2016). *Determination Method of aerosol radioactive particles size based on used the inertial separators. J. ANRI, № 3(86), pages 57-63.*  
Budyka A. K., Fedorov G. A. (1987). *Determination of the dispersed composition of radioactive aerosols in technological systems of research reactors. Isotopes in the USSR. M: Energoatomizdat, 1 (72), page 113.*

# COMPUTATIONAL COMPARISON OF DIFFERENT REAGENT IONS IN THE CHEMICAL IONIZATION OF OXIDIZED MULTIFUNCTIONAL COMPOUNDS

N. HYTTINEN<sup>1</sup>, R.V. OTKJÆR<sup>2</sup>, S. IYER<sup>1</sup>, H.G. KJAERGAARD<sup>2</sup>, M.P. RISSANEN<sup>3</sup>, P.O. WENNBORG<sup>4</sup>,  
and T. KURTÉN<sup>1</sup>

<sup>1</sup> Department of Chemistry and Institute for Atmospheric and Earth System Research, Faculty of Science, University of Helsinki, Finland

<sup>2</sup> Department of Chemistry, University of Copenhagen, Denmark

<sup>3</sup> Institute for Atmospheric and Earth System Research / Physics, Faculty of Science, University of Helsinki, Finland

<sup>4</sup> Division of Engineering and Applied Science and Division of Geological and Planetary Sciences, California Institute of Technology, United States

Keywords: CIMS, quantum chemistry, clustering

Chemical ionization, combined with a mass spectrometer (CIMS), is often used for the detection of neutral molecules in the gas phase. Using chemical ionization, the sensitivity of the measurements depends on how efficiently the reagent ion is able to charge the sample molecule. If the sample molecules are detected as ion-molecule clusters (Figure 1), the sensitivity also depends on the stability of the charged clusters (Iyer et al., 2016).

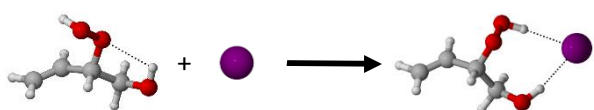


Figure 1: Cluster formation between  $C_4H_8O_3$  and  $I^-$ .

We compared the cluster stabilities of seven different reagent anions by calculating the formation free energies and enthalpies of the reagent ion – sample molecule clusters. As sample molecules we used several OH-initiated butadiene oxidation products that contain hydroxy and hydroperoxy functional groups. In addition, we investigated the effect of humidity on the detection efficiencies of the different reagent ions by calculating the formation free energies of hydrated reagent ions and ion-molecule clusters. All energies were calculated at DLPNO-CCSD(T) / def2-QZVPP //  $\omega$ B97X-D / aug-cc-pVTZ level of theory (aug-cc-pVTZ-PP basis set for  $Br^-$  and  $I^-$ ).

The calculated energies show a near linear correlation between the number of oxygen atoms in the sample molecule and the formation free energy of the ion-molecule cluster for each of the reagent ions (Figure 2). All of these sample molecules have 2, 3 or 4 hydrogen bond donating functional groups. However, in the lowest free energy conformers of the ion-molecule clusters, the reagent ions always form two hydrogen bonds with the sample molecule. This explains why the number of functional groups in the sample molecule is not in itself significant as long as the sample molecule has at least two hydrogen bond donating groups. (Hyttinen et al., 2018)

The formation free energies of the reagent ion hydrates indicate that a water molecule binds more strongly to a reagent ion monomer than to a reagent ion dimer. This could explain why reagent ions that are not able to form dimers generally have higher humidity dependence in CIMS measurements than for instance nitrate, which can form a strongly bound cluster with nitric acid. (Hyttinen et al., 2018)

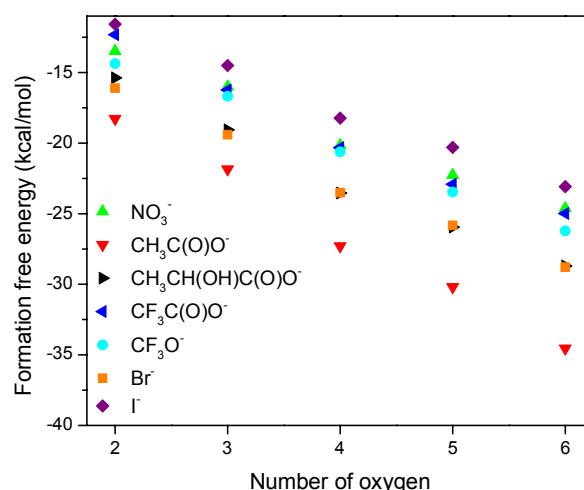


Figure 2: Formation free energies of ion-molecule clusters as a function of the number of oxygen atoms in the sample molecule.

## ACKNOWLEDGEMENTS

We thank the Academy of Finland for funding and CSC-IT Center for Science in Espoo, Finland, for computing time.

## REFERENCES

- Hyttinen, N., Otkjær, R. V., Iyer, S., Kjaergaard, H. G., Rissanen, M. P., Wennberg, P. O. and Kurtén, T. (2018). *J. Phys. Chem. A*, 122:269-279.
- Iyer, S., Lopez-Hilfiker, F., Lee, B. H., Thornton, J. A. and Kurtén, T. (2016). *J. Phys. Chem. A*, 120:576-587.

# STATISTICAL DIMENSION REDUCTION TECHNIQUES APPLIED TO MULTIVARIATE CAR EXHAUST EMISSION DATA

S. ISOKÄÄNTÄ<sup>1</sup>, E. KARI<sup>1</sup>, A. BUCHHOLZ<sup>1</sup>, A. VIRTANEN<sup>1</sup> and S. MIKKONEN<sup>1</sup>

<sup>1</sup>Department of Applied Physics, University of Eastern Finland, Finland

Keywords: dimension reduction, pmf, efa, pca, multivariate time series

Online measurements with mass spectrometers produce complex and large datasets. Statistical dimension reduction techniques are able to compress the information from complex composition data into a few latent factors, which can be interpreted further according to their properties. Currently the most exploited method in the analysis of AMS data is Positive Matrix Factorization (PMF) developed by Paatero and Tapper (1994). Recently, however, Wyche et al. (2015) applied Principal Component Analysis (PCA) to CIR-ToF-MS and cToF-AMS data from their chamber studies.

In this work, the statistical analysis was applied for the measurements where the effect of the exhaust from a modern gasoline car on the photochemistry of  $\alpha$ -pinene was studied in environmental chamber under atmospherically relevant conditions. The dimension reduction techniques were used to compress the information from the data measured with the PTR-ToF-MS (volatile organic compounds, VOCs) and with the ToF-CIMS (semi volatile organic compounds, SVOCs), because both instruments produced complex datasets during the measurement campaign.

Different variations of PMF, PCA and Exploratory Factor Analysis (EFA) were applied to the PTR-ToF-MS data. Factor time series presented in Fig. 1 are from the photo-oxidation experiments conducted with the car emission (without added  $\alpha$ -pinene). For EFA and PCA, the factors in concentration units were calculated by multiplying the original data with the loading values (i.e. the contribution of a variable to a factor) acquired from the EFA/PCA factorization. For both EFA and PCA, oblique rotations were used.

PMF differs conceptually from EFA and PCA as the errors for the data values must be known to proceed with PMF. The error matrix for PMF was calculated in two different ways. Constant errors were derived from the standard deviation of each ion trace in the measurement data, i.e. the error value for a specific ion does not change with time. Data dependent errors were calculated by first smoothing the time series of every variable with local regression and the error was determined as the difference between the smoothed time series and the original time series. Error calculated by this way varied between the time points.

The benefit of EFA and PCA compared to PMF is that these methods are generally better in find very small changes in the time series of the variables. This is because EFA/PCA use arbitrary units instead of the data units. This can be seen from Fig. 1, where EFA/PCA

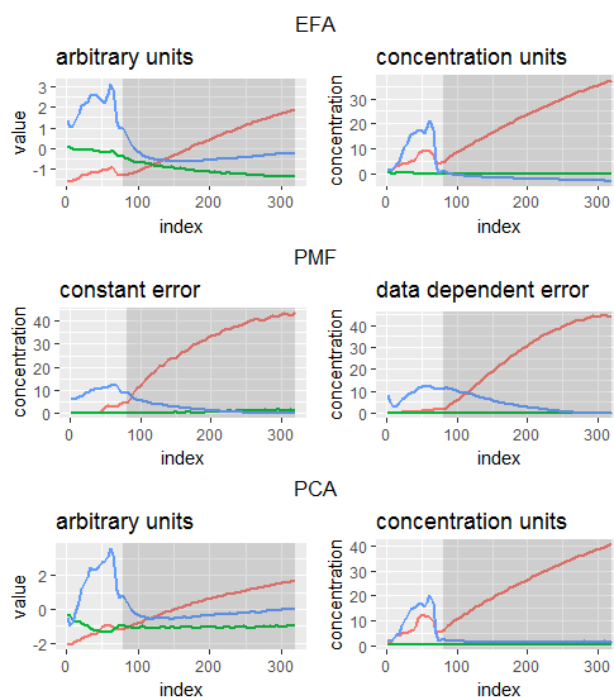


Figure 1: The factor time series from different methods. Index refers to time point. The shaded area indicates the period when UV-lights (centered at 340 nm) were on.

factors have generally more variation as the factors from PMF. Large differences in the order of magnitude between the variables may also cause problems for PMF whereas in EFA/PCA the values are scaled and only the relative changes are considered.

The factors were identified based on the results acquired from EFA as it created the most interpretable factors. The grouping of variables to distinct factors was also most explicit in EFA. The blue factor includes SOA precursors of the car exhaust, red factor includes most of the products formed during the photo-oxidation of the car exhaust and the green factor includes VOCs that mostly originated from the car exhaust but were not SOA precursors. It should be noted that the changes in the green factor are not visible in Fig. 1 when the concentration units are used, as the changes are very small.

Paatero, P. and Tapper, S. (1994). *Environmetrics*, 5, 111-126

Wyche et al. (2015). *Atmos. Chem. Phys.*, 15, 8077–8100

# COMPUTATIONAL INVESTIGATION OF RO<sub>2</sub> + HO<sub>x</sub> REACTIONS

S. IYER<sup>1,4</sup>, H. REIMAN<sup>1,4</sup>, K.H. MØLLER<sup>2</sup>, M.P. RISSANEN<sup>3,4</sup>, H. KJAERGAARD<sup>2</sup>, T. KURTÉN<sup>1,4</sup>

<sup>1</sup> Department of Chemistry, University of Helsinki, Finland

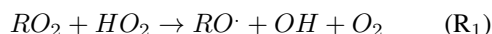
<sup>2</sup> Department of Chemistry, University of Copenhagen, Denmark

<sup>3</sup> Department of Physics, University of Helsinki, Finland

<sup>4</sup> Institute of Atmospheric and Earth System Research / Faculty of Science, University of Helsinki, Finland

Keywords: peroxy radicals, hydroperoxy radical, hydroxyl radical, monoterpene, oxidation

Peroxy radicals (RO<sub>2</sub>s) produced from the oxidation of biogenic volatile organic compounds (VOCs) are important in the formation of highly oxygenated multifunctional compounds (HOMs) (Mentel et al., 2015; Rissanen et al., 2014). These HOMs are known to play a critical role in the formation of secondary organic aerosols (SOAs) in the atmosphere. An important mechanism that affects the lifetimes of these RO<sub>2</sub>s (and subsequently their contribution to HOM formation) is their bimolecular reaction with the HO<sub>2</sub> and OH radicals. The reaction with HO<sub>2</sub> is mostly thought to be a radical sink process, producing closed-shell hydroperoxides (ROOH). However, the RO<sub>2</sub> + HO<sub>2</sub> reaction can also produce alkoxy radical products:



This channel can become relevant for large peroxy radicals formed from the oxidation of monoterpenes. Reactions that lead to the recycling of radical species in the atmosphere can potentially enhance HOM formation. Additionally, the bimolecular RO<sub>2</sub> + HO<sub>2</sub> reaction can also be a source of tropospheric ozone:



This is potentially an important ozone forming pathway in clean (low NO and NO<sub>2</sub>) environments. The reaction of peroxy radicals with the OH radical has recently garnered attention (Archibald et al., 2009; Assaf et al., 2016; Müller et al., 2016). This is potentially an important radical sink pathway in remote areas. In this work, the intermediates and products formed via RO<sub>2</sub> + OH reactions for 'R's with different atmospherically relevant functionalities were studied. The thermodynamic favorability of the alkoxy and ozone forming channels via RO<sub>2</sub> + HO<sub>2</sub> reaction for a set of RO<sub>2</sub>s generated by the oxidation of a set of monoterpenes was also computationally investigated. The monoterpenes considered in this study are  $\alpha$ -pinene,  $\beta$ -pinene, limonene, trans- $\beta$ -ocimene, and  $\Delta^3$ -carene (that account for more than 80% of the total monoterpene emission), and the oxidants considered are OH, NO<sub>3</sub>, and ozone. Calculated reaction free energies for the ozone oxidized peroxy radicals are shown in Table 1.

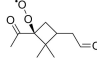
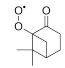
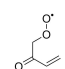
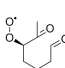
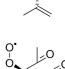
VOC	Isomer	$\Delta G(R_1)$	$\Delta G(R_2)$
$\alpha$ -pinene		-25.26	-8.34
$\beta$ -pinene		-25.40	-13.29
Trans- $\beta$ -ocimene		-5.54	-10.80
Limonene		-5.73	-10.59
$\Delta^3$ -carene		-4.77	-8.62

Table 1: Reaction Gibbs free energies ( $\Delta G$ ) of reactions R<sub>1</sub> and R<sub>2</sub> in kcal/mol calculated at the DLPNO-CCSD(T)/def2-QZVPP// $\omega$ b97xD/aug-cc-pVTZ level for the O<sub>3</sub> oxidized monoterpenes.

Mentel, T. F. et al. (2015). *Atmos. Chem. Phys.*,15:6745-6765.

Rissanen, M. P. et al. (2014). *J. Am. Chem. Soc.*, 136:15596-15606.

Archibald, A. T., et al. (2009). *Atmos. Sci. Let.*,10:102-108.

Assaf, E. et al. (2016). *J. Phys. Chem. A*, 120:8923-8932.

Müller, J-F., et al. (2016). *Nat. Comm.*, 7:13213.

# What can be learned about the lung from inhaled nanoparticles?

J. Jakobsson<sup>1</sup>, H. L. Aaltonen<sup>2</sup>, P. Wollmer<sup>2</sup> and J. Löndahl<sup>1</sup>

<sup>1</sup> Ergonomics and Aerosol Technology (EAT), Lund University, 221 00, Lund, Sweden

<sup>2</sup> Dept. of Translational Medicine, Lund University, 205 02, Malmö, Sweden

Keywords: Lung deposition, inhaled nanoparticles, in-vivo study, Airspace Dimension Assessment

## Introduction

Airspace Dimension Assessment (AiDA) is a technique to assess features of the distal lung by measuring the recovery of inhaled nanoparticles after varied residence times in the lungs (Löndahl et al. 2016, Jakobsson et al. 2016). It has previously been shown that airspace dimensions can be inferred by measuring the half-life time of inhaled nanoparticles (Löndahl et al. 2016). It has also been suggested that the estimated particle recovery for a zero second breath hold (the “intercept”) may provide information about the conducting airways.

The aim of this work was to investigate the characteristics and significance of the two AiDA parameters in healthy subjects.

## Method

For 19 healthy subjects we performed measurements of the recovery of inhaled nanoparticles for breath holding times between 5-20 s and volumetric sample depths between approx. 200-5000 mL. A simplified protocol, measuring recovery at a fixed (1300 mL) sample depth and breath-holding times between 5-10 s was performed by a larger group (N=668). The measurements were carried out with monodisperse 50 nm polystyrene nanospheres.

All subjects also underwent a detailed investigation of lung function, including measurement of vital capacity (VC), forced expiratory volume in 1 s (FEV<sub>1</sub>), lung diffusing capacity for carbon monoxide (D<sub>L,CO</sub>) and forced oscillation technique (FOT), which gives information about respiratory resistance (R<sub>5</sub>).

Typical characteristics of the derived airspace dimensions and the intercept (zero breath-hold recovery) were analysed in detail for the smaller group. Statistical analysis comparing the parameters to individual demographics and clinical lung function parameters was performed for the larger group to elucidate the parameters clinical significance.

## Results

The derived airspace dimensions captures the main features of the lung geometry from the onset of the anatomical dead-space to the distal lung. The dimension are root mean square (RMS) diameters of the airspaces and therefore larger than a normal arithmetic mean.

It was found that the derived airspace dimensions correlated mainly with lung function parameters known to be related to alveolar dimensions and diffusion properties (age, D<sub>L,CO</sub> and FEV<sub>1</sub>/VC) while

the intercept correlated mainly with parameters related to body (lung) size and respiratory flow characteristics (height, VC, FEV<sub>1</sub> and R<sub>5</sub>). Airspace dimensions and intercept did not correlate strongly (N.S. for N=19), (p=.02, r = -.09 for N=668).

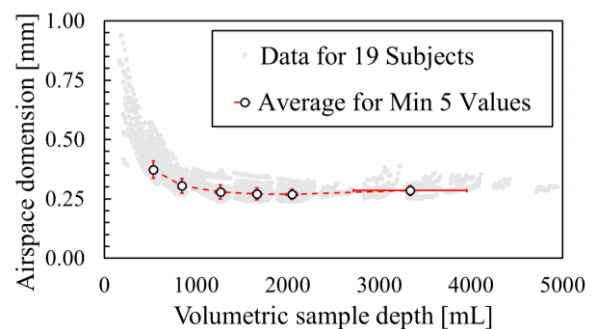


Figure 1. The AiDA airspace dimensions for 19 healthy subjects at various volumetric sample depths.

Table 1: Spearman's Rho and p for correlations between AiDA and clinical parameters, N=668.

	Intercept		Airspace dimension	
	P	Corr.	P	Corr.
Age	N.S.	-	< .001	-.14
D <sub>L,CO</sub>	N.S.	-	< .0001	.17
FEV <sub>1</sub> /VC	N.S.	-	< .0004	.14
Height	< 10 <sup>-8</sup>	.23	< .003	-.11
VC	< 10 <sup>-6</sup>	.19	< .03	-.01
FEV <sub>1</sub>	< 10 <sup>-11</sup>	.25	N.S.	-
FOT (R <sub>5</sub> )	< 10 <sup>-8</sup>	-.21	< .02	.08

## Conclusion

The results show that the AiDA-derived airspace dimension and the intercept conveys independent information about individual lung properties, which is likely to have clinical relevance.

This work was supported by Swedish Research Council, Vinnova, EU EuroNanoMed, The Swedish Heart and Lung Foundation, the Crafoord foundation and the Sten K Johnsson foundation.

Löndahl, J., J. Jakobsson, D. Broday, H. Aaltonen and P. Wollmer (2016). *Int J of Nanomed* 2017; 12: 41–51.

Jakobsson, J., J. Hedlund, J. Kumlin, P. Wollmer and J. Löndahl (2016). *Sci Rep* 6: 36147.

# TOWARDS A SOURCE LIBRARY FOR MODELLING – COMPARING SMALL AND LARGE CHAMBER CONCENTRATIONS

Authors: Jensen, ACØ<sup>1</sup>; Bertram, N<sup>1</sup>; Koponen, IK<sup>2</sup>; Koivisto, AJ<sup>1</sup>

<sup>1</sup>The National Research Centre for the Working Environment, Copenhagen, Denmark

<sup>2</sup>FORCE technology Copenhagen, Denmark

Keywords: Modelling, Chamber studies, Aerosol dispersion, Occupational health

Presenting author email: alj@nfa.dk

Modelling of indoor occupational aerosol concentrations is frequently used in exposure assessment tools. However, source strength information for the models is often lacking. The source strength can be based on dustiness or a theoretical mass release, which is not necessarily directly relatable to real life processes. Additionally for the dustiness value, the release has been shown to depend highly on storage conditions and handling factors. Establishing a source library as proposed by Koivisto *et al.*, 2017, based on experimental data of standardized sources and processes could be beneficial. However, this requires high quality data of source strength from a variety of different materials and that the sources are transferrable between different setups and different locations so that source strength measured in one setting is equivalent to the source from the same process in a different setting.

In this work the aim was to measure the same process in two different settings and compare the concentrations measured at the source and the concentrations measured in the remainder of the room with the concentrations obtained using the two source strengths in a simple mass balance model Jensen *et al.*, submitted.

Here we conduct sanding experiments on lime-based paint with embedded graphene nanofibres. Two identical experiments with each numerous repetitions were done in either a small unventilated chamber (0.55 m<sup>3</sup>) or a large chamber (20 m<sup>3</sup>). Source concentrations were measured with an ELPI+ (Dekati, Finland) as close as possible to the rotating head of the handheld sander (fig 1). The head was weighted to ensure uniform pressure on the surface. In the small chamber the engine of the sander was isolated from the chamber using a glove from a glovebox. In the large chamber we additionally monitored the concentrations and size distributions in 3 different positions with several aerosol instruments.

Figure 2 shows the particle total number concentration and size distributions measured at the source. Sanding of the lime-based paint caused in both cases a significant increase in the particle concentrations. Comparison of the two experiments showed that the source concentrations were equivalent in magnitude with the concentrations in the closed small chamber were around twice the concentrations of the large chamber source of  $1.6 \cdot 10^6 \text{ # cm}^{-3}$  and the source measured in the larger chamber  $9.5 \cdot 10^5 \text{ cm}^{-3}$ . In the large chamber there is generally lower concentration at

the source due to ventilation and dilution to the larger volume. The size distribution from the sanding process was similar. Highest release from the sanding process was above 200 nm particles while for the engine of the sander for the small chamber the particles smaller than 100 nm showed less machine contribution since it is isolated from the process.

Here we showed that the same process measured in different chambers were similar in magnitude and size distribution. This suggests that a source library based on small scale experiments is possible, however more investigation is needed.

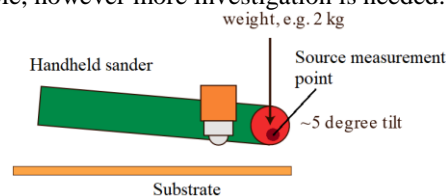


Figure 1, handheld sander set-up used in both the small and large chamber studies.

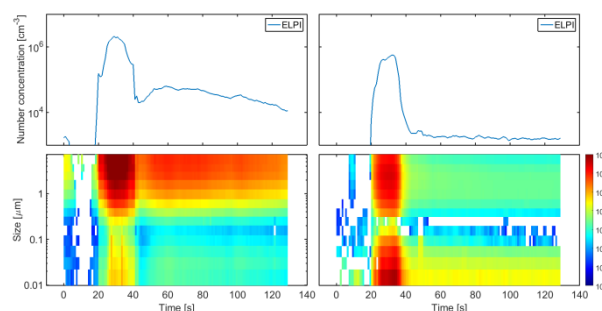


Figure 2, source number concentrations (upper) and particle size distributions (lower) measured in the small (left) and large (right) chamber. Concentrations have been subtracted averaged concentrations before the experiment started.

## References

Koivisto AJ, Jensen ACØ, Kling KI, Nørgaard A, Brinch A, Christensen F, et al. Quantitative material releases from products and articles containing manufactured nanomaterials: Towards a release library. *NanoImpact*, 2017; 5: 119–132.

Jensen ACØ, Dal Maso M, Koivisto AJ, Belut E, Meyer-Plath A, Van Tongeren M et al. Comparison of geometrical layouts for a multi-box aerosol model from a single-chamber dispersion study. *J Expo Sci Env Epid*. Submitted.

# IMPACTS OF FUTURE EUROPEAN EMISSION REDUCTIONS ON AEROSOL NUMBER CONCENTRATIONS WITH FOCUS ON ULTRAFINE PARTICLES

J. JULIN<sup>1,2</sup>, B.N. MURPHY<sup>3</sup>, D. PATOULIAS<sup>4</sup>, C. FOUNTOUKIS<sup>5</sup>, T. OLENIUS<sup>1</sup>, S.N. PANDIS<sup>4,6,7</sup> and I. RII-PINEN<sup>1</sup>

<sup>1</sup> Department of Environmental Science and Analytical Chemistry (ACES) and Bolin Centre for Climate Research, Stockholm University, Sweden

<sup>2</sup> Department of Applied Physics, University of Eastern Finland, Finland

<sup>3</sup> National Exposure Research Laboratory, US Environmental Protection Agency, United States

<sup>4</sup> Department of Chemical Engineering, University of Patras, Greece

<sup>5</sup> Qatar Environment and Energy Research Institute, Hamad Bin Khalifa University, Qatar

<sup>6</sup> Department of Chemical Engineering, Carnegie Mellon University, United States

<sup>7</sup> Institute of Chemical Engineering Sciences, Foundation for Research and Technology, Greece

Keywords: gas and particle emissions, sulfuric acid, ammonia, amines, organic species

Besides being a major contributor to atmospheric aerosol particle number and a source of cloud condensation nuclei, ultrafine aerosol particles below 100 nm are recognized as a health hazard. These small particles can be particularly harmful as they are able to penetrate deep into the lungs and blood circulation (e.g. Terzano et al., 2010), and thus monitoring and controlling ultrafine particulate pollutants is essential for air quality policies.

This work (Julin et al., 2018) presents simulations of the response of particle number concentrations over Europe to recent, country-resolved assessments of future emission reductions of particles and their precursor gases (Amann, 2015a,b). The reductions are guided by the European Commission's targets to decrease air-pollution-driven mortality by 2030. We consider three emission scenarios: current legislation (CLE), optimized emissions designed to meet the air quality improvements proposed in the Clean Air Policy Package (OPT), and maximum technically feasible reductions (MTFR). The reductions apply to SO<sub>2</sub>, NO<sub>x</sub>, ammonia, amines, volatile organic compounds and primary particles.

The simulations were performed with the chemical transport model PMCAMx-UF, which was updated with state-of-the-art descriptions of new particle formation (NPF) from sulfuric acid with ammonia and amine, and condensation of organic species onto particles. The NPF schemes were incorporated as look-up tables of particle formation rates generated by molecular clustering simulations using quantum chemical data. Organic condensation was implemented applying a volatility basis set covering volatilities from 10<sup>-3</sup> to 10<sup>3</sup> μg m<sup>-3</sup> (at 298 K) and considering oxidative aging. These updates enable more realistic predictions of particle size distributions than have been available before.

The results show notable impacts on ambient particle concentrations, dominated by the ultrafine sizes (Figure 1). All three scenarios result in substantial reductions of 10–50% in the median particle numbers in the European domain, with the absolute reduction depending on the location. Consistent decreases were predicted in Central Europe, while Northern Europe exhibited

smaller decreases or even slightly increased concentrations, likely due to decrease in the condensation sink caused by larger particles. These results highlight the need to (1) accurately assess changes in spatially resolved gas and particle emissions, and (2) model the often very non-linear effects on particle size distributions in sufficient detail.

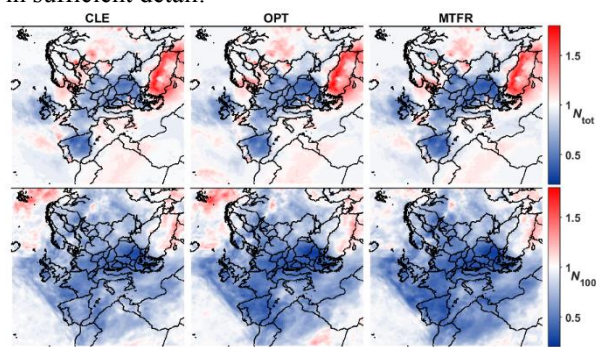


Figure 1: Predicted relative change in the median concentration of all particles  $N_{\text{tot}}$  (upper panels), and particles over 100 nm  $N_{100}$  (lower panels) between the CLE, OPT and MTFR scenarios and present-day conditions.

*Acknowledgements:* The authors thank the Swedish research council FORMAS (2015-749) and European Integrated Project PEGASOS (FP7-ENV-2010-265148) for funding, and the National Supercomputing Centre (NSC) for computational resources.

Amann, A., Ed. (2015a). *Adjusted historic emission data, projections, and optimized emission reduction targets for 2030 – A comparison with COM data 2013. Part A: Results for EU-28. TSAP Report 16a.*

Amann, A., Ed. (2015b). *Adjusted historic emission data, projections, and optimized emission reduction for 2030 – A comparison with COM data 2013. Part A: Results for Member States. TSAP Report 16b.*

Julin, J. et al. (2018). *Environ. Sci. Technol.*, 52:692–700.

Terzano, C. et al. (2010). *Riv. Eur. Sci. Med. Farmacol.*, 14:809–821.



# Mobile application based aerosol calculator for easing the life of students and researchers

P. Juuti<sup>1</sup>

<sup>1</sup> Aerosol Physics, Laboratory of Physics, Tampere University of Technology, Finland

Keywords: fundamentals, calculator, mobile application, ease-of-access

Aerosol specific calculators have been around for decades to ease research and help students. Whether they are physical or electronic, their main purpose is to make crucial information readily available without the need to carry an arsenal of books and reference manuals with you at all times.

One of the earliest physical calculators was prepared by V.A. Marple in 1981, and it could compute slip correction factor and diffusion coefficient, along with 3 other parameters as a function of particle diameter (Marple, 1981). Another noteworthy physical calculator was designed by E. Saukko in 2014, for calculating between classification voltage of a DMA and its output particle size (Saukko, 2014). Both of these are shown in Figure 1.

Electronic aerosol calculators, such as the spreadsheet made by P. Baron (shown in Figure 1), which can calculate over a hundred parameters (Baron, 2001), excel at providing vast amounts of data with an easily shareable format as it is not limited by physical dimensions. Other type of electronic calculators are the online website calculators, which are even more readily available.

In order to combine the portability and the information richness of these two approaches, a mobile application for calculating gas and particle properties in user specified situations was developed. The application platform also has the capability to perform task specific functions, such as calculating the DMA voltage for a certain particle diameter or helping students visualize parameters of a log-normal distribution. The information and equations for this application have been gathered from notable books in the field of aerosol science (Hinds, 1999; Seinfeld and Pandis, 2006; Baron and Willeke, 2011).

Mobile devices are ideal for this purpose as they are easy to use, always at hand and do not rely on the availability of internet access. The application also has the benefit of helping students in their studies, via easily accessible information and tailor-made visualization aids. Additionally, researchers can benefit from moving their repetitive calculations into the application to aid in e.g. TEM collection times.

A mobile application was introduced to give an easier access to aerosol related parameters and to help with everyday tasks by utilizing the mobile devices that are at everyone's disposal. The first version of the finished application is to be made publicly available by the time of NOSA 2018, and afterwards more features will be added based on the user feedback.



Figure 1: Selection of aerosol calculators from physical to electronic. Schematic view of the introduced application can be seen in the mobile phone screen.

Paxton Juuti acknowledges the TUT's graduate school for financial support.

Marple, V.A. (1981). *Aerosol properties -calculator disc*, TSI

Saukko, E., (2014). *Universal DMA slide rule*, Available at: <https://sites.google.com/site/dmacalculator/>, [Accessed 19.01.2018].

Baron, P., (2001). *Aerosol Calculator*, Available at: [www.tsi.com/uploadedFiles/Product\\_Information/Literature/Software/Aerocalc2001.xls](http://www.tsi.com/uploadedFiles/Product_Information/Literature/Software/Aerocalc2001.xls), [Accessed 19.01.2018].

Hinds, W., (1999). *Aerosol Technology. Properties, behaviour, and measurement of airborne particles*. John Wiley & Sons, Inc., 2nd edition.

Seinfeld, J. and Pandis, S. (2006). *Atmospheric Chemistry and Physics: From Air Pollution to Climate Change*. Wiley Interscience, 2nd edition.

Baron, P. and Willeke, K., (2011). *Aerosol Measurement: Principles, Techniques, and Applications*. John Wiley & Sons, Ltd.

# THE EFFECT OF METEOROLOGY ON POLLUTANT DISTRIBUTIONS WITHIN STREET CANYON NETWORK IN HELSINKI

L. JÄRVI<sup>1</sup>, L. PIRJOLA<sup>2</sup>, M. KURPPA<sup>1</sup>, H. KUULUVAINEN<sup>3</sup>, A. MALINEN<sup>2</sup>, A. BALLING<sup>4</sup>, S. KARTTUNEN<sup>1</sup>, T. RÖNKKÖ<sup>3</sup>, J.V. NIEMI<sup>5</sup>, and P. RANTALA<sup>1</sup>

<sup>1</sup> Institute for Atmospheric and Earth system research / Physics, University of Helsinki, Finland

<sup>2</sup> Department of Technology, Metropolia University of Applied Sciences, Helsinki, Finland

<sup>3</sup> Aerosol Physics, Faculty of Natural Sciences, Tampere University of Technology, Tampere, Finland

<sup>4</sup> Department of Atmospheric Chemistry, University of Bayreuth, Bayreuth, Germany

<sup>5</sup> Helsinki Region Environmental Services Authority, Helsinki, Finland

Keywords: air quality, meteorology, sniffer, street canyon, urban, ventilation

Urban areas are characterised with highly variable air pollutant fields both in time and space. Despite this, we are often forced to measure their concentrations in a single measurement point with coarse time resolution. More detailed data is, however, particularly needed to understand in detail pollution ventilation, advection and dispersion within complex urban canopies as well as in high-resolution model development. The purpose of this work is to understand how the prevailing meteorological conditions modify the pollutant distributions of both particulate matter and gaseous pollutants in Helsinki. This will be done with the aid of two 2-week measurement campaigns utilising mobile and drone observations.

The measurement campaigns were conducted around the Helsinki Regional Environmental Services Authority (HSY) supersite located in a street canyon, about 3 km North-East from Helsinki city centre, on 5–16 Jun 2017 and 27 Nov–8 Dec 2017 covering both summer and winter conditions. The street canyon is 42 m wide ( $W$ ) and the mean building height ( $H$ ) is 17 m creating  $H/W$  value of 0.41. During both campaigns, the Sniffer mobile laboratory (Pirjola et al., 2012) was measuring on three 2-hour time slots (morning and afternoon rush hours and noon/evening) on workdays with suitable weather conditions (i.e. not too rainy). The mobile laboratory circled in the main street canyon and side roads in addition to measuring background air and standing still in the street canyon. On two days on both campaigns, the vertical distribution of air pollutants was measured using a drone during the same 2-hour slots.

The mobile laboratory measured the particle number size distribution (ELPI, EEPS), particle mass (PM<sub>2.5</sub>/PM<sub>10</sub>, TEOM), black carbon (AE33), and concentrations of O<sub>3</sub>, NO<sub>x</sub> and NO (Horiba) with 1 s. The drone measured lung deposited particle surface area (LDSA, Partector), concentrations of NO, NO<sub>x</sub>, O<sub>3</sub>, air temperature and humidity (BH-8, Aeromon) with 1 s. Continuous air quality concentrations were provided by the supersite and the SMEARIII station (Järvi et al., 2009) located 800 m from the supersite. In latter, high-frequency wind and temperature (USA-1 Metek) were also continuously measured providing atmospheric stability and friction velocity, both of which are crucial

variables for atmospheric dispersion. During the campaigns, a similar instrument was also installed at the supersite providing local street canyon dispersion information. The ELPI measurements made at the supersite and with the mobile van will be converted to LDSA following Kuuluvainen et al. (2016).

The analyses of the campaign data are currently ongoing and as an example Figure 1 shows the LDSA measured by the mobile laboratory on the morning of 9th June. The next step is to classify data by means of meteorological conditions allowing us to examine the impact of these of the pollutant fields.

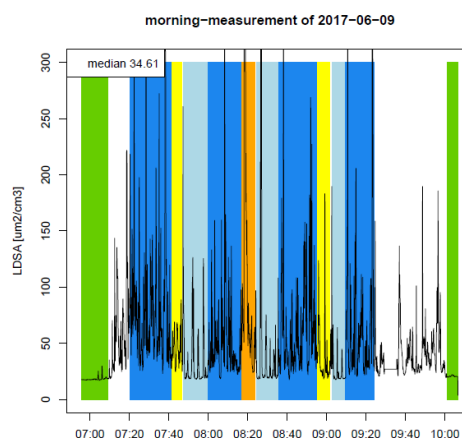


Figure 1: LDSA measured by the mobile laboratory on morning 9 June 2017. Different colours show the driving routes: green = background, dark blue = street canyon, yellow = standing at supersite, light blue = side roads and orange = standing opposite supersite.

Järvi, L., Hannuniemi, H., Hussein, T., et al. (2009). *Boreal Env. Res.*, 14:86–109.

Kuuluvainen, H., Rönkkö, T., Järvinen, A., et al. (2016). *Atmos. Env.*, 136:8105–113.

Pirjola, L., Lähde, A., Niemi, J.V., et al. (2012). *Atmos. Env.*, 63:156–167.

# THE VOLATILITY AND CHEMICAL COMPOSITION OF SUBMICRON PARTICLES IN A STREET CANYON IN HELSINKI

Joni Kalliokoski<sup>1</sup>, Hilikka Timonen<sup>2</sup>, Heino Kuuluvainen<sup>1</sup>, Riina Hietikko<sup>1</sup>, Mia Isotalo<sup>1</sup>, Niina Kuittinen<sup>1</sup>, Minna Aurela<sup>2</sup>, Jarkko Niemi<sup>3</sup>, Jorma Keskinen<sup>1</sup> and Topi Rönkkö<sup>1</sup>

<sup>1</sup> Aerosol Physics, Faculty of Natural Sciences, Tampere University of Technology, Tampere, FI33720, Finland

<sup>2</sup> Atmospheric Composition Research, Finnish Meteorological Institute, Helsinki, FI00101, Finland

<sup>3</sup> Helsinki Region Environmental Services Authority (HSY), FI00066 HSY, Finland

Keywords: urban aerosols, chemical composition, street canyon, volatility

Anthropogenic aerosols can cause adverse health effects and have a significant impact on global climate. The volatility of aerosol particles is linked to the chemical composition of particles. Therefore, the investigation of volatility may provide valuable information on the particle properties as well as their sources and impacts on global climate and human health. Here, we present preliminary results obtained from a field campaign carried out in Helsinki in May 2017. Our aim was to measure the volatility as a function of particle size and combine it with the chemical composition obtained by a mass spectrometer.

The measurement site was located at a kerbside in a street canyon in Helsinki, Finland (Mäkelänkatu 50). Mäkelänkatu is one of the main streets of Helsinki and it is leading towards city center. Measurements were conducted during daytime between May 22nd and May 29th in 2017. The chemical composition of submicron particles was measured with a soot particle aerosol mass spectrometer (SP-AMS, Aerodyne Research Inc.). The time resolution of SP-AMS measurements was one minute. Two electrical low pressure impactors (ELPI, Dekati Ltd.) were used to measure aerodynamic particle size distributions with a time resolution of one second. The sample was drawn from the roof of the measurement site 4 m above the ground. The volatility of aerosol particles was analyzed by using a thermodenuder. The thermodenuder was operated at four different temperatures (50, 80, 150 and 265 °C). One ELPI sampled upstream of the thermodenuder and the other was sampling downstream. The sampling location of SP-AMS was varied between upstream and downstream of the thermodenuder. A total of 13 temperature ramps were measured. One ramp consisted of measuring 10 minutes at each temperature (SP-AMS measured downstream) and one 10 minute measurement in which all instruments measured from the same point upstream of the thermodenuder.

The mass concentrations from the SP-AMS are shown in Figure 1 as a function of thermodenuder temperature. As shown in the figure, there is a very small change in concentrations from upstream to 50 °C, which is probably due to thermodenuder losses. 60 % of total aerosol mass seems to evaporate at 150 °C and almost 85 % at 265 °C. Sulphate in aerosol particles seems not to evaporate until at 265 °C when almost all sulphate

evaporates. In addition, ammonium and nitrate is completely evaporated in that temperature. The results indicate also that 15 % of the total aerosol mass is composed of particles which evaporate in temperatures higher than 265 °C. This particulate matter composes of black carbon (soot particles) and organic compounds with low volatility. The ELPI results revealed that, even though 85 % of the total mass evaporates at 265 °C, there is still almost 40 % of the total number remaining indicating the presence of low volatility compounds at ultrafine particle size range. Minimum evaporation efficiency was at an aerodynamic diameter of 40 nm which is close to the typical size of soot particles emitted by traffic. In general, the results of the study demonstrate the usefulness of combining the composition and size distribution in volatility studies.

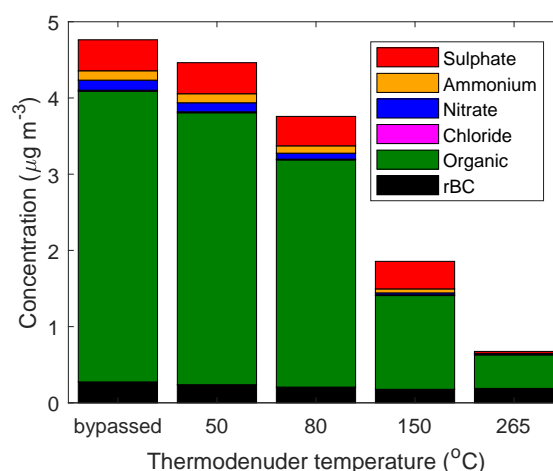


Figure 1: The chemical composition of submicron particles as a function of thermodenuder temperature. The measurement was conducted by the SP-AMS in the roadside environment.

This work was conducted in the CITYZER project funded by Tekes, HSY and Pegasor Oy. Joni Kalliokoski acknowledges the TUT Graduate School for its funding.

# IMPROVING THE ACCURACY AND PRECISION OF SUB-10 NM ATMOSPHERIC NANOPARTICLE MEASUREMENTS WITH A NEW HIGH FLOW DMPS

J. Kangasluoma<sup>1</sup>, L. R. Ahonen<sup>1</sup>, T. Laurila<sup>1</sup>, R. Cai<sup>1</sup>, J. Enroth<sup>1</sup>, S. Buenrostro Mazon<sup>1</sup>, F. Korhonen<sup>1</sup>, P.P. Aalto<sup>1</sup>, M. Kulmala<sup>1</sup>, M. Attoui<sup>1,2</sup>, T. Petäjä<sup>1</sup>

<sup>1</sup> Institute for Atmospheric and Earth System Research / Physics, Faculty of Science, University of Helsinki, Finland

<sup>2</sup> University Paris Est Creteil, University Paris-Diderot, LISA, UMR CNRS 7583, France

Keywords: DMPS, sub-10 nm, instrumentation, uncertainties

Measurement of atmospheric sub-10 nm nanoparticle number concentrations has been of substantial interest recently, which, however, is subject to considerable uncertainty that has not been examined thoroughly. We report a laboratory characterization of a high flow differential mobility particle sizer (HFDMPs), which is based on the SEADM Half-mini type differential mobility analyzer (DMA) (Fernández de la Mora and Kozlowski 2013) and Airmodus A11 nano condensation nuclei counter (Vanhanen et al. 2011), and show the first results from atmospheric observations from Hyytiälä, Finland during spring of 2017. The HFDMPs utilizes the state-of-the-art aerosol technology, and is optimized for particle size distribution measurements in the sub-10 nm size range by a moderate resolution DMA, optimized and characterized low-loss particle sampling line (Kangasluoma et al. 2016) and minimal dilution in the detector.

We present an exhaustive laboratory calibration to the HFDMPs (Figure 1) and compare the inverted atmospheric particle number concentrations to the long-term size segregated aerosol number size distribution measured with the Hyytiälä long-term DMPS. Because of the optimized sampling and higher sensitivity of the HFDMPs, it detects about two times more 3-10 nm particles than the long-term DMPS (Figure 2), and by having better counting statistics by a factor of 3.5-9 depending on the size, the counting uncertainties are reduced about 50% as compared to the long-term DMPS. The HFDMPs did not observe any sub-2.5 nm particles in Hyytiälä, and the reason for that was shown to be the inability of DEG to condense on such small biogenic particles, instead of lack of sensitivity. Last, we discuss the general implications of our results to the sub-10 nm DMPS based measurements.

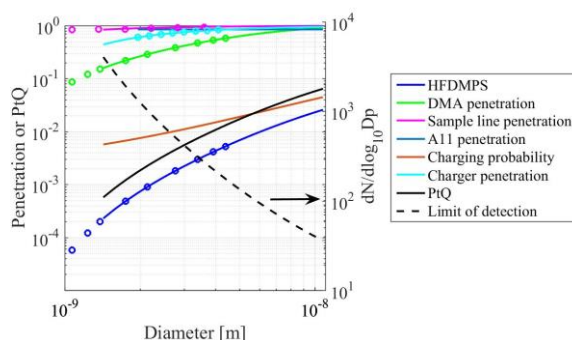


Figure 1. Characterization of the HFDMPs.

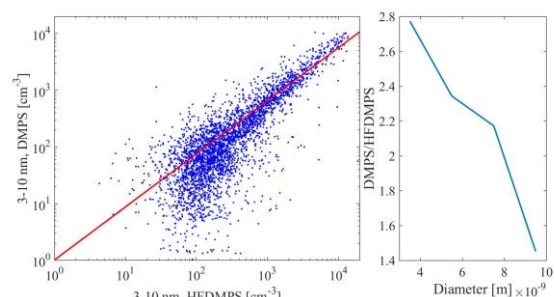


Figure 2. Comparison of the 3-10 nm particle concentrations measured by the HFDMPs and the Hyytiälä long-term DMPS.

Table 1. Size dependent median number of counts for the DMPS systems.

	3-4 nm	5-6 nm	7-8 nm	9-10 nm
DMPS	1	6	12	17
HFDMPs	9	21	40	81
Ratio	9.32	3.64	3.40	4.78

Table 2. Size dependent median relative counting uncertainties [%] for the DMPS systems.

	3-4 nm	5-6 nm	7-8 nm	9-10 nm
DMPS	86	53	45	39
HFDMPs	43	29	24	20
Ratio	0.50	0.54	0.54	0.52

## References:

- Fernández de la Mora, J. *et al. J Aerosol Sci* **57**, 45-53 (2013).  
 Kangasluoma, J. *et al. Atmos Meas Tech* **9**, 2977-2988 (2016).  
 Vanhanen, J. *et al. Aerosol Sci Tech* **45**, 533-542 (2011).

# LONG-RANGE TRANSPORTED AEROSOLS AT THE MALDIVES AND THE IMPACT OF WET DEPOSITION ON PARTICLE NUMBER AND SIZE

J. KESTI<sup>1</sup>, J. BACKMAN<sup>1</sup>, E. ASMI<sup>1</sup>, E. J. O'CONNOR<sup>1</sup>, Ö. GUSTAFSSON<sup>2</sup> and K. BUDHAVANT<sup>2,3</sup>

<sup>1</sup>Finnish Meteorological Institute, Helsinki, Finland

<sup>2</sup>Department of Applied Environmental Science and Bolin Centre for Climate Research, Stockholm University, Stockholm, Sweden

<sup>3</sup>Maldives Climate Observatory at Hanimaadhoo, Hanimaadhoo, Republic of the Maldives

Keywords: atmospheric aerosols, tropics, aerosol sources, wet deposition

Wet deposition is a significant removal process of aerosol particles from the atmosphere. Precipitation intensity, aerosol particle size and other microphysical properties are the factors that affect the efficiency of the process.

Precipitation is a significant climate variable in the Maldives. During summer, the Maldives is under the influence of the Indian monsoon, which brings warm and moist marine air consisting mostly of natural aerosols from the Indian Ocean. During winter, which is the dry season, the air masses measured at the Maldives are mainly coming from the Indian subcontinent and thus bringing polluted air.

To study the effect of precipitation on long-range transported aerosol particles in the Maldives, we used two different data sets measured at the Climate Observatory of Hanimaadhoo in the Maldives (MCOH), which is one of the Atmospheric Brown Cloud (ABC) observatories (Ramana and Ramanathan, 2006). The first measurements were conducted during 2004–2008 using a Scanning Mobility Particle Sizer (SMPS.) The second measurement period was during 2014–2017, and the instrument used was a Differential Mobility Particle Sizer (DMPS). In addition, we collected the meteorological observation data measured at MCOH for these periods and calculated hourly back trajectories and cumulative rainfall along the trajectory for the measurement periods using HYSPLIT 4.9 model (Draxler and Hess, 1998). The meteorological data, which provided both wind fields and precipitation for the model, was the GDAS 1° dataset from National Center for Atmospheric Research.

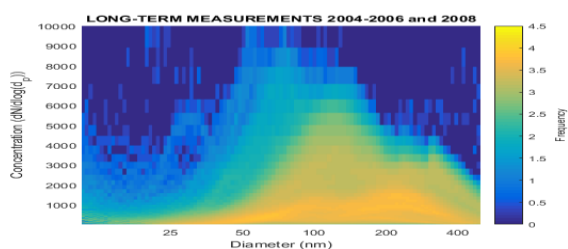


Figure 1: A histogram of aerosol particle size distributions measured with a SMPS at MCOH.

The results reveal different particle size distribution shapes depending on the source region of

aerosol particles (Figure 1); the highest concentrations were observed in outflow from India and the Indo-Gangetic plain. The particle size distributions were also affected by the precipitation intensity en route to the measurement site. The median particle number concentration during the dry season in the first measurement period 2004–2008 was 624 1/cm<sup>3</sup> and during monsoon season 178 1/cm<sup>3</sup>. For the second measurement period, during 2014–2017, the numbers were 1647 1/cm<sup>3</sup> for dry season and 408 1/cm<sup>3</sup> for monsoon season.

We also studied the change in the aerosol particle size distribution shape compared to different amounts of rainfall by using the cumulative rainfall from the model and in-situ measurements with the SMPS and DMPS. The analysis was divided to cover different source regions and seasons. Impact of precipitation on size distribution shape in the tropics for different aerosol types was then elucidated and compared with previous studies made in other locations (eg. Tunved et al., 2013). The results will be thoroughly discussed in the conference.

The staff working at the Climate Observatory of Hanimaadhoo is acknowledged for maintenance of the measurements.

Draxler, R. R., and Hess, G. D. (1998). *An overview of the HYSPLIT\_4 modelling system for trajectories, dispersion, and deposition*. Aust. Meteorol. Mag., 47, 295–308.

Ramana, M. V., and Ramanathan, V. (2006). *Abrupt transition from natural to anthropogenic aerosol radiative forcing: Observations at the ABC-Maldives Climate Observatory*. J. Geophys. Res. Atmos., 111(D20).

Tunved, P., Ström, J., and Krejci, R. (2013). *Arctic aerosol life cycle: linking aerosol size distributions observed between 2000 and 2010 with air mass transport and precipitation at Zeppelin station, Ny-Ålesund, Svalbard*. Atmos. Chem. Phys., 13, 3643–3660.

# STUDYING AEROSOL RADIATION FEEDBACK LOOP BASED ON SATELLITE DATA

M. KHANSARI. ONE<sup>1</sup>, A. NIKANDROVA. TWO<sup>1</sup>, P. PAASONEN. THREE<sup>1</sup>, V.-M. KERMINEN. FOUR<sup>1</sup> AND M. KULMALA. FIVE<sup>1</sup>

<sup>1</sup> Institute for Atmospheric and Earth System Research / Physics, Faculty of Science, University of Helsinki, Finland

Keywords: aerosol radiation, condensation sink, GPP

Apart from having an important role in defining air quality, atmospheric aerosols are found to affect the Earth's radiation budget. The aerosols impact radiation directly by scattering and absorbing incoming solar radiation and indirectly by changing cloud properties via formation of cloud condensation nuclei (CCN) (IPCC 2013). All these impacts are largely affected by the size of the aerosol particles. Thus, studying the parameters involved in the formation and growth of atmospheric particles is essential for understanding their role in our atmosphere.

Satellite measurements would be suitable tools to adopt in studying the effect of aerosols on the amount of radiation reaching the surface. Remote sensing provides information about the spatial distribution of aerosols and trace gases (Sundström et al, 2015), as well as the vegetation structure and photosynthesis, on a nearly global level.

In this study, our aim is to study the aerosol radiation feedback based on satellite data (Fig 1) in semi-clean boreal forest in southern Finland. The loop examines the effect of introducing a perturbation of +10ppm in CO<sub>2</sub> concentration, first on temperature. The temperature dependence of oxidation products of BVOCs is then investigated. SOA (secondary organic aerosols) concentrations would be affected by any changes to the level of these oxidation products, yet would also directly influence CS (condensation sink). The ratio of diffuse radiation to global radiation ( $R = R_d/R_g$ ) is defined to describe any possible effect on photosynthesis. Finally, to close the loop, the approximate nature of CO<sub>2</sub> concentration dependency on the level of photosynthesis is examined.

We focused on cloud-free conditions to diminish the effect of clouds (Kulmala et al, 2014). To achieve this purpose, we used MODIS cloud mask data in our study. Here, we used satellite-based radiation data from CERES instruments. Furthermore, re-analysis temperature from ERA- Interim (global atmospheric reanalysis) was used.

We found positive correlation between satellite-derived R and re-analysis temperature during clear day in Hyytiälä as it is shown in Fig 2.

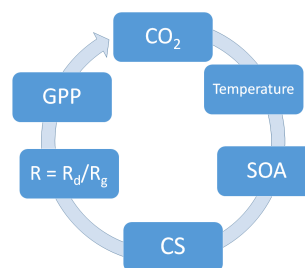


Figure 1: The aerosol radiation feedback loop. Where GPP is gross primary production, SOA is secondary organic aerosols, CS is the condensation sink and R is the ratio between diffuse radiation ( $R_d$ ) and global radiation ( $R_g$ ).

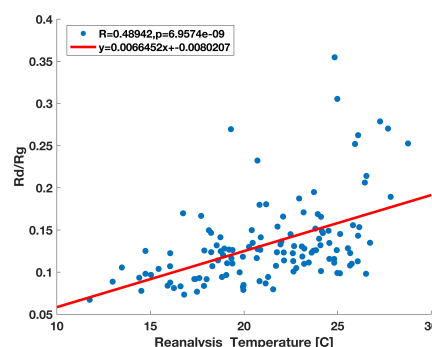


Figure 2: One hour median of R from Ceres instrument as a function of re-analysis temperature for Hyytiälä station during daytime on June and July from 2000 to 2016. We considered here clear days detected by MODIS cloud mask.

Kulmala, M., Nieminen, T., Nikandrova, A., Lehtipalo, K., Manninen, H. E., Kajos, M. K., ... & Hansson, H. C. (2014). C [O. sub. 2]-induced terrestrial climate feedback mechanism: From carbon sink to aerosol source and back. *Boreal Environment Research*, 19, SS122-SS122.

Sundström, A. M., Nikandrova, A., Atlaskina, K., Nieminen, T., Vakkari, V., Laakso, L., ... & Venter, A. D. (2015). Characterization of satellite-based proxies for estimating nucleation mode particles over South Africa. *Atmospheric Chemistry and Physics*, 15(9), 4983-4996.

# ACTRIS – Shaping the future of Atmospheric Research

N. Kivekäs<sup>1</sup> and S. Sorvari<sup>1</sup>

<sup>1</sup>Finnish Meteorological Institute, FI-00101, Helsinki, Finland

Keywords: ACTRIS, Research Infrastructure, Aerosols

## Introduction

During the latest decades the improvements in means of analysing and sharing big data sets have made it possible to easily analyse complex data from across the globe. This requires inter-comparable data. The production of such data sets calls for wide networks producing harmonized data sets over large geographical area, and storing and delivering the data in a common way. This requires a lot of coordination.

International Research Infrastructures are the European answer to these needs. They enable implementation of scientific instruments and networks that are too big for any nation to build alone. They also enable a more continuous funding scheme for large scale international operations.

## ACTRIS

In the field of aerosol the research infrastructure is ACTRIS (Aerosols, Clouds and Trace gases Research Infrastructure). It is a research infrastructure for observing and providing tools for research on the short-lived components of the atmosphere.

ACTRIS is planned to consist of National and Central Facilities. The National Facilities are the numerous existing and to-be-implemented measuring sites, mobile research platforms, simulation chambers and laboratories producing atmospheric data. The Central Facilities are Head Office, Data Centre and six Topical Centres for calibration and operational support for different measurement instruments.

ACTRIS is currently in preparation. Some of its parts are already providing data via EBAS and other data delivery services, but the provision of more harmonized ACTRIS data and services is planned to start in 2020, and ACTRIS aims to be fully operational in 2025. There are currently 24 countries involved in the preparation of ACTRIS, 15 of them also at the ministry level (Figure 1).

As a research infrastructure ACTRIS will be based on international agreements between the ACTRIS member states. The states commit themselves to fund their share of the national and international ACTRIS activities for five years at the time, and gain advantage to their scientific community via ACTRIS.

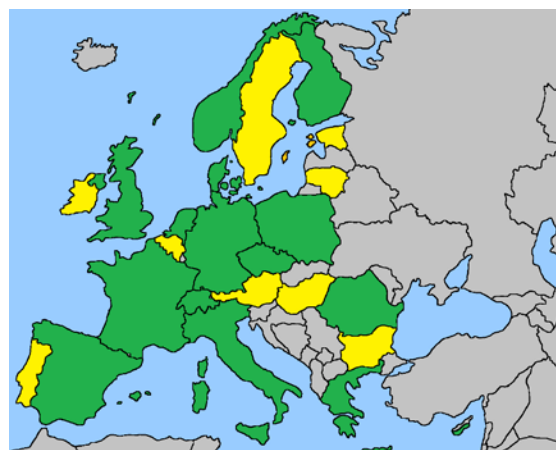


Figure 1. Countries participating in preparation of ACTRIS at both ministry- and research organization level (green) and at research organization level only (yellow).

## ACTRIS services

The first and most obvious ACTRIS service is the data, which will be available for free via the ACTRIS Data Centre. The data will be inter-comparable due to common measurement and data processing protocols, and quality controlled via regular calibrations of the instruments. Besides data delivery the Data Centre provides virtual tools for processing the data online.

Another ACTRIS service is to provide supported access to the Topical Centres and to selected National Facilities via a competitive selection process. This way the most promising research projects will always have access to the best facilities and expertise available.

ACTRIS also provides training and education related to instruments and processing of atmospheric data. Furthermore, ACTRIS gives a stronger voice in the policy making for the related scientific communities.

## Acknowledgements

ACTRIS has been / is currently supported by EC grants 262254 (ACTRIS, 2011-2015), 654109 (ACTRIS-2, 2015-2019), 730997 (EUROCHAMP 2020) and 739530 (ACTRIS PPP, 2017-2019). We also thank the numerous past and ongoing national projects and programs for providing immense support for long-term atmospheric and aerosol research throughout Europe.

# REGULATORY EXPOSURE MODELLING – CURRENT STATUS AND WORK NEEDED

A.J. KOIVISTO<sup>1</sup>, A.S. FONSECA<sup>1</sup>, I.K. KOPONEN<sup>1</sup>, and A.C.Ø JENSEN<sup>1</sup>

<sup>1</sup>National Research Centre for the Working Environment, Copenhagen, Denmark.

Keywords: near-field/far-field model, the Advanced REACH Tool, STOFFENMANAGER<sup>®</sup>, exposure modeling

The Registration, Evaluation, Authorization, and Restriction of Chemicals (REACH) regulation No 1907/2006 implemented by European Chemical Association (ECHA), demands that manufacturers or importers must report or estimate human exposure by all relevant routes to determine the appropriate risk management measures and prevent excessive exposure (EC, 2006). By the end of May 2018, this will apply to all chemicals that are manufactured or imported in quantities over 1 metric ton per year within the European Union. This means that exposure has to be assessed for hundreds of thousands of chemicals by all potential routes including environmental, occupational and consumer exposure scenarios. This can be fulfilled only by worst case or predictive exposure modelings.

STOFFENMANAGER<sup>®</sup> ([stoffenmanager.nl](http://stoffenmanager.nl)) and the Advanced REACH Tool (ART; [advancedreachttool.com](http://advancedreachttool.com)) are higher tier occupational exposure models recommended in REACH guidance for occupational exposure assessment. These models are primarily mechanistic models based on exposure determinants and are different from physical mass-balance models (Figure 1). Mechanistic models are more difficult to test for potential model errors than physical mass-balance models.

Recently, it was found that there was an error in the general ventilation multipliers in the STOFFENMANAGER<sup>®</sup> and the ART models. The general ventilation multipliers in the two models are calculated using a standard Near-Field/Far-Field (NF/FF) model (Hemeon, 1963). We recalculated the multipliers and found that those should be up to 280% higher than the values used in STOFFENMANAGER<sup>®</sup>. For 1- and 8-h exposure estimates using ART, the error resulted in <17 % and <41 % lower concentrations than with original ventilation data, respectively. The error has greatest influence on exposure calculated for small rooms with low ventilation rates. The exposure score calculated by the models is directly proportional to the general ventilation multipliers, but the personal exposure estimates is given using calibration factors to adjust relevant exposure measured data.

Eventhough the error results in more precautionary exposure scores, the wide use of especially STOFFENMANAGER<sup>®</sup> (>32.000 users), the observed error could have an impact on decisions made.. It needs to be assessed whether model evaluation, sensitivity testing, calibration and validation should be

revisited (see Savic et al. 2016 and its references; Landberg et al. 2017; Spinazzé et al. 2017).

Another approach for exposure assessment is direct use of mathematical mass balance models. These models consist of three parts: ventilation-dispersion model, emission source strengts, and controls (Figure 1). Emission source libraries are currently in development (Koivisto et al. 2017; Schneider and Jensen, 2008) and high quality emission control efficacy libraries exists (Fransman et al. 2008).

Examples will be given on use of both types of models for occupational exposure assessment to discuss potential consequences on results.

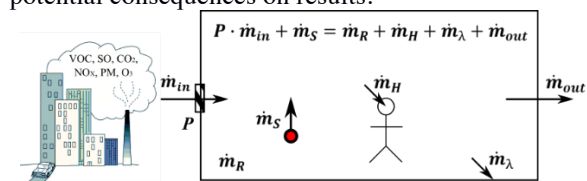


Figure 1: Scheme of mass flows in a single compartment mass balance model comprising filtered ( $P$ ) outdoor pollutions ( $\dot{m}_{in}$ ), source  $\dot{m}_s$ , room concentration ( $\dot{m}_R$ ), accumulation to human ( $\dot{m}_H$ ) and surfaces ( $\dot{m}_\lambda$ ), and mass flow to environment ( $\dot{m}_{out}$ ).

This work was supported by the European Union's H2020 under EC-GA No. 760840 'GRACIOUS' and 686239 'caLIBERate'.

- EC (2006). *Off. J. Eur. Commun.*, L136: 3–280.
- Fransman, W., Schinkel, J., Meijster, T., Van Hemmen, J., Tielemans, E., Goede, H. (2008). *Ann. Occup. Hyg.*, 52:567-575.
- Hemeon, W.C. (1963). *Plant and process ventilation*. 2nd. New York: Industrial Press. pp. 235–45.
- Koivisto AJ, Jensen ACØ, Koponen IKK. *In review at JOEH*.
- Koivisto A.J., Jensen A.C.Ø., Kling K.I., Nørgaard A., Brinch A., Christensen F., Jensen K. (2017). *Nanoimpact* 5:119-132.
- Savic, N., Racordon, D., Buchs, D., Gasic, B., Vernez, D. (2016). *Ann. Occup. Hyg.* 60:991-1008.
- Schneider, T., Jensen, K.A. (2008). *Ann. Occup. Hyg.* 52: 23–34.
- Landberg, H.E., Axmon, A., Westberg, H., Tinnerberg, H. (2017). *Ann. Work. Expo. Health.* 61:575-588.
- Spinazzé, A., Lunghini, F., Campagnolo, D., Rovelli, S., Locatelli, M., Cattaneo, A., Cavallo, D.M. (2017). *Ann Work Expo Health.* 61:284-298.



# MOLECULAR-RESOLUTION SIMULATIONS OF THE GROWTH OF ATMOSPHERIC CLUSTERS BY ORGANIC VAPORS

J. KONTKANEN<sup>1,2</sup>, T. OLENIUS<sup>1</sup>, M. KULMALA<sup>2</sup> and I. RIIPINEN<sup>1</sup>

<sup>1</sup>Department of Environmental Science and Analytical Chemistry and Bolin Centre for Climate Research, Stockholm University, Sweden

<sup>2</sup>Institute for Atmospheric and Earth System Research / Physics, University of Helsinki, Finland

Keywords: nucleation, new particle formation and growth, molecular clusters

Oxidized organic compounds are believed to be important in the formation and growth of atmospheric particles (Riipinen et al., 2012; Riccobono et al., 2014). However, a robust physical description of particle formation involving sulfuric acid, bases and organic vapors is missing. One of the mechanisms proposed to depict this process is nano-Köhler theory, which describes the activation of inorganic clusters to growth by condensation of soluble organic vapor (Kulmala et al., 2004). In this work, we use molecular-resolution cluster kinetics simulations to study if nano-Köhler theory can be used to describe the growth of atmospheric molecular clusters.

We simulated the time-development of atmospheric cluster concentrations starting from vapor monomers up to clusters with mass diameter of ~3 nm by solving the discrete general dynamic equation for each cluster (Olenius and Riipinen, 2017). The simulated systems included two model compounds: a quasi-unary sulfuric acid–base mixture and an oxidized organic compound. In most simulations the inorganic compound was set to have the mass of a sulfuric acid–dimethylamine cluster (SA–DMA) and saturation vapor pressure  $p_{\text{sat}} = 0$ . The properties of the organic compound were varied but in most simulations it was set to have a mass of 300 amu and  $p_{\text{sat}} = 10^{-8}$  Pa, representing a low-volatile organic compound (LVOC). We performed several sets of simulations to study 1) the effect of the volatility, mass and concentration ( $C_{\text{ORG}}$ ) of the organic vapor, 2) the effect of the volatility and concentration of the inorganic vapor ( $C_{\text{SA}}$ ), and 3) the effect of time-dependent vapor concentration profiles.

From the simulated cluster concentrations, we determined the contributions of different vapor monomers and clusters to the growth over selected threshold sizes. Figure 1 shows these for the simulations with different concentrations of SA–DMA and LVOC. When  $C_{\text{ORG}} = 10^6 \text{ cm}^{-3}$ , SA monomer dominates the flux at all sizes. However, when  $C_{\text{ORG}} = 10^7 \text{ cm}^{-3}$  LVOC monomer has a significant contribution to the flux at 1 nm and at 2 nm and above, but only a minor contribution at 1.5 nm. This behavior resembles nano-Köhler activation, where the critical size, corresponding to the peak of the Köhler curve, is around 2 nm. When  $C_{\text{ORG}} = 10^8 \text{ cm}^{-3}$ , a similar behavior can be observed. When  $C_{\text{ORG}} = 10^9 \text{ cm}^{-3}$ , LVOC dominates the growth at all sizes.

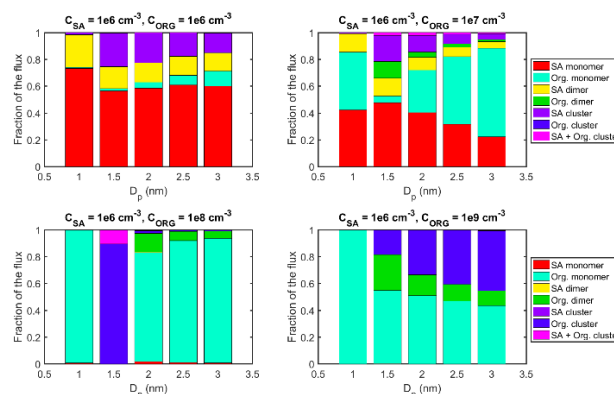


Figure 1: Contribution of different vapor monomers and clusters to the net flux past certain threshold sizes in simulations with SA–DMA and LVOC at  $C_{\text{SA}} = 10^6 \text{ cm}^{-3}$  and  $C_{\text{ORG}} = 10^6\text{--}10^9 \text{ cm}^{-3}$ . The values are at steady state.

We determined the apparent cluster growth rates (GR) using the method that is applied for measured data (Lehtipalo et al., 2014). We found that GR often increases at sizes where the organic vapor starts to contribute to the growth, but other dynamic processes can also cause a similar increase in GR. We also determined the cluster activation size from the nano-Köhler theory and compared it to the simulation results. The comparison suggests that the nano-Köhler theory cannot predict the exact size at which the organic vapor starts to contribute to the growth.

Overall, our results show that depending on the organic vapor saturation ratio ( $S_{\text{ORG}}$ ) and the ratio between organic and sulfuric acid concentrations, different growth mechanisms prevail. When  $S_{\text{ORG}} = \sim 4\text{--}40$  and  $C_{\text{ORG}}/C_{\text{SA}} = \sim 10\text{--}10000$ , nano-Köhler type behavior is observed. When  $S_{\text{ORG}}$  and  $C_{\text{ORG}}/C_{\text{SA}}$  are lower than these values, SA dominates the growth at the studied sizes, whereas with the larger values the organic compound dominates.

Kulmala, M. et al. (2004). *J. Geophys. Res.*, 109, D04205, doi:10.1029/2003JD003961.

Lehtipalo, K. et al. (2014). *Boreal Environ. Res.*, 19: 215–236.

Olenius T. and Riipinen I. (2016). *Aerosol Sci. Technol.*, doi: 10.1080/02786826.2016.1262530.

Riccobono, F. et al. (2014). *Science*, 344:717–721, doi:10.1126/science.1243527.

Riipinen, I. et al. (2012). *Nat. Geosci.*, 5:453–458, doi:10.1038/ngeo1499.

## **A comparison of long-term air concentration trends of PAH at the background regions of the Russian Federation and in some EMEP countries**

Maria Kotorova<sup>1</sup>, Sergey Gromov<sup>1,2</sup>

<sup>1</sup>Institute of Global Climate and Ecology of Roshydromet & RAS, Moscow, Russia   mkotorova.igce@gmail.com

<sup>2</sup>Institute of Geography RAS, Moscow

Key words: integrated background monitoring, biosphere reserve, long-term trends, persistent organic pollutants, statistical trend analysis.

The study is devoted to the global problem of environmental pollution with anthropogenic persistent organic compounds which now is increasingly attentive at national and international levels. The Integrated background monitoring network (IBMoN) was established and developed from 1980s in Eastern European countries to trace and evaluate the increasing anthropogenic impact on natural ecosystems by the emitted harmful pollutants. The IBMoN stations in the territory of the Russian Federation are operated by Roshydromet and they are located in pristine areas of biosphere reserves in European Russia.

The airborne polyaromatic hydrocarbons (PAH, mostly benz(a)pyren and benzperylene) are measured in air or precipitation samples collected at all stations through whole year under the unified program of observations (Izrael and Rovinsky, 1992). The mass concentrations in samples are determined by the high-performance liquid chromatography applied for the analysis of the priority PAH components. The datasets is concatenated year-by-year for the long period since early 1990s.

Our study covers investigation the PAH concentration levels in near surface atmosphere (in aerosol form) and their variations at four IBMoN stations on the European Russia over the period of 1995–2017. Along the recognition of indicative seasonal variability of benz(a)pyrene and benzperylene in air the statistical proceeding was done for the disclosure and evaluation of statistically reliable trends, their seasonal, harmonious and casual components.

The results demonstrated that the dynamics of PAH concentrations in the air have irregular changing character with non-evident seasonal variations. Maximum values always occur during the cold seasons. These findings were verified with the reference to the similar parameters obtained from EMEP observations and modelling results.

We compared trends of PAH observed at Russian IBMoN sites with the results of trend evaluation for other stations within region of EMEP (Co-Operative Program for Monitoring and Evaluation of the Long Range Transmission of Air Pollutants in Europe). The difference among the temporal changes of airborne PAH over areas of EMEP countries and IBMoN is discussed.

Izrael, Y. A. and F. Y. Rovinsky, 1992. Integrated background monitoring of environmental pollution in midlatitude Eurasia. WMO-GAW No 72, WMO TD No.434, 80 p.

# CONFIGURATIONAL SAMPLING OF ATMOSPHERIC MOLECULAR CLUSTERS

J. KUBEČKA<sup>1</sup>, T. KURTÉN<sup>2</sup> and H. VEHKAMÄKI<sup>1</sup>

<sup>1</sup>Department of Physics, University of Helsinki, Finland

<sup>2</sup>Department of Chemistry, University of Helsinki, Finland

Keywords: molecular clusters, interactions, computation, sulphuric acid, guanidine

Atmospheric air pollutants are responsible for plenty of human diseases and even for up to 7 million premature deaths per year (WHO, 2014). Not just pollutants but also other aerosol particles play important role in atmospheric chemistry and processes such as light scattering, absorption of radiation, cloud nucleation or ice crystallization. Approximately half of all particles in the Earth's atmosphere are formed from gaseous precursors, while the rest are emitted as particles. Unfortunately, the processes of formation are not still well understood. In this work, we focus on small acid-based clusters relevant to the atmosphere (Loukonen *et al.*, 2010; Torpo *et al.*, 2007, Herb *et al.*, 2011) [2-4] which seems to be driving particles growth.

For an accurate theoretical analysis of molecular clusters, a proper configurational sampling of clusters is required. Unfortunately, since the number of possible conformations (minima on a multidimensional potential energy surface (PES), see Figure 1) is growing exponentially with the size of molecular cluster, proper searching of the PES becomes computationally very expensive. Thus, we have to use some tricks for desired but still proper sampling.

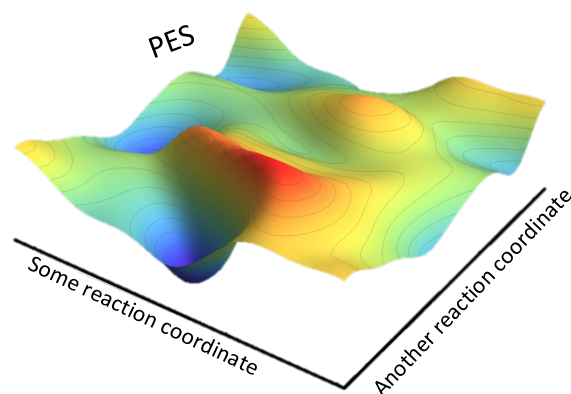


Figure 1: An illustrative example of a cut through a potential energy surface.

In this work, we would like to present a general way for theoretical configurational sampling of equilibrated molecular clusters containing mixtures of different molecules. This method is illustrated using molecular clusters containing mainly sulphuric acid ( $\text{H}_2\text{SO}_4$ ) and guanidine ( $\text{CH}_5\text{N}_3$ ) molecules in different

ratios. Since this pair of mentioned molecules often undergoes proton transfer (see Figure 2), it is very difficult to bring any effective approximation for

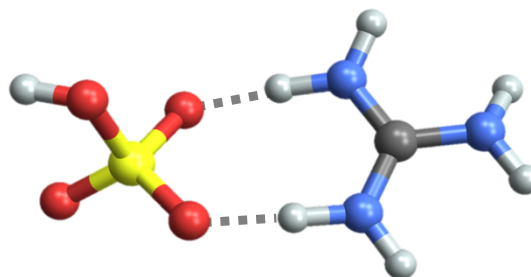


Figure 2: Illustration of the proton transfer between sulphuric acid ( $\text{H}_2\text{SO}_4$ ) and guanidine ( $\text{CH}_5\text{N}_3$ ).

theoretical description of these clusters. Thus, the exploring of the PES becomes even more expensive. We have developed a conformational sampling method employing molecular mechanics on rigid molecules, which is ultimately corrected by quantum methods. In equilibrium, protons, which undergoes the proton transfer, are closer to one of the sharing molecules. Thus, the preliminary selection of rigid molecules can contain also deprotonated or protonated versions of its neutral cases. For finding the minimum shown in Figure 2, the best initial selection would be based on one hydrogensulphate anion ( $\text{HSO}_4^-$ ) and one guanidium cation ( $\text{CH}_6\text{N}_3^+$ ). We would like to present also results for clusters containing more than 5 molecules. Moreover, we are comparing this method with some already existing methods to demonstrate its advantages.

World Health Organization (2014). *7 million premature deaths annually linked to air pollution.*, web: <http://www.who.int/mediacentre/news/releases/2014/air-pollution/en/>.

Loukonen, V., Kurtén, T., Ortena, I. K., Vehkamäki, H., Pádua, A. A. H., Sellegri, K., and Kulmala, M. (2010). *Atmos. Chem. Phys.*, 10: 4961–4974.

Torpo, L., Kurtén, T., Vehkamäki, H., Laasonen, K., Sundberg, M. R., and Kulmala, M. (2007). *J. Phys. Chem. A*, 111:10671–10674.

Herb, J., Nadykto, A. B., and Yu, F. (2011). *Chem. Phys. Lett.*, 518:7–14.

# NOVEL HIGH-RESOLUTION URBAN AIR QUALITY MODEL: DEVELOPMENT AND EVALUATION

M. KURPPA<sup>1</sup>, A. HELLSTEN<sup>2</sup>, M. AUVINEN<sup>1,2</sup>, S. KARTTUNEN<sup>1</sup>, P. KUMAR<sup>3</sup>, and L. JÄRVI<sup>1</sup>

<sup>1</sup> Institute for Atmospheric and Earth system research / Physics, University of Helsinki, Finland

<sup>2</sup> Finnish Meteorological Institute, Helsinki, Finland

<sup>3</sup> University of Surrey, Guildford, United Kingdom

Keywords: aerosol, modelling, LES, air quality, meteorology, street canyon

Air pollution is one of the greatest environmental threats to urban population, but still our capacities to study and understand the processes controlling pollutant distributions are limited. Dispersion and transformation of both aerosol particles and gaseous pollutants are ruled by local wind conditions, which in turn are modified by the presence of obstacles such as buildings and vegetation, their thermal properties as well as solar radiation. This urban complexity is, however, inadequately represented both by current air quality models and field measurements. For detailed modelling of urban air quality, the most promising method is the large-eddy simulation (LES), which resolves the three-dimensional turbulent fields of wind and scalars. With the increasing computing performance, application of computationally expensive LES can be extended to air quality modelling. Therefore, the objectives of this study are to develop and evaluate a computationally efficient, high-resolution urban LES-based air quality model, that can be used to understand the spatially and temporally varying air pollutant fields within complex urban structures. Here the focus will be on the aerosol scheme but the used model also includes a gas-phase chemistry module.

The study applies an LES model PALM (Maronga et al., 2015), which is especially suitable for simulations over a complex urban area owing to its features including schemes for a Cartesian topography, urban vegetation and solar radiation, and a land surface model to describe the physical and thermal properties of different surfaces. In this study, a sectional aerosol module SALSA (Kokkola et al., 2008) has been embedded to PALM to consider the evolution of particle concentrations and size distributions (PSD) as well as their chemical composition due to aerosol dynamic processes and local emissions. The coupled PALM-SALSA includes the processes of coagulation, condensation, dissolutional growth, nucleation and dry deposition of aerosol particles on surfaces, including vegetation. The aerosol scheme can be coupled with a gas chemistry module to acknowledge changes in the gas phase.

First evaluation of the aerosol scheme within an urban LES simulation is conducted against pseudo-simultaneous measurements of the vertical distribution of PSD in Cambridge, UK (Kumar et al., 2008). PSDs were measured on the leeward side of a street canyon as

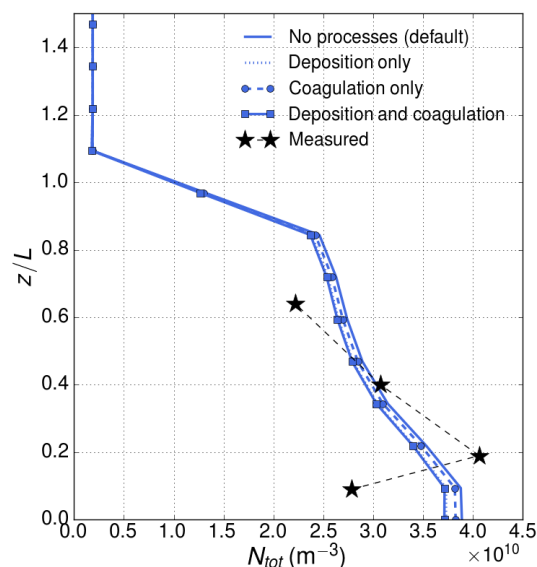


Figure 1: Vertical distribution of the total aerosol particle number concentration  $N_{tot}$  ( $\text{m}^{-3}$ ) in Cambridge, UK. Modelled profiles are given in blue and the measured with a black line with stars.

well as at a background site for consecutive 24 hours in March 2007. Simulations have been conducted for an idealistic topography including a single, infinitely long street canyon. Preliminary results show that PALM-SALSA can produce the vertical distribution of aerosol particles concentrations even with a simplified representation of the surrounding topography (Figure 1). However, simplified topography omits many turbulent scales and transport of air pollution from the surroundings. Therefore, next step is to run the model for a  $500 \text{ m} \times 500 \text{ m}$  domain with a 1-m resolution and a detailed description of the buildings and vegetation of the surrounding area.

Maronga, B., Gryschka, M., Heinze, R., et al. (2015). *Geosci. Mod. Dev.*, 8:2515–2551.

Kokkola, H., Korhonen, H., Lehtinen, K. E. J., et al. (2008). *Atmos. Chem. Phys.*, 8(9):2469–2483.

Kumar, P., Fennell, P., Langley, D., et al. (2008). *Atmos. Env.*, 42(18):4304–4319.

# USING COSMOTHERM TO EVALUATE PROPERTIES OF TERPENE OXIDATION PRODUCTS: PROMISES AND PITFALLS

T. KURTÉN<sup>1</sup>, N. HYTTINEN<sup>1</sup>, P. ROLDIN<sup>2</sup>, M. P. RISSANEN<sup>3</sup>, G. MICHALOUDI<sup>4</sup>, N. PRISLE<sup>4</sup>

<sup>1</sup>Department of Chemistry, University of Helsinki, Finland

<sup>2</sup>Division of Nuclear Physics, Lund University, Sweden

<sup>3</sup>Department of Physics, University of Helsinki, Finland

<sup>4</sup>Nano and Molecular Systems Research Unit, University of Oulu, Finland

Keywords: saturation vapor pressure, isoprene, autoxidation, quantum chemistry, COSMO-RS

A combination of statistical thermodynamics methodology with relatively simple quantum-chemical molecular data has proven useful for exploring the properties of compound types for which experimentally measured properties are scarce. We have recently applied the COSMO-RS approach (Klamt, 1995), as implemented in the COSMOTerm program (Eckert and Klamt, 2002), to explore the saturation vapor pressures and Henry's law constants of potential products formed in both sequential and peroxyradical-based autoxidation of  $\alpha$ -pinene (with either  $O_3$  or OH as the initiating oxidant), as well as to evaluate Setschenow constants for a large range of atmospherically relevant solute-salt combinations. Comparison to experimental data on a limited set of related compounds indicates that while these COSMOTerm results are far from quantitative, the predictions are systematic. For example, saturation vapor pressures are likely overestimated by up to one order of magnitude per intramolecular hydrogen bond even with the newest and highest-level parameterizations available (Krieger *et al.*, 2018), while Setschenow constants are systematically biased toward greater salting out (Toivola *et al.*, 2017). Nevertheless, COSMOTerm allows us to make useful order-of-magnitude predictions of both saturation vapor pressures, solubilities and salting behavior for systems for which no other modelling method is currently applicable. For example, our calculations strongly suggest that products of OH – initiated monoterpene autoxidation have significantly lower volatilities than the corresponding products of  $O_3$  – initiated autoxidation with identical numbers of carbon and oxygen atoms.

Isoprene dihydroxy dihydroperoxide (ISO(POOH)<sub>2</sub>; see Figure 1) provides a useful test system for evaluating volatility predictions of autoxidation products. ISO(POOH)<sub>2</sub> contains four hydrogen-bonding functional groups, and its saturation vapor pressure has recently been experimentally estimated as  $10^{-9}$  bar (D'Ambro *et al.*, 2017). ISO(POOH)<sub>2</sub> is chemically representative of larger (e.g. monoterpene) autoxidation products, yet small enough that all conformers of all structural and stereoisomers (about 70 000 in total) can be explicitly simulated. COSMOTerm-predicted saturation vapor pressures for the atmospherically dominant structural isomer ("iso1") of ISO(POOH)<sub>2</sub> are 1-2 orders of magnitude larger than the experimental estimate (see Figure 2), consistent with an overestimation of a factor of 2-3 for each of the four

intramolecular H-bonds. Unfortunately, test calculations also demonstrate that the default conformational sampling method implemented in the COSMOconf module is inappropriate for the ISO(POOH)<sub>2</sub> system, as the predicted saturation vapor pressure varies by up to a factor of 40 depending on the arbitrary input conformer. We also find large differences (up to a factor of 100) in saturation vapor pressures between stereoisomers, as well as between structural isomers, where the OH and OOH groups are located on different carbon atoms. For example, isomers with OOH groups on adjacent carbon atoms tend to have lower saturation vapor pressures, likely because of steric strain preventing efficient intramolecular H-bonding in these systems.

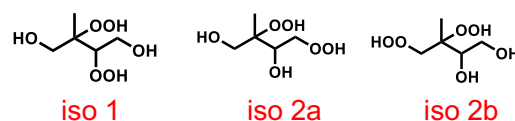


Figure 1: The three atmospherically relevant structural isomers (out of a total of 6 isomers) of ISO(POOH)<sub>2</sub>.

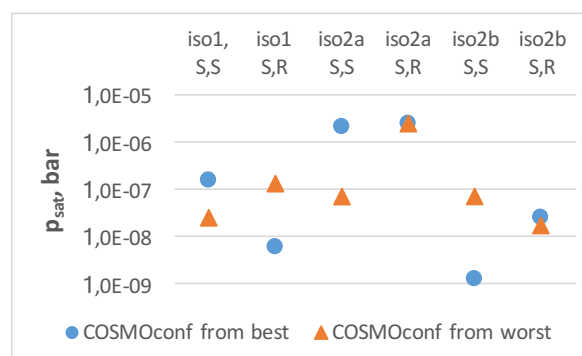


Figure 2: Predicted saturation vapor pressures (298 K) of different (stereo)isomers of ISO(POOH)<sub>2</sub>, using 100 conformers generated by COSMOconf, starting from the lowest-energy (spheres) or highest-energy (triangles) conformer from the full set (ca 2500-3000 per isomer), at the BP-TZVPD-FINE level, with COSMOTerm version C30-1705. The experimental value is ca  $10^{-9}$  bar.

D'Ambro, E., *et al.* (2017). *Atmos. Chem. Phys.* 17:159–174.

Eckert, F. and Klamt, A. (2002). *AIChE J.* 48: 369–385.

Klamt, A. (1995). *J. Phys. Chem.*, 99:2224–2235.

Krieger, U., *et al.* (2018). *Atmos. Meas. Tech.* 11:49–63

Toivola, M., *et al.* (2017). *J. Phys. Chem. A* 121:6288–6295.

# Response characterization of an inexpensive aerosol sensor

J. Kuula<sup>1</sup>, T. Mäkelä<sup>1</sup>, R. Hillamo<sup>1</sup> and H. Timonen<sup>1</sup>

<sup>1</sup>Department of atmospheric aerosols, Finnish Meteorological Institute, Erik Palmenin aukio 1, 00560, Helsinki, Finland

Keywords: inexpensive aerosol sensor, novel evaluation method, particulate matter

Particulate matter (PM) poses health risks to citizens, and therefore detailed understanding of spatial distribution of PM is desirable (Mayer, 1999). Currently, high unit cost of standardized monitoring equipment limits the availability of dense air quality monitoring networks. Inexpensive monitoring methods, such as sensors, have been therefore considered as a prospective tool for complementary air quality monitoring (Kumar et al., 2015). However, documentation about the accuracy and detailed response characteristics of the inexpensive sensors remains limited (Rai et al., 2017).

A novel laboratory evaluation method was developed to characterize the response properties of inexpensive Shinyei PPD42NS and PPD60PV sensors (Kuula et al., 2017). A continuously changing monodisperse size distribution was created by feeding two different solutions to the Vibrating Orifice Aerosol Generator (VOAG), one by one. The diffusion between the separate solutions creates a particle size gradient illustrated in Fig 1. This evaluation method is particularly useful in characterizing the sensor response as a function of particle size. A single test run lasts less than 15 minutes.

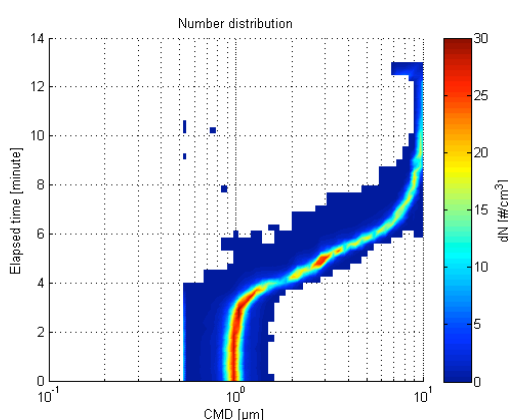


Figure 1. Generated number distribution of the novel evaluation method.

Two different particle compositions (crystalline white solid and transparent liquid) were accounted in order to examine whether the change in optical properties influenced the responses of the sensors.

Additionally, a field test was performed where the results of the laboratory tests were validated.

The Shinyei sensors responded to particulate mass concentration stimulus rather than number concentration. The highest detection efficiency for the PPD42NS was within particle size range of 2.5 – 4  $\mu\text{m}$ , and the respective optimal size range for the PPD60PV was 0.7 – 1  $\mu\text{m}$ . The field test yielded high PM mass correlations ( $R^2 = 0.962$  and  $R^2 = 0.986$ ) for viable detection ranges of 1.6 – 5 and 0.3 – 1.6  $\mu\text{m}$ , when compared to a medium cost optical dust monitor. As the size distribution of atmospheric particles tends to be bimodal, it is likely that indicatively valid results could be obtained for the  $\text{PM}_{10-2.5}$  size fraction with the PPD42NS sensor. And respectively, the PPD60PV could possibly be used to measure the  $\text{PM}_{2.5}$  size fraction.

This study was funded by TEKES funded INKA-ILMA/EAKR project (Tekes nro: 4588/31/2015) and by the Regional innovations and experimentations funds AIKO, governed by the Helsinki Regional Council (project HAQT, AIKO014).

Kumar, R., Morawska, L., Martani, C., Biskos, G., et al., (2015). The rise of Low-Costing Sensing for Managing Air Pollution in Cities *Environ. Int.*, 74, 199-205.

Kuula, J., Mäkelä, T., Hillamo, R. & Timonen, H. (2017). Response characterization of an inexpensive aerosol sensor. *Sensors*, 17(12), 2915; doi: 10.3390/s17122915.

Mayer H. (1999). Air Pollution in Cities. *Atmospheric Environment*. 33, 4029-4037.

Rai, A.C., Kumar, P., Pilla, F., Skouloudis, A.N., et al., (2017). End-User Perspective of Low-Cost Sensors for Outdoor Air Pollution Monitoring. *Science of the Total Environment*. 607, 691-705.

# TRAFFIC PRODUCES A SIGNIFICANT FRACTION OF ATMOSPHERIC NANOCLUSTER AEROSOL IN URBAN AREAS

H. Kuuluvainen<sup>1</sup>, R. Hietikko<sup>1</sup>, P. Karjalainen<sup>1</sup>, J. Keskinen<sup>1</sup>, R. Hillamo<sup>2</sup>, J. V. Niemi<sup>3</sup>, L. Pirjola<sup>4</sup>, H. J. Timonen<sup>2</sup>, S. Saarikoski<sup>2</sup>, E. Saukko<sup>1</sup>, A. Järvinen<sup>1</sup>, H. Silvennoinen<sup>1</sup>, A. Rostedt<sup>1</sup>, M. Olin<sup>1</sup>, J. Yli-Ojanperä<sup>1</sup>, P. Nousiainen<sup>5</sup>, A. Kousa<sup>3</sup>, M. Dal Maso<sup>1</sup> and T. Rönkkö<sup>1</sup>

<sup>1</sup> Aerosol Physics, Faculty of Natural Sciences, Tampere University of Technology, Tampere, Finland

<sup>2</sup> Atmospheric Composition Research, Finnish Meteorological Institute, Helsinki, Finland

<sup>3</sup> Helsinki Region Environmental Services Authority HSY, Helsinki, Finland

<sup>4</sup> Department of Technology, Metropolia University of Applied Sciences, Helsinki, Finland

<sup>5</sup> Faculty of Technology, Environment, and Business, Turku University of Applied Sciences, Turku, Finland

Keywords: nanocluster aerosol, traffic emissions, urban air

Traffic is known to emit a considerable amount of aerosol particles that influence on climate and human health. However, the knowledge on the smallest particles emitted by traffic is limited and e.g. the emission factors of such particles have not been largely studied. Modern aerosol instruments enable particle measurements down to approximately 1 nm, so the fraction of sub-3 nm particles, referred here as nanocluster aerosol (NCA), can be studied.

In our recent publication (Rönkkö et al., 2017), the NCA was studied through stationary roadside measurements in an urban street canyon and in a semiurban area, engine laboratory measurements with a modern diesel engine and on-road measurements in different environments while driving through the Europe with a mobile laboratory. The measurements were conducted during the years 2012–2015. In the spring of 2017, more measurements were carried out in a street canyon. In this abstract, we combine the old and the new results. A key instrument in all measurements was a particle size magnifier (PSM, Airmodus, Finland), which is capable of growing and detecting particles down to approximately 1 nm. The fraction of the NCA was obtained by either using a PSM in a step mode or measuring number concentrations simultaneously with a PSM and a condensation particle counter (CPC) with different cut-off sizes. In the experiments, the NCA measurement was supported e.g. by measurements for gaseous pollutants, particle size distribution and weather data.

The measurement data was sorted according to the wind direction to analyze the origin of the NCA. From the measurement data, the NCA concentrations in different urban environments were obtained, diurnal variation of the NCA on roadside was analyzed, and the emission factors of the NCA for different environments and engine loads were calculated with help of the simultaneously monitored CO<sub>2</sub> concentrations.

The fraction of the NCA varied with the measurement location but proved to be significant in all of the measurements, sometimes even over 50 % of the total particle number concentration in the air. Our results

show that the amount of the NCA varies with the wind direction, i.e., higher concentrations are observed when wind direction is from the road to the measurement site, and with the diurnal variation of traffic. The driving situations and the engine load also seem to affect the NCA concentrations. As an example of the results, Figure 1 shows the diurnal variation of the NCA concentration on weekdays during the roadside measurements in the spring of 2017.

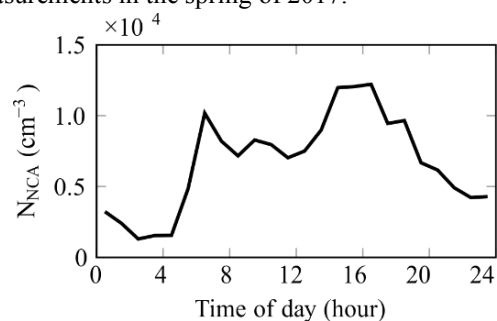


Figure 1: Diurnal variation of nanocluster aerosol (NCA) concentration in a street canyon on weekdays.

Previously the atmospheric NCA has been assumed to originate from atmospheric new particle formation, but our measurement results show that, in urban areas, the NCA can be directly emitted by traffic. NCA may form when hot gaseous precursors in engine exhaust cool rapidly or in combustion processes. In general, the NCA emissions of traffic may have a significant impact on air quality, climate and human health.

This work was funded by Tekes—the Finnish Funding Agency for Innovation, Academy of Finland Grants 283455, 259016, and 293437, Cleen Ltd. (MMEA project), Dinex Ecocat Oy, Neste Oyj, AGCO Power, Ab Nanol Technologies Oy, Helsinki Region Environmental Services Authority HSY and Pegasor Oy.

Rönkkö, T. et al. (2017). Traffic is a major source of atmospheric nanocluster aerosol. *Proceedings of the National Academy of Sciences*, 114, 7549–7554.

# FIRST RESULTS FROM “ENVISUM” PROJECT: EMISSION MEASUREMENTS ON-BOARD A RORO PASSENGER SHIP UNDER REAL OPERATING CONDITIONS

J. LAAKIA<sup>1</sup>, K. TEINILÄ<sup>1</sup>, H. TIMONEN<sup>1</sup>, S. SAARIKOSKI<sup>1</sup>, M. BLOSS<sup>1</sup>, P. KARJALAINEN<sup>2</sup>, N. KUITTINEN<sup>2</sup>, H. VESALA<sup>3</sup>, R. PETTINEN<sup>3</sup>, P. AAKKO-SAKSA<sup>3</sup> AND J.-P. JALKANEN<sup>1</sup>

<sup>1</sup>Finnish Meteorological Institute, Atmospheric Composition Research, FI-00560, Helsinki, Finland

<sup>2</sup>Tampere University of Technology, Faculty of Natural Sciences, Aerosol Physics, FI-33101 Tampere, Finland

<sup>3</sup>VTT Technical Research Centre of Finland Ltd., FI-02044 VTT, Finland

Keywords: ship emission measurements and chemical composition

Anthropogenic air pollutants emitted from Ocean-going vessels (OGVs) reach significant concentrations especially in coastal areas. The main focus of this study was to create accurate emission data for particulate matter and gases like SO<sub>2</sub>, NO<sub>x</sub> and volatile organic compounds (VOC). Chemical composition of submicron particles (< 1.0 μm) were also measured continuously. There are some literature available from on-board measurements on typical heavy fuel oil (HFO) engine at sea (Aakko-Saksa et al., 2016, Agrawal et al. 2010), but experimental measurements at realistic operation conditions and sufficient level of detail are scarce. The measured vessel was equipped with wet open loop SO<sub>x</sub> scrubber in order to reduce SO<sub>x</sub> emission levels comparable to 0.1 % sulfur content fuel also when using fuel with higher sulfur content. The vessel also had a Diesel Oxidation Catalyst (DOC) installed before the scrubber.

Real-time measurements were recorded for both the open sea cruising and harbor operation. The roro passenger ship used two different fuel types: Marine Gas Oil (MGO) and Heavy Fuel Oil (HFO). The emission measurements for particle chemical composition were conducted from exhaust pipe after the DOC and the scrubber, but gaseous compounds were measured both before and after the DOC and scrubber.

The particle sampling downstream the scrubber system was performed with a Fine Particle Sampler (FPS, Dekati Oy) equipped with a stack heater probe. In the FPS, the first stage dilution is performed with a perforated tube diluter whereas the second stage dilution unit is an ejector. The dilution air was set to the temperature of about 25 C. Total dilution ratio was determined with trace gas (CO<sub>2</sub>) measurements in both exhaust and diluted exhaust. The concentrations of total organic compounds, nitrate, sulphate, ammonium, chloride, and black carbon in particle phase (< 1 μm) were measured after dilution from fresh primary exhaust gas with high-resolution soot particle aerosol mass spectrometer (SP-AMS) (Onasch et al., 2012). In addition, black carbon concentrations was measured with a dual-spot aethalometer (AE33, Magee Scientific) (Drinovec et al., 2015). Particle number concentration and size distribution was measured using two SMPS-CPC systems (TSI Inc.) measuring particle size between 2.5-60 nm and 10-400 nm. Fourier transformation infrared

(Gasmeter DX-4000) was used to measure components from gas phase. Chemical composition of fine particulate matter of both fresh primary emissions and aged exhaust were measured to study the formation of secondary organic aerosols. Aging was simulated using a Potential Aerosol Mass (PAM) oxidation chamber (Aerodyne Research Inc.)

During open sea cruising when HFO was used sulphate and organics were main components in the submicron particulate matter, representing over 90 % of the PM<sub>1</sub>. Concentration of black carbon was low (typically < 3 mg m<sup>-3</sup>), although it increased when MGO was used and at low engine loads. FTIR measurements showed that the scrubber decreased SO<sub>2</sub> emissions to levels lower than the 0.1% Emission Control Area (ECA) requirement. VOC emissions were reduced by the DOC and very low concentrations were measured.

European Union (European Regional Development Fund) funded project Environmental Impact of Low Emission Shipping: Measurements and Modelling Strategies (EnviSuM), and Trafi (58942) are acknowledged for financial support.

Aakko-Saksa P., Aakko-Saksa P., Murtonen T, Vesala H, Nyssönen S., Puustinen H., Lehtoranta K, Timonen H, Teinilä K, Hillamo R, Karjalainen P, Kuittinen N, Simonen P, Rönkkö T, Keskinen J, Saukko E, Tutuianu M, Fischerleitner R, Pirjola L, Brunila O.-P. & E H. (2016). *28th CIMAC World Congress on Combustion Engines, At Helsinki, Finland, Volume: CIMAC, Paper no. 068.*

Agrawal, H., Welch, W.A., Henningsen S., Miller, J.W., Cocker, D.R., Emissions from main propulsion engine on container ship at sea, (2010), *J. Geophys. Res. Atmos.* 115 1–7. doi:10.1029/2009JD013346.

Drinovec, L., Mocnik, G., Zotter, P., Prévôt A., ruckstuhl, C., Coz, E., Rupakheti, M., Sciare, J., M, Müller, T., Wiedensohler, A., (2015). *Atmos. Meas. Tech.* 8 (5) 1965-1979.

Onasch, T.B., Trimborn, A., Fortner, E. D., Jayne, J.T., Kok, G.L., Williams, R.L., Davidovits, P., Worsnop, D.R. (2012). *Aerosol Sci. Tech.* 46 (7), 0278-6826 doi: 10.1080/02786826.2012.663948.



# Climate responses to Solar Radiation Management and Carbon Dioxide Removal in two Earth System Models

A. Laakso<sup>1,2</sup>, D. Millet<sup>2</sup>, S. Liess<sup>3</sup>, A.-I. Partanen<sup>4,5</sup>, H. Kokkola<sup>1</sup> and P. Snyder<sup>2</sup>

<sup>1</sup> Finnish Meteorological Institute, Atmospheric Research Centre of Eastern Finland, Kuopio, Finland

<sup>2</sup> Department of Soil, Water and Climate, University of Minnesota, Twin Cities, St. Paul, Minnesota, United States

<sup>3</sup> Department of Earth Sciences, University of Minnesota, Twin Cities, Minneapolis, Minnesota, United States

<sup>4</sup> Finnish Meteorological Institute, Climate System Research, Helsinki, Finland

<sup>5</sup> Department of Geography, Planning and Environment, Concordia University, Montreal, Canada

Keywords: geoengineering, earth system models, hydrological cycle, stratospheric aerosols

Solar Radiation Management (SRM) and Carbon Dioxide Removal (CDR) methods are proposed to prevent climate warming if fast enough carbon dioxide emission reductions are not put into action and the climate will warm in the near future. SRM methods are aiming to increase the Earth's solar reflectivity which would result in cooling at the surface. However, it has been shown that if the temperature increase due to increased greenhouse gases is compensated by SRM, it will lead to a decrease in the global mean precipitation. This is because of the changes in the radiative flux between the top of the atmosphere and the surface, which are then compensated by a reduced latent heat flux which in turn reduces the global mean precipitation Laakso et al. (2017) Samsset et al. (2016).

Here we have studied geoengineering scenarios in this century. These are compared against a representative concentration pathway 4.5 scenario which, compared to current climate, would lead to a 1.20-1.30 K warming and a 1.75 % increase in the global mean temperature and the precipitation, respectively, before the end of 21st century. All geoengineering scenarios are based on RCP 4.5 for the years 2010-2100. In the first two scenarios, the global mean temperature or precipitation is kept stable by SRM. In the third scenario, 1% of the atmospheric CO<sub>2</sub> load is removed each year until the year 2070. Model simulations are done by using MPI-ESM and CESM. In these models the stratospheric aerosol fields for SRM are included as prescribed fields, from an aerosol-climate model ECHAM-HAMMOZ simulation.

The results show that in average 110 Tg(S) and 104 Tg(S) sulfur is needed in MPI-ESM and CESM, respectively, for keeping the precipitation at the 2010 level until year 2100. However, keeping the temperature at the 2010 level requires almost double the amount of sulfur (306 Tg(S)) in MPI-ESM compared to the simulations with CESM (178 Tg(S)). Compared to the current climate, this will lead to -1.42% and -0.7% reductions in the global mean precipitation in MPI-ESM and CESM simulations, respectively. Thus, temperature and precipitation responses of SRM depend on the model used and how the radiation will change at the top of the atmosphere and at the surface. For example if a different ocean albedo for diffused and direct radiation is taken

into account, in the case of SRM, responses in the radiative budget and climate are significantly different.

Modelled CDR scenarios prevent warming which is seen in scenario RCP 4.5 with no geoengineering and the global mean temperature is roughly the same in the last decades in the 21st century as in the beginning of the simulation (2010). Surprisingly, the global mean precipitation is still 0.5% larger in 2100 than in 2010, even though global mean temperature is the same. This is because of the difference in the radiative fluxes in 2010 and end of the simulation in the CDR scenario, which further leads to a different latent heat flux and an increase in global mean precipitation.

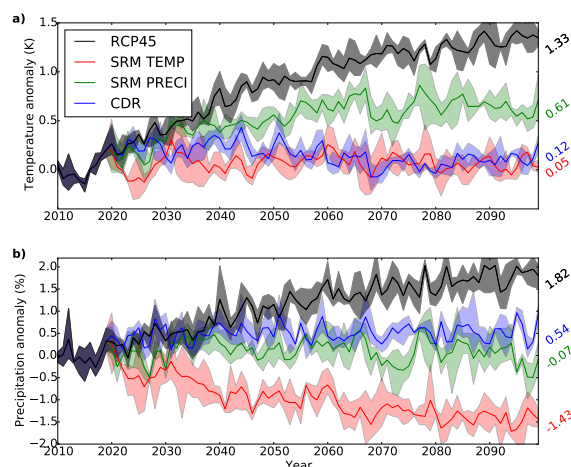


Figure 1: Global mean a) temperature and b) precipitation anomaly

Laakso, A., Korhonen, H., Romakkaniemi, S., and Kokkola, H. (2017). *Atmos. Chem. Phys.*, 117, 6957-6974

Samsset, B. H., G. Myhre, P. M. Forster, Ø. Hodnebrog, T. Andrews, G. Faluvegi, D. Fläschner, M. Kasoar, V. Kharin, A. Kirkevåg, et al. (2016). *Geophys. Res. Lett.*, 43, 2782-2791

## FRESHLY FORMED PARTICLES IN THE CAPPING INVERSION

J. LAMPILAHTI<sup>1</sup>, K. LEINO<sup>1</sup>, L. BECK<sup>1</sup>, A. MANNINEN<sup>1</sup>, P. POUTANEN<sup>1</sup>, H. JUNNINEN<sup>2</sup>, A. NIKANDROVA<sup>1</sup>, M. PELTOLA<sup>1</sup>, P. HIETALA<sup>1</sup>, L. DADA<sup>1</sup>, L. QUÉLÉVER<sup>1</sup>, I. PULLINEN<sup>3</sup>, S. SCHOBESBERGER<sup>3</sup>, T. PETÄJÄ<sup>1</sup>, M. KULMALA<sup>1</sup>

<sup>1</sup>Institute for Atmospheric and Earth System Research / Physics, Faculty of Science, University of Helsinki, Finland.

<sup>2</sup>Institute of Physics, University of Tartu, Ülikooli 18, 50090 Tartu, Estonia.

<sup>3</sup>Department of Applied Physics, University of Eastern Finland, 70211 Kuopio, Finland.

Keywords: nucleation, atmospheric aerosols, boundary layer

New particle formation (NPF) is an important yet poorly understood source of aerosol particles and cloud condensation nuclei in the atmosphere. In order to gain a more complete picture of NPF in the lower troposphere, we measured vertical profiles of aerosol particles down to 1.5 nm using an instrumented small airplane.

A Cessna 172 was equipped with a particle size magnifier (>1.5 nm particle number concentration), TSI 3776 CPC (>3 nm particle number concentration), scanning mobility particle sizer (10–400 nm particle number-size distribution) and meteorological sensors. In May 2017 the measurement flights (6 days and 40 hours in total) were performed around Hyytiälä, southern Finland and in August 2017 the flights (12 days and 63 hours in total) were around Väriö or Pallas in northern Finland.

We found elevated number concentrations of 1.5–3 nm particles and 3–10 nm particles in the interface between the residual layer and the free atmosphere, also known as the capping inversion (CI), suggesting that NPF was taking place in the layer. The subsiding particles were entrained into the developing convective boundary layer (CBL) and a growing nucleation mode was observed at the field station. The new mode was missing the initial growth phase of the particles, which supposedly happened in the CI. A simultaneously flying second Cessna with an onboard APi-TOF was measuring during the May 2017 campaign. These measurements might be able to shed more light on the particle formation process.

A suddenly appearing growing nucleation or Aitken mode without the initial particle growth is a common finding in the number size distribution measured at the SMEAR II station. A comparison with lidar measurements and soundings should elucidate if the particles indeed originate from entrained capping inversions. Our findings are in line with previous observations from Germany (Platis et al., 2015) and recent observations from the US (Chen et al., 2018; Dadashazar et al., 2017).

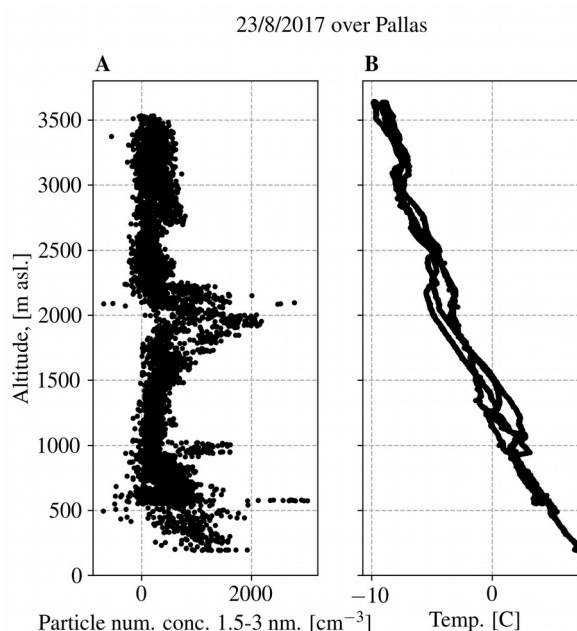


Figure 1: Panel A shows the particle number concentration between 1.5–3 nm and panel B the temperature measured on board the airplane over Pallas on the morning of August 23, 2017. A temperature inversion at 1 km, below which the particle concentration was increased, suggests the presence of a boundary layer. A capping inversion is left from the previous day's CBL at 2 km, which is where the number concentration is elevated.

Platis, A. et al. (2015). *Bound.-Layer Meteorol.* 158:67–92.

Chen, H. et al. (2018). *Atmos. Chem. Phys.* 18:311–326.

Dadashazar, H. et al. (2017). *Atmos. Chem. Phys. Discuss.*

# EXPANDING FIELD STUDY CCN MEASUREMENTS WITH CLUSTER ANALYSIS OF LONG TERM SMPS DATA

R. LANGE<sup>1</sup>, M. DALL'OSTO<sup>2</sup>, R. HARRISON<sup>3</sup>, D. C. S. BEDDOWS<sup>3,4</sup>, H. SKOV<sup>1</sup> and A. MASSLING<sup>1</sup>

<sup>1</sup>Center for Arctic Research, ICLIMATE, Department of Environmental Science, Aarhus University, Denmark

<sup>2</sup>Institute of Marine Sciences, Barcelona, Spain

<sup>3</sup>National Center for Atmospheric Sciences, University of Birmingham, United Kingdom

<sup>4</sup>Department of Environmental Sciences, King Abdulaziz University, Saudi Arabia

Keywords: CCN, Arctic aerosol, SMPS, k-means cluster analysis

In this work we use k-means cluster analysis of long term particle number size distribution data to expand measurements of Arctic aerosol CCN concentrations, from two field studies. Thereby gaining insights into longer term patterns and seasonal variation of Arctic aerosol CCN populations.

Measurements of Arctic aerosol CCN concentrations were conducted at the high Arctic research site of Villum Research station (VRS) (81°36' N, 16°40' W) during two field studies in 2016. The first field study took place in March-June, probing the aerosol of the Arctic spring (anthropogenically impacted), while the second field study was carried out in August-September (biogenically impacted).

A SMPS dataset (9-900 nm) spanning the period 2010-2016, also from VRS, was undertaken k-means cluster analysis (Beddows et al., 2009) with daily time resolution. Hereby, eight significantly different clusters were isolated. The cluster number size distributions are shown in figure 1. The average CCN concentration associated with each cluster was extrapolated to each time the respective cluster appeared during the SMPS measurement period.

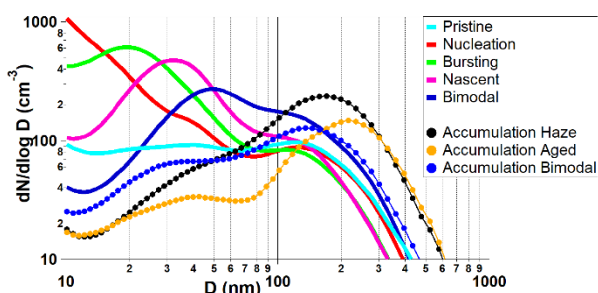


Figure 1: Average particle number size distribution of the eight clusters that were identified with k-means cluster analysis of SMPS data from VRS.

We termed the clusters according to their size distribution characteristics. The clusters have a clear seasonal pattern, where clusters: Haze, Aged and Bimodal mostly appear in winter and springtime and relate to accumulation mode aerosol. The clusters associated with higher ultrafine aerosol concentrations: Nucleation, Bursting, Nascent and Bimodal dominate the summertime aerosol. Note that a Bimodal cluster

occurs in both the ultrafine and accumulation mode group.

As each cluster appeared during our two CCN measurement periods, we were able to calculate the average CCN concentration associated with each cluster. Based on the cluster average CCN concentration and the monthly appearance of each cluster, we derive annual evolution of CCN concentrations at this high Arctic site.

The monthly average yearly CCN concentrations at three different supersaturations (SS) are presented in figure 2.

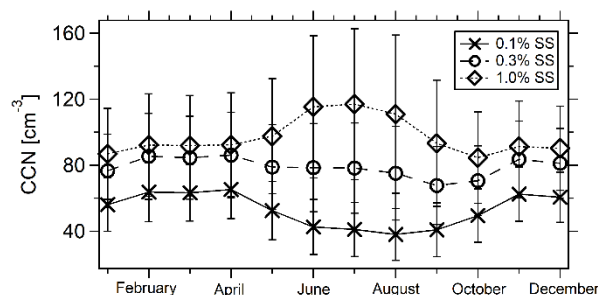


Figure 2: Yearly evolution of CCN concentrations at three different supersaturations, based on monthly size distribution cluster appearance.

The generally low CCN concentrations do not exceed 100 cm<sup>-3</sup> most of the year. Strikingly, opposite yearly trends are observed for the considered supersaturations. At low SS of 0.1% the CCN concentration decreases during summer months, while for 1.0% SS the CCN concentration increases notably during June-August. During summer the aerosol at VRS is biogenic.

Depending on the supersaturation actually achieved during natural cloud formation in the high Arctic, the CCN population might show very different trends over the course of a full year. Different CCN scenarios potentially have a large impact on the cloudiness, as the high Arctic can be a CCN-limited regime (Mauritsen et al., 2011).

Beddows, D. C. S., Dall'Osto, M., Harrison, R. M. (2009). *Environ. Sci. Technol.*, 43 (13), 4694–4700  
Mauritsen, T. et al., (2011). *Atmos. Chem. Phys.*, 11, 165–173

# NEW PARTICLE FORMATION FROM BIOGENIC PRECURSORS - EFFECT OF SO<sub>2</sub>, NO<sub>x</sub> and NH<sub>3</sub>

K. LEHTIPALO<sup>1,2</sup>, C. YAN<sup>1</sup>, L. DADA<sup>1</sup>, F. BIANCHI<sup>1</sup>, R. WAGNER<sup>1</sup>, J. DUPLISSY<sup>1</sup>, J. KIRKBY<sup>3,4</sup>, U. BALTENSBERGER<sup>2</sup>, M. KULMALA<sup>1</sup>, D. R. WORSNOP<sup>5</sup> and THE CLOUD COLLABORATION

<sup>1</sup>Institute for Atmospheric and Earth System Research, Faculty of Science, University of Helsinki, FINLAND

<sup>2</sup>Laboratory of Atmospheric Chemistry, Paul Scherrer Institute, Villigen, SWITZERLAND

<sup>3</sup>CERN, Geneva, SWITZERLAND

<sup>4</sup>Goethe University of Frankfurt am MAIN, GERMANY

<sup>5</sup>Aerodyne Research Inc., Billerica, MA, USA

Keywords: nucleation, atmospheric aerosols, chamber experiments

New particle formation (NPF) is known to be a major source of atmospheric aerosols and cloud condensation nuclei, but the exact physical and chemical mechanisms behind it are poorly understood. Due to a large number of co-varying factors in the atmosphere, laboratory experiments are crucial in isolating the effect of different chemical compounds and environmental parameters. The aim of this study was to investigate NPF under realistic daytime atmospheric conditions resembling the observations in boreal forest. This was achieved by conducting experiments in the CLOUD chamber at CERN (Kirkby et al. 2011) in the simultaneous presence of multiple precursor vapors and oxidation pathways.

Although both pure biogenic nucleation (Kirkby et al. 2016) and ternary acid-base nucleation (Dunne et al. 2016) are plausible mechanisms for new particle formation, neither of them can explain all of the observed NPF events in the boreal forest. We started the particle formation experiments from a mixture of the two most abundant monoterpenes in the boreal forest environment: alpha-pinene and delta-3-carene, and then added varying levels of SO<sub>2</sub> to produce sulphuric acid (H<sub>2</sub>SO<sub>4</sub> from less than 1e5 cm<sup>-3</sup> up to 5e7 cm<sup>-3</sup>) and repeated the experiments at different levels of NO<sub>x</sub> (from 0 to 5 ppbv) and NH<sub>3</sub> (up to 3 ppbv). To study the influence of ion-induced particle formation pathways, all experiments were conducted both without ions (neutral conditions) and with ions present, produced mainly by the ionization from galactic cosmic rays. A comprehensive suite of instruments including state-of-the-art particle counters and mass spectrometers were used to detect the forming clusters and their precursors, and to determine the particle formation and growth rates.

We will present results illustrating the interactions between different vapours in the NPF process. We show that oxidized organics, sulfuric acid and ammonia are all needed for replicating the observed nucleation and growth rates, and their variability in the boreal forest environment. We will also discuss the effect of NO<sub>x</sub> and ions on the NPF process in the different chemical systems.

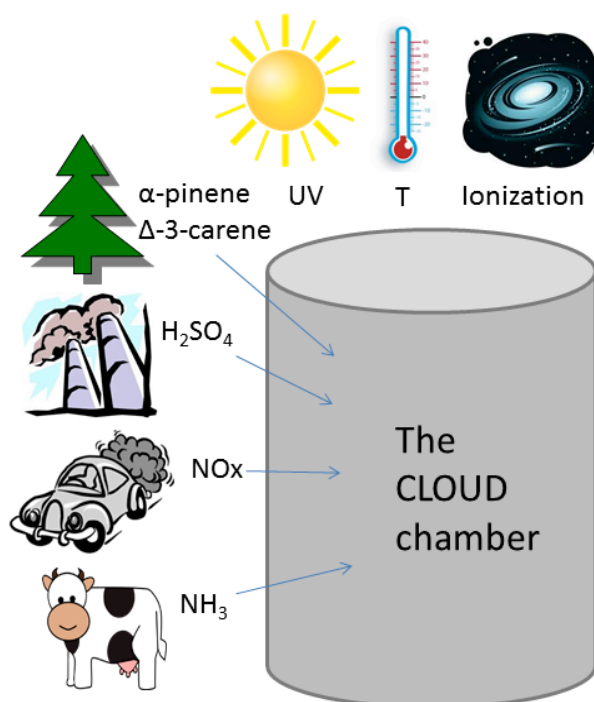


**Figure 1.** Conceptual picture of the CLOUD experiments simulating new particle formation in boreal forest.

We thank CERN for supporting CLOUD with important technical and financial resources, and for providing a particle beam from the Proton Synchrotron. This research received funding from the EC Seventh Framework Programme MC-ITN "CLOUD-TRAIN" grant no. 316662, ERC-Advanced "ATMNUCLE" grant no. 227463 and European Union's Horizon 2020 research and innovation programme under the Marie Skłodowska-Curie agreement "Nano-CAVa" grant no. 656994.

Dunne, E.M. et al. (2016). *Science* 6316, 1119-1124.

Kirkby, J. et al. (2011). *Nature* 476, 429-433.

Kirkby, J. et al. (2016). *Nature*, 533, 521-526.

# Size distributions of water-soluble ions in atmospheric aerosols in the eastern China and the implications for the formation mechanism of heavily polluted days

ANNA LI<sup>1</sup>

<sup>1</sup>Laboratory of Atmospheric Physico-Chemistry, Anhui Institute ,China

Keywords: atmospheric aerosols, Size distributions,haze, SWSI

abstract

To investigate the characteristics of aerosols in typical haze days, water-soluble inorganic ions in 8 size-segregated particle fractions, are collected by an Anderson sampler from Dec.2016 to Jan.2017 in the eastern China. The results of chemical composition analysis showed that secondary water soluble ions  $\text{NO}_3^-$ ,  $\text{SO}_4^{2-}$ ,  $\text{NH}_4^+$  (SWSI) composed more than half the total ions, and are mainly found in fine particles (aerodynamic diameters less than 2.1  $\mu\text{m}$ ), while  $\text{Ca}^{2+}$  and  $\text{Mg}^{2+}$  contributed to a large fraction of the total water-soluble ions in coarse particles (aerodynamic diameters greater than 2.1  $\mu\text{m}$  and less than 9.0  $\mu\text{m}$ ). The SWSI showed a bimodal size distribution with the

peak mass concentration of particles shifted from 0.43–0.65  $\mu\text{m}$  on clear days to 0.65–1.1  $\mu\text{m}$  on lightly polluted days and to 1.1–2.1  $\mu\text{m}$  on heavily polluted days.  $\text{NH}_4^+$  played an important role in the size distributions and the formations of  $\text{NO}_3^-$ ,  $\text{SO}_4^{2-}$ . Heterogeneous reaction is the main formation mechanism of  $\text{NO}_3^-$  and  $\text{SO}_4^{2-}$ , which tended to be enriched in the coarse mode of aerosol. Local sources played a more important role in the formation of particles. Clear evidence is presented indicating that the secondary formation of particulate was one important mechanism in the formation of the heavy pollution episodes. Meteorological conditions contributed to influence the secondary formation and regulate the size distributions of SWSI.

# EFFECT OF TEMPERATURE ON EVAPORATION OF $\alpha$ -PINENE SECONDARY ORGANIC AEROSOL

Z. LI<sup>1</sup>, A. BUCHHOLZ<sup>1</sup>, O.-P. TIKKANEN<sup>1</sup>, E. KARI<sup>1</sup>, L. HAO<sup>1</sup>, T. YLI-JUUTI<sup>1</sup> and A. VIRTANEN<sup>1</sup>

<sup>1</sup> Department of Applied Physics, University of Eastern Finland, Kuopio, Finland

Keywords: temperature, volatility, evaporation, secondary organic aerosol,  $\alpha$ -pinene

Secondary organic aerosol (SOA) consists of various organic species differing in chemical and physical characteristics. This challenges describing the condensation or evaporation of aerosol particles (Hallquist et al., 2009). One key aspect to be investigated is the volatility of SOA constituents, which governs their partitioning between gas and particulate phase. The Volatility Basis Set (VBS) framework, which categorizes organic compounds based on their saturation mass concentration ( $C^*$ ), has been coupled with the equilibrium gas-particle partitioning theory to describe both gas and aerosol composition (Donahue et al., 2006). However, previous studies have reported slower SOA evaporation than expected from VBS parametrizations, suggesting considerable impacts from particle-phase diffusion and from condensed phase reactions such as oligomer degradation (Vaden et al., 2011; Yli-Juuti et al., 2017). To date, aerosol measurements have revealed that lower temperature can significantly hinder molecular diffusion (Bastelberger et al., 2017) and suppress oligomer decomposition (DePalma et al., 2013). Given the importance of these physical and chemical processes on SOA evaporation, investigations on SOA evaporation at low temperature are needed.

Here, evaporation of  $\alpha$ -pinene SOA was studied in a relative humidity (RH) range from 0 to 80%, both at warm (20 °C) and at cold temperature (10 °C). Briefly, a continuous flow tube reactor was used to generate SOA by oxidizing  $\alpha$ -pinene with either hydroxyl radicals ( $\alpha$ pinOH) or ozone ( $\alpha$ pinO<sub>3</sub>) at room temperature. The  $\alpha$ pinOH and  $\alpha$ pinO<sub>3</sub> SOA had O:C ratio of 0.58 and 0.52, respectively. SOA was size selected by two parallel Differential Mobility Analyzers (DMAs, model 3085, TSI) operated with open loop configuration. This setup effectively removed most gas-phase compounds and promoted particle evaporation. A sample flow of 80 nm SOA was either lead directly to the instruments via a bypass line or fed into two 100-L Residence Time Chambers (RTCs). Short residence time data points were collected by varying the bypass tube length, while intermediate and long residence time data were collected from the RTCs during the filling period and in one hour intervals after SOA filling, respectively.

Characterization of particles was conducted by a Scanning Mobility Particle Sizer (SMPS, TSI) and a High Resolution Time-of-Flight Aerosol Mass Spectrometer (AMS, Aerodyne Inc.). Size selection, evaporation and size change measurement were conducted in the temperature and RH controlled environment.

Evaporation of  $\alpha$ -pinene SOA was hindered at lower temperature. This is consistent with the temperature dependence of saturation vapor pressures, but it may additionally suggest a temperature effect in the diffusion limitations in SOA particle bulk and the degradation of oligomers. Different evaporation behavior was observed for  $\alpha$ pinOH and  $\alpha$ pinO<sub>3</sub> SOA. This different volatility distribution most likely stems from a change in the particle chemical composition which is not represented by the very similar O:C ratio derived for the two SOA types.

A kinetic-based evaporation model, coupled with Clausius–Clapeyron relation, was employed to reproduce the observed evaporation and derive the enthalpy of vaporization. These simulations showed that the derived enthalpy of vaporization was higher than the typical values assumed (30–40 kJ/mol) in global aerosol models (Pye et al., 2010).

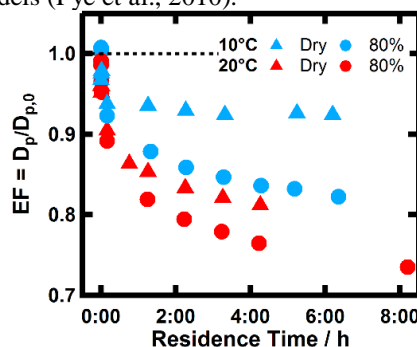


Figure 1: Measured evaporation of  $\alpha$ -pinene ozonolysis SOA with initial mobility diameter 80 nm as function of residence time under dry and 80% RH at 10 °C and 20 °C. The y-axis presents the evaporation factor (EF).

This work was supported by European Research Council (ERC starting grants 335478) and Academy of Finland (grant no. 259005 and 299544).

- S. Bastelberger, et al. (2017). *Atmos. Chem. Phys.*, 17:8453-8471.  
J. W. DePalma, et al. (2013). *Phys. Chem. Chem. Phys.*, 15:6935-6944.  
N. Donahue, et al. (2006). *Environ. Sci. Technol.*, 40:2635-2643.  
M. Hallquist, et al. (2009). *Atmos. Chem. Phys.*, 9:5155-5236.  
H. O. Pye, et al. (2010). *Atmos. Chem. Phys.*, 10:4377-4401.  
T. D. Vaden, et al. (2011). *Proc. Natl. Acad. Sci.*, 108:2190-2195.  
T. Yli-Juuti, et al. (2017). *Geophys. Res. Lett.*, 44:2562-2570.

# CCN ACTIVITY OF SIX POLLENKITTS AND THE INFLUENCE OF THEIR SURFACE ACTIVITY

J.J. LIN<sup>1,2</sup>, S.K. PURDUE<sup>2</sup>, H. LIN<sup>3</sup>, J.C. Meredith<sup>3</sup>, A. Nenes<sup>2,3,4,5</sup>, and N.L. Prisle<sup>1,2,3,6</sup>

<sup>1</sup> Nano and Molecular Systems Research Unit, University of Oulu, Oulu, 90014, Finland

<sup>2</sup> School of Earth & Atmospheric Sciences, Georgia Institute of Technology, Atlanta, 30332, USA

<sup>3</sup> School of Chemical & Biomolecular Engineering, Georgia Institute of Technology, Atlanta, 30332, USA

<sup>4</sup> Institute of Chemical Engineering Sciences (ICE-HT), FORTH, Patras, GR-26504, Greece

<sup>5</sup> Institute for Environmental Research and Sustainable Development, NOA, Athens, GR-15236, Greece

<sup>6</sup> Department of Physics, University of Helsinki, Helsinki, 00014, Finland

Keywords: bioaerosols, pollenkitt, surface activity, cloud activation

Pollen is an important class of bioaerosol with annual emissions into the atmosphere of 47–84 Tg. Both whole grains of pollen (5–150  $\mu\text{m}$ ) and fragments of pollen (0.03–5  $\mu\text{m}$ ) can act as nuclei for cloud droplets and ice crystals and therefore potentially impact Earth's hydrological cycle and radiative balance (Frohlich-Nowoisky et al., 2016). The pollen of entomophilous and zoophilous plant species are often coated with a viscous, hydrophobic liquid called pollenkitt that is thought to play important roles in pollen dispersion and adhesion (Lin et al., 2013). The exact composition of pollenkitt is thought to vary between species but is generally a hydrophobic mixture of saturated and unsaturated lipids, carotenoids, flavonoids, proteins, and carbohydrates (Pacini and Hesse, 2005). The molecular and functional composition of pollenkitt suggest that pollenkitt may be surface active in aqueous solution analogous to the surface active behavior of marine fatty acids (Prisle et al., 2008, 2010). Hydration of pollenkitt at high relative humidity has been found to change pollenkitt properties and its capillary adhesion that may in turn affect the atmospheric lifetime of pollen and ability of pollen to act as atmospheric condensation nuclei (Lin et al., 2015).

In this work, we present measurements of surface tension and supersaturated hygroscopicity of pollenkitt extracted from the pollen of six different species. Binary solutions of pure pollenkitt in water and ternary solutions of pollenkitt and ammonium sulfate in water were measured. Surface tension of the solutions were measured via axisymmetric drop shape analysis of pendant drops in air with a ramé-hart goniometer (Model 250). Scanning Mobility CCN Analysis (SMCA) is used to make rapid measurements of size-resolved CCN distributions of the pollenkitt extract for a number of supersaturations between 0.1–1.4% enabling the calculation of critical diameters and hygroscopicity parameter  $\kappa$  of pure pollenkitt and pollenkitt–ammonium sulfate mixtures. Various thermodynamic models that describe surface tension depression and bulk-to-surface partitioning of surface-active compounds were employed to predict the CCN activity and droplet surface tension at the moment of activation for mixtures of pollenkitt solutions.

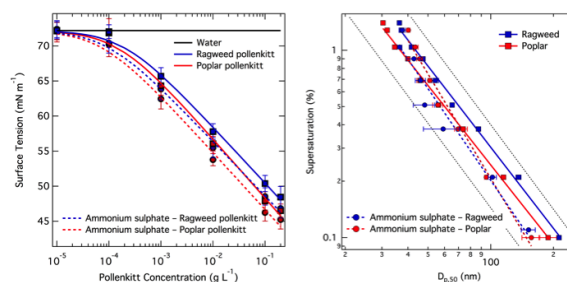


Figure 1: Surface tension depression as a function of pollenkitt concentration (left) and critical supersaturation as a function of dry diameter for two pollenkitts and their mixtures with ammonium sulfate (right).



This work was supported by the Finnish Academy of Sciences (257411), a Georgia Power Faculty chair, and a Cullen-Peck Fellowship from the Georgia Institute of Technology. This project has received funding from the European Research Council (ERC) under the European Union's Horizon 2020 research and innovation programme (grant agreement 717022).

Frohlich-Nowoisky, J., et al. (2016). *Atmos. Res.*, 182:346–376.

Lin, H., Gomez, I., and Meredith, J. C. (2013). *Langmuir*, 29:3012–3023.

Pacini, E. and Hesse, M., 2005. *Flora*, 200:399–415.

Prisle, N., et al. (2008). *Tellus B*, 60B:416–431.

Prisle, N. L., et al., (2010). *Atmos. Chem. Phys.*, 10:5663–5683.

Lin, H., et al., (2015). *J. Colloid Interf. Sci.*, 442:133–139.

# CLEANING SPRAY AEROSOLS: CHARACTERIZATION OF AIRBORNE PARTICLES

K. LOVÉN<sup>1</sup>, C. ISAXON<sup>1</sup>, A. WIERZBICKA<sup>1</sup> and A. GUDMUNDSSON<sup>1</sup>

<sup>1</sup> Department of Design Sciences, Ergonomics and Aerosol Technology, Lund University, Sweden

Keywords: cleaning spray, aerosol characterization, particle size distribution, mass median aerodynamic diameter, respiratory deposition

Cleaning workers belong to a large occupational group, which is exposed to many risk factors, including handling of cleaning products. Documented risks for professional cleaners include development of asthma and other respiratory symptoms (Unge *et al.*, 2007; Lillienberg *et al.*, 2013). Spray is a cleaning method with the advantage of easy use and even and precise dosage. A survey ( $n=225$ ) conducted within this study confirmed that spray cleaning products are used by about 78 % of the Swedish professional cleaning workers that participated in the survey. There are some studies (e.g. Zock *et al.*, 2007) linking the specific use of cleaning sprays to high occurrence of development of new-onset asthma as well as other respiratory symptoms. In order to determine how aerosols from cleaning sprays are deposited in the respiratory tract and why they cause airway symptoms, knowledge of the particle characteristics is needed.

In this study, cleaning spray aerosols were characterized in terms of size distributions and new particle formation from ozone reactions. The respiratory deposition fraction was calculated for the measured particles.

Seven different cleaning sprays were characterized. The different aerosol particle size distributions were measured in a 1.33 m<sup>3</sup> stainless steel chamber with controlled temperature, relative humidity and air exchange rate, provided through a conditioning system. Particle concentrations and size distributions (0.5-20 μm) were measured using an Aerodynamic Particle Sizer (APS model 3321, TSI Inc., USA).

In a 21.6 m<sup>3</sup> stainless steel chamber, with air provided through the same conditioning system, new particle formation from cleaning spray use in the presence and absence of ozone was studied. Three of the seven products were chosen for these measurements. A Fast Aerosol Mobility Size Spectrometer (DMS500 MkII, Cambustion, UK) was used to measure particle concentrations and size distributions (0.005-1 μm).

From the particle number concentration and size distributions measured with the APS, the particle mass median aerodynamic diameter (MMD<sub>ac</sub>) could be calculated for the different sprays. The MMD<sub>ac</sub> for the seven different sprays ranged from 1.9 μm to 3.9 μm. The mass size distributions of three of the cleaning sprays (Window B, Bathroom A and Bathroom B) can be seen in Figure 1. The MMD<sub>ac</sub> did not change significantly over time, indicating an extensive and rapid natural evaporation for all the tested cleaning sprays.

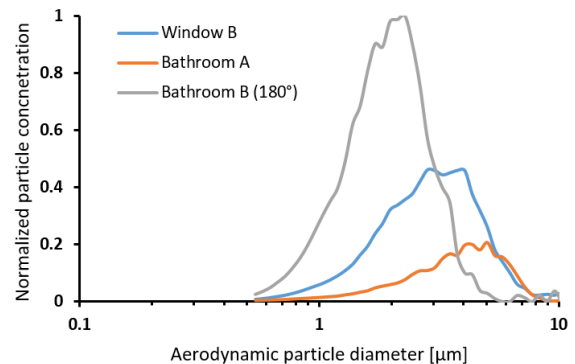


Figure 1. Particle mass size distributions for three of the seven cleaning sprays tested based on APS measurements (0.5-20 μm). The particle concentration was normalized against the maximum concentration value.

During the experiments conducted with and without ozone present, the changes in particle number concentration and size distribution over time were measured with the DMS. A particle number concentration increase (0.005-1 μm) could be seen for all three cleaning spray products, however, a difference in the amount of increase was observed between the different products. These results indicate a difference in potential for new particle formation for different products, probably due to differences in volatile organic compound (VOC) concentrations generated during spray use. From the size distributions, a slight size shift can be seen over time, demonstrating not only new particle formation, but also growth in particle size in the presence of ozone.

Calculations of the respiratory deposition fractions show dominating deposition in the alveolar and nasal regions.

Outcomes of this study implies that particles generated from the use of cleaning sprays, due to their pattern of deposition in the respiratory system, can contribute to the observed health effects.

This work was supported by Swedish AFA Insurance.

Lillienberg *et al.* (2013) *Annals of Occupational Hygiene* **57**(4):482-492.

Unge *et al.* (2007) *International Archives of Occupational and Environmental Health* **81**:209-220.

Zock *et al.* (2007) *American Journal of Respiratory and Critical Care Medicine* **176**:735-741.



# TRENDS OF AEROSOL OPTICAL PROPERTIES AT THE SMEAR II STATION

K. LUOMA<sup>1</sup>, A. VIRKKULA<sup>1,2</sup>, P. AALTO<sup>1</sup> and T. PETÄJÄ<sup>1</sup>

<sup>1</sup> Department of Physics, University of Helsinki, Finland

<sup>2</sup> Finnish Meteorological Institute, Helsinki, Finland

Keywords: atmospheric aerosols, optical properties, trends

Measurement of aerosol optical properties are needed in determining the radiative forcing related to the aerosol particles. Due to the large temporal and spatial variation, the effect of aerosol particles on the climate is still one of the biggest uncertainties in determining the global radiative forcing (Boucher *et al.*, 2013).

The absorption, scattering and backscattering coefficient of aerosol particles at multiple wavelengths have been measured at the SMEAR II station since 2006. The SMEAR II station is located in Hyytiälä, Finland (61°51'N, 24°17'E) and it represents boreal forests. The measurements presented in this study have been conducted for particles smaller than 10 µm (PM10). The measurements were conducted for dried air (RH < 40 %).

The scattering and backscattering coefficients ( $\sigma_{sca}$  and  $\sigma_{bsca}$ ) on three wavelengths were measured with an integrating nephelometer (TSI model 3563) and the absorption coefficient ( $\sigma_{abs}$ ) on seven wavelengths were measured with an aethalometer (Magee Scientific model AE-31). The trends and the significance of the trends were determined by using the seasonal Kendall test described in Gilbert (1987). The trends were calculated by using monthly medians.

The resulted trends and their significance are presented in Table 1. All of the extensive properties ( $\sigma_{sca}$ ,  $\sigma_{bsca}$  and  $\sigma_{abs}$ ) have a significant negative trend, which is caused by a decrease in the aerosol number concentration.

For the intensive properties, significant trends were found for the backscattering fraction ( $b$ ), scattering Ångström exponent ( $\alpha_{sca}$ ), imaginary part of the complex refractive index ( $k$ ) and for the aerosol forcing efficiency ( $\Delta F\delta^{-1}$ ). The trends for  $b$  and  $\alpha_{sca}$  describe the change in the size distribution. Increasing trend in the  $b$  and  $\alpha_{sca}$  indicates that the weight in the size distribution of aerosol particles is moving towards smaller particles. Since the  $k$  describes how much the particles are absorbing light, the negative trend for the  $k$  indicates that the particles are not as efficient absorbers as before.

The  $\Delta F\delta^{-1}$  describes the difference the aerosol particles would make to the radiating forcing ( $\Delta F$ ) per unit of aerosol optical depth ( $\delta$ ). The  $\Delta F\delta^{-1}$  was calculated according to the equation by Charlson *et al.* and the values were chosen according to Haywood and Shine (1995). The negative trend in  $\Delta F\delta^{-1}$  means that the particles are more efficiently cooling the climate. It must be noted that the  $\Delta F\delta^{-1}$  was calculated for dried aerosol particles and that the values used in the equation were constant, so the  $\Delta F\delta^{-1}$  doesn't describe ambient aerosol.

	Trend (yr <sup>-1</sup> )	Trend (% yr <sup>-1</sup> )	p-value
$\sigma_{sca}$ (Mm <sup>-1</sup> )	-0.25	-2	< 0.05
$\sigma_{bsca}$ (Mm <sup>-1</sup> )	-0.029	-2	< 0.05
$\sigma_{abs}$ (Mm <sup>-1</sup> )	-0.050	-3	< 0.05
$\omega$	2.2e-3	-0.3	0.10
$b$	1.3e-3	1	< 0.01
$\alpha_{sca}$	0.021	1	< 0.01
$\alpha_{abs}$	-3.3e-3	-0.3	0.23
$n$	-1.3e-4	0.0	0.86
$k$	-7.4e-4	4	< 0.01
$\Delta F\delta^{-1}$ (W m <sup>-2</sup> )	-0.28	1	< 0.01

Table 1: Trend for different optical properties of aerosol particles. Also the annual change in percentages is shown as well as the p-value. If the p-value is above 0.05 the trend is not statistically important.

- Boucher, O., Randall, D., Artaxo, P., Bretherton, C., Feingold, G., Forster, P., ... & Rasch, P. (2013) Clouds and aerosols. In Climate change 2013: The physical science basis. Contribution of working group I to the fifth assessment report of the intergovernmental panel on climate change (pp. 571-657). Cambridge University Press.
- Charlson, R.J., Laugher J., Rodhe, H., Leovy, C.B., Warren, S.G., Perturbation of the Northern Hemisphere Radiative Balance by Backscattering from Anthropogenic Sulfate Aerosols. *Tellus*, J3AB, 152-163, 1991.
- Gilbert, R. O.: Statistical methods for environmental pollution monitoring, John Wiley & Sons, 1987.
- Haywood, J. and Shine, K.: The effect of anthropogenic sulfate and soot aerosol on the clear sky planetary radiation budget, *Geophysical Research Letters*, 22, 603–606, 1995.

# SEAMLESS MULTI-SCALE AND -PROCESSES MODELLING ACTIVITIES AT INAR

A. MAHURA<sup>1</sup>, R. MAKKONEN<sup>1</sup>, M. BOY<sup>1</sup>, T. PETÄJÄ<sup>1</sup>, M. KULMALA<sup>1</sup>, S. ZILTINKEVICH<sup>1</sup>  
and “ENVIRO-PEEX ON ECMWF” MODELLING TEAM

<sup>1</sup>Institute for Atmospheric and Earth System Research (INAR) / Physics, Faculty of Science, University of Helsinki (UHEL), Finland

Keywords: seamless modelling, processes, components, scales, Enviro-PEEX on ECMWF HPC project

The Pan-Eurasian EXperiment (PEEX) Modelling Platform (MP) presents a strategy for best use (<https://www.atm.helsinki.fi/peex/index.php/modelling-platform>) of current generation modeling tools to improve process understanding and improve predictability on different scales in the PEEX domain. At INAR, as part of the research project “Enviro-PEEX on ECMWF” (2018-2020) a number of application areas of new integrated modelling developments are expected, including research and developments for: (i) improved numerical weather prediction and chemical weather forecasting with short-term feedbacks of aerosols and chemistry on meteorological variables; (ii) two-way interactions between atmospheric pollution/composition and climate variability/ change; (iii) better prediction of atmosphere and/or ocean state through closer coupling between the component models to represent the two-way feedbacks and exchange of the atmospheric and ocean boundary layer properties; (iv) more complete/ detailed simulation of the hydrological cycle, through linking atmospheric, land surface, ecosystems, hydrological and ocean circulation models. The overall objectives of the special project will be to analyse the importance of the meteorology-chemistry-aerosols interactions and feedbacks and to provide a way for development of efficient techniques for on-line coupling of numerical weather prediction and atmospheric chemical transport via process-oriented parameterizations and feedback algorithms, which will improve the numerical weather prediction, climate and atmospheric composition forecasting.

The on-line integrated/ seamless coupling includes different processes, components, scales and tools (schematics is shown in Figure 1). At INAR, among the research tools to be applied are the EC-Earth, Enviro-HIRLAM, ASAM, SOSAA, MALTE-box and other models. The scales to be considered cover scales from micro- to local, urban, sub-regional, regional, hemispheric, global; and from box-model to large eddy simulations, meso- and climate scales. The horizontal resolutions for models runs are ranging from a few meters to more than a degree in the latitudinal-longitudinal domain. The processes, at the current moment studied at different degree of understanding and to be considered include meteorological and climatological, chemical and aerosols, biological, hydrological, and others as well as taking into account society interactions (see Figure 1).

The simulations are expected for: (i) short-term case studies with physical and chemical weather forecasting

(downscaling from hemispheric-regional-subregional to urban/ city scales) in order to evaluate sensitivity of aerosol feedback effects on meteorology, atmospheric composition and climate; (ii) episodes simulations for weather, climate and air quality applications to evaluate possible effects; (iii) testing of parameterisations, meteorological and chemical initial and boundary conditions, and chemical data assimilation.

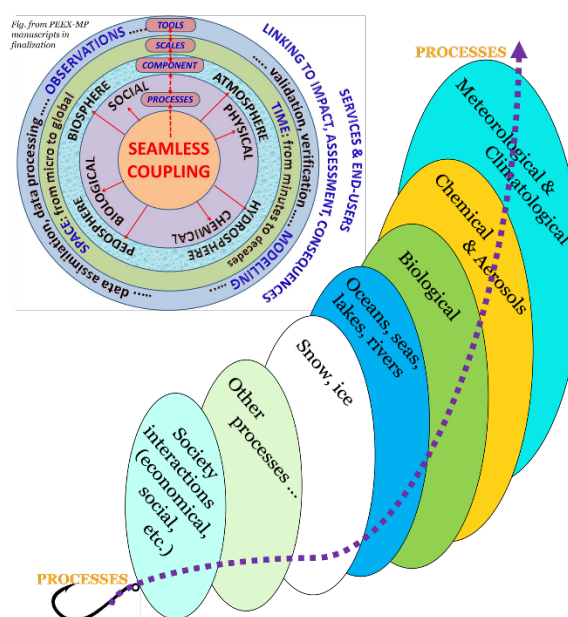


Figure 1: Seamless coupling and considered processes (left figure – Baklanov, Mahura et al. PEEX-MP, in finalization, 2018)

Available observations for atmosphere and ecosystems (in particular, from the SMEAR-II and PEEX metadatabase stations) are to be used for data assimilation and data processing as well as for the models validation and verification studies.

The IT Center for Science (CSC, Finland; <https://www.csc.fi>) and European Center for Medium-range Weather Forecasting (ECMWF, UK; <https://www.ecmwf.int>) will be in a close collaboration with INAR, where CRAY’s supercomputing facilities, mass storage systems, meteorological and atmospheric composition data archives are to be used extensively.

**Enviro-PEEX on ECMWF (2018-2020): Pan-Eurasian EXperiment (PEEX) Modelling Platform research and development for online coupled integrated meteorology-chemistry-aerosols feedbacks and interactions in weather, climate and atmospheric composition multi-scale modelling.** HPC ECMWF project, PI – A. Mahura.

# IDENTIFYING GLOBAL AEROSOL-CLIMATE INTERACTIONS THROUGH GEOSPATIAL NETWORK ANALYSIS

R. MAKKONEN<sup>1</sup> and M. KULMALA<sup>1</sup>

<sup>1</sup>Institute for Atmospheric and Earth System Research / Physics  
Faculty of Science, University of Helsinki, Finland

Keywords: global modeling, aerosol-cloud interactions, network analysis

Climate models provide a fruitful platform for generating Big Data: Coupled Model Intercomparison Project Phase 5 (CMIP5) produced already several petabytes of data, while ongoing CMIP6 is expected to surpass with potentially tens of petabytes. The large climate datasets allow for application of novel data science methods, and increasing model complexity and interactivity allows exploration of undisclosed patterns, interactions and feedbacks mechanisms.

Fountalis et al. (2014) proposed network-analysis framework for studying climate variable patterns. The process involves identification of geographical regions based on e.g. homogeneity of a certain variable. The established regions can further be considered as nodes, and network analysis can be used to find interconnections in the coupled system.

Global aerosol-climate models produce easily several terabytes of data even during one-year simulation. During subsequent post-processing, there is urgent need to reduce amount of data, usually by reduction of temporal resolution. However, temporal averaging distorts the data, hindering analysis of e.g. aerosol-cloud-climate interactions. Constructing spatial nodes based on variable homogeneity is one mechanism for spatial dimension reduction, while it also allows for analyzing interactions between aerosol and precursor sources, aerosol formation, and clouds. Furthermore, cluster detection helps to assess model performance against observations: does the model and observations show similar spatial clusters and do they behave consistently, or are there spatial shifts in the model response?

We have developed a software package which contains modules for 1) automatic cluster (node) detection from geospatial datasets and 2) network generation from detected clusters. The Python software package reads in NetCDF-files as input, and outputs data and figures (maps) of detected clusters. The same software can then be applied to detect networks between established nodes or to analyze node correlation to separately given time series (e.g. climate indices).

Here we present selected results of potential applications of network analysis of aerosol-climate connection. For example model input, we use ECHAM-HAM aerosol-climate model (Zhang et al., 2012). As an example of observations, we show results on MODIS Level 3 product *PSML003\_Ocean* (Terra, Collection 6).

In our example, we have chosen to cluster single vertical level (atmospheric column integral) data acquired from models and observations during the period 2001-2010. We deseasonalize the data throughout the period and consider only monthly anomalies. Figure 1 shows an example of clustering based on simulated cloud condensation nuclei (CCN) data (0.2% supersaturation) over oceans. In this case, the algorithm requires a minimum correlation between any two gridcell timeseries. The size of the domains is a direct consequence of selected parameter values for required homogeneity (minimum correlation).

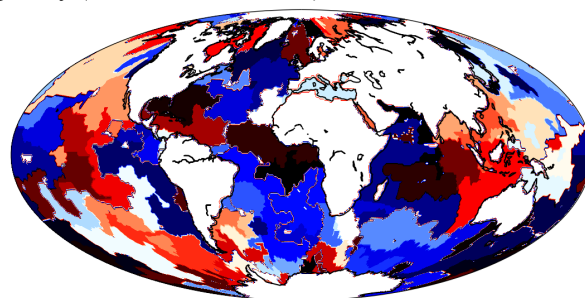


Figure 1: Example of detected clusters of monthly CCN concentration anomalies simulated by ECHAM-HAM during 2001-2010. An individual cluster would show similar response to e.g. emission or climate changes.

We have applied the algorithm to anomalies in climate (temperature, precipitation) aerosol sources (anthropogenic and biogenic emissions, sea spray, dust), aerosol concentrations, and cloud properties. This allows us to detect spatial responses to perturbations and later, given a set of sensitivity simulations, attributing the aerosol-climate responses to e.g. emission sectors. Further, we have used the methodology to pinpoint certain issues in the model not being able to capture the observed anomalies.

This work has been supported by Nordic Centre of Excellence eSTICC and the EU FP7 project BACCHUS. R.M. would like to thank Athanasios Nenes for fruitful discussions.

Fountalis, I., Bracco, A. & Dovrolis, C (2014). *Clim. Dyn.*, 42: 879.

Zhang, K. et al. (2012). *Atmos. Chem. Phys.* 12: 8911-8949.

# A PHYSICALLY CONSISTENT PARTITIONING SCHEME FOR TREATMENT OF SURFACTANTS IN AQUEOUS AEROSOLS

J. MALILA and N.L. PRISLE

Nano and Molecular Systems Research Unit, University of Oulu, Finland

Keywords: partitioning, surfactants, atmospheric aerosols

The role of surface active organic compounds in hygroscopic responses of aerosol particles has been a recurrent issue in the atmospheric sciences, as such responses modulate not only aerosol–cloud interactions, but also effects of particulate matter on plant and animal health (Brimblecombe and Latif, 2004). Over the years, various schemes have been proposed for the treatment of this issue in models describing aerosol microphysics, including Gibbsian thermodynamic concept of surface excess quantities (e.g. Sorjamaa et al., 2004; Prisle et al., 2010) and physical surface layer (or film) models, either with fixed surface thickness  $\delta$  (e.g. Ovadnevaite et al., 2017) or composition (e.g. Ruehl et al., 2016). While the Gibbsian model is in principle completely general, in contrast to other proposed approaches, it can be prone to numerical issues related to the functional forms that are assumed for parameterisations of various thermodynamic quantities. Here we propose an alternative partitioning scheme, which consists of a surface monolayer with composition depending thickness and mass-conserving partitioning between bulk and surface.

The pivotal relation for the partitioning scheme is the equation relating surface tension  $\sigma$  to the composition of the surface: we extend the so-called modified Eberhart model for ternary mixtures,

$$\sigma(\mathbf{x}^B) = \frac{\sum_{i=1}^3 v_i \sigma_i x_i^S}{\sum_{i=1}^3 v_i x_i^S}. \quad (1)$$

Here  $\mathbf{x}^B = (x_1^B, x_2^B, x_3^B)$  are the bulk mole fractions,  $v_i$  and  $\sigma_i$  the partial molecular volume and surface tension of pure compound  $i$ , respectively, and  $\mathbf{x}^S$  the surface mole fractions. This model has earlier been found to give a good description of surface enrichment in binary water–alcohol mixtures (Raina et al., 2001; Salonen et al., 2005), and can naturally be extended to any number of components (although obviously no analytic solution for  $\mathbf{x}^S$  cannot be obtained in ternary or higher cases). In spirit of Eq. (1), the thickness of the surface layer is estimated as

$$\delta = \left( \frac{6 \sum_{i=1}^3 v_i x_i^S}{\pi} \right)^{1/3}. \quad (2)$$

The partitioning of molecules between bulk and surface is calculated using a mass-conserving approach, where densities of bulk and surface phases are taken to be those of macroscopic liquid with the same composition than the given phase.

In initial calculations, this new partitioning scheme has been found to agree reasonably well with

direct measurements of surface enrichment in ternary water–surfactant–salt/acid solution droplets (Bzdek and Reid, unpublished data; cf. Bzdek et al., 2016), often giving an improved description when compared to the Gibbsian droplet model (Prisle et al., 2010). Successful application of the partitioning scheme requires, however, thermodynamically consistent parameterisations of the ternary and unary surface tensions and ternary, binary and unary densities potentially extending beyond stable liquid regime, as the composition of the surface phase may differ from those accessible in equilibrium samples. Further development of the model is aimed to provide a better description of the cloud condensation activity of aerosol particles containing surface active organic species.



This project has received funding from the European Research Council (ERC) under the European Union’s Horizon 2020 research and innovation programme (grant agreement no. 717022).

- Brimblecombe, P. and Latif, M. T. (2004). *Environ. Chem.*, 1:11–12.
- Bzdek, B. R., Power, R. M., Simpson, S. H., Reid, J. P. and Royall, C. P. (2016). *Chem. Sci.*, 7:274–285.
- Ovadnevaite, J., Zuend, A., Laaksonen, A., Sanchez, K. J., Roberts, G., Ceburnis, D., Decesari, S., Rinaldi, M., Hodas, N., Facchini, M. C., Seinfeld, J. H. and O’Dowd, C. (2017). *Nature*, 546:637–641.
- Prisle, N. L., Raatikainen, T., Laaksonen, A. and Bilde, M. (2010). *Atmos. Chem. Phys.*, 10:5663–5638.
- Raina, G., Kulkarni, G. U. and Rao, C. N. R. (2001). *J. Phys. Chem. A*, 105:10204–10207.
- Ruehl, C. R., Davies, J. F. and Wilson, K. R. (2016). *Science*, 351:1447–1450.
- Salonen, M., Malila, J., Napari, I. and Laaksonen, A. (2005). *J. Phys. Chem. B*, 109:3472–3479.
- Sorjamaa, R., Svenningsson, B., Raatikainen, T., Henning, S., Bilde, M. and Laaksonen, A. (2004). *Atmos. Chem. Phys.*, 4:2107–2117.

# CONSEQUENCES OF AEROSOL ABSORPTION BY BEKOKO MINES EMPLOYEES IN SOUTH WEST CAMEROON

EBENEZER Jacquard Mallon<sup>1</sup>, Maurice CHUAMOU<sup>2</sup>, and Dr. Paul AGBE<sup>3</sup>

<sup>1</sup>Ecosystem and Environmental Risk Office, Freedom Life NGO, Cameroon

<sup>2</sup>Department of Environmental sciences, institute NGASSI, Cameroon

<sup>3</sup>Cameroon Institute of Specialization, Douala, Cameroon

Keywords: climate, atmospheric aerosols, water, sulphuric acid, ammoniac, health

## **Background:**

The industrial revolution has caused the transformation of society, and atmospheric pollution and greenhouse gases contribute to the warming of the earth. Atmospheric aerosols are at the heart of scientific concerns because of their proven but not yet controlled impacts on global climate change, air quality and human health. In addition, the African continent is recognized as a major source of atmospheric aerosols globally. Our study focuses on the impact of dust particles from the Békoko mines in the South region of Cameroon being absorbed by employees.

## **Objectives:**

To identify the risk factors involved in the absorption of dust particles in employees working on the Bekoko mines, in southwest Cameroon

## **Method:**

This is a descriptive quantitative study retrospective during a period of 6 months (September to February 2017) in the Bekoko mines. We used SPSS and Excel 2007 software to analyze the data collected.

## **Results:**

484 cases were searched, of which 52 cases of illness were identified. 20 women and 32 men. They suffered heart palpitation, tuberculosis, pulmonary infection, loss of eyesight and strong cough.

## **Conclusion:**

These results demonstrate the severity and magnitude of the situation. Occupational health and safety measures must be put in place for good performance and especially for the health of the employees. However, the state through the ministry of labor and public policies do not invest enough for the protection of the worker. What are the government measures implemented in these cases?

## **References:**

Olivier Boucher (2015). Atmospheric Aerosols: Properties and Climate Impacts. Pages

<http://www.aerodrug.com/News-from-the-European-Aerosol.html>

Course support Dr. Agbe, environmental pollution, Cameroon Institute of Specialization (2017)

# RELATING AEROSOL MASS SPECTRA AND THERMAL OPTICAL ANALYSIS (OC/EC) FOR PRIMARY BROWN CARBON EMISSIONS

V.B. Malmborg<sup>1</sup>, A.C. Eriksson<sup>1</sup>, C. Andersen<sup>1</sup>, S. Török<sup>2</sup>,  
C. Boman<sup>3</sup>, R. Lindgren<sup>3</sup>, K. Lovén<sup>1</sup>, M. Tuner<sup>4</sup>, P-E. Bengtsson<sup>2</sup> and J. Pagels<sup>1</sup>

<sup>1</sup>Division of Ergonomics and Aerosol Technology, Lund University, Sweden

<sup>2</sup>Department of Combustion Physics, Lund University, Sweden

<sup>3</sup>Thermochemical Energy Conversion Laboratory, Umeå University, Sweden

<sup>4</sup>Division of Combustion Engines, Lund University, Sweden

Keywords: Fullerenes, Brown Carbon, Soot, Combustion Particles

Black carbon (BC), or soot, requires high formation temperatures and forms in most incomplete combustion processes. Emissions of primary brown carbon (BrC) in combustion processes are documented but relationships between BrC emissions and combustion conditions are missing, as well as knowledge about the chemical composition of BrC emissions. We studied BrC emissions and optical, physical and chemical properties of soot from different combustion sources under varying operating conditions.

Soot was generated by common combustion sources: cook stoves, a wood stove, a heavy-duty diesel engine, and a diffusion flame burner. Particle emissions were collected on quartz filters for thermal-optical organic and elemental carbon analysis (OC/EC) according to the EUSAAR 2 protocol. The soot was probed by an aethalometer (AE33) to derive information on the optical properties, and a soot particle aerosol mass spectrometer (SP-AMS; Aerodyne Research Inc.) to study the chemical composition. The SP-AMS detects the chemical composition of non-refractory and refractory soot particle components. In some experiments semi-volatile particulate matter was removed in a thermodenuder (250°C for 5-10s) prior to sampling, allowing refractory particle components to be studied separately from the major part of non-refractory components.

BrC was identified in emissions during air-starved flaming combustion at reduced temperatures from the wood stove, several of the cook stoves, the burner, and the diesel engine. For these combustion conditions, particle emissions were commonly characterized by large amounts of particle bound polycyclic aromatic hydrocarbons (PAHs) and were for selected cases linked to poorly graphitized soot with short carbon lamellae and highly amorphous nanostructures. Soot particles from these conditions were all associated with high mass fractions of larger polycyclic aromatic hydrocarbons (PAHs), with five or more rings, and strong wavelength dependent light absorption with absorption Ångström exponents larger than 1.5.

The SP-AMS analysis showed that non-refractory components were commonly shifted from aliphatic-dominated for BC soot to aromatic-dominated for the brown, amorphous soot. Thermal-optical OC to EC analysis separates both OC and EC in four sub-

groups of decreasing volatility (OC1-4, EC1-4). Some OC may form pyrolysis products and a separate class termed pyrolytic OC is also included. For the BC dominated soot, EC emissions were high, while OC emissions were low, and mainly of low volatility (OC1-3). The BrC rich soot was associated with higher OC to EC ratios, OC of lower volatility (OC4) and more pyrolytic OC.

SP-AMS mass spectra of the BrC rich soot were all associated with refractory carbon fragments of fullerenes and other large refractory carbon clusters ( $rC_{>5}$ ; Malmborg et al. 2017). Figure 1 displays EC to total carbon (TC) fractions of BC dominated soot (1, 3) and BrC rich soot (5, 6, 7) derived from thermo-optical and SP-AMS analysis from the burner. The large carbon clusters ( $rC_{>5}$ ) are associated with pyrolytic OC and OC4 of the corresponding thermal-optical analysis

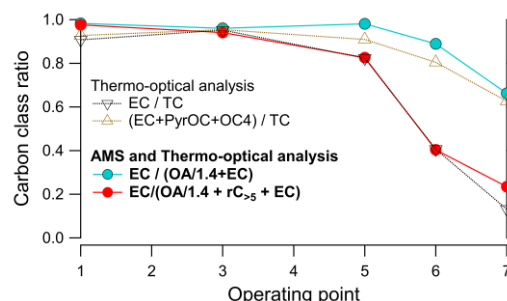


Figure 1: Relation between thermal optical analysis and SP-AMS carbon classes for BC (1, 3) and BrC (5-7) rich burner soot.

We found relationships between combustion conditions and refractory BrC emissions. Associated changes in emissions of genotoxic compounds such as PAHs will be studied in detail. The primary hypothesis for further investigation is that amorphous or fullerenic carbon nanostructures are principal components of refractory primary BrC causing increased light absorption at shorter wavelengths. Future work should aim at quantifying the importance of semi-volatile vs refractory BrC emissions.

This work has received financial support from the Swedish research councils VR and FORMAS.

Malmborg, V. B., et al. Environmental science & technology 51.3 (2017): 1876-1885.

# FOCUS ON 1 NM PARTICLES – CHALLENGES AND POSSIBILITIES OF MEASUREMENTS

E. MIETTINEN<sup>1</sup>, P. SALO<sup>1</sup> and J. VANHANEN<sup>1</sup>

<sup>1</sup> Airmodus Ltd., Finland

Keywords: 1 nm, nCNC, sampling, nucleation

Particles close to 1 nm in diameter have been observed in various environments from as pristine locations as Antarctica and boreal forest zone in northern hemisphere to highly polluted mega cities like Shanghai (Kulmala et al., 2012; Kontkanen et al., 2017), from cleanroom environments to vehicle emissions (Ahonen et al., 2017; Rönkkö et al. 2017). The same studies have further shown that the processes forming the nano cluster aerosol (NCA), with particle diameters close to 1 nm, are often different from the processes that grow the clusters to 2 nm particles and larger. Atmospheric NCA particles can be charged or neutral as they form, and their charge state can change when growing to larger sizes (Wagner et al., 2017).

To determine the sources and growth rates of nucleation mode aerosol particles in different environments and applications, the number concentration and size information is needed starting from the critical sizes of 1-2 nm in diameter (Sipilä et al., 2010). Nano Condensation Nucleus Counter (nCNC) is already widely used to measure particles starting from 1.3 nm in size (Kontkanen et al., 2017). Sampling can cause nearly 100% losses of such small particles or distort measurement results in other ways. Also neglecting basic maintenance of measurement instruments can have an effect on the quality of the results. This presentation will introduce the most common challenges and ways to overcome them, regarding measurement of sub-3 nm particles.

The first thing in measurements is getting the sample to the instruments unaltered. Diffusion losses of sub-3 nm particles in sampling lines can be significant, and different to larger particles; this proposes a challenge to sampling systems (Kumar et al., 2008). Increased flow rate in the sampling line can help in getting sub-3 nm particles to the instruments without losing them on the way. In turn, overly increasing the flow rate in the sampling line can result in diffusion losses due to turbulence. The possible losses in sampling lines need to be taken into account in data handling, to avoid underestimating the number of the smallest particles in the sampled aerosol.

It is also important to consider sample conditions from the point of view of the technology in use. Sample conditions such as relative humidity, pressure and extreme temperatures, as well as particle composition can affect the detection efficiencies of particle counter systems (Kangasluoma et al., 2014 & 2016) and also charger performance (Leppä et al., 2017). The sample

concentration needs to be noted in relation to the concentration range of the instrument in question. To gain the most reliable results possible, the sample can for example be diluted to reach the single particle counting range of a CPC, where the instrument is naturally the most accurate, with least corrections used to obtain the concentration data.

Liquid handling and accuracy of flow rates are key factors in ensuring stable operation of instruments and accurate data. Contamination of operating liquids and accumulation of the liquids in different parts of instruments may cause reduced detection efficiencies. As the CPC technology's basic principle is condensation, in addition to the operating fluid, also other substances like water from the sampled air and fluids from other instruments can condensate inside the instrument and interfere with the operation. Proper liquid handling procedures help minimize the issues. It is crucial to note that a 5% error in CPC flow rate results in 5% error in concentration. The actual flow rate must be measured regularly and taken into account in data handling.

The behavior of the sample can affect the selection of measurement method. To obtain good size distribution data, the sample needs to be stable for the duration of the scan, which is often a few minutes. Transient data in turn calls for the type of measurement capable of detecting concentration changes with higher temporal resolution.

Kulmala, M. et al. (2012). *Nature Protocols*, 7;1651-1667.

Kontkanen, J. et al. (2017). *Atmos. Chem. Phys.*, 17;2163-2187.

Ahonen, L. et al. (2017). *Aerosol Sci. Technol.*, 51;685-693.

Rönkkö, T. et al. (2017). *Proc. Natl. Acad. Sci. U.S.A.*, 114;7549-7554.

Wagner, R. et al. (2017). *Atmos. Chem. Phys.*, 17;15181-15197.

Sipilä, M. et al. (2010). *Science*, 327;1243-1246.

Kumar, P. et al. (2008). *Atmos. Environ.*, 42;8819-8826.

Kangasluoma, J. et al (2014). *Atmos. Meas. Tech.*, 7;689-700.

Kangasluoma, J. et al (2016). *Atmos. Meas. Tech.*, 9;2977-2988.

Leppä, J. et al. (2017). *Aerosol Sci. Technol.*, 51;1168-1189.

# PM<sub>2.5</sub> CONCENTRATION AND COMPOSITION BEFORE, DURING, AND AFTER THE 2014 YOUTH OLYMPIC GAMES IN NANJING, CHINA

M. Miettinen<sup>1</sup>, A. Leskinen<sup>2</sup>, G. Abbaszade<sup>3</sup>, J. Orasche<sup>3,6</sup>, K. Kuuspallo<sup>1</sup>, M. Sainio<sup>1</sup>, H. Koponen<sup>1</sup>, P. Jalava<sup>1</sup>, L. Hao<sup>4</sup>, J. Ruusunen<sup>1</sup>, D. Fang<sup>5</sup>, Q. Wang<sup>5</sup>, C. Gu<sup>5</sup>, Y. Zhao<sup>5</sup>, J. Schnelle-Kreis<sup>3</sup>, K.E.J. Lehtinen<sup>2,4</sup>, R. Zimmermann<sup>3,6</sup>, M. Komppula<sup>2</sup>, J. Jokiniemi<sup>1</sup>, M-R. Hirvonen<sup>1</sup>, and O. Sippula<sup>1</sup>

<sup>1</sup>Department of Environmental and Biological Sciences, University of Eastern Finland, Kuopio, Finland

<sup>2</sup>Finnish Meteorological Institute, Kuopio, Finland

<sup>3</sup>Joint Mass Spectrometry Centre – Cooperation Group “Comprehensive Molecular Analytics”, Helmholtz Zentrum München, Neuherberg, Germany

<sup>4</sup>Department of Applied Physics, University of Eastern Finland, Kuopio, Finland

<sup>5</sup>Nanjing University, School of the Environment, Nanjing, China

<sup>6</sup>Joint Mass Spectrometry Centre – Institute of Chemistry, Division of Analytical and Technical Chemistry, University of Rostock, Rostock, Germany

Keywords: fine particles, chemical composition, China, emission control measures, health effects

Emission control measures have been frequently implemented during large events in China in order to improve air quality. This may result in changes in the levels, composition, and temporal and spatial distribution of the emissions. One such period took place during the 2014 Youth Olympic Games (YOG) in Nanjing, the second largest city in central east China with a population over 8.2 million. More than 900 industrial plants account for 97 % of the city’s coal consumption (Zhao et al., 2015). In addition, other industry, such as chemical production, and transportation increases emissions of air pollutants in the city.

Here, concentration and chemical composition of PM<sub>2.5</sub> (particulate matter with aerodynamic diameter ≤ 2.5 μm) in Nanjing were studied before, during, and after the 2014 YOG to find out possible changes arising from emission control measures, meteorological parameters, or regional atmospheric transport. Fourteen polycyclic aromatic hydrocarbons (PAH), eight oxygenated PAHs (OPAH), ten hopanes, and twenty-one n-alkanes were analyzed with in-situ derivatization thermal desorption followed by gas chromatography and time-of-flight mass spectrometry (Orasche et al., 2011). Various metals and other elements were analyzed with inductively coupled plasma mass spectrometry.

Total 112 PM<sub>2.5</sub> filter samples were collected at the Nanjing University Xianlin campus (N32°07.152', E118°56.918') with an impactor (DPS PM2.5, SKC Inc.) in six measurement campaigns between January 2014 – August 2015 (Table 1). The YOG was held from 16 to 28 August 2014 (campaign 3). The samples were collected separately during day and night.

Table 1: Dates of the measurement campaigns.

Campaign	Date
1	5.–14.1.2014
2	28.5–8.6.2014
<b>3</b>	<b>16.–27.8.2014 (YOG)</b>
4	25.–29.10.2014
5	8.–19.1.2015
6	16.–30.8.2015

Mean PM<sub>2.5</sub> mass concentration was the highest (93±48 μg m<sup>-3</sup>) during campaign 2 in May–June. Zhao et al. (2015) have reported that over 90 % of biomass open burning (BB) in Nanjing occurs in May–July. This

results in high organic carbon and potassium emissions that may explain the observation. PM<sub>2.5</sub> concentration decreased 31 % during the YOG compared to August 2015 (campaign 6). Iron and steel, and cement production are the largest sources of particles in Nanjing (Zhou et al., 2017). Restrictions during the YOG may have affected the PM<sub>2.5</sub> emissions from these sources. Furthermore, declined precursor emissions may have decreased secondary inorganic aerosol formation (Fu et al., 2016).

High concentration of lead (Pb) was observed especially during the winter campaigns 1 and 5. During the YOG, Pb concentration decreased noticeably (55 %) compared to August 2015 that is in line with the results of Li et al. (2016). Concentrations of total PAHs and OPAHs were the highest in campaign 5 and decreased 63 % and 44 % during the YOG compared to August 2015, respectively. The PAHs were dominated by sum-Benzo[b,k]fluoranthene and fluoranthene, and OPAHs by 1,8-Naphthalic anhydride and 9,10-Anthracenedione. Concentration of total OPAHs was lower than concentration of total PAHs in all campaigns except campaign 2 that may be explained by BB emissions (Hays et al., 2005). Hopanes are used as markers for fossil fuel combustion. The most abundant hopanes were 30ab, 29ab and 31abS. Hopane indexes pointed to vehicular transport as the major fossil fuel source, while the contribution of coal combustion to organic aerosols was obviously minor. The main n-alkanes were tetracosane (campaigns 1, 3, 5, 6) and nonacosane (campaigns 2, 4). Carbon preference index (CPI) and the contribution of wax n-alkanes from plants (WNA%) indicated that alkanes were mainly from biogenic sources in the campaign 2, and from anthropogenic sources in the other campaigns.

Emission control measures affected PM<sub>2.5</sub> concentration and composition during the YOG. Part of the observed differences between the campaigns, however, arose from regional atmospheric transport and/or meteorological parameters.

Fu, X., et al. (2016). *Sci. Rep.*, 6:35992.

Hays, M., et al. (2005). *Atmos. Environ.*, 39:6747–6764.

Li, S-W., et al. (2016). *Environ. Internat.*, 94:69–75.

Orasche, J., et al. (2011). *Atmos. Chem. Phys.*, 11:8977–8993.

Zhao, Y., et al. (2015). *Atmos. Chem. Phys.*, 15:12623–12644.

Zhou, Y. et al. (2017). *Atmos. Chem. Phys.*, 17:211–233.



# OXIDIZED ORGANIC COMPOUNDS IN THE INITIAL STEPS OF PARTICLE FORMATION

N. MYLLYS<sup>1</sup>, J. ELM<sup>2</sup>, T. OLENIUS<sup>3</sup>, and T. KURTÉN<sup>4</sup>

<sup>1</sup> Institute for Atmospheric and Earth System Research, University of Helsinki, Finland

<sup>2</sup> Department of Chemistry, Aarhus University, Denmark

<sup>3</sup> Department of Environmental Science and Analytical Chemistry, Stockholm University, Sweden

<sup>4</sup> Department of Chemistry, University of Helsinki, Finland

Keywords: cluster formation, quantum chemistry, oxidized organic compounds

We have investigated the molecular interaction between sulfuric acid and various oxidized organic compounds at atmospheric conditions. We have used state-of-the-art quantum chemical methods, which details can be found in each references listed here. We identified that multi-carboxylic acids are the most prominent candidates to enhance sulfuric acid driven new-particle formation (Elm *et al.*, 2017a). We have studied clustering of 3-methyl-1,2,3-butanetricarboxylic acid (MBTCA) and sulfuric acid molecules up to the cluster size of 2 nm (see Figure 1).

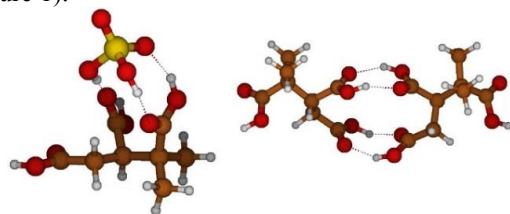


Figure 1: Molecular structures of (MBTCA)(sulfuric acid) (left) and (MBTCA)<sub>2</sub> (right) clusters.

Medium-sized clusters are particularly stable, but cluster growth is limited by a weak formation of the largest sulfuric acid–MBTCA clusters (Elm *et al.*, 2017b). We have investigated the ability of bisulfate, ammonium, and ammonia to enhance cluster formation and growth by decreasing the overall evaporation rates of the clusters containing sulfuric acid and multi-carboxylic acids. We showed that it is very unlikely that organic multi-carboxylic acids and sulfuric acid, even together with common stabilizing compounds, can drive new-particle formation via clustering mechanisms (Myllys *et al.*, 2017).

We have demonstrated that non-basic organic compounds are unlikely to have a strong enhancing role in sulfuric acid driven new-particle formation at atmospheric conditions. However, experimental studies have shown that oxidized organic compounds participate in the initial steps of new-particle formation (Riccobono *et al.*, 2014). Due to the disagreement between theoretical and experimental findings, some other mechanisms or compounds are needed to explain the experiments.

One possible reason for the discrepancy between experimental and theoretical results might be the formation of covalently-bound dimers. The formed dimer products very likely have a lower saturation vapor pressure than the reacting monomers due to a higher molecular mass and a larger number of functional

groups. We have showed that these clusters would be more stable against evaporation; therefore, cluster-phase reactions might play a significant role in atmospheric new-particle formation and growth (Hirvonen *et al.*, 2018).

Furthermore, we have demonstrated that not only the atmospheric abundance but also the basicity and ability to form hydrogen bonds are important when estimating the ability of bases to form stable clusters (Xie *et al.*, 2017). For instance, guanidine (a normal product of protein metabolism) binds with sulfuric acid four times stronger than dimethylamine, and thus even at low concentration it can enhance new-particle formation (Myllys *et al.*, 2018). Figure 2 presents the mesh-like structure of very stable (sulfuric acid)<sub>4</sub>(guanidine)<sub>4</sub> cluster. Due to a high stability against evaporation, sulfuric acid–guanidine clusters could act as seeds for further growth via the uptake of other vapor molecules such as oxidized organic compounds.

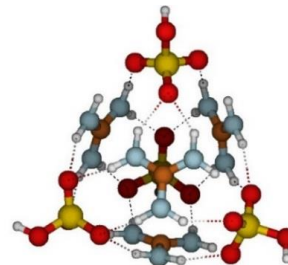


Figure 2: Molecular structure of cluster containing 4 sulfuric acid and 4 guanidine molecules.

We thank the Academy of Finland, AtMath, and ERC project 692891-DAMOCLES for funding, and CSC for computational resources.

Elm, J., Myllys, N., Kurtén, T. (2017a). *J. Phys. Chem. A*, 121:4578.

Elm, J., Myllys, N., Olenius, T., *et al.* (2017b). *Phys. Chem. Chem. Phys.*, 19:4877.

Hirvonen, V., Myllys, N., Kurtén, T., Elm, J. (2018), *J. Phys. Chem. A*, in review.

Myllys, N., Olenius, T., Kurtén, T., *et al.* (2017). *J. Phys. Chem. A*, 121:4812.

Myllys, N., Ponkkonen, T., Elm, J., *et al.* (2018), in preparation.

Riccobono, F., Schobesberger, S., Scott, C., *et al.* (2014). *Science*, 344:717.

Xie, H.-B., Elm, J., Halonen, R., *et al.* (2017). *Environ. Sci. Technol.*, 51:8422.

# MODELING THE IMPACT OF BACKGROUND GAS PRESSURE ON THE FRAGMENTATION OF MOLECULAR CLUSTERS INSIDE THE APi-TOF

N. Myllys<sup>1</sup>, M. Panssananti<sup>1</sup>, A. Shcherbacheva<sup>1</sup> and E. Zapadinsky<sup>1</sup>

<sup>1</sup> Institute for Atmospheric and Earth System Research /Physics, Faculty of Science, University of Helsinki, Finland

Keywords: fragmentation, molecular clusters, mass spectrometers, COMSOL modeling, gas pressure

The role of atmospheric particles in phenomena ranging from urban photochemical smog to potential climate change indicates that it is crucial to study and model the processes of new particle formation and growth in the atmosphere. Indeed, particles can reflect, scatter or absorb solar radiation to varying degrees depending on their physical properties.

In the last years, mass spectrometers (e.g. APi-TOF) have been developed to detect, at ambient low concentration, molecules and clusters involved in new particle formation. However the Atmospheric Pressure interface Time Of Flight (APi-TOF) mass spectrometer is a powerful instrument to detect clusters, it has been shown that these clusters could undergo transformations (fragmentation and/or evaporation) inside the instrument due to the low pressure and energetic collisions. Therefore, in order to correctly interpret the experimental data and retrieving the initial cluster distribution, we decided to carefully study the parameters that influence the cluster fragmentation inside the APi and build a model to predict it. In this particular study, we focus the attention on the effect of the pressure on the fragmentation.

Experiment have been carried on indicating that the pressure of background gas has a substantial impact on the fragmentation of molecular clusters inside the APi-TOF. Specifically, experiments were conducted using an Electrospray Ionization Differential Mobility Analyser Atmospheric Pressure interface Time Of Flight (ESI-DMA-APi-TOF) system implemented with an additional pump in order to regulate the pressure inside the APi. In particular, the results provided convincing evidence that higher cluster fragmentation is observed in the experiments conducted under the higher pressure.

In order to carefully model the processes inside the APi, that lead to cluster fragmentation, we modelled the pressure gradient inside the APi-TOF using finite element based calculations implemented in the software package Comsol Multiphysics ver. 5.3. The experimental setup consisted of three chambers (APi) and the mass spectrometer (TOF) connected with the small orifices, where each of the chambers is differentially pumped. The process of pumping happens in two stages: switching on the scroll pump (Anest iwata oilfree scroll vacuum pump ISP-500C) and reaching the pressure levels almost similar for two first chambers and a subsequent pumping of the second and the third chambers using a turbopump Pfeiffer SplitFlow 310.

Particularly, in this study we are interested in spatial variation of gas pressure and velocity inside of the instrument. Based on reference pressure levels and geometric dimensions, APi-TOF chambers feature different gas flow regimes, characterized by a Knudsen number: a ratio of the mean free path to characteristic length scale. As a fluid flow model for solving Navier-Stokes equations we consider a continuous flow based on calculated Knudsen number. Specifically, the flow in Chamber I and Chamber II features continuous regime, while the flow in third chamber is characterized by the slip regime, with reduced number of collision between the particles.

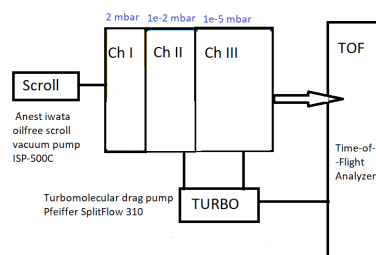


Figure 1: Schematic representation of the vacuum system in the APi-TOF

- Seinfeld, J. and Pandis, S. (2006). *Atmospheric Chemistry and Physics: From Air Pollution to Climate Change*. Wiley Interscience, 2nd edition.
- Olenius, T. and Kupiainen-Määttä, O. and Ortega, I. K. and Kurtén, T. and Vehkamäki, H. (2013) *J. Chem. Phys.*,139(8):084312.
- Gallis, M.A.and Torczynski, J.R. *J. Phys. Fluids*, 24:012005

# LONG-TERM TRENDS IN PARTICLE NUMBER SIZE-DISTRIBUTIONS AND NEW PARTICLE FORMATION OBSERVED AT SAN PIETRO CAPOFIUME, ITALY

T. NIEMINEN<sup>1</sup>, J. JOUTSENSAARI<sup>1</sup>, V. LEINONEN<sup>1</sup>, S. MIKKONEN<sup>1</sup>, T. YLI-JUUTI<sup>1</sup>, P. MIETTINEN<sup>1</sup>, A. VIRTANEN<sup>1</sup>, K. E. J. LEHTINEN<sup>1</sup>, A. LAAKSONEN<sup>2</sup>, S. DECESARI<sup>3</sup>, L. TAROZZI<sup>3</sup> and M. C. FACCHINI<sup>3</sup>

<sup>1</sup>Department of Applied Physics, University of Eastern Finland, Kuopio, Finland

<sup>2</sup>Finnish Meteorological Institute, Helsinki, Finland

<sup>3</sup>Institute of Atmospheric Sciences and Climate (ISAC) of the Italian National Research Council, Bologna, Italy

Keywords: atmospheric aerosols, particle number size-distributions, particle formation and growth, long-term trends

Atmospheric aerosols have a large impact on air quality, human health and even the global climate. Both the aerosol number concentration and their size have influence on the climatic effects of aerosols. Formation and growth of secondary aerosol particles is a major source of atmospheric aerosols (Merikanto et al., 2009), and has been a subject of active research during the past two decades. However, only few long-term datasets (over 10 years of measurements) of atmospheric aerosol number size distributions exist (Hamed et al., 2010; Asmi et al., 2011; Kyrö et al., 2014; Nieminen et al., 2014).

In this work, we characterize trends in aerosol number size distributions and in new particle formation (NPF) at San Pietro Capofiume in Po Valley, Northern Italy. Number size distributions of 3–630 nm particles have been measured there continuously since March 2002 with a twin-DMPS setup. The site is influenced by emissions of local anthropogenic pollutants (such as SO<sub>2</sub>) as well as long-range transport from Central and Eastern Europe (Sogacheva et al., 2007), and thus can provide information on the impact of anthropogenic activity on aerosol size-distributions and NPF.

The particle number size distribution data was classified into NPF event, non-event and undefined days (Kulmala et al. (2012)). The formation and growth rates of nucleation mode particles (defined here as particles of 3–25 nm in diameter) were calculated based on the time-evolution of the measured number size-distribution data. To quantify the trends in particle concentrations, we have used two methods. The first method fits the concentration time series as a sum of constant linear trend and seasonally varying component. The statistical significance of the fitted trend is estimated by performing the fitting multiple times with bootstrap sampling. The second method is a Dynamic Linear Model (DLM; see e.g. Durbin and Koopman, 2012), where the particle number concentration timeseries is decomposed into level, trend, seasonality, and noise. These components are allowed to change as functions of time, and the magnitude of this change is modelled and estimated (Mikkonen et al., 2015).

There has been a longer break in the measurements from November 2010 until June 2011, during which time the twin-DMPS setup was repaired. Before this break, statistically significant decreasing linear trends are observed in nucleation, Aitken and accumulation mode particle concentrations. The largest decrease (–10%/year) occurs in the nucleation mode par-

ticle concentration. After the measurement break, only the nucleation mode particle concentration shows a statistically significant trend (decreasing –4.9%/year). The DLM method indicates that these changes occurred in 2008–2009. The particulate mass concentrations (PM<sub>10</sub> and PM<sub>2.5</sub>) have also been reported to decrease throughout the Po Valley region, and it is attributed to decreases both in primary emissions and in precursors of secondary inorganic aerosol emissions mostly from vehicular traffic (Bigi and Ghermandi, 2016). However, unlike the change in the trends of the particle number concentrations after 2007–2008 seen in our study, the PM concentrations seem to have continued their decrease until at least 2014.

The annual frequency of NPF event occurrence did not show any clear trend, varying between 20% and 40% of the days in a year. Both the formation and growth rates of nucleation mode particles had a decreasing trend of –3%/year and –2%/year, respectively. This would indicate that even though the sink for the newly formed particles has decreased (due to decrease in PM concentrations), a simultaneous decrease in precursor vapour emissions (sulphur dioxide, ammonia, amines, organics) has also occurred.

This work was supported by the Academy of Finland Centre of Excellence (grants no. 272041 and 307331).

- Asmi, E. *et al.* (2011). *Atmos. Chem. Phys.* 11, 12959–12972.
- Bigi, A. and Ghermandi, G. (2016). *Atmos. Chem. Phys.* 16, 15777–15788.
- Durbin, T. J. and Koopman, S. J. (2012). *Time Series Analysis by State Space Methods*. Oxford University Press.
- Hamed, A., Birmili, W., Joutsensaari, J., *et al.* (2010). *Atmos. Chem. Phys.* 10, 1071–1091.
- Kulmala, M. *et al.* (2012). *Nat. Protocols* 7, 1651–1667.
- Kyrö, E.-M. *et al.* (2014). *Atmos. Chem. Phys.* 14, 4383–4396.
- Merikanto, J. *et al.* (2009). *Atmos. Chem. Phys.* 9, 8601–8616.
- Mikkonen, S. *et al.* (2015). *Stoch. Environ. Res. Risk Assess.* 29, 1521–1529.
- Nieminen, T. *et al.* (2014). *Boreal Env. Res.* 19 (suppl. B), 191–214.
- Sogacheva, L. *et al.* (2007). *Atmos. Chem. Phys.* 7, 839–853.

# COMBINING AIRBORNE IN SITU AND GROUND-BASED LIDAR MEASUREMENTS FOR ATTRIBUTION OF AEROSOL LAYERS

A. NIKANDROVA<sup>1</sup>, K. TABAKOVA<sup>1</sup>, A. MANNINEN<sup>1</sup>, R. VÄÄNÄNEN<sup>1</sup>, T. PETÄJÄ<sup>1</sup>, M. KULMALA<sup>1</sup>, V.-M. KERMINEN<sup>1</sup> AND E. O'CONNOR<sup>2</sup>

<sup>1</sup> Institute for atmospheric and earth system research, Faculty of Science, University of Helsinki, Finland

<sup>2</sup> Finnish Meteorological Institute, Helsinki, Finland

Keywords: atmospheric aerosols, airborne measurements, lidar, HSRL

Aerosol particles are not distributed uniformly in the atmosphere; their concentrations and properties vary significantly in space and time. Therefore, implementation of aerosol schemes in global climate models remains a challenge (Glassmeier et al., 2017), and aerosols continue to constitute one of the largest sources of uncertainty in future climate estimates (IPCC, 2013).

In this study, we explored aerosol layers aloft in the rural environment, their evolution and origin as well as atmospheric boundary layer (BL) dynamics. We used combination of ground-based remote sensing, airborne aerosol measurements, radiosonde observations and back trajectories. The high spectral resolution lidar (HSRL, Shipley et al., 1983) was deployed at SMEAR II station (Hyytiälä, Finland) as a part of the US DoE ARM (Atmospheric Radiation Measurement) mobile facility during Biogenic Aerosols – Effects on Cloud and Climate (BAECC) campaign during 2014 (Petäjä et al., 2016), and radiosondes were launched every six hours during this period. The airborne measurements utilizing a Scanning Mobility Particle Sizer (SMPS) and Optical Particle Counter (OPC) took place in April and August. Two case studies were chosen for the analysis: sequential three days of clear sky and one partly cloudy day, with air masses for both cases arriving from the North.

We observed several elevated aerosol layers during both case studies. The highest particle concentration in all size ranges was found predominantly in the BL. The shape of the size distribution in the upper layer often resembled the shape of the distribution in the BL but with overall lower concentrations due to dilution of particles into a larger volume of air. Variability in the number concentrations was the lowest in the BL due to turbulent mixing, while there was more variability in the elevated layers. 96-hours back trajectories for every 50 m for the altitudes from 0 to 4 km showed slight difference in the origin of the air masses. Origin of the air masses, as well as mixing and deposition, affect aerosol size distribution in different layers. Compared to the clear sky case, the BL during the cloudy case was not as well mixed, even though there was a clear presence of a convective BL, which is expected to stimulate mixing. Furthermore, we compared particle size distribution in the aerosol layers

during three days of the clear sky case and observed that there was almost no mixing of particles between the middle layer and neighboring layers, since particle concentrations stayed similar during the days. Therefore, we concluded that nucleation mode particles, that were observed in the middle layer, could have been formed there.

This work was supported by the Academy of Finland Centre of Excellence program (grant no. 272041). We also acknowledge the use of HSRL data in collaboration with the U.S. Department of Energy as part of the Atmospheric Radiation Measurement (ARM) Climate Research Facility during BAECC (AMF campaign in Hyytiälä, Finland).

Glassmeier, F., Possner, A., Vogel, B., Vogel, H., and Lohmann, U. (2017). *Atmos. Chem. Phys.*, 17, 8651-8680.

Intergovernmental Panel on Climate Change (2013). Stocker, T.F., D. Qin, G. K. Plattner, M. Tignor, S.K. Allen, J. Boschung, A. Nauels, Y. Xia, V. Bex and P.M. Midgley (eds.). Cambridge University Press.

Petäjä et al. (2016) *Bulletin of the American Meteorological Society*, 97(10), 1909-1928.

Shipley, S.T., Tracy, D.H., Eloranta, E.W., Trauger, J.T., Sroga, J.T., Roesler, F.L. and Weinman, J.A. (1983) *Appl. Opt.*, 22, 3716-3724.

# ESTIMATION OF NUCLEATION AND CONDENSATION RATES FROM SIZE DISTRIBUTION MEASUREMENTS USING STATISTICAL INVERSE METHODOLOGY

M. OZON<sup>1</sup>, A. SEPPÄNEN<sup>1</sup>, J.P. KAIPIO<sup>3,1</sup> and K.E.J. LEHTINEN<sup>1,2</sup>

<sup>1</sup> Department of Applied Physics, University of Eastern Finland, Kuopio, Finland

<sup>2</sup> Finnish Meteorological Institute, Kuopio, Finland

<sup>3</sup> Department of Mathematics, University of Auckland, Auckland, New Zealand

Keywords: aerosol, nucleation, condensation, growth rate, New Particle Formation, parameter estimation, Extended Kalman Filter, General Dynamic Equation

**Motivation** Aerosols play a key role in the global radiative balance of the earth. Their number concentration, size distribution (SD) and chemical composition affect their ability to scatter and absorb solar radiation as well as the formation, properties and lifetimes of clouds Pachauri et al. (2014). The same properties determine how particles enter the human lung and cause various public health problems Guerreiro et al. (2016). To quantify these effects, we need to be able to determine the rates of the key microphysical processes, aerosol formation and growth, from measurements of aerosol SD evolution.

**Methods** The estimation of nucleation rate and condensation rates still typically relies on rather simple visual analysis, regression methods or balance equations involving crude approximations Kulmala (2012). So far, e.g. determining both size and time dependence of condensation rates has been a challenge. In addition, the methods have not considered measurement uncertainty in a rigorous way. We propose an automated method based on the Extended Kalman Filter (EKF) similar to the one used in Viskari et al. (2012). However, instead of using the EKF only for filtering the SD, it is tweaked to also estimate the nucleation and condensation rates. This method requires no assumption of SD shape as it relies only on a physical evolution model — the aerosol General Dynamic Equation — and a measurement model — DMPS — that are both combined in the EKF framework.

**Results** As a proof of concept of our method and a test of its performance we analyze synthetic data — SD — that are generated by solving the GDE with a sectional method. We simulate eight days with four having a new particle formation event. The size spectrum ranges from an arbitrary critical cluster size of  $2nm$  to  $2\mu m$ . One single vapor is responsible for condensational growth. The simulated data are corrupted by additive and multiplicative noise in order to resemble actual measured data. An example of the estimation of the nucleation rate and the vapor concentration is shown in Fig. 1 where the true — input for the synthetic data generation — and the estimated parameters are compared. The results for both nucleation rate and vapor concentration are promising, even if not perfect. Negative values can be avoided by further tuning of the method — variable change.

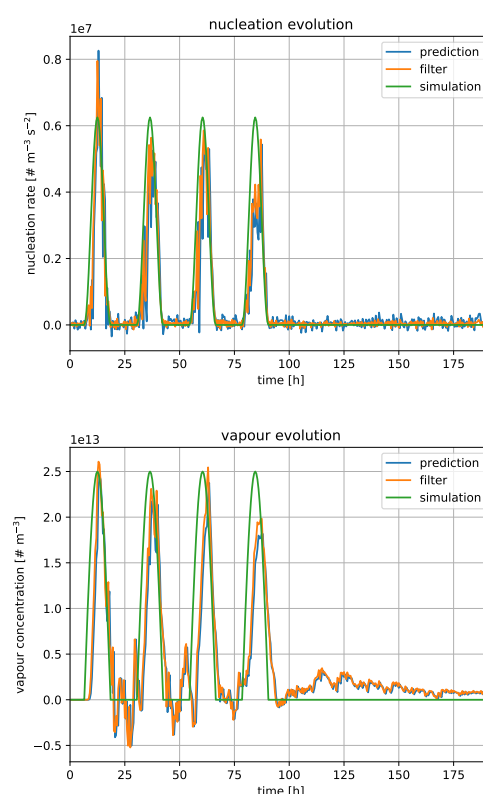


Figure 1: The evolution of the nucleation rate (top) and the overall vapor concentration: in green, the input feed to the simulation (noiseless) and in blue and orange the estimates given by the Kalman filter for the prediction and filtering steps respectively.

Pachauri, R., Allen, M., Barros, V., and others (2014). *Climate change 2014: synthesis report*. IPCC.

Guerreiro, C., Ortiz, A. G., de Leeuw, F. and others (2016). *Air Quality in Europe-2016 Report*. Publications Office of the European Union.

Kulmala, M., Petäjä, T., Nieminen, T., and others (2012). *Nature protocols*, 7:1651–1667.

Viskari, T., Asmi, E., Kolmonen, P., and others (2012). *Atm. Chem. and Phys.*, 12:11767–11779.

# PARTICLE GROWTH RATES FROM NUCLEATION MODE TO CLOUD CONDENSATION NUCLEI SIZES

P. PAASONEN, M. PELTOLA, J. KONTKANEN, H. JUNNINEN, V.-M. KERMINEN and M. KULMALA

Institute for Atmospheric and Earth System Research / Physics, Faculty of Science, University of Helsinki, Finland

Keywords: particle growth rate, organic condensation, Aitken mode, accumulation mode

Aerosol particles play a key role in our lack of understanding of the climate system, largely due to uncertainties in aerosol-cloud interactions (Stocker et al., 2013). In the lower troposphere, particles with diameters ( $d_p$ ) larger than 50–100 nm are capable of acting as cloud condensation nuclei (CCN). A major fraction of CCN seems to be formed by condensational growth of smaller aerosol particles (Paasonen et al., 2013; Wang et al., 2017). The condensable vapours typically originate from emissions of volatile organic compounds from plants (Hallquist et al., 2009).

We developed an automatic method, which searches for roughly monotonic growth periods of particle modes in particle number size distributions and calculates particle growth rates (GR) for these periods. The method considers not only the nucleation mode ( $d_p < 25$  nm), but also the Aitken ( $25 \text{ nm} < d_p < 100$  nm) and accumulation mode ( $d_p > 100$  nm) particles, and the growth periods do not need to follow immediately after a new particle formation event.

We determined GRs for a 21-year-long data set recorded at the SMEAR II station in Hyytiälä, Finland (Hari and Kulmala, 2005). GRs were compared with other measured variables presumably related to the formation and concentration of condensable vapours, such as air temperature, concentrations of monoterpenes and their oxidants, condensation sink (CS), radiation and diameter of the growing particles.

The growth rates of particles in nucleation and Aitken modes were observed to increase with increasing temperature, whereas in accumulation mode the relation was opposite. The dependencies were very similar when GR was compared, instead of temperature, with the oxidation rate of monoterpenes (OxRate, Fig. 1) or CS). The correlations were strongest with OxRate, which was calculated using the monoterpene concentration proxy and oxidation rates as presented in Kontkanen et al. (2016).

The positive correlation between CS and GR in nucleation and Aitken modes presumably stems from the strong coupling between temperature, monoterpene concentrations and CS. However, we find surprising that even in narrow OxRate bins, the GR was not observed to decrease with increasing CS. This would be expected because condensable vapour concentrations are presumed to decrease with increasing sink. Such relation was, however, observed only in accumulation mode.

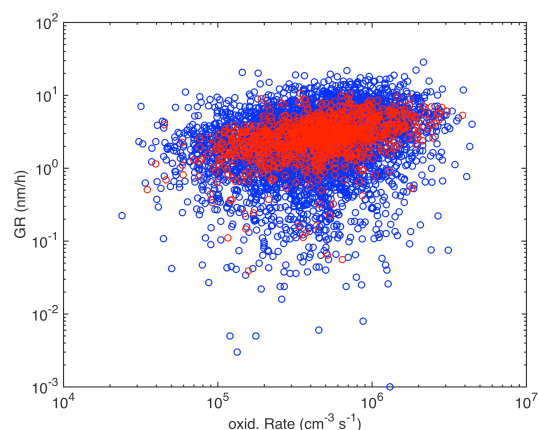


Figure 1: Growth rate of nucleation and Aitken mode particles as a function of monoterpene oxidation rate in April-September. Blue dots show growth periods longer than 2 h and red longer than 5 h.

Additionally, GR was observed to increase with increasing particle diameter. For growth events starting at  $d_p = 10$  nm, the highest GRs were around 10 nm/h, whereas for the events that started at  $d_p = \sim 100$  nm GRs reached 30 nm/h. The same was observed when simultaneous growth periods in different sizes were inspected. We also show using a single particle growth model that this increase of GR with increasing  $d_p$  can be explained by aerosol phase dimer formation, where originally semi-volatile vapours form practically non-volatile compounds.

Hallquist et al. (2009). *Atmos. Chem. Phys.*, 9, 5155–5236.

Hari, P., and Kulmala, M. (2005). *Boreal Environ. Res.*, 10, 315-322.

Kontkanen, J. et al. (2016). *Atmos. Chem. Phys.*, 16, 13291-13307.

Paasonen, P. et al. (2013). *Nature Geoscience*, 6, 438–442.

Stocker, T. F. et al. (2013). Technical Summary, in: *Climate Change 2013: The Physical Science Basis. Contribution of Working Group I to the Fifth Assessment Report of the Intergovernmental Panel on Climate Change*, Cambridge University Press, Cambridge, UK, and New York, NY, USA.

Wang, Z. et al. (2017). *Science of the Total Environment*, 577, 258-266.

# EFFECT OF SURFACE GEOMETRY ON HETEROGENEOUS ICE NUCLEATION

O. H. PAKARINEN<sup>1</sup>, G. ROUDSARI<sup>1</sup> and H. VEHKAMÄKI<sup>1</sup>

<sup>1</sup>Institute for Atmospheric and Earth System Research (INAR) / Physics, University of Helsinki, Finland

Keywords: ice nucleation, water, simulation, molecular dynamics

Understanding the way in which ice forms is of great importance to many fields of science. Pure water droplets in the atmosphere can remain in the liquid phase to nearly -40° C. Crystallization of ice in the atmosphere therefore typically occurs in the presence of aerosol particles, such as mineral dust, soot or organic particles. These ice nucleating particles (INPs) trigger heterogeneous ice nucleation at clearly higher temperatures than possible through homogeneous ice nucleation. Therefore, a better understanding of how the various types of aerosol particles present in the atmosphere affect ice nucleation (IN) in clouds would improve our ability to measure, model and parameterize the key processes related to ice- and mixed-phase cloud formation, and would advance the field of atmospheric science.

Experiments have shown in great detail what is the IN activity of different types of compounds, and recently also clarified the importance of small surface features such as surface defects. The molecular-scale processes responsible for ice nucleation are still not well known, however, and difficulties in atomic-scale characterization of complex and imperfect surfaces means that a full understanding of these processes from solely experimental evidence is still a distant goal. In recent years, several computational studies have been published on heterogeneous ice nucleation, advancing our understanding of the details of ice nucleation in many materials. The role of defects has been studied less, but recently the importance of feldspar microstructure and different crystallographic faces of feldspar were shown to be responsible for IN activity of feldspars (Kiselev *et al.*, 2017). Simulations also showed enhanced ice nucleation efficiency in confined geometry such as wedges or pits (Bi, Cao and Li, 2017).

We are studying these topics by utilizing the monatomic water model (Molinero and Moore, 2009) for unbiased molecular dynamics (MD) simulations, where a system including a defected surface, such as pyramidal pits, steps or surface cracks, immersed in water, is cooled continuously below the melting point over tens of nanoseconds of simulation time and crystallization is followed.

Results of simulations on pyramidal pits on Si (100) surfaces, for example, show a clear ( $\Delta T > 10^\circ \text{C}$ ) enhancement of ice nucleation compared to flat Si (100) or Si (111) surfaces. Understanding the enhanced activity in such confined geometry may lead to characterization of active sites on some ice nucleating materials, as well as to development of optimal cloud seeding materials.

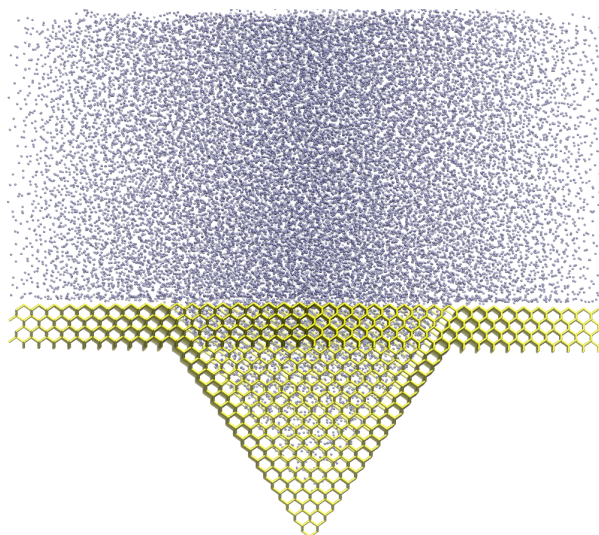


Figure 1: Experimentally realizable etched Si (001) pits increase ice nucleation activity due to geometric confinement.

Kiselev, A. *et al.* (2017). *Science* **355**, 367.

Bi, Y., Cao, B. and Li, T. (2017). *Nat. Commun.* **8**, 15372.

Molinero, V. and Moore, E. B. (2009). *J. Phys. Chem. B* **113**, 4008.

This work was supported by the Academy of Finland Center of Excellence programme (grant no. 307331) and ARKTIKO project 285067 ICINA, by ERC Grant 692891-DAMOCLES, by University of Helsinki, Faculty of Science ATMATH project, and by supercomputing resources at CSC - IT Center for Science Ltd.

# Distribution of atmospheric aerosols and trace gases over Finland modelled with high resolution

Y. PALAMARCHUK<sup>1</sup> and M. SOFIEV<sup>1</sup>

<sup>1</sup> Finnish Meteorological Institute, Helsinki, Finland

Keywords: SILAM, atmospheric aerosols, concentrations, seasonality

The distribution of air pollution over Finland was computed with several spatial resolutions for the year of 2015, aiming at complex assessment of atmospheric composition and air quality in Finland. The multi-scale simulations for three nested domains were performed with the SILAM atmospheric composition model (Sofiev et al., 2015). Since Finland is largely a receptor of pollution from Central Europe, the simulations started from the European domain with 50 km zoomed towards Fennoscandia (10km grid). The high-resolution domain had grid spacing of 1 km covering the whole Finland. For the computations the Copernicus European emission database was expanded with the 250m emission information from the Finnish Environment Institute (SYKE) and the Ship Traffic Emission Assessment Model (STEAM) (Jalkanen et al., 2014).

The SYKE database for Finland also contains the exhaustive list of point sources with the sectoral separation of emitted substances. The STEAM inventory of ship emissions was based on bottom-up compilation of individual vessels using anti-collision (AIS) system reports and converted to time-resolving emission fields with 1km grid spacing.

The SILAM analysis covered the entire year 2015 for all main reactive gases, primary and secondary organic and inorganic aerosols. The seasonal variations of concentrations are similar for all grid resolutions but absolute levels differed substantially. In particular, even small cities resolved by the fine-scale computations were characterized by up to a factor of times higher concentrations than over surrounding sub-urban/rural regions. City-scale emissions, plumes from roads and point sources were quite well expressed in both hourly patterns and at annual averaging. Since most observational stations are located in proximity of local sources or inside populated areas, reproducing the local rise of PM and trace gases concentrations was important for low-biased model-measurement comparison. Coarser-grid simulations showed noticeably higher biases in small cities and near small local sources.

Possibilities for AQ improvement via emission abatement was explored via a set of sensitivity runs. The impact of 10% emission reduction in different sectors was computed showing non-linear and season-dependent response of air components concentrations. Thus, the reduction of NO<sub>x</sub> emission results in increase of ozone in cities in summer with simultaneous reduction over rural areas. In winter, the O<sub>3</sub> growth was predicted over the whole country. For PM, different components showed different behavior.

Jalkanen, J.-P., Johansson, L., & Kukkonen, J. (2014). *A Comprehensive Inventory of the Ship Traffic Exhaust Emissions in the Baltic Sea from 2006 to 2009*. *Ambio*, 43 (3), 311 – 324. <http://doi.org/10.1007/s13280-013-0389-3>.

Sofiev, M., Vira, J., Kouznetsov, R., Prank, M., Soares, J., Genikhovich, E. (2015). *Construction of the SILAM Eulerian atmospheric dispersion model based on the advection algorithm of Michael Galperin*, *Geosci. Model Developm.* 8, 3497-3522, doi:10.5194/gmd-8-3497-2015



# CARBON BUDGET UNCERTAINTY DUE TO UNCERTAINTY IN AEROSOL FORCING AND TRANSIENT CLIMATE RESPONSE

A.-I. PARTANEN<sup>1</sup>, N. MENGIS<sup>2</sup>, J. JALBERT<sup>3</sup> and H.D. MATTHEWS<sup>1</sup>

<sup>1</sup>Climate System Research, Finnish Meteorological Institute, Helsinki, Finland

<sup>2</sup>Department of Geography, Planning and Environment, Concordia University, Montreal, Canada

<sup>3</sup>Department of Mathematical and Industrial Engineering, Polytechnique Montréal, Montreal, Canada

Keywords: aerosol forcing, transient climate response, carbon budgets, probabilistic modelling

In Paris, nations agreed to limit the increase in global mean surface temperature relative to the preindustrial era below 2 degrees Celsius and pursue efforts to a more ambitious goal of 1.5 degrees Celsius. To achieve these goals, it is necessary to estimate the amount of cumulative carbon emissions compatible with these temperature targets, i.e. so called carbon budgets (e.g., Matthews et al., 2017). Many previous estimates of carbon budgets are based on arbitrary assumptions on the strength of aerosol forcing. However, there is a considerably uncertainty in present-day and future aerosol forcing, and this uncertainty, together with uncertainty in transient climate response to CO<sub>2</sub> emissions, creates previously unquantified uncertainty in carbon budgets.

In this work, we use the intermediate complexity University of Victoria Earth System Climate Model (UVic ESCM) (Eby et al., 2013) to assess how uncertainty in aerosol forcing and transient climate response transfers to uncertainty in the carbon budget for keeping the global mean temperature increase below 1.5 degrees. We create a perturbed parameter ensemble of model simulations by scaling aerosol forcing and transient climate response, and assess the likelihood of each simulation by comparing the simulated historical cumulative carbon emissions to observations.

By weighting the results of each simulation with the likelihood of the simulation, the preliminary results give a carbon budget of 178 Pg C to reach 1.5 degree Celsius temperature increase. The small weighted mean is due to large fraction of simulations with strong aerosol forcing and transient climate response giving negative carbon budgets for this time period (Fig. 1). The carbon budgets after temperature stabilization at 1.5 degrees are even smaller with a weighted mean of -42 Pg C until the year 2200. The main reason for the negative carbon budgets after temperature stabilization is an assumed strong decrease in aerosol forcing in the 21st century. Conversely, simulations with weak aerosol forcing and transient climate response give positive carbon budgets after temperature stabilization. Our results highlight both the importance of reducing uncertainty in aerosol forcing and transient climate response, and of and of taking the non-CO<sub>2</sub> forcings into

account when estimating carbon budgets.

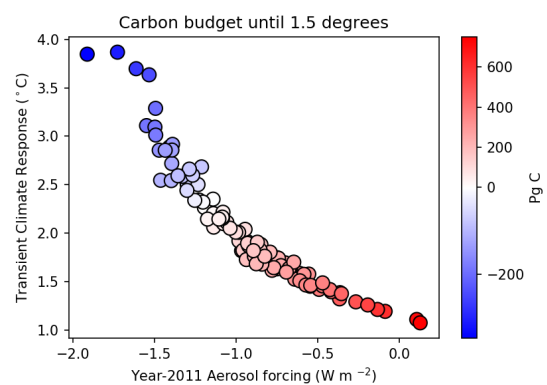


Figure 1: Carbon budget (Pg C) from 2015 until temperature stabilization at 1.5 °C above 1861-1880 global mean temperature as a function of transient climate response and year-2011 aerosol forcing.

Eby et al. (2013). *Clim. Past* 9, 1111–1140.

Matthews, H. D., Landry, J.-S., Partanen, A.-I., Allen, M., Eby, M., Forster, P. M., Friedlingstein, P., Zickfeld, K. (2017). *Curr. Clim. Change Rep.*, doi: 10.1007/s40641-017-0055-0.

# STUDY ON FRAGMENTATION OF ATMOSPHERIC CLUSTERS INSIDE A MASS SPECTROMETER

M. PASSANANTI<sup>1</sup>, E. ZAPADINSKY<sup>1</sup>, J. KANGASLUOMA<sup>1</sup>, N. MYLLYS<sup>1</sup>, B. REISCHL<sup>1</sup>, R. HALONEN<sup>1</sup>, M. ATTOU<sup>2</sup> and H. VEHKAMÄKI<sup>1</sup>

<sup>1</sup>Institute for Atmospheric and Earth System Research / Physics, Faculty of Science, University of Helsinki, Finland

<sup>2</sup>LISA, University Paris Est Creteil, Creteil, 94010, France

Keywords: clusters, APi-TOF, sulfuric acid, Differential Mobility Analyzer, fragmentation

It is crucial to collect experimental data from field campaigns and laboratory measurements in order to understand and simulate atmospheric processes. However, the analysis and the interpretation of the experimental data should always be done very carefully. Artefacts and phenomena such as wall loss should be considered and taken into account in the data analysis. A common problem that atmospheric scientists face is to retrieve the correct composition and concentration of atmospheric clusters measured by the Atmospheric Pressure interface Time Of Flight (APi-TOF) mass spectrometer. Indeed, clusters can undergo transformations (fragmentation and/or evaporation) inside the instrument, mainly in the APi, due to the low pressure and energetic collisions (Kürten et al., 2014; Olenius et al., 2013). If not accounted for, this leads to a systematic error in the observed cluster size distribution.

We tested a new tandem instrument in order to study the fragmentation and the stability of small clusters inside the APi-TOF. We used a flat differential mobility analyser (DMA) coupled with the APi-TOF and we produced charged clusters by ElectroSpray Ionization (ESI). This DMA has a high resolution for small ions and clusters, making it ideal to measure the mobility of small clusters involved in new particle formation. Moreover, with this tandem system (DMA-APi-TOF) we can obtain 2D mobility-mass spectra that can allow us to account for the fragmentation of clusters inside the APi-TOF. Using the DMA with a fast scanning mode, we can analyse several clusters in a short time and for each of them we can evaluate the fragmentation inside the mass spectrometer. Another advantage of this set-up is the presence of an electrometer after the DMA and before the APi-TOF. The electrometer provides the concentration of ions in real time and these data can be compared with the mass signal to easily calculate the transmission of the APi-TOF.

We analysed sulfuric acid clusters, and sulfuric acid-bases clusters in both negative and positive mode, which are particularly relevant in the early stages of atmospheric particle formation. The experiments provided a set of data on the stability of charged clusters and their fate inside the atmospheric pressure interface. With an accurate analysis of the data it is possible to define the fragmentation pathways of clusters inside the APi. The data will be used to

develop and validate different model approaches (Monte Carlo and molecular dynamics simulations) that can be used to describe the collisions between charged clusters and neutral molecules (of the carrier gas). Developing such accurate fragmentation models will be useful to retrieve the correct composition and concentration of the clusters measured with APi-TOF mass spectrometers.

This work was supported by the European Research Council (Grant 692891-DAMOCLES), the University of Helsinki, Faculty of Science ATMATH project and Academy of Finland (ARKTIKO project 285067 ICINA).

Kürten, A., Jokinen, T., Simon, M., Sipilä, M., Sarnela, N., Junninen, H., Adamov, A., Almeida, J., Amorim, A., Bianchi, F., Breitenlechner, M., Dommen, J., Donahue, N.M., Duplissy, J., Ehrhart, S., Flagan, R.C., Franchin, A., Hakala, J., Hansel, A., Heinritzi, M., Hutterli, M., Kangasluoma, J., Kirkby, J., Laaksonen, A., Lehtipalo, K., Leiminger, M., Makhmutov, V., Mathot, S., Onnela, A., Petäjä, T., Praplan, A.P., Riccobono, F., Rissanen, M.P., Rondo, L., Schobesberger, S., Seinfeld, J.H., Steiner, G., Tomé, A., Tröstl, J., Winkler, P.M., Williamson, C., Wimmer, D., Yei, P., Baltensperger, U., Carslaw, K.S., Kulmala, M., Worsnop, D.R. and Curtius, J. (2014) *PNAS*, 111:15019-15024.

Olenius, T., Schobesberger, S., Kupiainen-Määttä, O., Franchin, A., Junninen, H., Ortega, I.K., Kurtén, T., Loukonen, V., Worsnop, D.R., Kulmala, M. and Vehkamäki, H. (2013) *Faraday Discuss.*, 165:75-89.

# DETERMINING THE UNDERLYING REASONS FOR BIASES IN PARTICLE NUMBER CONCENTRATIONS IN AN AEROSOL-CLIMATE MODEL

M. PELTOLA<sup>1</sup>, P. PAASONEN<sup>1</sup>, F. XAUSA<sup>1</sup>, R. MAKKONEN<sup>1</sup>, and M. KULMALA<sup>1</sup>

<sup>1</sup>Institute for Atmospheric and Earth System Research / Physics, Faculty of Science, University of Helsinki, Finland

Keywords: atmospheric aerosols, model-measurement comparison

More information on the complex interactions between aerosol particles and the changing climate is needed. To know how the particles will affect the climate in the future, we have to know the sources and processes affecting the particle population. Here, we study how well the global aerosol-climate model ECHAM5.5-HAM2 predicts the concentrations of particles with diameters above 50 or 100 nm (N50 and N100) by comparing the model results to ambient measurements done in different environments around the world. These diameters represent the minimum diameters of particles that are able, under different conditions, to act as cloud condensation nuclei (CCN) and thus affect the climate indirectly. In order to determine what causes the observed discrepancies between the model and the measurements, we evaluate how different variables, such as temperature and the sources and the composition of the particles, affect the observed particle number biases.

Here, ECHAM5.5-HAM2 (Zhang et al., 2012) with nudged meteorology for year 2013 is used. The model describes the particle size distribution with 7 log-normal modes, including 4 soluble modes and 3 insoluble modes. The particles can be composed of black carbon, organic carbon, sulphate, dust and sea salt.

Ambient particle size distributions have been measured with a Differential/Scanning Mobility Particle Sizers (DMPS/SMPS) for several sites. Here, we use as an example data measured at SMEAR II station in Hyytiälä, Finland (Hari and Kulmala, 2005). Figure 1 shows both the measured and modelled particle concentrations (N50) as a function of temperature for Hyytiälä. It can be seen that even though both concentrations correlate positively with temperature, the effect is weaker for the model and the model underestimates the concentrations systematically.

Temperature could be used to explain the differences between modelled and observed concentrations, because many of the processes affecting the particle population are temperature dependant. For example, the amount of CCN produced by condensational growth caused by biogenic vapours increases as a function of temperature (Paasonen et al., 2013). As SMEAR II is situated in a pine forest, underestimating the effects of biogenic sources could be a potential explaining factor for the observed difference. For Hyytiälä, we are also able to use other measured variables, such as concentrations of different gases and the composition of the particles to better quantify what causes the biases.

As the sources of the particles are very different in different environments, in order to obtain the global picture, we made a similar comparison for several other stations around the world. For most stations, only particle and temperature measurements are available, which is why the focus for those stations will be on the effects of temperature and modelled emissions.

To estimate the contribution of different anthropogenic sources on the particle concentrations, we utilise GAINS (Greenhouse gas - Air pollution Interactions and Synergies) model (Amann et al., 2011). For example anthropogenic sulphur, nitrate and volatile organic compound emissions can affect the formation and growth of the particles and thus their regional emissions could be related to the observed particle number biases.

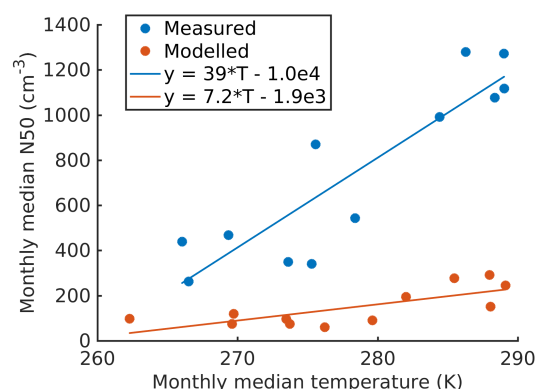


Figure 1: The number of particles with diameters above 50 nm increases as function of temperature for both model and measurements for Hyytiälä. However, for the modelled concentrations, the effect is weaker and the concentrations are clearly underestimated.

- Amann, M et al. (2011). *Environmental Modelling & Software*, 26:116–1501
- Hari, P and Kulmala, M (2005). *Boreal Environment Research*, 10:315–322
- Paasonen, P. et al (2013). *Nature Geoscience*, 6:438–442
- Zhang, K. et al (2012). *Atmospheric Chemistry and Physics*, 12:8911–8949

# SOURCES AND CHARACTERISTICS OF CARBONACEOUS AEROSOLS IN NORTHERN PART OF INDIA

Atar Singh Pipal<sup>1&2\*</sup>, P. Gursumeeran Satsangi<sup>2</sup>, Ajay Taneja<sup>2</sup> and Suresh Tiwari<sup>3</sup>

<sup>1</sup>Department of Chemistry, Dr. B. R. Ambedkar University, Agra, India-282002

<sup>2</sup>Department of Chemistry, University of Pune, Pune, India - 411007,

<sup>3</sup>Indian Institute of Tropical Meteorological, New Delhi Branch, India-110060

**Keywords:** PM<sub>2.5</sub>, carbonaceous aerosols, secondary organic aerosol, India

Presenting author email\*: aspippal@gmail.com

## Abstract

Carbonaceous aerosol is a large fraction of atmospheric aerosols, played a crucial role in air pollution, adverse health, visibility reduction and climate effects. They constitute a significant fraction in fine particles (PM<sub>2.5</sub>), and it could be accounted for up to 40% of mass of PM<sub>2.5</sub> in urban atmosphere (Seinfeld and Pandis 1998). Agra, which is one of the oldest cities “World Heritage site” and Delhi, is the capital city of India; both are located in the border of Indo-Gangetic Plains (IGP) and heavily loaded with atmospheric aerosols due to tourist place, anthropogenic activities and its topography respectively.

The present study was carried out at Agra (AGR) as well as Delhi (DEL) during winter period from Nov. 2011 to Feb. 2012 of fine particulate (PM<sub>2.5</sub>; d < 2.5 µg) and associated carbonaceous aerosols. PM<sub>2.5</sub> was collected at both places using medium volume air sampler and analyzed for organic carbon (OC), and elemental carbon (EC). Average mass concentration of PM<sub>2.5</sub> was 165.42±119.46 µg m<sup>-3</sup> at AGR while at DEL, it was 211.67±41.94 µg m<sup>-3</sup> which is ~ 27 % higher at DEL than AGR. Concentrations of OC and EC were 69.96±34.42 and 9.53±7.27 µg m<sup>-3</sup> at Agra and 50.11±11.93 and 10.67±3.56 µg m<sup>-3</sup> respectively. The OC/EC ratio was 13.75 at (AGR) and 5.45 at (DEL). Significant correlation between PM<sub>2.5</sub> and its carbonaceous species were observed indicating similarity in sources at both sites.

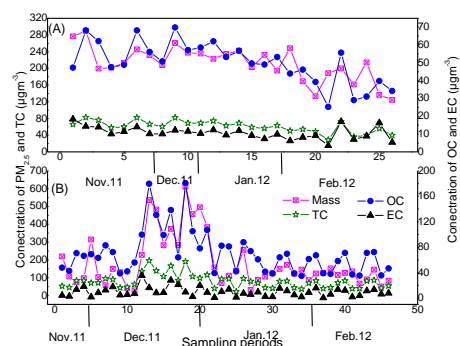


Fig. 1: Day to day variability of mass PM<sub>2.5</sub> and carbonaceous species at DEL (A) and AGR (B)

In the case of POC, similar concentrations were observed at both places but in the case of SOC higher over AGR by 24 in comparison to DEL, it is due to the high concentration of OC over AGR. Secondary organic aerosol (SOA) was 42% higher at AGR than DEL which confirms the formation of secondary aerosol. The SOA contribution in PM<sub>2.5</sub> was also estimated and was ~32% and 12% at AGR and DEL respectively. Being high loading of fine particles along with carbonaceous aerosol, it is suggested to take necessary and immediate action in mitigation of the emission of carbonaceous aerosol in the northern part of India.

## References

Seinfeld JH, Pandis SN (1998) Atmospheric Chemistry and Physics: from Air Pollution to Climate Change. Wiley, New York.

# MOLECULAR LEVEL STUDIES OF AQUEOUS OXIDIZED ORGANICS AND THEIR SALTING INTERACTIONS USING SYNCHROTRON RADIATION X-RAY ABSORPTION SPECTROSCOPY AND QUANTUM-CHEMISTRY BASED COSMO-RS

N.L. Prisle<sup>1</sup>, G. Michailoudi<sup>1</sup>, M. Toivola<sup>2</sup>, M. Patanen<sup>1</sup>, H. Yuzawa<sup>3</sup>, M. Nagasaka<sup>3</sup>, N. Hyttinen<sup>2</sup>, M. Huttula<sup>1</sup>, N. Kosugi<sup>3</sup>, and T. Kurten<sup>2</sup>

<sup>1</sup> Nano and Molecular Systems Research Unit, University of Oulu, Oulu, 90014, Finland

<sup>2</sup> Department of Chemistry, University of Helsinki, Helsinki, 00014, Finland

<sup>3</sup> UVSOR Synchrotron, Institute for Molecular Science, Okazaki 444-8585, Japan

Keywords: glyoxal, salting interactions, synchrotron spectroscopy, COSMOTerm

Humidified aerosol particles and cloud droplets provide the media for aqueous-phase chemistry in the atmosphere. Solubility of organic and inorganic mixtures in aerosol water is therefore a key component in atmospheric processing. In particular, aqueous-phase molecular interactions, such as salting in and out, between different solute components impact aerosol composition via gas-particle partitioning and precipitation processes. However, such aqueous-phase phenomena are still very poorly constrained for complex atmospheric mixtures. Our previous work has demonstrated large impacts of interactions between organic and inorganic aerosol components on their gas-particle partitioning and water uptake properties (Kurten et al., 2014; Hansen et al., 2015). In particular, we studied the successive hydration equilibria of glyoxal in aqueous sulfate solutions using quantum chemical methods and found that the overall Henry's law solubility of glyoxal is greatly enhanced by strong, specific complex formation with sulfate ions stabilizing the hydrates in aqueous solution (Kurten et al., 2014). This mechanism would potentially greatly enhance availability of glyoxal for aqueous SOA formation in regions dominated by sulfate rich aerosol.

We then used COSMO-RS, a method combining quantum chemistry with statistical thermodynamics, to compute aqueous salting interactions for a large array of organic solutes and salts, including highly oxidized organics glyoxal, methylglyoxal, and glycerol (Toivola et al., 2017). While glycerol has no immediate atmospheric relevance, it provides an autonomously characterized analogue to the glyoxal hydrates. COSMOTerm generally overpredicts salting out and/or underpredicts salting in (overpredicts both positive and negative Setschenow constants, respectively) and in particular was unable to replicate the strong salting in of glyoxal in sulfate solutions predicted in our previous work, and observed experimentally by Kampf et al. (2008). For methylglyoxal, experimentally observed salting out was qualitatively predicted.

Subsequently, we used soft X-ray absorption spectroscopy (XAS) to study aqueous interactions of oxidized organics with sulfate in-situ. XAS experiments were carried out using the liquid flow cell end-station at the BL3U beamline at UVSOR synchrotron

facilities, Okazaki, Japan. Synchrotron radiation provides very high sensitivity to the chemical environment of absorbing atoms and enables us to probe molecular structure and inter-molecular interactions in near real-time. The highly oxidized organics were probed via the carbon and oxygen K-edges at photon energies between 280 and 305 eV and 525 to 550 eV, respectively, with a resolution of approximately 0.2-0.4 eV. The absorbance  $\ln(I_0/I)$ , where  $I_0$  is the absorbed intensity of empty cell without sample and  $I$  is the intensity of sample, is recorded over the entire energy region.

We measured SR-XAS spectra for binary aqueous glyoxal, methylglyoxal, and glycerol and their ternary mixtures with  $\text{Na}_2\text{SO}_4$ . We observe glyoxal entirely in its tetrol dihydrate form, whereas methylglyoxal exists as both mono- and dihydrate. Glycerol only shows features attributed to C-OH, as expected. Careful analysis of spectral changes with addition of increasing amounts of salt reveal features of organic-inorganic interactions in the aqueous phase. For each of the studied organics, the effect of sulfate is at best modest, in apparent contrast to both quantum-chemical and COSMOTerm calculations, and experimental observations. Our adventures with glyoxal thus seem far from over yet.



This project has received funding from the European Research Council (ERC) under the European Union's Horizon 2020 research and innovation programme (grant agreement 717022). The authors are ever grateful to the Academy of Finland for financial support.

Kampf, C. J., et al. (2013). *Env. Sci. Tech.*, 47:4236-4244.

Kurten, T., et al. (2014). *J. Phys. Chem. A*, 119:4509D4514.

Hansen, A. M., et al. (2015). *Atmos. Chem. Phys.*, 15:14071-14089.

Toivola, M., et al. (2017). *J. Phys. Chem. A*, 121:6288-6295.

# SECONDARY ORGANIC AEROSOL FORMATION FROM $\alpha$ -PINENE VERSUS REAL PLANT EMISSIONS: CHEMICAL AND PHYSICAL PROPERTIES

I. PULLINEN<sup>1</sup>, A. YLISIRNIÖ<sup>1</sup>, O. VÄISÄNEN<sup>1</sup>, L. Q. HAO<sup>1</sup>, A. BUCHHOLZ<sup>1</sup>, S. SCHOBESBERGER<sup>1</sup>, Z. LI<sup>1</sup>, E.KARI<sup>1</sup>, P. MIETTINEN<sup>1</sup>, P. YLI-PIRILÄ<sup>1,2</sup>, and A. VIRTANEN<sup>1</sup>

<sup>1</sup>Department of Applied Physics, University of Eastern Finland, P.O. Box 1627, 70211 Kuopio, Finland.

<sup>2</sup>Department of Environmental and Biological Sciences, University of Eastern Finland, P.O. Box 1627, 70211 Kuopio, Finland.

Keywords: SOA,  $\alpha$ -pinene, BVOC, hygroscopicity

Atmospheric aerosols (particles and the surrounding gas medium) in general have effect on human health and on climate (Nel, 2005; IPCC, 2013). They can scatter and absorb solar radiation, and act as cloud condensation nuclei (CCN), and regulate cloud properties (e.g. Rosenfeld *et al.*, 2008; Clement *et al.*, 2009). Aerosol particles are also counted as pollution deteriorating air quality (Nel, 2005). A large fraction (up to 90%) of atmospheric sub-micrometre particle mass consists of organic compounds (Jimenez *et al.*, 2009).

Due to the complexity of the biogenic volatile organic compound (BVOC) mixtures emitted by trees and other plants,  $\alpha$ -pinene has often been used for simplicity as a reference compound for boreal forest emitted BVOCs. The aim of this study was to look at some of the physical and chemical properties of secondary organic aerosol (SOA) formed from  $\alpha$ -pinene, and compare them to SOA formed from a BVOC mix taken from real plants, specifically Scots pines. Main focus was on the chemical composition of the particles, and their hygroscopicity.

All the experiments were conducted at the facilities of University of Eastern Finland. The experiment campaign consisted of two main parts: BVOC collection, and chamber studies. The first phase was conducted by selecting five healthy pines (*Pinus sylvestris*), and bringing them into the laboratory space, where BVOC were collected on Tenax tubes. To analyse the actual sampled BVOC mix, three Tenax tubes were analysed with a gas chromatography mass spectrometer (GC-MS) immediately after collection.

The main part of the experiments was conducted in a 10 m<sup>3</sup> Teflon chamber, which was operated as a batch reactor. The chamber was filled with humidified air (45% relative humidity at 22 °C). In the cases of photochemical experiments, H<sub>2</sub>O<sub>2</sub> was added as OH precursor, and butanol-D9 was added as a tracer for OH. After target conditions were reached in the chamber, selected VOC ( $\alpha$ -pinene or real plant BVOC mix) was added, and ozone injected to begin the reactions. In photochemical experiments UV-lights were turned on to signal the start of the experiments. Experiments lasted on average six hours.

Five experiments were conducted in total, four with  $\alpha$ -pinene as a precursor, and one real plant reference. With  $\alpha$ -pinene both pure ozonolysis and low

NO<sub>x</sub> photochemical conditions were probed, while the real plant experiment was in ozone regime only.

The two main instruments used in this study were the Filter Inlet for Gas and Aerosols, (FIGAERO-CIMS, Aerodyne Research Inc., USA and ToFwerk AG, Thun, Switzerland, see Lopez-Hilfiker *et al.*, 2014) for analysing the chemical composition of the particles, and hygroscopic tandem differential mobility analyser (HTDMA, custom made, described in Väisänen *et al.*, 2016) to measure the hygroscopicity of the particles.

Supporting instruments included a high sensitivity proton-transfer-reaction time-of-flight mass spectrometer (PTR-MS, Ionicon) to measure VOC concentrations during chamber experiment, aerosol mass spectrometer (AMS, Aerodyne Research Inc., USA) to get information on particle composition and organic fraction, scanning mobility particle sizer (SMPS, TSI Incorporated, USA) for particle size distribution and number concentration, and ozone monitor (TE49i, Thermo Fischer Scientific).

This work was supported by the Academy of Finland Center of Excellence programme (grant no. 307331), and by the European Research Council (ERC starting grant 335478).

Clement, A. C., Burgman, R., and Norris, J. R. (2009) *Science*, 325, 460-464.

Jimenez, J. L., *et al* (2009) *Science*, 326, 1525-1529.

Lopez-Hilfiker, F. D., Mohr, C., Ehn, M., Rubach, F., Kleist, E., Wildt, J., Mentel, Th. F., Lutz, A., Hallquist, M., Worsnop, D., and Thornton, J. A (2014) *Atmos. Meas. Tech.*, 7, 983-1001.

Nel, A. (2005) *Science*, 308, 804-806.

Rosenfeld, D., Lohmann, U., Raga, G. B., O'Dowd, C. D., Kulmala, M., Fuzzi, S., Reissell, A., and Andreae, M. O. (2008) *Science*, 321, 1309-1313.

Väisänen, O., Ruuskanen, A., Ylisirniö, A., Miettinen, P., Portin, H., Hao, L., Leskinen, A., Komppula, M., Romakkaniemi, S., Lehtinen, K. E. J., and Virtanen, A. (2016) *Atmos. Chem. Phys.*, 16, 10385-10398.

# THE EFFECT OF CHEMISTRY AND PARTICLE TOTAL SURFACE AREA ON LOSS RATE OF HIGHLY OXIDIZED MULTIFUNCTIONAL ORGANIC MOLECULES (HOM)

I. PULLINEN<sup>1,2</sup>, J. WILDT<sup>2,3</sup>, E. KLEIST<sup>3</sup>, M. SPRINGER<sup>2</sup>, C. WU<sup>2,4</sup>, S. ANDRES<sup>2</sup>, S.H.SCHMITT<sup>2</sup>, A. WAHNER<sup>2</sup> and T.F. MENTEL<sup>2</sup>

<sup>1</sup>Department of Applied Physics, University of Eastern Finland, Finland

<sup>2</sup>Institute of Energy and Climate Research, IEK-8: Troposphere, Forschungszentrum Jülich, Germany

<sup>3</sup>Institute for Bio- and Geosciences, IBG-2, Forschungszentrum Jülich, Germany

<sup>4</sup>Department of Environmental Science and Analytical Chemistry, Stockholm University, Sweden

Keywords: HOM, loss rates, uptake coefficient

Highly oxidized multifunctional organic molecules (HOMs) are a group of organic molecules produced by oxidation of VOC, and are generally considered to have low to extremely low vapour pressures (Ehn et al., 2014). These features make them potentially important in particle formation and growth processes in the atmosphere. Understanding the formation and loss processes of these molecules is thus important for a better understanding of particle formation.

It has been shown that HOM formation can be explained by peroxy radical chemistry: first, a HOM peroxy radical (HOM-RO<sub>2</sub>) is formed by autoxidation; and second, termination occurs via classical peroxy radical pathways (e.g. Mentel et al., 2015). The main stable end product pathways are those leading to formation of ketones or alcohols (RO<sub>2</sub>+RO<sub>2</sub>'), and hydroperoxides (RO<sub>2</sub>+HO<sub>2</sub>).

When studying the formation and loss processes of HOMs in chamber experiments we discovered that there were indications that the particles were participating photochemistry, in that they provided a condensation sink to both HO<sub>2</sub> and HOM-RO<sub>2</sub>. This could be seen when analysing the data and calculating the uptake coefficients of HOM molecules. At high particle surface (> 1.0 · 10<sup>-3</sup> m<sup>2</sup>m<sup>-3</sup>), the loss rates of hydroperoxides were increasing, but the loss rates for ketones were decreasing. Our hypothesis is that the apparent increase in loss rate of hydroperoxides is in fact a decrease in production rate, and the decrease in ketone loss rate comes from increased production rate. As losses of HO<sub>2</sub> to particles cannot be excluded (e.g. Brune et al., 1999; Carslaw et al., 2002) we suggest that this loss explains our observations. Lower HO<sub>2</sub> with higher particle loading would lead to fewer HOM-RO<sub>2</sub> terminating with HO<sub>2</sub>, and more with other HOM-RO<sub>2</sub>, leading to higher ketone formation and lower hydroperoxide formation.

Dimer formation is another major termination pathway for HOM-RO<sub>2</sub>. In dimers determining an effective uptake coefficient lead to unrealistically high values above 1, which is the upper limit from the kinetic gas theory. We conclude that if the chemical lifetime of peroxy radicals is in range of its lifetime with respect to losses on particles, further increasing

particle surface will decrease formation rates of dimers and thus pretend a too high condensational sink of dimers. This is then manifested as unrealistically high uptake coefficient at high particle surface loading.

The loss of HOM peroxy radicals on existing particle surface as found here might have implications on atmospheric chemistry. Particle densities used in the experiments mentioned here correspond to mass loadings observed in the Troposphere. HOM-RO<sub>2</sub> lifetimes in the atmosphere are also likely to be longer than in our experiments, leading to proportionally higher importance of condensational loss onto particles.

Brune, W. H., Tan, D., Faloon, I. F., Jaeglé, I., Jacob, D. J., Heikes, B. G., Snow, J., Kondo, Y., Shetter, R., Sachse, G. W., Anderson, B., Gregory, G. L., Vay, S., Singh, H. B., Davis, D. D., Crawford, J. H., and Blake, D. R.(1999). *Geophysical Research Letters*, 26, 3077-3080.

Carslaw, N., Creasey, D. J., Heard, D. E., Jacobs, P. J., Lee, J. D., Lewis, A. C., McQuaid, J. B., Pilling, M. J., Bauguitte, S., Penkett, S. A., Monks, P. S., and Salisbury, G.(2002). *Journal of Geophysical Research*, 107, ACH 5-16.

Ehn, M., Thornton, J. A., Kleist, E., Sipila, M., Junninen, H., Pullinen, I., Springer, M., Rubach, F., Tillmann, R., Lee, B., Lopez-Hilfiker, F., Andres, S., Acir, I. H., Rissanen, M., Jokinen, T., Schobesberger, S., Kangasluoma, J., Kontkanen, J., Nieminen, T., Kurten, T., Nielsen, L. B., Jorgensen, S., Kjaergaard, H. G., Canagaratna, M., Maso, M. D., Berndt, T., Petaja, T., Wahner, A., Kerminen, V. M., Kulmala, M., Worsnop, D. R., Wildt, J., and Mentel, T. F.(2014). *Nature*, 506, 476-479.

Mentel, T. F., Springer, M., Ehn, M., Kleist, E., Pullinen, I., Kurtén, T., Rissanen, M., Wahner, A., and Wildt, J.(2015). *Atmos. Chem. Phys.*, 15, 6745-6765.

# Modelling study on HOM concentrations and their contributions to new particle formation at the boreal forest and polluted urban

X. M. Qi<sup>1,2</sup>, A. J. Ding<sup>1</sup>, P. Roldin<sup>2,3</sup> and M. Boy<sup>2</sup>

<sup>1</sup>School of Atmospheric Sciences, Nanjing University, China

<sup>2</sup>Department of Physics, University of Helsinki, Finland

<sup>3</sup>Division of Nuclear Physics, Lund University, Sweden

Keywords: SMEAR II station, SORPES station, MALTE-BOX model, HOM

Highly oxidized multifunctional organic compounds (HOM) play key roles in new particle formation (NPF) and thereby influence the climate and air quality. HOM formation and NPF mechanism is well studied at SMEAR II station, a boreal forest site. However, as one of the most economically invigorating and densely populated countries, China, the measurements of HOM are rare. This study uses the MALTE-BOX model (Boy et al., 2006) with newest HOM formation mechanism described by Ehn et al. (2016) to simulate the HOM and NPF at SMEAR II and SORPES. By comparing the modeling results at two sites, the differences of HOM concentrations and their contributions to initial growth are investigated.

As tabulated in Table 1, although having high condensation sink, the NPF events are frequently observed in urban of China like SORPES (Qi et al., 2015). The formation rate and growth rate at SORPES are much higher than at SMEAR II. The environmental condition during the NPF are substantially different, with higher condensation sink, atmospheric oxidant ( $O_3$ ) and anthropogenic pollutants ( $SO_2$ ,  $NO_x$ ).

	SMEAR II	SORPES
$J_6$ [ $cm^{-3}s^{-1}$ ]	0.1	1.6
GR [nm/h]	2.8	8.0
CS [ $10^{-2}s^{-1}$ ]	0.14	2.7
$O_3$ [ppbv]	36.6	43.3
$SO_2$ [ppbv]	0.1	8
$NO_x$ [ppbv]	0.2	13.4

Table 1: The differences of NPF characters and corresponding environmental conditions between SMEAR II and SORPES

Five days (four NPF events days and one non-event day) at each sites were chosen for simulations with MALTE-BOX. As shown in Fig. 1, by comparing the observed and simulated sulfuric acid and HOM at SMEAR II, the model provides an acceptable agreement between simulated and measured gas vapors

concentrations. By comparing the simulated sulfuric acid and HOM at two sites, one can see that higher concentrations of sulfuric acid and HOM organonitrate but much lower HOM monomer and dimer concentrations are at SORPES.

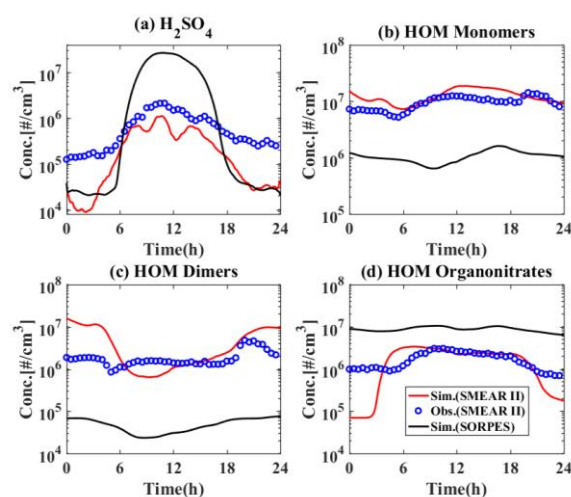


Figure 1: The observed and simulated  $H_2SO_4$  and HOM from monoterpene oxidation at SMEAR II and SORPES.

Different concentrations of gas vapor lead to the discrepancy of their contributions to NPF and even NPF mechanisms at SMEAR II and SORPES. In general, sulfuric acid and HOM from aromatics (not shown in Fig 1) play a dominant role in NPF at SORPES.

Boy, M., O. Hellmuth, H. Korhonen, E. D. Nilsson, D. ReVelle, A. Turnipseed, F. Arnold, and M. Kulmala (2006), MALTE - model to predict new aerosol formation in the lower troposphere, *Atmos. Chem. Phys.*, 6, 4499-4517.

Ehn, M., et al. (2014), A large source of low-volatility secondary organic aerosol, *Nature*, 506(7489), 476-+.

Qi, X. M., et al. (2015), Aerosol size distribution and new particle formation in the western Yangtze River Delta of China: 2 years of measurements at the SORPES station, *Atmos. Chem. Phys.*, 15(21), 12445-12464.



# EFFECT OF TEMPERATURE ON THE FORMATION OF HIGHLY OXYGENATED MOLECULES (HOMS) FORMED FROM $\alpha$ -PINENE OZONOLYSIS

L. L. J. QUÉLÉVER<sup>1</sup>, K. KRISTENSEN<sup>2</sup>, L. NORMANN JENSEN<sup>2</sup>,  
B. ROSATI<sup>2,3</sup>, R. TEIWES<sup>2,3</sup>, H. B. PEDERSEN<sup>3</sup>, M. BILDE<sup>2</sup> and M. EHN<sup>1</sup>

<sup>1</sup> Institute for Atmospheric and Earth System Research/ Physics, P.O. Box 64, 00014 University of Helsinki, Finland.

<sup>2</sup> Aarhus University, Department of Chemistry, Langelandsgade 140, DK-8000 Aarhus C, Denmark.

<sup>3</sup> Aarhus University, Department of Physics and Astronomy, Ny Munkegade 120, DK-8000 Aarhus C, Denmark.

Keywords: HOMs, Temperature, AURA chamber, CI-APi-TOF

The oxidation of  $\alpha$ -pinene by ozone and other oxidants has been extensively studied as it a major source of secondary organic aerosol (SOA) in the atmosphere. Several studies have shown the existence of highly oxygenated molecules (HOMs) produced by autoxidation reactions from the same initiators (Ehn et al, 2014), in chambers and in natural environments, such as the boreal forest. These molecules are now considered to greatly contribute to SOA but are also interesting for their contribution to new particle formation processes. Despite all the newly obtained knowledge on HOM formation, we presently lack understanding of how temperature impacts these processes. Herein, we present the results of HOM measurements in the AURA (Aarhus University Research on Aerosol) chamber during  $\alpha$ -pinene ozonolysis experiments performed at 20 °C, 0 °C and -15 °C.

A description of the chamber can be found in Kristensen et al. (2017). Briefly, it consists of a 5 m<sup>3</sup> Teflon chamber bag run in batch sampling mode where the temperature was set within a range from 20 °C to -15 °C. Initialized at a stable temperature, the chamber was fed with ozone (100 ppb) dispersed in filtered air, exempt of particles, then,  $\alpha$ -pinene was injected reaching a concentration of 50 ppb. The gas phase HOMs were measured using the high-resolution nitrate-based Chemical Ionization Atmospheric Pressure interface Time-Of-Flight (CI-APi-TOF) mass spectrometer (Tofwerk AG, Aerodyne Research), extensively described in Jokinen et al. (2012).

With a high number of oxygen atoms,  $\alpha$ -pinene derived HOMs are usually seen in the mass range 300-600 Th and typically have a chemical composition of C<sub>10</sub>H<sub>14-16</sub>O<sub>7-11</sub> (monomers) and C<sub>19-20</sub>H<sub>28-32</sub>O<sub>10-18</sub> (dimers). **Figure 1** shows the averaged time traces of the HOMs monomers detected during  $\alpha$ -pinene experiments at 3 different temperatures. It also includes the extremum values obtained when the experiments were repeated.

Here the temperature is seen to mainly impact the amount of HOMs formed, leading to higher signals, by more than 2 orders of magnitude, from -15 to 20 °C.

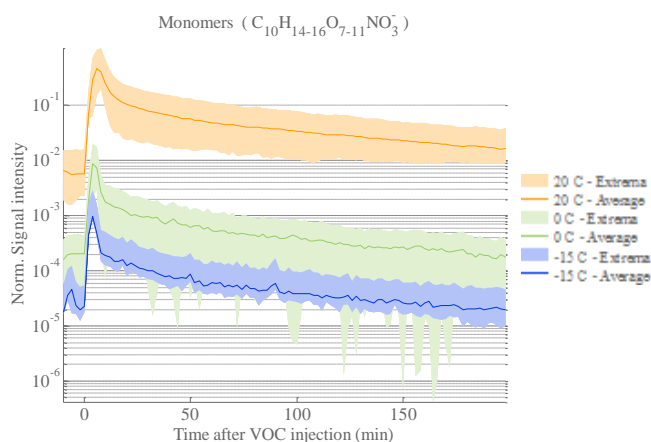


**Figure 1:** Time series of HOMs monomers for the 50 ppb  $\alpha$ -pinene experiments, averaged were done according temperatures (at 20 °C, 0 °C and -15 °C).

As the majority of HOMs are low or extremely low-volatility species already at 20 °C, the loss rates will not be greatly affected by the decrease in temperature, and our results show that the temperature is mostly affecting the formation of HOMs.

With this work investigating the variability of the HOMs production at different temperatures, we clearly show that colder temperatures drastically slow down the rate of HOM production, presumably due to less efficient autoxidation. More details and various aspects of this study, also involving chemical composition analysis, will be presented during the symposium.

This work was supported by the European Research Council (Grant 638703-COALA), the Academy of Finland Centre of Excellence program (project n<sup>o</sup>. 307331), and the Aarhus University Research Foundation.

Ehn et al. (2014), *Nature* **506**, 476-479.

Jokinen et al. (2012), *Atmos. Chem. Phys.* **12**, 4117-4125.

Kristensen et al. (2017), *Environ. Sci. Processes Impacts.* **19**, 1220-1234.

# MOLECULAR DYNAMICS SIMULATIONS OF SULFURIC ACID CLUSTER COLLISIONS

B. REISCHL, M. PASSANANTI, N. MYLLYS, R. HALONEN, E. ZAPADINSKY and H. VEHKAMÄKI

Institute for Atmospheric and Earth System Research / Physics, Faculty of Science, University of Helsinki, Finland

Keywords: atmospheric aerosols, cluster collision, sulfuric acid, molecular dynamics

The first steps in atmospheric particle formation involve small clusters, in particular sulfuric acid and ammonia (or amine) clusters (Vehkamäki and Riipinen, 2012). The detection and quantification of these clusters has recently been made possible due to the development of the chemical ionization atmospheric pressure interface mass spectrometers (CI-APi-TOF). While this technique can detect clusters at environmental low concentration (Jokinen et al., 2012), the fate of atmospheric clusters inside the instrument is unclear: clusters can undergo fragmentation due to chemical ionization, low pressure and energetic collisions with neutral molecules. All these processes can lead to a misinterpretation of the data, in particular the measurement of the concentration and composition of clusters. Therefore modeling of cluster collision and fragmentation is an essential prerequisite for understanding the processes occurring inside the APi during the measurement – as well as in nature.

Interactions between small molecular clusters cannot accurately be modeled as hard sphere collisions: first, the scattering cross-section is not well defined, as clusters already interact through Coulomb or Van der Waals interactions well before a collision takes place, and second, because of the energy transfer to internal rotational and vibrational degrees of freedom of the clusters' constituent molecules or ions during collision.

*Ab initio* molecular dynamics simulations could reveal the atomistic details of the cluster collisions. However, while the system size is small, a large number of individual trajectories with different initial conditions and parameters such as cluster composition, conformer, velocity, and impact parameter, is required to obtain statistically significant results. In practice, we have to resort to classical force fields to describe atomistic interactions, which need to be both accurate and transferable, to enable studies of a wide range of atmospherically relevant clusters, e.g. containing sulfuric acid and water, amines, or other organic molecules. The General AMBER and GROMOS force fields (Wang et al., 2004; Schmid et al., 2011) are both reasonable choices.

We present equilibrium configuration and energy benchmarks for sulfuric acid clusters, using GAFF and GROMOS force fields, against *ab initio* calculations using PW91/aug-cc-pVQZ level of theory, as well as initial results on the molecular dynamics simulations of the cluster collision and fragmentation.

In order to validate the theoretical model we carried out laboratory experiments coupling an APi-TOF mass spectrometer with a separation technique: a high resolution Differential Mobility Analyser (DMA). The DMA classifies charged particles (and clusters) as a function of their electrical mobility, hence with this instrument it is possible to measure the clusters' size and separate them based on their size. In our experimental set-up, sulfuric acid clusters are produced in negative mode with the ElectroSpray Ionization (ESI) source and injected into the DMA. The DMA settings used allow only the negatively charged sulfuric acid trimer ((SA)<sub>3</sub>, [(H<sub>2</sub>SO<sub>4</sub>)<sub>2</sub>HSO<sub>4</sub>]<sup>-</sup>) to enter in the APi-TOF, in this way, we are able to separate (SA)<sub>3</sub> clusters from other sulfuric acid clusters and easily study and quantify their fragmentation inside the instrument. Inside the APi-TOF the sulfuric acid trimer cluster is mainly fragmented in a neutral sulfuric acid molecule (not detectable by the TOF) and a negatively charged sulfuric acid dimer ((SA)<sub>2</sub>, [H<sub>2</sub>SO<sub>4</sub>HSO<sub>4</sub>]<sup>-</sup>). We measured the ratio between the (SA)<sub>3</sub> and its fragmentation product (SA)<sub>2</sub> under different experimental condition and compare the results with the theoretical model.

This work was supported by the European Research Council (Grant 692891-DAMOCLES), the Academy of Finland (ARKTIKO project 285067 ICINA), and the University of Helsinki, Faculty of Science ATMATH project. Computational resources have been provided by CSC – IT Center for Science, Ltd., Finland.

- Jokinen, T., Sipilä, M., Junninen, H., Ehn, M., Lönn, G., Hakala, J., Petäjä, T., Mauldin III, R. L., Kulmala M. and Worsnop, D. R. (2012). *Atm. Chem. Phys.* 12:4117–4125.
- Schmid, N., Eichenberger, A. P., Choutko, A., Riniker, S., Winger, M., Mark, A. E. and Van Gunsteren, W. F. (2011). *Eur. Biophys. J.* 40:843–856.
- Vehkamäki, H. and Riipinen, I. (2012). *Chem. Soc. Rev.* 41:5160–5173.
- Wang, J., Wolf, R. M., Caldwell, J. W., Kollman, P. A. and Case, D. A. (2004). *J. Comput. Chem.* 25:1157–1174.

# THE EFFECT OF SEA SPRAY AEROSOL AGEING ON ITS HYGROSCOPIC AND CLOUD FORMING POTENTIAL

B. ROSATI<sup>1</sup>, R. LANGE<sup>2</sup>, A. MASSLING<sup>2</sup> and M. BILDE<sup>1</sup>

<sup>1</sup>Department of Chemistry, Aarhus University, Aarhus, 8000, Denmark

<sup>2</sup>Arctic Research Centre, Department of Environmental Science, Aarhus University, Roskilde 4000, Denmark

Keywords: sea spray aerosol, ageing, smog chamber, hygroscopicity, cloud droplet activation

Sea spray aerosols (SSA) are continuously emitted into the Earth's atmosphere and play a significant role in the planetary energy budget, by interacting directly with solar radiation and by affecting the formation and lifetime of clouds. This has a major effect on climate since 70% of the planet is covered by the ocean, which thereby is the largest single source of aerosol mass in the atmosphere (e.g. de Leeuw et al. 2011). The atmospheric lifetime of SSA varies from seconds to weeks. During this time, SSA is exposed to oxidants, condensable vapours, light and changing conditions of relative humidity and temperature, which in summary induce so-called ageing effects. Hence, the properties of SSA may be significantly altered, which leads to changes in their role for climate.

The hygroscopic behaviour of SSA, at sub-saturated relative humidities (RH), influences the type and magnitude of the aerosol-radiation interactions by changing the optical properties of the aerosol particles due to water uptake. The hygroscopicity may also affect the particles' efficiency to act as cloud condensation nuclei (CCN) at supersaturated conditions. Commonly, the hygroscopicity and CCN-activity of SSA is assumed to be comparable to that of sodium chloride (NaCl; Lewis and Schwartz, 2004), which is the major component of SSA particles overall (Lewis and Schwartz, 2004). Previous laboratory studies have investigated reactions of aqueous NaCl with ozone and the presence of UV-light, hereby mimicking ageing conditions occurring in the marine boundary layer (Knipping et al., 2000, Laskin et al., 2003). These experiments demonstrated changes in the chemical and physical properties of the particles and hence the authors hypothesize a possible effect on the hygroscopic and cloud activation potential.

Previous studies have mainly addressed aspects of nascent SSA or proxies like NaCl but changes in the particles' hygroscopic and cloud activation potential due to ageing are still poorly characterized. Therefore, in this study we examine atmospheric ageing processes of SSA. To simulate different atmospheric conditions we use the constrained conditions of the Aarhus University Research on Aerosol (AURA) smog chamber, which provides a temperature regulation between 257 and 299 K. In our experiments, the complex chemical composition of SSA is first simplified by using pure NaCl particles generated with a TSI atomizer. These particles are then investigated with regard to their

hygroscopic as well as cloud forming potential and alterations occurring as a result of oxidation processes. Hygroscopicity is measured with a humidified tandem differential mobility analyser (Brechtel) while a cloud condensation nucleus counter (DMT) is used to investigate the cloud forming potential of the fresh and aged particles. Additionally, the particle number size distribution is monitored with a scanning mobility particle sizer (SMPS; TSI) and an optical particle sizer (OPS; TSI).

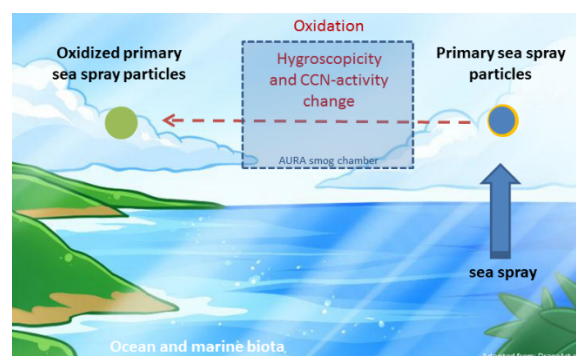


Figure 1: Schematic figure of the ageing of sea spray aerosols.

We will present first results of ageing experiments carried out at the AURA chamber. As illustrated in Figure 1, in this study primary SSA undergo oxidation due to gases and UV-radiation as present in the atmosphere while their hygroscopic and cloud forming potential are constantly monitored.

This work is supported by the Austrian Science Fund (FWF): J 3970-N36.

de Leeuw, G., et al. (2011), *Rev. Geophys.*, 49, RG2001.

Knipping, E. M., M. J. Lakin, K. L. Foster, P. Jungwirth, D. J. Tobias, R. B. Gerber, D. Dabdub, B. J. Finlayson-Pitts, (2000). *Science*, 14: 301-306.

Kristensen, K., Jensen, L.N., Glasius, M., Bilde, M. (2017). *Environ. Sci.: Processes Impacts*, 19:1220-1234.

Laskin, A, Gaspar, D.J., Wang, W.H., Hunt, S.W., Cowin, J.P., Colson, S.D., Finlayson-Pitts, B.J. (2003), *Science*, 301: 340-344.

Lewis, E. R. and Schwartz, S. E. (2004). *Sea Salt Aerosol Production*, American Geophysical Union.

# Heterogeneous Ice Nucleation by Mineral Dusts in Mixed Phased Clouds: Molecular Dynamics Simulations

G. ROUDSARI<sup>1</sup>, O. H. PAKARINEN<sup>1</sup>, AND H. VEHKAMÄKI<sup>1</sup>

<sup>1</sup>(INAR)/ Physics, University of Helsinki, Finland

Keywords: ice nucleation, kaolinite, k-feldspar, molecular dynamics simulations.

Clouds play a substantial role in the modification of climate. Interaction with radiation, influence on wind patterns, transportation of water and precipitation are some of their roles. The formation of ice in clouds has a major effect on their properties, especially in precipitation. Ice crystal may form either homogeneously or heterogeneously. In the former process, ice does not nucleate until  $-38$  °C, whereas in the latter process, ice nucleates at higher temperature with the aid of aerosol seed particles. (Murray et al., 2012) Although, the impact of airborne particles in ice nucleation is poorly understood.

Among these ice nucleating particles, the high ability of mineral dust to nucleate ice has led this particle type to be one of the most studied agents in cloud ice and precipitation formation. There are several types of mineral dusts such as feldspar, kaolinite and illite that are revealed experimentally to be effective ice nuclei. Kaolinite is an aerosol particle that helps water freeze through heterogeneous ice nucleation, but understanding the effect is limited regarding the microscopic level of ice formation on the substrates of kaolinite. Molecular dynamics simulations can help us discover the underlying mechanism of ice formation in the presence of kaolinite (Zielke et al., 2016). Our study focuses on ice structures on the surface of kaolinite. Kaolinite has both a flexible Al-surface and a rigid Si-surface. The results showed that the structure of these surfaces have an effect on the ice structures, and ice nucleation is different between flexible and rigid surfaces. Figure 1 shows two kaolinite surfaces which mirror each other, and TIP4P/Ice water model which is used in this system.

Studies have shown that ice nucleating efficacy of mineral dusts is related to their specific crystallographic features. Atmospheric aerosols have different active sites and surface structures, so it is important to identify which crystallographic features and surface structures are most efficient in ice formation. Therefore the role of imperfections on K-feldspar, for instance, cracks and steps in ice nucleation is being studied to investigate their effect on ice formation. This study will help us identify which structural materials are more efficient as ice nucleating particles, and consequently we will be able to suggest designs of artificial materials optimized for cloud seeding for the rain enhancement application.

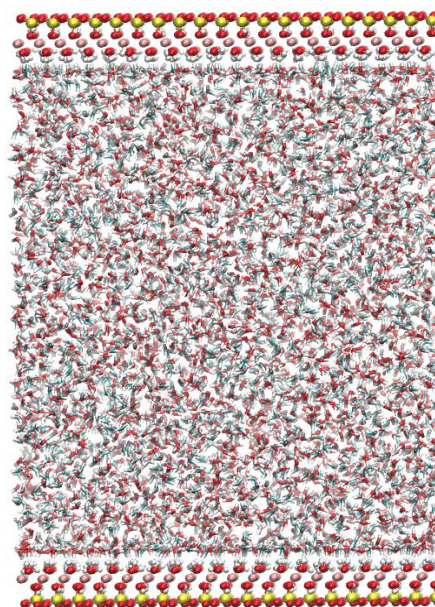


Figure 1: Mirrored kaolinite slabs are at the top and bottom of the simulation cell, hydrogen, aluminum, silicon and oxygen atoms are white, pink, yellow and red, respectively.

Murray, B. J., Sullivan, D., Atkinson, J. D. and Webb, M. E. (2012). *Chem. Soc. Rev.*, 41:6519-6554.

Zielke, S. A., Bertram, A. K. and Patey, G. N. (2016). *J. Phys. Chem. B.* 120:17266-1734.

Acknowledgments:

Work is supported by the National Center of Meteorology & Seismology, Abu Dhabi, UAE under the UAE Research Program for Rain Enhancement Science and by supercomputing resources at CSC – IT Center for Science Ltd, ERC Grant 692891-DAMOCLES, and University of Helsinki, Faculty of Science ATMATH project.

# DEVELOPMENT OF SMEARCORE

A. RUSANEN<sup>1</sup>, P. KOLARI<sup>1</sup>, M. KAUKOLEHTO<sup>1</sup>, M. KULMALA<sup>1</sup> and H. JUNNINEN<sup>1,2</sup>

<sup>1</sup> Institute for Atmospheric and Earth System Research / Physics, Faculty of Science, University of Helsinki, Finland

<sup>2</sup> Institute of Physics, University of Tartu, Estonia

Keywords: software, measurements, data management, data analysis

We are developing a new data management and analysis system SMEARCORE. A challenge in data management of SMEAR type stations is the comprehensiveness of the measurements. For example the SMEAR II station continuously measures over 1000 variables and during 2014 this produced 8 TB of raw data. Managing and refining this data takes a large amount of work even if it is only one station. Thus the motivation behind this development is to clearly document current practices, simplify setting up new measurement campaigns and stations and make the system replicable in case of failure.

We also aim to produce a high level interface to the stored data, which would allow independent development of further analysis and data transform tools, similar to (Junninen *et al.*, 2009). An example of such a tool would be routine and automated processing of complex instruments, such as DMPS measurement systems. Similarly one could also define software instruments based on the data of one or more real ones. The complete system will consist of three subcomponents and configuration files, their connections are shown in Figure 1.

- A collection component that copies data from measurement computers.
- A storage component that stores the data and indexes it. Essentially an interface to the raw data and metadata in a machine readable format.
- An analysis component which builds upon the index provided by storage. For example preprocessing of instrument data or any other routine calculations.

The idea is that end users can use the system through interfaces that represent their problem domain. When setting up measurements the user can input relevant info and metadata about measurement into a configuration file through a web interface. The configuration for that measurement then generates the required database definitions & code to transport the files between the measurement computer and the SMEARCORE server. This reduces the all too common duplication of information. For calibration and analysis code, the user would define what data is needed and would get it in a standardized format out from the storage component. This allows the creation of generic routines that could be used at different stations for similar

instruments. This also makes writing code for exporting to various other data formats easier, since the code only needs to be written once.

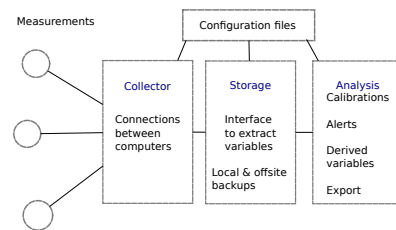


Figure 1: Schematic representation of the responsibilities of the different components of the system at a research station.

The system is still in development. We aim to have the first new deployment running this spring. We also aim to start running it in parallel at a current SMEAR station during this year to evaluate system performance.

Work was supported by the Academy of Finland Center of Excellence programme (grant no. 307331).

Junninen, H., Lauri, A., Keronen, P., Aalto, P., Hiltunen, V., Hari, P., Kulmala, M. (2009). *Smart-SMEAR: on-line data exploration and visualization tool for SMEAR stations*. Boreal Environment Research 14, 447-457.

# RELATIONS OF CLOUD DROPLET PROPERTIES AND IN-CLOUD ICING

A.RUUSKANEN<sup>1</sup>, A. LESKINEN<sup>1,2</sup>, S. ROMAkkANIEMI<sup>1</sup>, M. KOMPPULA<sup>1</sup>

<sup>1</sup>Finnish Meteorological Institute, Kuopio, Finland

<sup>2</sup>Department of Applied Physics, University of Eastern Finland, Finland

Keywords: cloud droplet, atmospheric aerosols, liquid water content, in-cloud icing

Icing is an atmospheric process where ice accumulates on surfaces of any kind. While couple of different icing processes exists, the most interesting related to atmospheric aerosol studies is in-cloud icing. This icing process can be caused either by liquid rain drops or cloud droplets. The most important differences between the two are droplet concentration and size.

Icing can cause damage to structures or financial losses. For example, wind energy power plants might have unplanned shutdown or flights might get delayed/cancelled. With well-structured forecasting models these kinds of unplanned events could be avoided.

Current forecasting models typically have simplified representation of droplets due to the lack of reliable measurement data for verifying the models (Makkonen et al., 2010). The size distributions with typical droplet size are the most important parameters that are needed for reliable icing forecasts.

We have studied cloud droplet properties and icing conditions (Figure 1) for several years at the Puijo measurement station (306 m a.s.l. and 224 m above the surrounding lake level)(Leskinen et al., 2009). The main focus of the study is to investigate connection between cloud microphysical properties, meteorology and icing rate. The study includes several icing detectors (on/off and accumulation speed), cloud droplet probe (CDP) and meteorological instruments for air temperature and wind speed/direction.

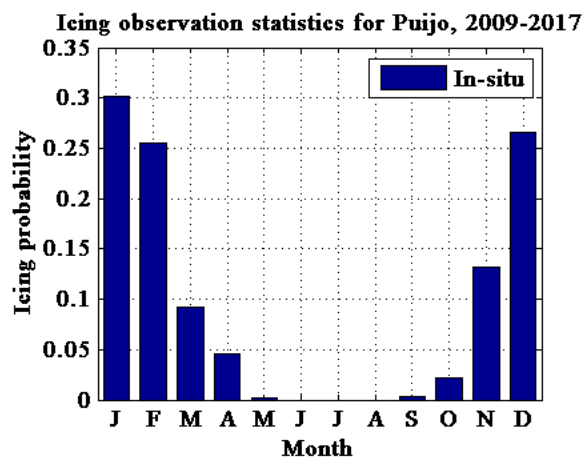


Figure 1: Occurance of icing events at Puijo measurement station, measured with an icing detector.

Preliminary results from 2009 icing events show that average icing rate over all the occurred events was 1.4 mm/h. There was 65 days when icing occurred. Some of the events were short, measured in minutes while others lasted several hours.

In Figure 2 an icing event is shown as an example. Cloud droplet number concentration and mean diameter are presented with icing information. Icing and non-icing events are marked with blue and red, respectively. The temperature during this icing event was almost constant  $-2.5^{\circ}\text{C}$ . The data shows that the icing starts after mean size of the droplets has grown a bit, up to  $8\ \mu\text{m}$  in this case. The size continues growing even during the event, but begins to decrease after concentration drops. During the event the icing rate varies between 2 mm/h and 3 mm/h.

Similar cases of droplet growth and icing were observed from the data set and the detailed analysis will provide the statistics for the assumed relation between the droplet population and in-cloud icing.

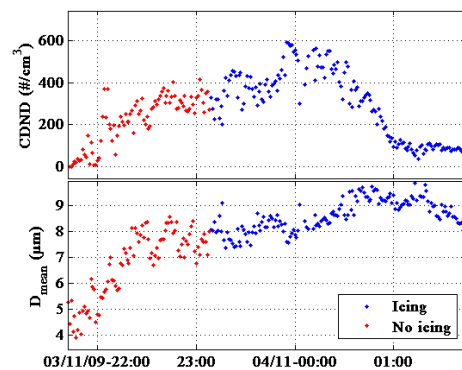


Figure 2: Cloud droplet number concentration (CDNC) and mean droplet diameter ( $D_{\text{mean}}$ ) during an icing event. The data during icing conditions is marked with blue colour while the non-icing one is marked with red.

Leskinen, A., Portin, H., Komppula, M., Miettinen, P., Arola, A., Lihavainen, H., Hatakka, J., Laaksonen, A., Lehtinen, K. E. J. (2009) *Overview of the research activities and results at Puijo semi-urban measurement station*, Boreal Env. Res., 14, 576–590

Makkonen, L., Laakso, T., Marjaniemi, M., Finstad, K. J. (2010) *Modelling and prevention of ice accretion on wind turbines*. Wind Engineering, 25:3-21

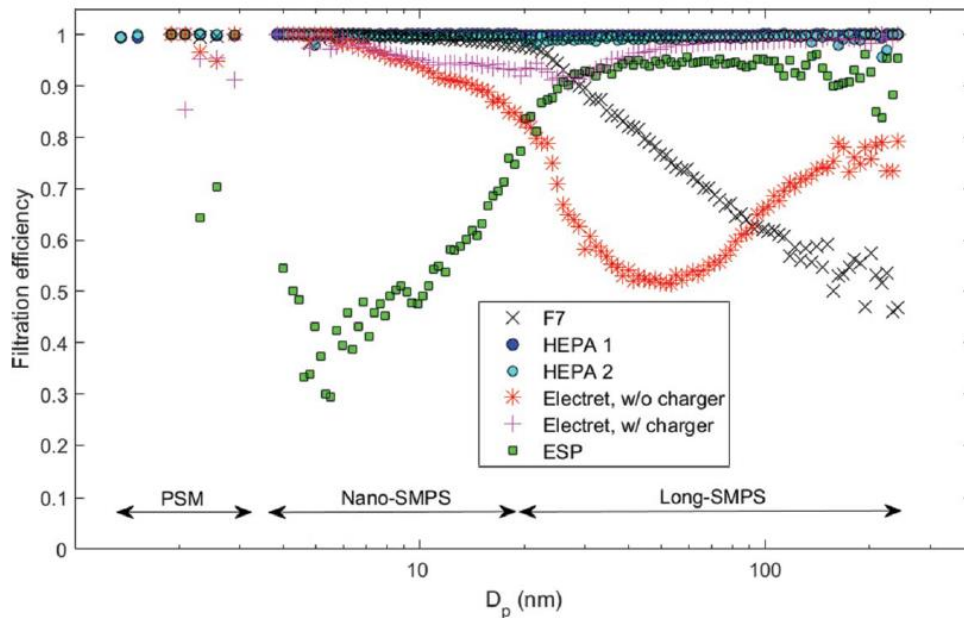
# INDOOR FILTRATION AND TRAFFIC RELATED ULTRAFINE NANOPARTICLES

S. SAARI<sup>1,2</sup>, P. KARJALAINEN<sup>1</sup>, H. KUULUVAINEN<sup>1</sup>, A. TAIPALE<sup>2</sup> and T. RÖNKKÖ<sup>1</sup>

<sup>1</sup> Aerosol Physics, Tampere University of Technology, Finland

<sup>2</sup> Clean Air Solutions, VTT Technical Research Centre of Finland, Finland

Keywords: indoor, filtration, ultrafine particles, traffic



In cities and on traffic lanes, the outdoor particulate number concentration is typically dominated by small nanoparticles, which can penetrate deep into human lungs and cause various health problems. These particles can penetrate into nearby buildings and affect the exposure of humans indoors. There is lack of knowledge how these ultrafine nanoparticles can penetrate through different air filters and affect the indoor air and human health.

In this study, we present an aerosol generation system that mimics the aerosol generated in traffic having typical nucleation and soot aerosol modes. The aerosol generation system was used to determine the particle filtration efficiency of five typical commercial ventilation filters in the particle size range of 1.3-240 nm. The full story of the study is reported in a paper by Karjalainen et al. (2017).

The results showed that the two tested HEPA filters were found to be effective in all particle sizes. The fiber filter (F7) was effective for the traffic related nucleation particles, but its efficiency decreased to 60 percent with the larger particles. The filtration efficiency of the electrostatic precipitator filter (ESP) increased as a function of the particle size and was more effective for traffic related soot particles than for nucleation particles. The electret filter was relatively effective (filtering efficiency > 85%) on all detected particle sizes. The HEPA, F7, and electret filters were found to effectively

remove nano-cluster particles smaller than 3 nm. Overall, filtration efficiency was found to be heavily dependent on particle size and significant differences were observed between different filters.

This study recommend that traffic related nanoparticles should be included in the quality criteria and testing standards of ventilation filters. Information on nanoparticle filtration is needed for manufacturers and end users of filters and ventilation machines as well as for designers of buildings and ventilation in new and refurbishment construction.

Karjalainen, P., Saari, S., Kuuluvainen, H., Kalliohaka, T., Taipale, A., Rönkkö, T. (2017). *Performance of ventilation filtration technologies on characteristic traffic related aerosol down to nanocluster size*. *Aerosol Science and Technology*, 51(12), 1398-1408.

# CHARACTERIZATION OF SECONDARY PARTICULATE EMISSIONS FROM ENGINE OPERATED BY NATURAL GAS AND PROPANE

S. SAARIKOSKI<sup>1</sup>, J. ALANEN<sup>2</sup>, H. VESALA<sup>3</sup>, T. MURTONEN<sup>3</sup>, M. ISOTALO<sup>2</sup>, S. MARTIKAINEN<sup>2</sup>, M. BLOSS<sup>1</sup>, M. AURELA<sup>1</sup>, T. MAUNULA<sup>4</sup>, K. KALLINEN<sup>4</sup>, J. TORRKULLA<sup>5</sup>, H. TIMONEN<sup>1</sup>, T. RÖNKKÖ<sup>2</sup> AND K. LEHTORANTA<sup>3</sup>

<sup>1</sup>Atmospheric Composition Research, Finnish Meteorological Institute, Helsinki, Finland

<sup>2</sup>Aerosol Physics, Faculty of Natural Sciences, Tampere University of Technology, Tampere, Finland

<sup>3</sup>VTT Technical Research center of Finland, Espoo, Finland

<sup>4</sup>Dinex-Ecocat Oy, Oulu, Finland

<sup>5</sup>Wärtsilä Finland Oy, Helsinki, Finland

Keywords: emission measurements, secondary particulate matter, gas engine, natural gas, propane

Natural gas (NG) is used world-wide as a fuel in vehicle engines and energy production, and due to the increased availability, competitive cost and lower CO<sub>2</sub> emissions compared to conventional liquid fossil fuels, its usage is expected to increase in the future. However, similar to other fuels, also NG engines produce emissions that can have impact on environment and human health. Particle mass emissions from NG engines are low compared to conventional diesel engines because of lower soot particle formation in combustion but particle number emissions of NG engines, especially nanoparticle emissions, are not necessarily low (Alanen et al., 2015). In addition to primary particulate emissions, NG engines emit gaseous species that act as precursors for secondary particulate emissions (Alanen et al., 2017).

In some power generation applications, it is more advantageous to use other gas compositions, like ethane and propane, instead of NG that is composed mostly of methane. Changing the gas composition is likely to alter the emissions from gas combustion and also the impact of emissions on environment and human health. Similar to other fuels, the emissions from gas engines are reduced by using exhaust after-treatment systems. The aim of this study was to examine the influence of different catalyst systems (oxidation catalysts and Selective Catalytic Reduction, SCR) in the gas engine operating with NG and propane on exhaust particles. The special focus in this study was on secondary particulate emissions.

The measurement campaign was conducted in November 2017 at VTT engine test facility. The test engine was a passenger car gasoline engine modified to run with NG and propane (Murtonen et al., 2016). The driving conditions were selected based on the emission levels and two different engine driving modes were used. Two catalyst setups were tested, the first one consisting of a combination of an oxidation catalyst and a SCR and the other setup having of only one oxidation reactor. Exhaust gas temperature was varied from 350 to 500 °C and exhaust gas flow was 80 kg/h or 40 kg/h.

The chemical composition of emission particles was studied by using a Soot Particle Aerosol Mass

Spectrometer (SP-AMS, Aerodyne Research Inc.). In addition to the particle chemistry, inorganic and organic gases, particle number concentration and size distribution were measured by an extensive set of instruments. The potential of emission to form secondary particles was examined by Potential Aerosol Mass (PAM) chamber. Two different dilution systems were tested. Exhaust was diluted by a factor from 100 to 1000 depending on the dilution system.

There was no clear difference in the secondary aerosol mass concentrations produced by NG and propane. Additionally, the chemical composition of secondary particles was similar for both gases consisting mostly of sulfate (60–70%), organic matter (25–30%), ammonium (3–4%) and nitrate (1–4%). However, the concentration and chemistry of secondary particles depended on the engine and catalyst conditions. Also the dilution system had an effect on secondary aerosol. It was found that, even after the dilution ratio corrections, the smaller dilution ratio caused larger concentrations of organic matter in secondary particles. Compared to secondary particles, the mass concentrations of primary particles were very small being close to the detection limits of the SP-AMS.

This work was funded by the Tekes – the Finnish Funding Agency for Innovation project no 770/31/2016 (NewGas), Wärtsilä Finland Oy, Dinex-Ecocat Oy, Dekati Oy, Neste, Oilon Oy and Airmodus Oy.

Alanen, J., Saukko, E., Lehtoranta, K., Murtonen, T., Timonen, H., Hillamo, R., Karjalainen, P., Kuuluvainen, H., Harra, J., Keskinen, J. and Rönkkö, T. (2015) *Fuel* 162, 155-161.

Alanen, J., Simonen, P., Saarikoski, S., Timonen, H., Kangasniemi, O., Saukko, E., Hillamo, R., Lehtoranta, K., Murtonen, T., Vesala, H., Keskinen, J. and Rönkkö, T. (2017). *Atmos. Chem. Phys.* 17, 8739–8755.

Murtonen, T., Lehtoranta, K., Korhonen, S., and Vesala, H. (2016) CIMAC congress.



# ATMOSPHERIC EFILTER MEASUREMENTS IN BEIJING, CHINA

L. Salo<sup>1</sup>, Z. Liu<sup>2</sup>, Y. Xie<sup>2</sup> and T. Rönkkö<sup>1</sup>

<sup>1</sup> Aerosol Physics, Faculty of Natural Sciences, Tampere University of Technology, Tampere, Finland

<sup>2</sup> Institute of Atmospheric Physics, Chinese Academy of Sciences, Beijing, China

Keywords: air quality, PM<sub>2.5</sub>, real-time measurement

The eFilter, introduced in 2016 by Dekati, simultaneously collects particles onto a filter and measures the current imparted by the particles. We used the eFilter to measure atmospheric particle mass concentrations in Beijing, China, in the spring of 2017. The results are compared to a TEOM (Thermo Fisher Scientific).

The eFilter has a main flow through the filter and a secondary flow through the electrical portion. The electrical portion has a separate pump, which takes 0.5 lpm from the main flow. The particles entering the electrical portion are charged with a unipolar diffusion charger, and their current is measured from a filter. This two-pronged approach allows data to be obtained with a high time-resolution (1 s), while average mass concentration is determined gravimetrically.

Calculations are necessary to obtain the mass concentration for a specified time period  $t1$  to  $t2$ . The total mass  $m_{total}$  is the mass obtained by weighing the filter before and after collection. The corresponding current  $I_{total}$  is the total current measured during the mass collection.  $A$  is the ratio of the total mass to the total current (equation 1). To calculate the mass collected during any time period  $m_{t1,t2}$ , the sum of the current during the given time period  $I_{t1,t2}$  is multiplied by  $A$  (equation 2). Finally, mass is converted to mass concentration  $M$  by dividing by the corresponding sampled volume  $V$  (equation 3).

$$A = \frac{m_{total}}{I_{total}} \left[ \frac{\mu\text{g}}{\text{fA}} \right] \quad (1)$$

$$m_{t1,t2} = AI_{t1,t2} \quad [\mu\text{g}] \quad (2)$$

$$M_x = \frac{m_x}{V_x} \left[ \frac{\mu\text{g}}{\text{m}^3} \right] \quad (3)$$

The instrument was setup on the third floor of an office building, with a vertical PM<sub>2.5</sub> inlet to remove coarse particles from the outdoor air. The reference instrument, TEOM for PM<sub>2.5</sub>, was located a few meters away from the eFilter. The flow rate through the filter stage was set to 30 lpm, and the filter was changed approximately every 24 hours. Eleven filter samples were taken in total. The filters were stored in a controlled environment for at least a full day before weighing.

Figure 1 shows the mass concentration results for each of the eleven filter samples, along with values measured with the reference TEOM and the eFilter recorded current. We calculated the coefficient  $A$  for each sample. The mean value was  $3.2 \times 10^{-4} \mu\text{g}/\text{m}^3$  and the standard deviation from the mean was 23 %. The results in Figure 2 were calculated for 2 hour periods,

using the mean value of  $A$ . The mass concentration measured by TEOM is also shown for comparison.

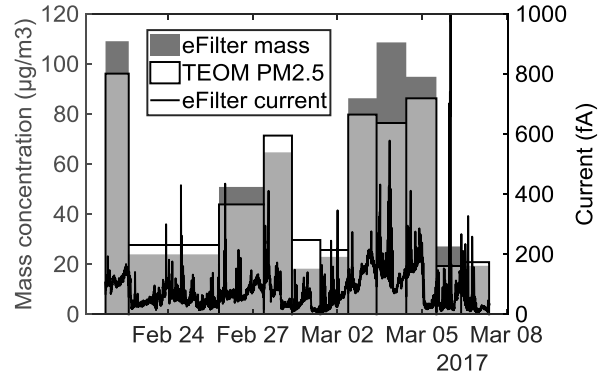


Figure 1: Mass concentration results from each filter for the eFilter (grey bars) and corresponding TEOM results (white bars), along with the eFilter current (black line).

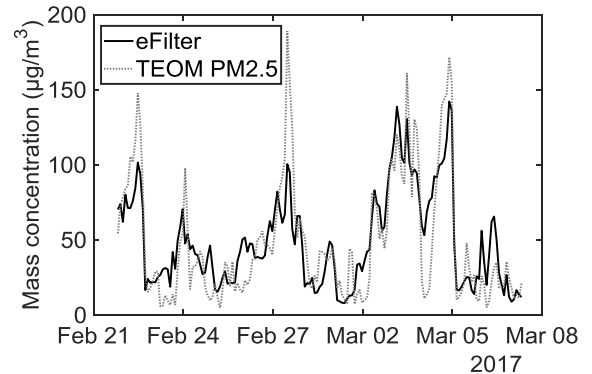


Figure 2: Mass concentration average for every 2 hours, calculated from eFilter data (black line) and the corresponding data from TEOM (grey dotted line) for reference.

The mass concentration measurement method employed by the eFilter worked well. The results presented in Figure 2 had a good correlation with the reference TEOM (correlation curve  $y = 0.65x + 17.9$ ,  $R^2 = 0.71$ ). Results may have been improved by using the nearest measured  $A$  value for each point (instead of the mean); however, even this simple method gave valid results.

## Acknowledgements

This work was conducted in the INKA-ILMA/EAKR project funded by Tekes, European Union, Helsinki Region Environmental Authority (HSY), City of Tampere, City of Kuopio, Dekati Ltd., Genano Ltd., Nordic Envicon Ltd., Pegasor Ltd., Sandbox Ltd., Suomen Terveysilma, TreLab Ltd., and Vallox Ltd.

# OBSERVATIONS OF AEROSOL PRECURSOR VAPOURS IN BOREAL FOREST

N. SARNELA<sup>1</sup>, M. SIPILÄ<sup>1</sup>, T. PETÄJÄ<sup>1</sup>, M. KULMALA<sup>1</sup> and T. JOKINEN<sup>1</sup>

<sup>1</sup> Institute for Atmospheric and Earth System Research / Physics, Faculty of Science, University of Helsinki, Finland

Keywords: low-volatility vapours, sulfuric acid, highly oxygenated organics, mass spectrometry

The process where molecular clusters form from atmospheric vapours by condensation and/or chemical reactions is called new particle formation. In favourable conditions the clusters can grow into larger particle sizes and act as cloud condensation nuclei. The presence of suitable low-volatility compounds is crucial for new particle formation. New measurement techniques have enabled the on-site measurements for low-volatility compounds but due to the expenses and high maintenance of the measurements, these low-volatile compounds have not been comprehensively measured. Here we present the combined results of three spring campaigns conducted in boreal forest site.

We have measured the vapour concentrations during three subsequent spring campaigns at SMEAR II measurement station in Hyytiälä, Finland. The campaigns were conducted in March – April 2011, March – May 2012 and April – June 2013. We used Chemical Ionization Atmospheric Pressure interface Time of Flight Mass Spectrometer (CI-APi-TOF, Jokinen et al., 2012) to measure low-volatility vapours and molecular clusters. In particular sulfuric acid (Sipilä et al., 2010) and highly oxygenated molecules (Ehn et al., 2014; Kirkby et al., 2016) have been identified being responsible of new particle formation. In addition of those we studied the appearance of iodic acid and methyl sulfonic acid. The ambient ions and ion-clusters were measured with APi-TOF (Junninen et al., 2010). The measured vapour and ion concentrations were studied together with meteorological parameters and calculated proxy concentrations (Fig. 1 and Fig. 2). More detailed discussion of the results will be presented in the conference.

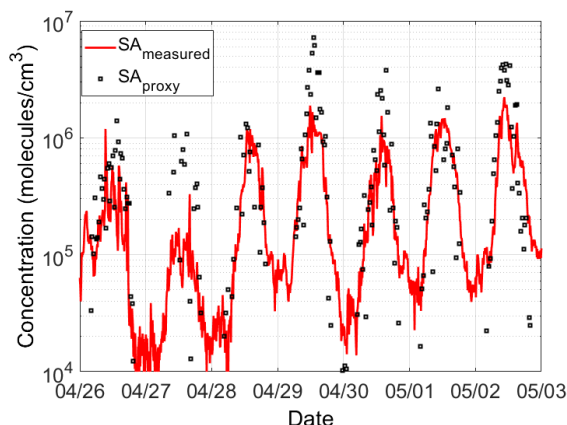


Figure 1. Example of time series of sulfuric acid and sulfuric acid proxy during spring campaign 2013.

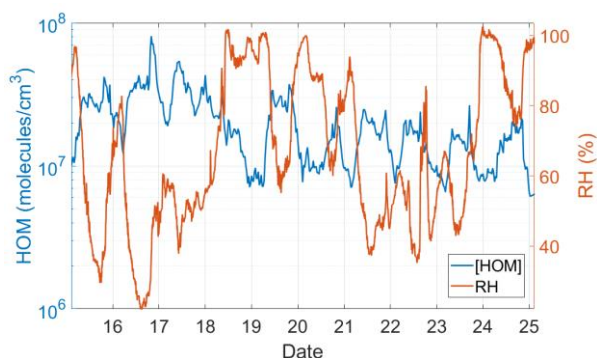


Figure 2. The total concentration of Highly Oxygenated Molecules and relative humidity in May 2013.

All the researchers contributing to the Hyytiälä spring campaigns 2011–2013 and Hyytiälä personnel are acknowledged for their help in conducting the measurements. We thank the tofTools team for providing tools for mass spectrometry data analysis. This work was supported by the Centre of Excellence program of the Academy of Finland (project 272041) and the Advanced Grant program of the European Research Council (project 227463).

- Ehn, M., *et al.* (2014). *Nature*, 506:476–479.
- Jokinen, T., Sipilä, M., Junninen, H., Ehn, M., Lönn, G., Hakala, J., Petäjä, T., Mauldin, R. L., Kulmala, M. and Worsnop, D. R. (2012). *Atmos. Chem. Phys.*, 12:4117–4125.
- Junninen, H., Ehn, M., Petäjä, T., Luosujärvi, L., Kotiaho, T., Kostianen, R., Rohner, U., Gonin, M., Fuhrer, K., Kulmala, M. and Worsnop, D. R. (2010) *Atmos. Meas. Tech.*, 3:1039–1053.
- Kirkby, J., *et al.* (2016). *Nature*, 533:521–526.
- Sipilä, M., Berndt, T., Petaja, T., Brus, D., Vanhanen, J., Stratmann, F., Patokoski, J., Mauldin, R. L., Hyvarinen, A.-P., Lihavainen, H. and Kulmala, M. (2010) *Science*, 327:1243–1246.

# THE EFFECT OF TEMPERATURE AND SEED AEROSOL ACIDITY ON THE FORMATION AND COMPOSITION OF SECONDARY ORGANIC AEROSOLS FROM ISOPRENE OXIDATION

P. M. SHAMJAD<sup>1</sup>, K. WANG<sup>2</sup>, T. HOFFMANN<sup>2</sup>, R. J. HUANG<sup>3</sup>, M. GLASIUS<sup>1</sup> and M. BILDE<sup>1</sup>

<sup>1</sup> Department of Chemistry, Aarhus University, Aarhus, Denmark

<sup>2</sup> Institute of Inorganic and Analytical Chemistry, Johannes Gutenberg-Universität Mainz, Germany

<sup>3</sup> Key Lab of Aerosol Chemistry & Physics, Chinese Academy of Sciences, Beijing, China

Keywords: isoprene, OH oxidation, organosulfates, sulfate seed

## Introduction

Isoprene (C<sub>5</sub>H<sub>8</sub>) is a major biogenic volatile organic compound known to contribute up to 70% of global secondary organic aerosol (SOA) concentration (Li et al., 2018). In the atmosphere, isoprene reacts with hydroxyl radicals (OH), ozone (O<sub>3</sub>) and nitrate radicals (NO<sub>3</sub>) producing various SOA compounds. The formation and chemical composition of these SOA compounds depends on the temperature, relative humidity (RH) and presence of other aerosol species known as seed particles. Isoprene oxidation reactions at high temperature and RH condition produces lower SOA yield (Zhang et al., 2011). Preexisting sulfate aerosols are known to increase the SOA yield depending on the acidity. Highly acidic sulfate aerosols produce more SOA compared to low acidic conditions (Surratt et al., 2008). In this study, we report the formation and chemical composition of SOA formed during the photo-oxidation of isoprene using OH radicals at different temperatures.

## Methods

Experiments were conducted using AURA smog chamber facility in Aarhus University (Kristensen et al., 2017) at 3 different temperatures, 258, 278, and 293 K respectively and a RH of 50%. Experiments were conducted under low NO<sub>x</sub> conditions (conc. < 1 ppb) with and without sulfate seeds of two pH values below 7. An Agilent gas chromatograph with flame ionization detector (GC-FID-7820A) and High Resolution Time of Flight Aerosol Mass Spectrometer (HR-ToF-AMS) were used to measure gas phase and particle phase concentrations respectively. Concentration of O<sub>3</sub> was measured using UV photometric (O<sub>3</sub> 42 Module, Environment S.A). A scanning mobility particle sizer (SMPS) system including electrostatic classifier (EC, TSI-3082) coupled with a water-based condensation particle counter (WCPC, TSI-3788) was used to record particle size distributions between size range 10 to 420 nm. Two filter samples (fresh and aged) were collected during the experiments which are then analyzed in an ultrahigh performance liquid chromatography coupled to electrospray ionization source of quadrupole time-of-flight mass spectrometer (UHPLC/ESI-qTOF-MS, microTOF II, Bruker Daltonik) to identify the chemical composition of the isoprene-derived SOA.

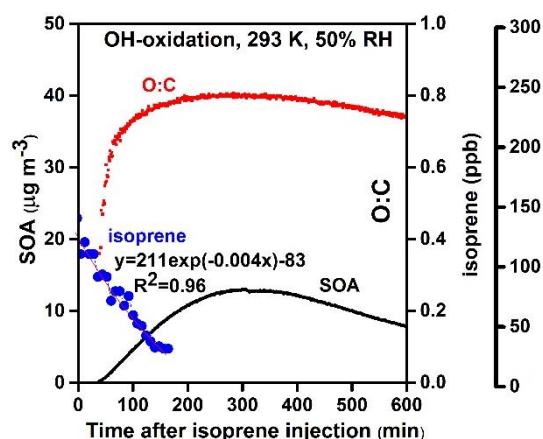


Figure 1: Concentration of isoprene consumed and SOA produced along with O:C ratio for an isoprene OH oxidation experiment at 293 K and 50% RH.

## Conclusions

Preliminary data and analysis shows change in SOA formation and composition depending on the experimental temperature and relative humidity. The influence of aerosol seed acidity on organosulfate production is also examined and will be discussed.

We acknowledge the support from Aarhus University for conducting this research.

Kristensen, K., Jensen, L.N., Glasius, M., Bilde, M. (2017). *Environ. Sci. Process. Impact.*, 19, 1220-1234.

Li, J., Wang, G., Wu, C., Cao, C., Ren, Y., Wang, J., Li, J., Cao, J., Zeng, L., Zhu, T. (2018). *Sci. Rep.*, 8, 535.

Surratt, J.D., Gómez-González, Y., Chan, A.W.H., Vermeylen, R., Shahgholi, M., Kleindienst, T.E., Edney, E.O., Offenberg, J.H., Lewandowski, M., Jaoui, M., Maenhaut, W., Claeys, M., Flagan, R.C., Seinfeld, J.H. (2008). *J. Phys. Chem. A.*, 112, 8345-8378.

Zhang, H., Surratt, J.D., Lin, Y.H., Bapat, J., Kamens, R.M. (2011). *Atmos. Chem. Phys.*, 11, 6411-6424.

# MODELING STUDY ON IMPORTANCE OF ANTHROPOGENIC AMONNIA AND ORGANICS ON NEW PARTICLE FORMATION IN NORTH CHINA PLAIN

D. J. Shang<sup>1</sup>, M. Hu<sup>1</sup>, K. D. Lu<sup>1</sup>, P. Roldin<sup>2</sup>, J. Größ<sup>3</sup>, S. Kecorius<sup>3</sup>, Y. S. Wu<sup>1,4</sup>,  
T. Olenius<sup>5</sup>, B. Birger<sup>6</sup>, L. M. Zeng<sup>1</sup>, Y. H. Zhang<sup>1</sup>, A. Wiedensohler<sup>2</sup>, M. Boy<sup>4</sup>

<sup>1</sup> College of Environmental Sciences and Engineering, Peking University, China

<sup>2</sup> Division of Nuclear Physics, Lund University, Sweden

<sup>3</sup> Leibniz Institute for Tropospheric Research, Leipzig, Germany

<sup>4</sup> Institute for Atmospheric and Earth System Science / Physics, Helsinki University, Finland

<sup>5</sup> Department of Environmental Science and Analytical Chemistry (ACES) and Bolin Centre for Climate Research, Stockholm University, Sweden

<sup>6</sup> Institute of Energy and Climate Research, IEK-8: Troposphere, Forschungszentrum Jülich GmbH, Jülich, Germany

Keywords: nucleation, atmospheric aerosols, model simulation, ammonia, organics

Atmospheric new particle formation (NPF) is an important source of aerosol particles globally. Especially in polluted atmosphere, the efficient nucleation and continuous growth of particles can increase the number concentration of cloud condensation nuclei (CCN), and even cause the deterioration of air quality by elevating particle mass (PM) concentration (Guo et al, 2014). In order to achieving a better quantification of those climate and air quality effects, detailed investigation of chemical mechanism of new particle formation is needed.

Recent laboratory studies revealed that ammonia, amine and highly oxygenated multifunctional organic compounds could be participants in stabilization of sulfuric acid clusters under the scale of ~1.7 nm, as well as in the condensational growth of the particles. However, these conclusions were hardly inspected in polluted atmosphere of China, because of the technical limitation in measuring those precursors. On the other hand, anthropogenic VOCs including aromatics are abundant in polluted atmosphere, but their contributions in growth through OH oxidation and HOMs formation were rarely studied.

This studied aimed at emphasizing anthropogenic ammonia and VOCs' contribution in the NPF process in polluted atmosphere through a combination of in-situ measurements and model simulation.

A comprehensive measurement was conducted at Wangdu station, a regional site in North China Plain (NCP). A twin-differential mobility particle sizer (TDMPMS) and an aerodynamic particle sizer (APS) were employed in achieving particle (3nm-10 $\mu$ m) number size distribution. OH, HO<sub>2</sub> radicals and NH<sub>3</sub> were measured by a laser-induced fluorescence (LIF) technique and an online ion-chromatography system, respectively. VOCs data consisting of 70 compounds was from a proton-transfer mass chromatography (PTR-MS). SO<sub>2</sub>, NO<sub>x</sub>, CO and other gaseous pollutants were also measured.

MALTE-box model developed by Boy et al (2006) was employed and modified in this research. Atmospheric cluster dynamics code (ACDC), including the sulfuric acid and ammonia in clusters, was used to solve the nucleation rate in the model. Biogenic HOMs was simulated based on lab results of monoterpene and

isoprene oxidation. Also, a simplified chemical mechanism of HOMs formation from OH-oxidation of aromatic VOCs was introduced. Three NPF days were simulated in this study, as shown in Table 1.

Table 1 Parameters of simulated NPF events.

Date	FR [cm <sup>-3</sup> s <sup>-1</sup> ]	GR [nm h <sup>-1</sup> ]	CS [s <sup>-1</sup> ]
June 12	7.8	8	0.017
June 27	20.5	4.4	0.02
June 28	10	5.7	0.014

The results showed that, the nucleation mode particle concentration during NPF was well captured by the model with ACDC considering the sulfuric-ammonia clustering, and no artificially corrected coefficient is needed. On the growth phase, the model failed in reproducing the particle volume concentration (Fig. 1) and CCN raising by NPF in NCP when considering only the biogenic HOMs. While the model set considering a 15% yield of first OH-oxidation products of aromatics into HOMs showed a very promising simulation results, in which HOMs-aromatics contributed 40% of sub-10 nm particle growth.

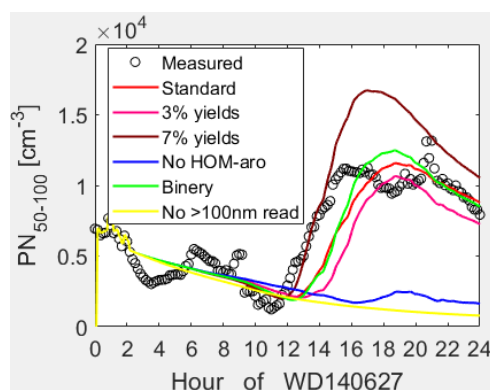


Fig. 1 Measured particle volume (PV<sub>0.1</sub>) concentration, and the simulation results from different model sets.

Guo S., et al. (2014). *Proc Natl Acad Sci USA*. 111:17373-17378.

Boy, M., et al. (2006). *Atmos. Chem. Phys.* 6(12):4499-4517.

# LONG TERM MEASUREMENT OF AEROSOL OPTICAL PROPERTIES AT SORPES, NANJING

Y. SHEN<sup>1</sup>, A. VIRKKULA<sup>1,2,3,4</sup>, A. DING<sup>1,2</sup>, J. WANG<sup>1</sup>, X. CHI<sup>1,2</sup>, W. NIE<sup>1,2</sup>, X. QI<sup>1,2</sup>, X. HUANG<sup>1,2</sup>, Q. LIU<sup>1</sup>, L. ZHENG<sup>1,2</sup>, Z. XU<sup>1,2</sup>, T. PETÄJÄ<sup>4</sup>, P. P. AALTO<sup>4</sup>, C. FU<sup>1,2</sup>, AND M. KULMALA<sup>4</sup>

<sup>1</sup>Joint International Research Laboratory of Atmospheric and Earth System Sciences, and School of Atmospheric Sciences, Nanjing University, 210023, China

<sup>2</sup>Collaborative Innovation Center of Climate Change, Jiangsu Province, China

<sup>3</sup>Finnish Meteorological Institute, FI-00560, Helsinki, Finland

<sup>4</sup>Department of Physics, University of Helsinki, FI-00014, Helsinki, Finland

Keywords: scattering, single scattering albedo, pollution, Nanjing

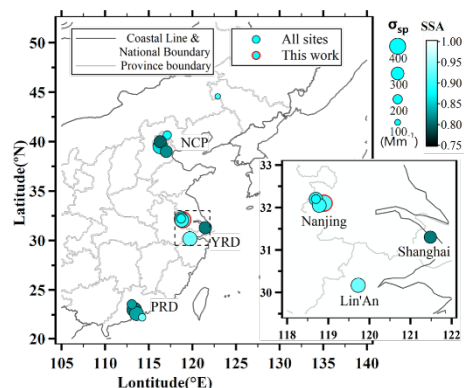
Long term measurement of Aerosol Optical Properties (AOPs) includes Scattering coefficient ( $\sigma_{sp}$ ), Absorption coefficient ( $\sigma_{ap}$ ), Single Scattering Albedo (SSA), backscattering fraction ( $b$ ) Ångstrom Exponent for scattering (SAE) and absorption (AAE) were conducted between June 2013 and May, 2015 at SORPES, a regional background station located inside Yangtze River Delta urban agglomeration.

The spatial and temporal variation of AOPs, the relationship between AOPs and other parameter, the potential effect on radiation forcing are analyzed for the same period. The aerosol was highly scattering with an average scattering coefficient of  $\sigma_{sp} = 410 \pm 320 \text{ Mm}^{-1}$  and an average SSA of 0.93 for the green light. The scattering coefficient in study is comparable to published values from several other sites in China, while SSA appears to be slightly higher than published values from those sites and elsewhere. The AOPs had typical seasonal cycles with high  $\sigma_{sp}$  and  $\sigma_{ap}$  in winter and lower in summer: the averages were  $\sigma_{sp} = 545 \pm 425 \text{ Mm}^{-1}$  and  $\sigma_{ap} = 36 \pm 24 \text{ Mm}^{-1}$  in winter and  $\sigma_{sp} = 364 \pm 294 \text{ Mm}^{-1}$  and  $\sigma_{ap} = 20 \pm 13 \text{ Mm}^{-1}$  in summer.

The seasonal cycles for intensive AOPs are less clear, the variations of them were more related to the evolution of pollution episodes. The diurnal cycles of the AOPs were clear and in agreement with the cycle of boundary layer height, radiation, human activities the particle number size distribution, however, is still unable to compare with multi-day scale cycle. Synoptic weather dominated the cycle of AOPs in a temporal scale of 3-7 days, or defined as 'pollution episode'. During pollution episodes, PM<sub>2.5</sub> and external AOPs usually go through several days continuously increasing and drops rapidly within several hours to one day. The extend of the growth usually up to half even one order of magnitude.

The continuous secondary formation process is considered to be the cause of growth, during which, particles grow larger, light-scattering increases and hence SSA increases. Back scattering fraction as an indicator of particle size, decreases significantly from  $\sim 1.6$  to  $\sim 1$  during some episodes, hence present negative correlated with SSA. The aerosol radiative forcing efficiency (RFE) is theoretically negatively correlated with both SSA and  $b$ , in other words, darker

aerosol and/or larger particles lead to higher RFE. The negative correlation between SSA and  $b$  (i.e. the darker aerosol usually smaller) consequential cancel out their individual effect on REF. The RFE probability distribution at SORPES was clearly more narrow than at a clean background site which is in agreement with a



published RFE climatology.

Figure 1, the location of SORPES and some studies in China. Colorcode represent SSA and marker size represent  $\sigma_{sp}$

## ACKNOWLEDGEMENTS

The research was supported by the Jiangsu Provincial Natural Science Fund (No.BK20140021), National Science Foundation of China (D0512/91544231, D0512/41422504) and National Key Research and Development Program of China (2016YFC0200500), and Academy of Finland's Centre of Excellence program (Centre of Excellence in Atmospheric Science - From Molecular and Biological processes to The Global Climate, project no. 272041) .

## REFERENCES

Shen, Y., Virkkula, A., Ding, A., Wang, J., Chi, X., Nie, W., Qi, X., Huang, X., Liu, Q., Zheng, L., Xu, Z., Petäjä, T., Aalto, P. P., Fu, C., and Kulmala, M.: Aerosol Optical Properties at SORPES in Nanjing, East China, Atmos. Chem. Phys. Discuss., <https://doi.org/10.5194/acp-2017-863>, in review, 2017.

# EFFECT OF SHIP SULPHUR EMISSION REDUCTION ON GLOBAL AEROSOL LOAD

M. SOFIEV<sup>1</sup>, J. WINEBRAKE<sup>2</sup>, L. JOHANSSON<sup>1</sup>, E.CARR<sup>3</sup>, R. KOUZNETSOV<sup>1</sup> J.-P. JALKANEN<sup>1</sup>, J. CORBETT<sup>4</sup>

<sup>1</sup>Finnish Meteorological Institute, Finland

<sup>2</sup>College of Liberal Arts, Rochester Inst. of Technology, USA

<sup>3</sup>Energy and Environmental Research Associates, LLC, USA

<sup>4</sup>University of Delaware, USA

Keywords: ship-induced aerosols, air quality modelling, emission reduction

Emission from shipping constitutes about 13% of the global totals for Sulphur oxides, one of the major precursors for secondary aerosols in the atmosphere. New global standards of sulphur content in the ship fuels come into force on 1 January 2020 reducing the maximum permissible sulphur mass fraction in the fuel 7 times – from 3.5% down to 0.5%. In some areas (Baltic and North Sea, zones near the US coast and China), restrictions have already been implemented as regional pollution abatement measures but still the planned reduction will cut the global annual SO<sub>x</sub> emission from ships from 11,5 Mt yr<sup>-1</sup> to 2.5 Mt yr<sup>-1</sup>.

The impact of this reduction on global distribution of aerosols and the related radiative forcing was studied with coupled STEAM (ship emission) and SILAM (atmospheric composition) models by Sofiev et al. (2018). With this talk, we discuss the main conclusions of that work.

The simulations were made with the interfaced STEAM ship emission and SILAM atmospheric composition models. STEAM provided the 3-hourly emission fluxes from ships using their actual locations, speed and physical characteristics as described in (Jalkanen et al. 2016) and passed this information to SILAM. Since ships, especially oceanic vessels, are strong point sources moving over pristine areas but sometimes passing by densely populated places, the simulations were performed at the resolution of 0.1° (~10km) over the whole globe for the full year of 2015. Input meteorological fields were taken from ECMWF with resolution of approximately 0.125°.

Owing to high spatial and temporal resolution, the simulations produced very detailed patterns of the pollution distribution. For instance, Figure 1 depicts SO<sub>2</sub> concentrations predicted 16.12.2015 near South Africa. One can distinguish dense routes near the African coast, individual ships ceiling offshore, coastal effects, and concentrations over populated areas.

It was shown that the MARPOL-VI regulations result in substantial reduction of PM concentrations: up to 50% of PM<sub>2.5</sub> can be shaved out in the vicinity of busy ship routes (Figure 2). We estimated that it can save up to 100,000 premature deaths, mainly in Africa and Asia (Europe and America already control fuel sulphur content).

From the other side, the measures will result in 50-100 mW m<sup>-2</sup> of lost cooling due to diminishing aerosol concentrations. The bulk of the effect comes from reduction of the cloud droplet number concentrations and associated reduction of cloud albedo (the first aerosol indirect effect).

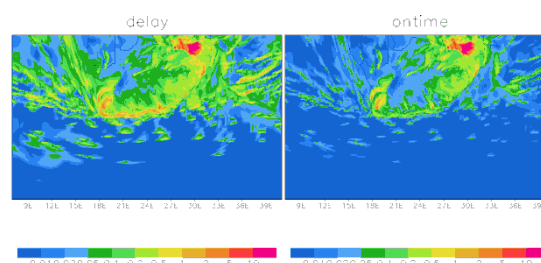


Figure 1: MARPOL VI effect: SO<sub>2</sub> concentrations [ $\mu\text{g S m}^{-3}$ ] on 16.12.2015 at 21:00 with current (left) and reduced (right) sulphur content of the fuel.

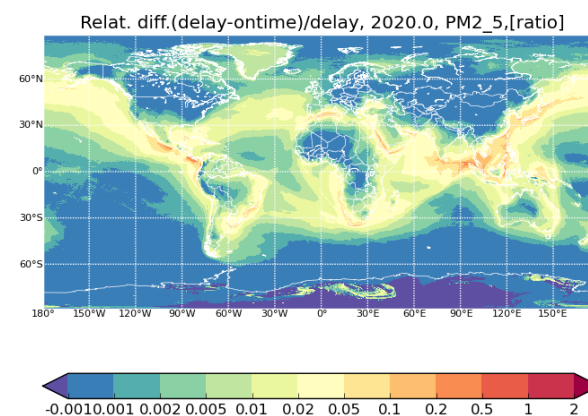


Figure 2: Relative reduction of PM<sub>2.5</sub> annual concentrations due to MARPOL VI implementation.

Jalkanen, J.P., Johansson, L. & Kukkonen, J., 2016. A comprehensive inventory the ship traffic exhaust emissions in the European sea areas in 2011. *Atmospheric Chemistry and Physics*, 16, pp.71–84  
Sofiev, M., Winebrake, J.J., Johansson, L., Carr, E.W., Prank, M., Soares, J., Vira, J., Kouznetsov, R., Jalkanen, J.-P., Corbett, J. J. (2018) Global health

and climate impacts from international shipping.  
Nature Comm. *In press*.

# UNDERSTANDING LINK BETWEEN TRAFFIC AND AIR QUALITY IN INDIA, FIRST RESULTS OF “TAQIITA” PROJECT: CHEMICAL CHARACTERIZATION OF EXHAUST PARTICLES FROM PASSENGER CARS

K. TEINILÄ<sup>1</sup>, H. TIMONEN<sup>1</sup>, S. SAARIKOSKI<sup>1</sup>, R. HOODA<sup>1</sup>, M. BLOSS<sup>1</sup>, M. AURELA<sup>1</sup>, E. ASMI<sup>1</sup>, A. MALINEN<sup>2</sup>, L. PIRJOLA<sup>2</sup>, B. LAL<sup>3</sup>, A. DATTA<sup>3</sup>, S. SUBUDHI<sup>3</sup>, R. SURESH<sup>3</sup>, Md. H. RAHMAN<sup>3</sup>, D. VERMA<sup>3</sup>, L. SALO<sup>4</sup>, P. SIMONEN<sup>4</sup>, P. KARJALAINEN<sup>4</sup>, H. KUULUVAINEN<sup>4</sup>, K. KULMALA<sup>5</sup>, J. NUOTTIMÄKI<sup>5</sup>, J. KESKINEN<sup>4</sup>, T. RÖNKKÖ<sup>4</sup> AND H. LIHAVAINEN<sup>1</sup>,

<sup>1</sup>Finnish Meteorological Institute, Atmospheric Composition Research, FI-00560, Helsinki, Finland

<sup>2</sup>Department of Technology, Metropolia University of Applied Sciences, FI-00180 Helsinki, Finland

<sup>3</sup>The Energy and Resources Institute, New Delhi, India

<sup>4</sup>Tampere University of Technology, Faculty of Natural Sciences, Aerosol Physics, FI-33101 Tampere, Finland

<sup>5</sup>Neste Corporation, Research and Development, Products and Applications, Technology Centre, FI-06101 Porvoo, Finland

Keywords: Air quality in India, exhaust emission, chemical composition

Traffic emissions are the most important contributor to air pollution in Indian cities where the number of vehicles continues rapid increase (Ramanathan et al., 2014). The main goal of TAQIITA (Traffic and Air Quality In India: Technologies and Attitudes) project is to improve Indian capabilities for air quality monitoring and measurements, and to provide knowledge and tools for vehicle emission reductions in order to improve the air quality in cities.

Important part of this project is detailed characterization of primary and secondary emissions from heavy-duty vehicles and passenger cars. Laboratory measurements in Finland were made on Metropolia chassis dynamometer (AVL, Zöllner GmbH, 48” -Compact) and chasing measurements were conducted using TUT’s mobile laboratory van and Metropolia’s Sniffer van. Laboratory and chase measurements made in Finland focused on the passenger car (diesel Toyota Corolla, Euro 4 and gasoline Suzuki SX4, Euro 4) emissions. The aim of the measurements was to get information how lubricants and used fuels affect the chemical composition of particles. The used fuels were Finnish 98E5 gasoline, regular Finnish diesel, regular Indian diesel, and paraffinic renewable diesel fuel - commonly known as Hydrogenated Vegetable Oil (HVO).

The driving cycles used on chassis dynamometer were WLTC (Worldwide harmonized Light vehicles Test Procedure), NEDC (New European Driving Cycle) and on-road cycles (designed to simulate Indian driving patterns). Measurements with these cycles were made with both cold and hot engine. In the chase measurements, exhaust emissions of a road cycle, including steady driving, accelerations and engine motoring conditions, were studied.

The concentrations of total organics, nitrate, sulphate, ammonium, chloride, black carbon and certain metals of submicron particles of both fresh primary emissions and aged exhaust were measured using a high-resolution soot particle aerosol mass spectrometer

(SP-AMS) (Onasch et al., 2012). SP-AMS gives also the size distribution of these compounds. Concentration of black carbon was also measured using a dual-spot aethalometer (AE33, Magee Scientific) (Drinovec et al., 2015). To gain information whether particle chemical composition affects particle density; the particle effective density was measured using CPMA-DMA-CPC (Cambustion/TSI) system on the chassis dynamometer studies.

The main chemical components of particulate matter for diesel passenger car exhaust were organics and black carbon. The black carbon emissions for gasoline were significantly lower compared to diesel. The higher sulphate emissions observed for regular Indian diesel were directly connected to its higher sulphur content. Used lubricant oil had also effect on the exhaust chemical composition.

TAQIITA project was financially supported by TEKES (2634/31/2015, 2763/31/2015 and 2840/31/2015) in Finland and by Department of Biotechnology in India.

Drinovec, L., Mocnic, G., Zotter, P., Prévôt A., ruckstuhl, C., Coz, E., Rupakheti, M., Sciare, J., M, Müller, T., Wiedensohler, A., (2015). *Atmos. Meas. Tech.* 8 (5) 1965-1979.

Onasch, T.B., Trimborn, A., Fortner, E. D., Jayne, J.T., Kok, G.L., Williams, R.L., Davidovits, P., Worsnop, D.R., (2012). *Aerosol Sci. Tech.* 46 (7), 0278-6826 doi: 10.1080/02786826.2012.663948.

Ramanathan V, Sundar S, Harnish R, Sharma S, Seddon J, Croes B, Lloyd A, Tripathi S N, Aggarwal A, Al Delaimy W, Bahadur R, Bandivadekar A, Beig G, Burney J, Davis S, Dutta A, Gandhi K K, Guttikunda S, Iyer N, Joshi T K, Kirchstetter T, Kubsh J, Ramanathan N, Rehman I H, Vijayan A, Waugh M, Yeh S., (2014). *India California Air Pollution Mitigation Program.*



# TIME-RESOLVED ANALYSIS OF SOA FORMATION FROM LOGWOOD COMBUSTION UPON PHOTOCHEMICAL AGING IN PEAR FLOW TUBE REACTOR

P. TIITTA<sup>1</sup>, A. HARTIKAINEN<sup>1</sup>, M. IHALAINEN<sup>1</sup>, P. YLI-PIRILÄ<sup>1</sup>, M. KORTELAINE<sup>1</sup>, J. TISSARI<sup>1</sup>, H. LAMBERG<sup>1</sup>, A. LESKINEN<sup>2,3</sup>, J. JOKINIEMI<sup>1</sup>, AND O. SIPPULA<sup>1</sup>

<sup>1</sup>Fine Particle and Aerosol Technology Laboratory, Department of Environmental and Biological Sciences, University of Eastern Finland, P.O. Box 1627, Kuopio, FI-70211, Finland

<sup>2</sup>Department of Applied Physics, University of Eastern Finland, Kuopio, FI-70211, Finland

<sup>3</sup>Finnish Meteorological Institute, P.O. Box 1627, 70211 Kuopio, Finland

Keywords: aerosols, photochemical aging, flow tube, wood combustion

The lifetime of atmospheric aerosols ranges from hours to weeks. Oxidation processes during this long time range can be simulated using a flow tube reactor with a wide degree of oxidant exposure times (e.g. Kang et al., 2007). In a flow tube reactor the aging process is continuous, which is beneficial for highly variable sources, such as the combustion cycle of logwoods. In this work, the most important combustion phases for SOA formation are revealed by the time-resolved analysis of both primary and aged emissions in the photochemical emissions aging flow tube reactor (PEAR).

The oxidant (hydroxyl radical, OH) exposure times were estimated by measuring D9-butanol gas decay with an HR-PTR-ToF-MS (Ionicon) during the experiments. The ozone concentration and lamp intensities in PEAR were adjusted to achieve the desired OH exposures of  $(0.8\text{--}6) \times 10^{11}$  molec.  $\text{cm}^{-3}\text{s}$  which correspond to an equivalent atmospheric aging time of 0.9–7 days at typical boundary-layer OH concentrations of  $1 \times 10^6$  molec.  $\text{cm}^{-3}$ . A soot particle aerosol mass spectrometer (SP-HR-ToF-AMS, Aerodyne Research, Inc.) was applied to determine the changes in concentrations and composition of submicron particles over the burning cycle (ignition, flaming and residual char burning).

The SOA production ratio (OA/POA) during aging in PEAR was between 2.1 – 2.7 for dry wood logs (moisture content of 5%). In particular, insertion of a new wood batch on the glowing embers leads to a very high momentary SOA emission. Long aging, in turn, the SOA mass decreased slightly compared to shorter aging times, likely due to increasing fragmentation reactions. The SOA chemical composition was found to change remarkably with increasing OH exposure times, which was pointed out by the oxidation state of OA spectra (Figure 1).

Two AMS mass spectra can be compared by inspecting the angle  $\theta$  between two corresponding vectors as follows (Kostenidou et al., 2009)

$$\cos\theta = \frac{MS_A MS_B}{|MS_A||MS_B|} \quad (1)$$

where  $MS_A$  and  $MS_B$  are two AMS mass spectra. The angle  $\theta$  is used in mass spectra comparison between flow tube and chamber experiments together with OA elemental analyses.

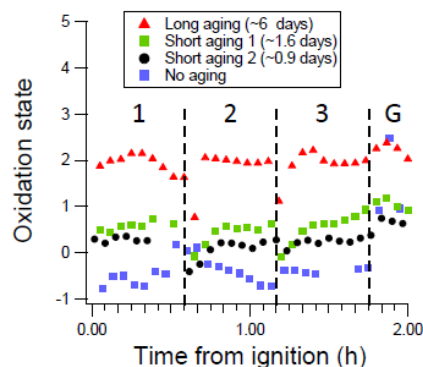


Figure 1: Oxidation state of combustion-related OA over three first combustion cycles (1-3) and glowing embers (G).

The composition of the aged OA in PEAR agreed well with the aged OA in the Ilmari smog chamber (Tiitta et al., 2016) with the same wood combustion source and comparable OH exposures. This was indicated by the low angle  $\theta$  value of  $5^\circ$  (Eq. 1) of the two AMS OA mass spectra. In general, values less than  $15^\circ$  indicate good agreement between two mass spectra (Kostenidou et al., 2009).

This work was supported by the Academy of Finland (Grants: 304459 & 296645).

Tiitta, P., Leskinen, A., Hao, L., Yli-Pirilä, P., Kortelainen, M., Grigonyte, J., Tissari, J., Lamberg, H., Hartikainen, A., Kuusalo, K., Kortelainen, A., Virtanen, A., Lehtinen, K. E. J., Komppula, M., Pieber, S., Prevot, A. S. H., Onasch, T. B., Worsnop, D., Czech, H., Zimmermann, R., Jokiniemi, J., and Sippula, O. (2016) *Atmos. Chem. Phys.* 16, 13251–13269.

Kang, E., Root, M. J., Toohey, D. W., and Brune, W. E. (2007) *Atmos. Chem. Phys.* 7, 5727–5744.

Kostenidou, E., Lee, B.-H., Engelhart, G. J., Pierce, J. R., and Pandis, S. N. (2009) *Environ. Sci. Technol.*, 43, 4884–4889.

# QUANTIFYING THE PROPERTIES OF SECONDARY ORGANIC AEROSOL THROUGH OPTIMIZING PROCESS-BASED MODELS

O.-P. TIKKANEN<sup>1</sup>, V. HÄMÄLÄINEN<sup>1</sup>, A. LIPPONEN<sup>2</sup>, A. BUCHHOLZ<sup>1</sup>, Z. LI<sup>1</sup>, A. VIRTANEN<sup>1</sup>, K.E.J. LEHTINEN<sup>1,2</sup> AND T. YLI-JUUTI<sup>1</sup>

<sup>1</sup> Department of Applied Physics, University of Eastern Finland, Kuopio, Finland

<sup>2</sup> Finnish Meteorological Institute, Kuopio, Finland

Keywords: secondary organic aerosol, optimization, volatility

A major fraction of organic aerosol in the atmosphere is formed through a pathway where gaseous volatile organic compounds transform through chemical reactions to less volatile species which can further partition into liquid or solid phases. This secondary organic aerosol (SOA) consists of a multitude of different chemical species, many of which have not been identified (Hallquist et al. 2009). Besides the distinct composition of SOA generated from a known precursor, there also exists uncertainty in the impact of many factors which are needed to understand the dynamics of SOA in the atmosphere, e.g. the condensed phase chemistry, viscosity and temperature.

At the University of Eastern Finland we have studied the evaporation of  $\alpha$ -pinene derived SOA at different relative humidities (RH) and temperatures. Once the SOA was generated, particles with diameter of 80 nm were selected with a nano-Differential Mobility Analyzer and led either to the instruments via a bypass or the Residence Time Chamber (RTC). The particle size distribution was determined by sampling the SOA in the RTC with ~1h intervals. The size distribution of the particles led to bypass was also measured to provide size information from the first minutes of the evaporation.

Besides direct information obtained from the measurement instruments we have also utilized process-based models coupled with novel optimization techniques to capture the properties which are not directly measurable with current techniques, like the volatility and viscosity of the particles at various relative humidities (Yli-Juuti et al. 2017). This is done by optimizing the input of process-based model to match the output to the observed rate of evaporation.

Here we have studied evaporation experiments performed in high relative humidity conditions to further explore the uncertainty related to the method of optimizing process model input. Utilizing the 1-D volatility basis set (VBS; Donahue et al. 2006) to describe the evaporating organic compounds, we searched for a volatility distribution that reproduces the measured particles' size change.

We tested two different schemes to optimize the initial composition of the SOA particles. One where the saturation concentrations of the compounds were predefined and only the dry particle mole fractions were optimized and an alternative scheme where both the composition and the saturation concentrations were the free parameters. With the first scheme the optimization was done with the the Monte

Carlo Genetic Algorithm (Berkemeier et al. 2017) and with the latter scheme methods based on the Bayesian inference and Markov Chain Monte Carlo were applied. Both schemes yield similar results. Figure 1 shows an example saturation concentrations and related dry particle mole fractions where the two schemes were applied to the same experimental data.

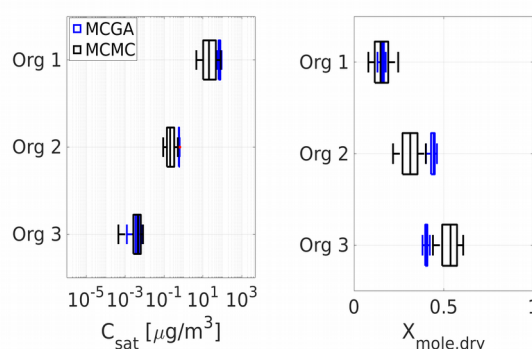


Figure 1: Distribution of saturation concentrations and dry particle mole fractions which best describe the measured particle size change in an experiment. Both methods include several independent optimization runs.

Our results show that using process-based models and optimization techniques to constrain SOA properties, like volatility, produce reliable estimates. However, only the size change data might not be adequate to constrain cases where multiple physical quantities in addition to volatility are to be optimized. In these studies additional constraints are needed. These constraints can come, for example, from coupling multiple models to simulate different parts of the experiment or from the mass spectrometric analysis of the particles.

This work was supported by the Academy of Finland (no. 307331, 259005 and 299544), the European Research Council (ERC Starting Grant 335478), the University of Eastern Finland Doctoral Program in Environmental Physics, Health and Biology.

- Berkemeier, T., et al. (2017). *Atmos. Chem. Phys.*, 17:8021-8029  
Hallquist, M., et al. (2009). *Atmos. Chem. Phys.*, 9:5155- 5236.  
Donahue, N., et al. (2006). *Environ. Sci. Technol.*, 40:2635-2643.  
Yli-Juuti, T., et al. (2017). *Geophys. Res. Lett.*, 44:2562- 2570.

# COMPOSITION AND PROPERTIES OF PARTICULATE EMISSIONS FROM MINING ACTIVITIES

H. TIMONEN<sup>1</sup>, M. BLOSS<sup>1</sup>, J. KUULA<sup>1</sup>, A. ARFFMAN<sup>2</sup>, J. ALANEN<sup>2</sup>, K. TEINILÄ<sup>1</sup>, M. AURELA<sup>1</sup>, L. SALO<sup>2</sup>, R. HILLAMO<sup>1</sup>, S. SAARI<sup>2</sup>, P. OYOLA<sup>3</sup>, F. REYES<sup>3</sup>, Y. VÁSQUEZ<sup>3</sup>, R. SALONEN<sup>4</sup>, J. KESKINEN<sup>2</sup>, T. RÖNKÖ<sup>2</sup>, E. ASMI<sup>1</sup>, S. SAARIKOSKI<sup>1</sup>

<sup>1</sup>Atmospheric Composition Research, Finnish Meteorological Institute, Helsinki, Finland

<sup>2</sup> Aerosol Physics, Faculty of Natural Science, Tampere University of Technology, Tampere, Finland

<sup>3</sup> Centro Mario Molina Chile Ltd, Santiago de Chile, Chile

<sup>4</sup> National Institute for Health and Welfare, Department of Health Security, Kuopio, Finland

Keywords: mining emissions, particulate matter composition, aerosol mass spectrometry,

The mining industry has expanded in recent years, especially in northern Finland. Mining and its associated early refining processes release particulate matter (PM) into the surrounding air. Previous studies have shown, that the main sources of particulate matter in mines are operations associated with deposit extraction (drilling, crushing etc.), blasting and vehicular engine emissions (used in mining machines, ore hauling and for transportation of people) (e.g. Saarikoski et al., 2017).

In this study, emissions from mining activities were investigated at the Kemi Mine (Outokumpu Ltd, Kemi underground mine) in 2014 and 2017, and at the Kevitsa Boliden open pit mine during spring 2014. A large variety of instruments was used to measure the chemical composition and properties of PM near actively operating mining environments. Key instruments of this study include the Soot Particle Aerosol Mass Spectrometer (SP-AMS, Aerodyne Research Inc., Onasch et al. (2012), the Multiangle absorption photometer (MAAP) and a scanning mobility particle sizer (SMPS). In addition, a mobile laboratory and low cost sensors were applied in the Kemi mine to study the spatio-temporal variation of PM in the mine.

Large variations in PM mass concentration, chemical composition and size distribution were observed at different locations (maintenance level, blasting, crushing, transfer belt and dumping site) at the underground mine (Figure 1). Sensors were successfully used to monitor the PM levels at different locations of the mine.

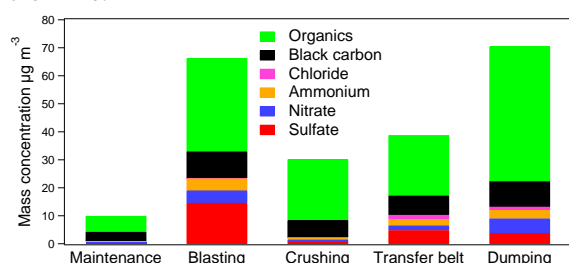


Figure 1. Average chemical composition of submicron particulate matter measured with SP-AMS at different locations in the underground Kemi mine.

In the boreal arctic environment, next to the actively operating open pit mine area, three distinct PM sources

with different chemical composition were identified: mining activities, long-range transported PM and clean arctic air. On average, the PM levels next to the mine were low, although higher concentrations were occasionally observed when wind brought particulate matter from mining area (Figure 2).

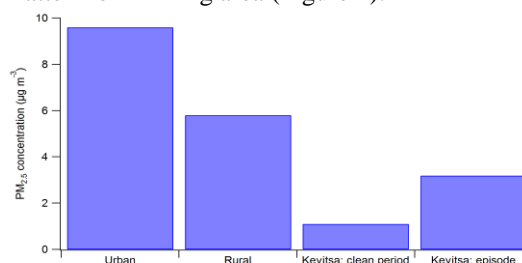


Figure 2. Submicron PM concentrations observed in the Kevitsa open pit mine compared to ambient PM concentrations in urban and rural areas (Laakso et al., 2003)

This project provides important information about the composition of PM and sources in underground and open pit mines, novel tools (e.g. sensors) for PM monitoring in mining areas as well as information about environmental impacts of mining. This information can be used to assess environmental, health and climate impacts of mining in future.

This work was supported by Academy of Finland, (PARMAT, Grant nro 297804), Tekes (HIME project 2011-2014) and CONICYT, Chile. The great help of the Kemi Mine and Kevitsa Boliden mine staff during the measurement campaigns is highly appreciated.

Laakso, L., Hussein, T., Aarnio, P., Komppula, M., Hiltunen, V., Viisanen, Y., and Kulmala, M., 2003. *Atmos. Environ.* 37, 2629-2641.

Onasch, T.B., Trimborn, A., Fortner, E.C., Jayne, J.T., Kok, G.L., Williams, L.R., Davidovits, P., Worsnop, D.R., 2012). *Aer. Sci. Technol.* 46, 804-817.

Saarikoski, S., Teinilä, K., Timonen, H., Aurela, M., Laaksovirta, T., Reyes, F., Vásques, Y., Oyola, P., Artaxo, P., Pennanen, A. S., Juntila, S., Linnainmaa, M., Salonen, R. O. and Hillamo, R. (2017). *Aerosol Sci Technol.*, DOI: 10.1080/02786826.2017.1384788.

# Cloud-scale modelling of aerosol-cloud-precipitation interactions with UCLALES-SALSA

J. TONTTILA<sup>1</sup>, H. KOKKOLA<sup>1</sup>, I. KUDZOTSA<sup>1</sup>, T. RAATIKAINEN<sup>2</sup>, J. AHOLA<sup>2</sup>, A. AFZALIFAR<sup>1</sup>, H. KORHONEN<sup>2</sup> and S. ROMAKKANIEMI<sup>1</sup>

<sup>1</sup>Finnish Meteorological Institute, Atmospheric Research Centre of Eastern Finland, Kuopio, Finland

<sup>2</sup>Finnish Meteorological Institute, Climate System Research, Helsinki, Finland

Keywords: large-eddy simulation, semivolatile aerosol, clouds, precipitation

In recent years there has been strongly increasing interest towards developing high-resolution models to study aerosol-cloud interactions at cloud-scale. The Large-Eddy Simulation (LES) approach provides a very attractive modelling platform for aerosol-cloud studies, where the turbulent flow is explicitly resolved for all but the smallest eddies.

UCLALES-SALSA (Tonttila et al. 2017) is a prominent example of such development, combining a straightforward method for simulating the boundary layer circulation with state-of-the-art spectral bin model for aerosol, cloud droplets, precipitation and ice. One of the unique aspects of the model is, that the bin system allows tracking the dry aerosol size distribution in both activated and non-activated particles with minimal loss of information. While this comes with a cost of losing some details of the water content for individual particles, experimenting with the model has shown that the wet size distribution is nevertheless represented with adequate accuracy for subsequent physical processes. This permits a sophisticated representation of many important processes, such as aerosol wet deposition, that have caused significant challenges in earlier modelling work.

The composition of the aerosol is explicitly modelled for all size bins in all particle categories. The available aerosol species comprise sulfate, organic and black carbon, sea salt, dust, and the recently added semivolatile ammonium and nitrate aerosols. The model includes a detailed representation for the key microphysical processes, i.e. coagulation and condensation. Collision processes are computed between all bins and categories. The partitioning of water and the semivolatile compounds is calculated dynamically by solving the condensation equations. Cloud activation is determined directly from the wet growth of aerosol particles and the resuspension of aerosol particles from evaporating hydrometeors is inherently included in the model processes.

These aspects and the direct coupling with atmospheric dynamics make UCLALES-SALSA a very attractive tool to study many of the contemporary questions related to aerosol-cloud interactions. As a descriptive example, the model has been applied in studying the effects of semivolatile aerosol on aerosol-cloud interactions and on the wet removal efficiency of different aerosol species: Figure 1 shows model results with a clear difference in the number of activated cloud droplets between simulations with and without semivolatile aerosol species. This difference subse-

quently affects the wet removal of aerosol through precipitation as well. Related to this, other examples include investigations into aerosol effects on precipitation formation. There, the skillful representation of cloud processing as well as the resuspension and recirculation of aerosol particles back into the cloud layer by UCLALES-SALSA offers a particular benefit. This enables realistic simulation of the effects of e.g. giant particle emissions, both from natural and artificial sources, to precipitation and cloud lifetime.

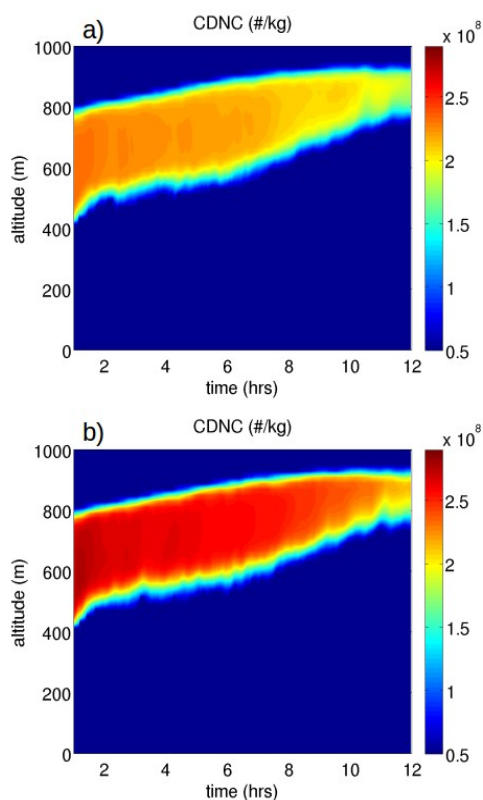


Figure 1: Domain mean time-height cross-section of the cloud droplet number concentration in UCLALES-SALSA in an experiment a) without semivolatile compounds and b) in another experiment initialized with 1 ppb HNO<sub>3</sub> and 5 ppb NH<sub>3</sub> in the gas phase.

Tonttila, J., Maalick, Z., Raatikainen, T., Kokkola, H., Kühn, T., and Romakkaniemi, S.: UCLALES-SALSA v1.0: a large-eddy model with interactive sectional microphysics for aerosol, clouds and precipitation, *Geosci. Model Dev.*, 10, 169-188, <https://doi.org/10.5194/gmd-10-169-2017>, 2017.

# FORMATION OF HIGHLY OXYGENATED MOLECULES (HOMs) DURING THE OXIDATION OF 1,3,5 TRIMETHYLBENZENE (TMB)

E. TSILIGIANNIS<sup>1</sup>, J. HAMMES<sup>1</sup>, M. LE BRETON<sup>1</sup>, T. MENDEL<sup>1,2</sup> and M. HALLQUIST<sup>1</sup>

<sup>1</sup> Department of Chemistry & Molecular Biology, University of Gothenburg, Sweden

<sup>2</sup> Institute for Energy and Climate Research, IEK-8, Forschungszentrum Jülich, Germany

Keywords: TMB, HOMs, VOC oxidation, SOA

Understanding the properties and formation of secondary organic aerosol (SOA) is of great importance, as there is still insufficient knowledge about them (Hallquist et al., 2009). In order to investigate the role of organic vapours in the production of atmospheric nanoparticles, experiments were conducted using the Gothenburg potential aerosol mass chamber (Go:PAM) by oxidation of anthropogenic as well as biogenic SOA precursors. The efficiency of the formation of highly oxygenated molecules (HOMs) (Ehn et al., 2014) by ozonolysis and reaction with the hydroxyl radical (OH) was tested for all the precursor compounds. A chemical ionization atmospheric pressure interface time-of-flight mass spectrometer (CI-API-TOF) coupled to a nitrate inlet was used in order to identify HOMs.

1,3,5 trimethylbenzene (TMB), toluene, methyl salicylate (MeSA) and  $\alpha$ -pinene were used during the experiments, but herein we focus on the TMB results. Different ozone as well as different NO<sub>x</sub> conditions were applied during the experiment, while the concentration of TMB remained constant (see Table 1). The oxidation products of TMB were identified and the HOMs – containing only carbon, hydrogen and oxygen – were classified into monomers and dimers.

The NO<sub>x</sub> to VOC ratio ranged from zero to above two. It is noticed that with increasing NO<sub>x</sub> the production of dimers was suppressed. This could be that the production of nitrogen-containing HOMs or organonitrates (ONs) (Bianchi et al., 2017) may be favoured under these conditions.

TMB [ppb]	Ozone [ppb]	NO <sub>x</sub> :VOC
~29	~10	0, ~1, >1
~29	~100	0, ~1, >1

Table 1: Ozone and NO<sub>x</sub> conditions during the experiments.

The TMB ozonolysis/OH oxidation generally leads to the production of monomers and dimers with the following molecular formulas: C<sub>9</sub>H<sub>12-16</sub>O<sub>2-11</sub> and C<sub>18</sub>H<sub>24-30</sub>O<sub>10-15</sub>, respectively. A typical mass spectrum of the oxidation products of TMB, in absence of NO<sub>x</sub> is depicted in Figure 1. Monomers range from m/Q about

270 to 370, while dimers range between m/Q 450 to 550. The high peak at m/Q 426 is due to the cluster of perfluoroheptanoic acid (PFHA) with NO<sub>3</sub><sup>-</sup>, which was used as a tracer during the mass calibration.

In total 41 compounds were identified as monomers and 42 as dimers, in absence of NO<sub>x</sub>. The 10 dominant monomers contributed to about 69% of the total monomer signal, while the 10 dominant dimers contributed to about 46% of the total dimer signal.

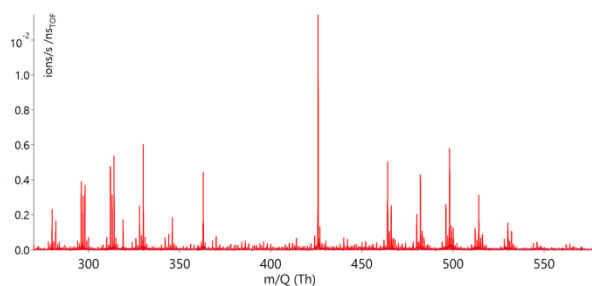


Figure 1: Typical mass spectrum of oxidation of TMB under no NO<sub>x</sub> conditions.

The results of the measurements with the ToF-CIMS are discussed in relation to the HOMs potential to form particles and the mechanism in their formation.

The research presented is a contribution to the Swedish strategic research area Modelling Regional and Global Earth system, MERGE. This work was supported by the Swedish Research Council (grant number 2014-5332) and Formas (grant number 2015-1537).

Bianchi, F. et al. (2017). *Atmos. Chem. Phys.*, 17: 13819-13831.

Ehn et al. (2014). *Nature*, 506: 476-479.

Hallquist M. et al. (2009). *Atmos. Chem. Phys.*, 9: 5155-5236.

## FINAL RESULTS OF A PROJECT ON ANTARCTIC AEROSOLS IN 2013 - 2016

A. VIRKKULA<sup>1,2</sup>, V.-M. KERMINEN<sup>2</sup>, T. PETÄJÄ<sup>2</sup>, G. DE LEEUW<sup>1,2</sup>, E. ASMI<sup>1</sup>, D. BRUS<sup>1</sup>, T. LAURILA<sup>1</sup>, H. TIMONEN<sup>1</sup>, K. TEINILÄ<sup>1</sup>, E. RODRIQUEZ<sup>1</sup>, J. SVENSSON<sup>1</sup>, V. AALTONEN<sup>1</sup>, J. BACKMAN<sup>1</sup>, R. HILLAMO<sup>1</sup>, M. SIPILÄ<sup>2</sup>, T. JOKINEN<sup>2</sup>, E. JÄRVINEN<sup>2</sup>, T. NIEMINEN<sup>2</sup>, R. VÄÄNÄNEN<sup>2</sup>, H. MANNINEN<sup>2</sup>, X. CHEN<sup>2</sup>, P.P. AALTO<sup>2</sup>, H. GRYPHE<sup>4,5</sup>, M. BUSETTO<sup>3</sup>, C. LANCONELLI<sup>3</sup>, A. LUPU<sup>3</sup>, V. VITALE<sup>3</sup>, R. WELLER<sup>6</sup>, A.C. SAULO<sup>7</sup>, AND M. KULMALA<sup>2</sup>

<sup>1</sup>Finnish Meteorological Institute, FI-00560, Helsinki, Finland

<sup>2</sup>Department of Physics, University of Helsinki, FI-00014, Helsinki, Finland

<sup>3</sup>Institute of Atmospheric Sciences and Climate of the Italian National Research Council, Bologna, Italy

<sup>4</sup>Department of Applied Environmental Science, Stockholm University, S-10691 Stockholm, Sweden

<sup>5</sup>Norwegian Institute for Air Research (NILU), N-2027 Kjeller, Norway

<sup>6</sup>Alfred-Wegener Institute, D-27570 Bremerhaven, Germany

<sup>7</sup>Servicio Meteorológico Nacional, Buenos Aires, Argentina

Keywords: Antarctic, Number size distribution, Aerosol optical properties, Greenhouse gases

It has been suggested that the discrepancy between global models and measurements could best be reduced through the study of natural aerosols in environments with negligible anthropogenic influence. Antarctica is such an environment, anthropogenic emissions are smaller there than on any other continent. Antarctica is also a negligible contributor to global greenhouse gas (GHG) emissions, due to the cold and dry climate with year-round snow cover. However, open seas surrounding Antarctica are actively exchanging CO<sub>2</sub> with the atmosphere due to ocean circulation and biological activity of the marine organisms.

The primary goal of the four-year (2013 – 2016) project Atmospheric Composition and Processes relevant to climate change in ANTArctica (ACPANT), funded by the Academy of Finland, was to provide new scientific insight into atmospheric composition and associated processes relevant to climate change in the Antarctic atmosphere. The project was a consortium of the University of Helsinki and the Finnish Meteorological institute. ACPANT consisted of four thematic issues: i) atmospheric new-particle formation, ii) properties and sources of cloud condensation nuclei, iii) aerosol optical properties and iv) oceans and coastal shelf areas around Antarctica as sources and sinks of carbon dioxide and methane.

The work was based on continuous measurements at three research stations located in Antarctica: the joint Italian-French Concordia station at Dome C in the upper plateau of East Antarctica, the German station Neumayer in coastal Antarctica, and the Argentinian station in Marambio – a small island at the northern tip of the Antarctic Peninsula. The continuous measurements were supported by intensive field campaigns at Neumayer and at the Finnish station Aboa, both in Queen Maud Land. Particle size distributions, optical properties, and chemical composition of aerosols well as greenhouse gas concentrations were measured.

Recent results of the work conducted by the consortium at the various measurement sites have been presented, e.g., by Järvinen et al. (2013), Kyrö et al.

(2013), Teinilä et al. (2014), Chen et al. (2017), and Asmi et al. (2018) In this presentation selected results from all sites will be shown.

### ACKNOWLEDGEMENTS

The project was supported by the Academy of Finland (projects no. 264375 and 264390), the Nordic Centre of Excellence CRAICC (Cryosphere-atmosphere interactions in a changing Arctic climate), and the Academy of Finland's Centre of Excellence program (Centre of Excellence in Atmospheric Science – From Molecular and Biological processes to the Global Climate, project no. 272041).

### REFERENCES

- Asmi, E., Neitola, K., Teinilä, K., Rodriguez, E., Virkkula, A., Backman, J., Bloss, M., Jokela, J., Lihavainen, H., de Leeuw, G., Paatero, J., Aaltonen, V., Mei, M., Gambarte, G., Copes, G., Albertini, M., Fogwill, G. P., Ferrara, J., Barlasina, M.E., and Sánchez, R. (2018). *Tellus B*, 70(1), 1414571, 2018.
- Chen, X., Virkkula, A., Kerminen, V.-M., Manninen, H. E., Busetto, M., Lanconelli, C., Lupi, A., Vitale, V., Del Guasta, M., Grigioni, P., Väänänen, R., Duplissy, E.-M., Petäjä, T., and Kulmala, M. (2017). *Atmos. Chem. Phys.*, 17, 13783-13800.
- Järvinen, E., Virkkula, A., Nieminen, T., Aalto, P. P., Asmi, E., Lanconelli, C., Busetto, M., Lupi, A., Schioppa, R., Vitale, V., Mazzola, M., Petäjä, T., Kerminen, V.-M., and Kulmala, M. (2013). *Atmos. Chem. Phys.*, 13, 7473-7487.
- Kyrö, E.-M., Kerminen, V.-M., Virkkula, A., Dal Maso, M., Parshintsev, J., Ruiz-Jimenez, J., Forsström, L., Manninen, H. E., Riekkola, M.-L., Heinonen, P., and Kulmala, M. (2013) *Atmos. Chem. Phys.*, 13, 3527–3546.
- Teinilä K., Frey, A., Hillamo, R., Tülp, H.C., Weller, R. (2014) *Atmos. Environ.*, 96, 11-19

# EXPERIMENTAL INVESTIGATION OF AEROSOL PARTICLE COMPOSITION AND GROWTH RATES

D. WIMMER<sup>1</sup>, P. WINKLER<sup>2</sup>, L.R. AHONEN<sup>1</sup>, K. LEHTIPALO<sup>1,3</sup>, J. KANGASLUOMA<sup>1</sup>, M. KULMALA<sup>1</sup> and T. PETÄJÄ<sup>1</sup>

<sup>1</sup>Institute for Atmospheric and Earth System Research, Faculty of Science, University of Helsinki, Finland

<sup>2</sup>University of Vienna, Faculty of Physics, Institute for Aerosol and Environmental Physics, Vienna, Austria

<sup>3</sup>Finnish Meteorological Institute, Helsinki, Finland

Keywords: nucleation, atmospheric aerosols, CPC battery,

The chemical composition of naturally charged and neutral clusters can be determined using high resolution mass spectrometry. Clusters with masses up to roughly 1000 amu (=2 nm in mobility) can be chemically analyzed with high resolution. When studying new particle formation phenomena, the chemical composition and the formation rates of aerosol particles between 1.5 and 3 nm are crucial (Kulmala *et al.*, 2014). Even though smaller clusters can exist, the relevance is determined by whether those clusters grow to larger sizes or not. The instrument we present here is aimed at bridging the size gap between high resolution mass spectrometry and other mass spectrometers.

We use three different CPCs, each using a different working fluid. The liquids used are water, butanol and DEG. The CPCs used in the CPC battery are tuned to the smallest sizes possible without generating homogeneous nucleation background in the instrument itself following a similar procedure as in Kuang *et al.*, 2012. A previous study has shown that the hygroscopicity of atmospheric aerosol particles can be resolved (Kulmala *et al.*, 2007) by using two CPCs with different working fluids.

In this study, upstream of the CPC battery, a Differential Mobility Analyzer (DMA) is used, which has two advantages. First, the particle growth rates can be determined. Second, as the diameters are fixed at any given time during the measurement cycle, the detected signal in each CPC can be attributed to the interaction between the aerosol particle and the condensing liquid.

Various studies have shown that the activation efficiency of an ultrafine CPC strongly depends on the interaction between the condensing liquid and the chemistry of the aerosol particles that are measured (Iida *et al.*, 2009). The results in Kangasluoma *et al.*, 2014, showed that salt like aerosol particles are activated easier with the water based CPC compared to the butanol based CPC. The opposite was true for the other aerosol particle types (e.g. limonene ozonolysis products). By carefully characterizing the CPCs in the laboratory using different aerosol particle types, their response with respect to aerosol particle composition is explored

Figure 1 shows an example of a nucleation event at the SMEAR II station in Hyttiälä, Finland. The ratio between water and butanol as a function as size are shown. The ratio is higher during than before/after the event, which shows that the particles are more hygroscopic during the nucleation event.

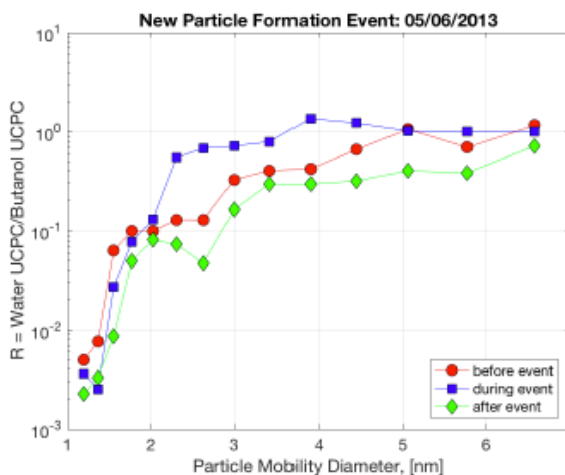


Figure 1: Concentration ratio vs aerosol diameter of ultrafine water/butanol CPC before (red line), during (blue line) and after (green line) nucleation event in Hyttiälä, Finland.

- Kulmala, M., Petäjä T., Ehn M., Thornton J., Sipilä M., Worsnop D. R., Kerminen V.-M. (2014). *Annu Rev. Phys. Chem.* 65:21–37
- Kuang C., Chen M., McMurry P. H. and Wang J. (2012). *Aerosol Sci Technol*, 46:3, 309-315.
- Kulmala M., Mordas G., Petäjä T., Grönholm T., Aalto P. P., Vehkamäki H., Hienola A. I., Herrmann E., Sipilä M., Riipinen I., Manninen H. E., Hämeri K., Stratmann F., Bilde M., Winkler P. M., Birmili W. and Wagner P. E. (2007) *J. Aerosol. Sci.*, 3:289-304
- Iida K., Stolzenburg M. R., McMurry P. H. (2009), *Aerosol Sci Technol*, 43:81-96.
- Kangasluoma J., Kuang C., Wimmer D., Rissanen M. P., Lehtipalo K., Ehn M., Worsnop D. R., Wang J., Kulmala M. and Petäjä T. (2014). *Atmos. Meas. Tech.*, 7, 689–700.

# Aerosol yields for selected BVOC as a function of different parameters

C. Xavier<sup>1</sup>, P. Roldin<sup>2</sup>, R. Makkonen<sup>1</sup> and M. Boy<sup>1</sup>

<sup>1</sup> Institute for Atmospheric and Earth System Research / Physics, Faculty of Science, University of Helsinki, Finland

<sup>2</sup> Division of Nuclear Physics, Lund University, Box 118, SE-22100, Lund, Sweden.

Keywords: Secondary Organic Aerosol, Mass yields, Master Chemical Mechanism, MALTE-BOX

Biogenic Volatile Organic Compounds (BVOCs) are a significant source of Secondary Organic Aerosols (SOA) but quantifying their aerosol forming potential still remains an active and challenging task (Hao et al., 2011). This work presents the results of SOA mass loadings derived from model simulations of BVOCs (isoprene, alpha-pinene, limonene and Beta-caryophyllene) with the main atmospheric oxidants (OH, O<sub>3</sub> and NO<sub>3</sub>) using the zero-dimensional model MALTE-BOX (Boy et al., 2006). We utilize the most common and widely used Master Chemical Mechanism (MCM), an explicit chemical mechanism detailing the gas phase processes involved in the tropospheric degradation of volatile organic compounds (<http://mcm.leeds.ac.uk/MCM>). The aim of this work is to parametrize the SOA mass yields applied in Large scale models (e.g. EC-EARTH, ECHAM etc.) as a function of precursor and oxidant concentrations, temperature, humidity and NO-levels.

The process is initiated by extracting the complete mechanism subset for the interested VOC species from the MCM website including the molecular weights and SMILES (Simplified Molecular Input Line Entry System), a chemical notation which facilitates the chemical structure to be read by the computer. The SMILES are used to derive the required molecular information needed to derive the pure liquid saturation vapor pressures by combining the boiling point method by (Nannoolal et al, 2004) and the vapor pressure method by (Nannoolal et al., 2008). To simulate SOA formation the MCM is coupled to an aerosol module as the compounds partitioning to the condensed phase vary as a function of vapour pressure.

The onset of semi or low volatile organic vapour condensation onto the inorganic seed particles are determined inside the aerosol module, which is described e.g in (Hermansson et al., 2014). The motivation is now to quantify and evaluate the SOA mass yields derived from the oxidation of individual precursor BVOCs with an aim to obtain temperature, relative humidity and NO-level dependent function with respect to varying initial precursor and oxidation concentrations.

Figure 1 shows the variation of mass yields with different concentrations of reacted alpha-pinene. The simulation was run for 12 hours with an initial VOC concentration of 50 ppb and fixed oxidant concentration that varied with each run. The table 1 shows the oxidants concentrations used for the runs. The VOC was added from the beginning of the run at every time step up until 10 hours (50 ppb in total for the entire 10 hours)

while the oxidant was added for the duration of the entire run.

Oxidant	Concentration [cm <sup>-3</sup> ]
OH (*10 <sup>6</sup> )	2, 5, 10, 50, 100
O <sub>3</sub> (*10 <sup>11</sup> )	1, 5, 10, 50, 100
NO <sub>3</sub> (*10 <sup>7</sup> )	1, 5, 10, 50, 100

Table 1: Concentrations of the oxidants.

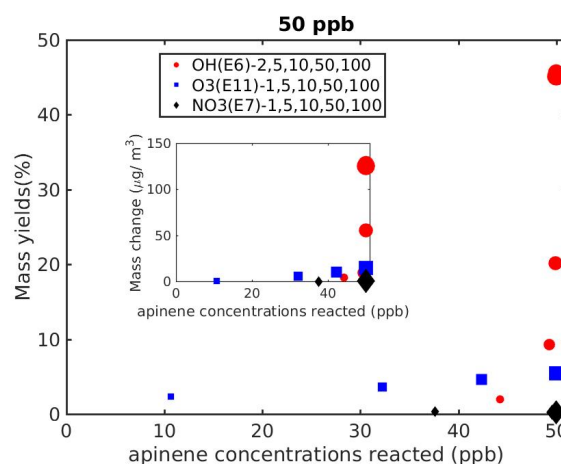


Figure 1: Reaction of alpha-pinene with the three oxidants OH, O<sub>3</sub> and NO<sub>3</sub>. The inset figure shows the SOA mass change variation with alpha-pinene concentration. The progressive sizes for the markers indicates the increasing oxidant concentrations.

Hao L. Q., et al., Atmos. Chem. Phys., 11, 1367-1378, 2011

Boy M., et al., Atmos. Chem. Phys., 6, 4499-4517, 2006

Hermansson, E., et al., Atmos. Chem. Phys., 14, 11853-11869, 2014

Nannoolal, Y., et al., Fluid Phase Equilibr., 226, 45-63, 2004

Nannoolal, Y., et al., Fluid Phase Equilibr., 269, 117-133, 2008



# FIRST MEASUREMENTS FROM SMEAR BEIJING STATION: NEW PARTICLE FORMATION IN URBAN BEIJING

C. Yan<sup>1,2</sup>, J. Kangasluoma<sup>1,2</sup>, F. Bianchi<sup>1,2</sup>, T. Chan<sup>2</sup>, B. Chu<sup>2</sup>, L. Dada<sup>2</sup>, K. Dällenbach<sup>2</sup>, C. Deng<sup>3</sup>, Y. Fu<sup>3</sup>, X. He<sup>2</sup>, L. Heikkinen<sup>2</sup>, H. Junninen<sup>2,4</sup>, Y. Liu<sup>5</sup>, Y. Lu<sup>5</sup>, Q. Ma<sup>6</sup>, X. Qiao<sup>3</sup>, P. Rantala<sup>2</sup>, A. Rusanen<sup>2</sup>, W. Wang<sup>7</sup>, Y. Wang<sup>2</sup>, M. Xue<sup>3</sup>, G. Yang<sup>5</sup>, R. Yin<sup>3</sup>, Y. Zhou<sup>1</sup>, J. Kujansuu<sup>1,2</sup>, T. Petäjä<sup>2,8</sup>, Y. Liu<sup>1</sup>, M. Ge<sup>7</sup>, H. He<sup>6</sup>, L. Wang<sup>3</sup>, J. Jiang<sup>3</sup>, M. Kulmala<sup>1,2,8</sup>

<sup>1</sup> Aerosol and Haze Laboratory, Beijing Advanced Innovation Center for Soft Matter Science and Engineering, Beijing University of Chemical Technology, Beijing, China

<sup>2</sup> Institute for Atmospheric and Earth System Research / Physics, Faculty of Science, University of Helsinki, Finland

<sup>3</sup> State Key Joint Laboratory of Environment Simulation and Pollution Control, School of Environment, Tsinghua University, Beijing, China

<sup>4</sup> Institute of Physics, University of Tartu, Ülikooli 18, EE-50090 Tartu, Estonia

<sup>5</sup> Department of Environmental Science & Engineering, Fudan University, Shanghai, China

<sup>6</sup> Research Center for Eco-Environmental Sciences, Chinese Academy of Science, Beijing, China

<sup>7</sup> Institute of Chemistry, Chinese Academy of Sciences, Beijing, China

<sup>8</sup> Joint International Research Laboratory of Atmospheric and Earth System Sciences, Nanjing University, Nanjing, China

Keywords: SMEAR Beijing, new particle formation, air quality, urban atmospheric chemistry

New particle formation (NPF) contributes a significant fraction to the total atmospheric particle load and affects the air quality. NPF proceeds via gas-to-particle conversion, which is governed by the availability of precursor vapors and existing particle surface area that the vapors can condense onto. In an urban environment, they are strongly affected by the local sources and micrometeorology. To obtain a comprehensive view on the processes governing air quality and NPF, long-term continuous measurements are needed (Kulmala 2018). Continuous measurements allow monitoring of response of the atmosphere to the various forcings, which the short-term campaign-type measurements cannot observe.

Because of recent rapid urbanization of the developing countries such as China and India, severe air quality problems and haze episodes have taken place in large cities, such as Beijing and Delhi. The exact mechanisms responsible for the worst haze episodes still remain unclear, but they are linked to at least increased emissions from the industry, traffic and heating. To monitor the air quality in urban Beijing area, a new SMEAR Beijing station has been established close to the western third ring road at the Beijing University of Chemical Technology.

The current measurement capabilities of the station include inorganic trace gases, volatile organic compounds, low-volatility vapors, particle and ion size distributions, particle chemical composition and meteorological parameters (Table 1). At the beginning of 2018, the first measurement was performed with collaborations with Tsinghua University, Fudan University, and several research centers of Chinese Academy of Science.

Table 1. SMEAR Beijing instrumentation

Instrument	Measured variable
DMPS	Particle size distribution 6 – 700 nm
NAIS	Particle size distribution 2 – 40 nm Ion size distribution 1 – 40 nm
PSM	Particle size distribution 1 – 3 nm
PSD	Particle size distribution 3 – 10000 nm
DEG SMPS	Particle size distribution 1 – 3 nm

CI-API-TOF	Low volatility vapors e.g. SA, HOMs
SPI-MS	Volatile organic compounds
ACSM	Aerosol chemical composition
Trace gases	SO <sub>2</sub> , NO <sub>x</sub> , O <sub>3</sub> , CO

From the brief existing data set we focused on a NPF event on 17.1.2018. The beginning of the day was characterized with a high concentration of existing accumulation mode particles. During the time period until 1pm, the concentration of accumulation mode v the decreased sink a strong NPF event took place, characterized with high concentrations of nucleation mode particles and immediate particle growth.

Further analysis of the data set will be the identification of the species contributing to the particle formation and growth, and air mass analysis on the micrometeorological conditions triggering the NPF event. Similar events from the extending continuous data set allows a deeper understanding on the processes governing NPF in urban Beijing (Cai et al. 2017, Kulmala et al. 2017).

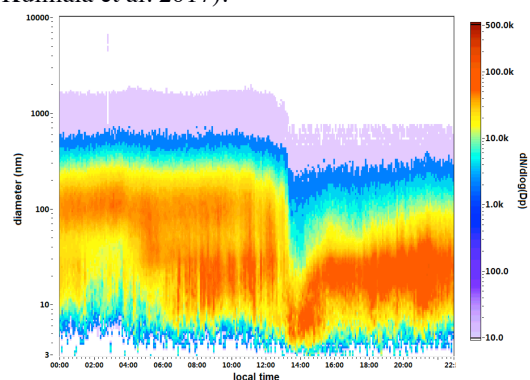


Figure 1. New particle formation event on Jan.17 2018.

## References:

- Cai, R, *et al.*. *Atmos. Chem. Phys.* 17(20):12327-12340 (2017).  
Kulmala, M. *Nature* **553**, 21-23 (2018).  
Kulmala, M. *et al.* *Faraday Discuss* **200**, 271-288 (2017).

# GROWTH AND VOLATILITY OF SECONDARY AEROSOL PARTICLES AT HYYTIÄLÄ IN SPRING 2014

T. YLI-JUUTI<sup>1</sup>, C. MOHR<sup>2</sup>, A. HEITTO<sup>1</sup>, F. D. LOPEZ-HILFIGER<sup>3</sup>, J. HONG<sup>4</sup>, E. L. D'AMBRO<sup>5</sup>, S. SCHOBESBERGER<sup>1,6</sup>, U. MAKKONEN<sup>7</sup>, M. RISSANEN<sup>4</sup>, R. L. MAULDIN III<sup>4,8</sup>, M. SIPILÄ<sup>4</sup>, N. M. DONAHUE<sup>9</sup>, M. KULMALA<sup>4</sup>, T. PETÄJÄ<sup>4</sup>, I. RIIPINEN<sup>2</sup> and J. THORNTON<sup>6</sup>

<sup>1</sup>Department of Applied Physics, University of Eastern Finland, Finland.

<sup>2</sup>Department of Environmental Science and Analytical Chemistry, University of Stockholm, Sweden.

<sup>3</sup>Laboratory of Atmospheric Chemistry, Paul Scherrer Institute, Switzerland.

<sup>4</sup>Department of Physics, University of Helsinki, Finland.

<sup>5</sup>Department of Chemistry, University of Washington, USA

<sup>6</sup>Department of Atmospheric Sciences, University of Washington, USA.

<sup>7</sup>Finnish Meteorological Institute, Helsinki, Finland.

<sup>8</sup>Department of Atmospheric and Oceanic Sciences, University of Colorado Boulder, USA.

<sup>9</sup>Departments of Chemistry, Chemical Engineering, Engineering and Public Policy, and Center for Atmospheric Particle Studies, Carnegie Mellon University, USA.

Keywords: organics, SOA, growth, volatility, atmospheric aerosols

Growth of secondary aerosol particles towards climatically relevant sizes is observed frequently in various atmospheric environments (Kulmala et al., 2004). However, the mechanisms related to the growth and the identity of the participating species are not known in detail. This reflects as uncertainty in aerosol-cloud interactions in climate predictions. Here we investigate the growth of secondary aerosol particles by combining atmospheric measurements of organic vapors, particle size distribution and volatility with a particle growth model in order to identify compounds that contribute to the particle growth.

We studied secondary aerosol particle growth in the boreal forest at Hyytiälä, Finland, during April-May 2014. We measured the gas phase concentrations of oxidized organic species with a chemical ionization high-resolution time-of-flight mass spectrometer with a filter inlet for gases and aerosols (FIGAERO-CIMS) using iodide as the reagent ion (Mohr et al., 2017). We calculated saturation concentrations ( $C_{\text{sat}}$ ) of each species with a parametrization based on the number of carbon, oxygen and nitrogen atoms in the species, and grouped the species in a 1-D volatility basis set (VBS). We used the time series of the organic concentrations grouped in the VBS together with measured gas concentrations of sulfuric acid and ammonia, relative humidity and temperature as inputs for the particle growth model MABNAG (Yli-Juuti et al. 2013). With the model, we simulated the change in size and composition of a freshly formed particle given the ambient conditions. We compared the predicted change in particle size and composition with the time evolution of particle size distribution measured with a differential mobility particle sizer and the volatility of 30 nm particles measured with a volatility tandem differential mobility analyzer (Hong et al., 2017).

The simulated particle growth rate matched within the uncertainties or overestimated the observed growth rate for most of the growth events. The results

therefore suggest that the detected gas phase concentrations of the condensable vapors could explain the observed particle growth. The majority of the simulated growth was due to condensation of low- or extremely low-volatile organic compounds (Fig. 1), and nitrate containing organic compounds contributed significantly. The simulated particle composition agreed on average well with the volatility measurements. The comparison of the model simulations to both the observed particle growth and volatility allowed investigating the sensitivities to the uncertainties in e.g. measured gas concentrations and estimated  $C_{\text{sat}}$ .

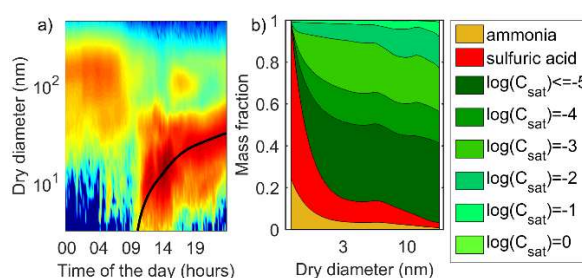


Figure 1: a) Simulated particle growth and measured particle size distribution. b) Simulated particle composition.

This work was supported by Academy of Finland Center of Excellence programme (grant no. 307331) and Academy of Finland grant no. 299544.

Hong, J. et al. (2017). *Atmos. Chem. Phys.*, 17:4387-4399.

Kulmala, M. et al. (2004). *Aerosol Sci.*, 35:143-176.

Mohr, C. et al. (2017). *Geophys. Res. Lett.*, 44:2958-2966.

Yli-Juuti, T. et al. (2013). *Atmos. Chem. Phys.*, 13:12507-12524.

# TRACKING SOA COMPOSITION AND THERMAL DESORPTION BEHAVIOR WITH OXIDATIVE AGING: $\alpha$ -PINENE VS. REAL PLANT EMISSIONS

A. YLISIRNIÖ<sup>1</sup>, A. BUCHHOLZ<sup>1</sup>, C. MOHR<sup>2,3</sup>, A. LAMBE<sup>4</sup>, C. FAIOLA<sup>1,5</sup>, E. KARI<sup>1</sup>, T. YLI-JUUTI<sup>1</sup>, S.A. NIZKORODOV<sup>6</sup>, D. R. WORSNOP<sup>4</sup>, S. SCHOBESBERGER<sup>1</sup> and A. VIRTANEN<sup>1</sup>

<sup>1</sup>Department of Applied Physics, University of Eastern Finland, Kuopio, Finland.

<sup>2</sup>Institute of Meteorology and Climate Research, Karlsruhe Institute of Technology, Karlsruhe, Germany.

<sup>3</sup>Department of Environmental Science and Analytical Chemistry, Stockholm University, Stockholm, Sweden.

<sup>4</sup>Center for Aerosol and Cloud Chemistry, Aerodyne Research, Inc., Billerica, MA, USA.

<sup>5</sup>Department of Ecology and Evolutionary Biology, University of California, Irvine, Irvine, CA 92697, USA.

<sup>6</sup>Department of Chemistry, University of California, Irvine, Irvine, CA 92697, USA.

Keywords:  $\alpha$ -pinene oxidation, Scots pine emissions, secondary organic aerosol, Potential Aerosol Mass reactor, FIGAERO

Chemical and physical properties of secondary organic aerosol (SOA) particles forming from oxidation products of volatile organic compounds (VOCs) are determined by the initial chemical composition of said VOCs and the oxidative conditions they experience (Glasius and Goldstein, 2016, Hallquist, et al, 2009). Important physical property of the oxidized compounds is their volatility, which has impact on formation and life time of SOA particles and thus their impact on climate.

In this study we set out to investigate differences in chemical composition and volatility of SOA formed from oxidation of  $\alpha$ -pinene and Scots Pine emissions using a Filter Inlet for Gases and AEROSols – Time of Flight – Chemical Ionization Mass Spectrometer, (FIGAERO-ToF-CIMS), (Lopez-Hilfiker, et al, 2014). SOA particles were formed inside a Potential Aerosol Mass reactor (PAM) (Kang, et al, 2007, Lambe, et al, 2011). Emissions from Scots Pine seedlings were monitored using a Proton-Transfer-Reaction Time of Flight Mass Spectrometer (PTR-ToF-MS) and Gas Chromatography – Mass Spectrometry (GC-MS). A representative emissions profile can be seen in Figure 1.

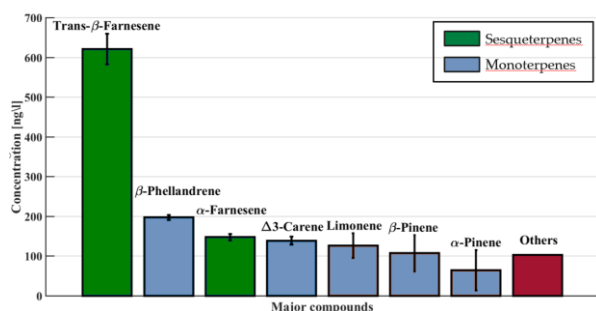


Figure 1: Emission profile from Scots Pine seedlings.

Figure 2. shows total ion counts (TIC) versus heating temperature and average chemical composition of three different  $\alpha$ -pinene experiments and one Scots Pine experiment.  $\alpha$ -Pinene experiments are termed “low”, “medium” and “high” indicating oxidative conditions inside PAM-reactor. Oxidative conditions in Scots Pine experiment are similar to “medium”  $\alpha$ -pinene

experiment. The results clearly show how the peak value of the TIC changes to higher temperature when oxidative level increases in the  $\alpha$ -pinene experiments. Results also show a high peak value for the Scots Pine experiment, even though oxidative conditions were weaker.

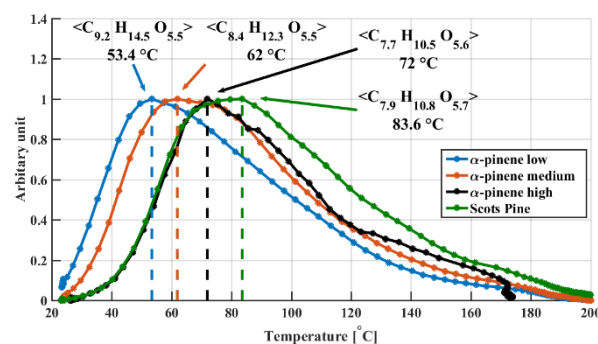


Figure 2. Total ion count vs. heating temperature of three different  $\alpha$ -pinene experiments and one Scots Pine experiment.

This work was supported by the Academy of Finland (259005, 272041, 299544), the European Research Council (ERC-StQ QAPPA 335478) and the University of Eastern Finland Doctoral Program in Environmental Physics, Health and Biology. We thank the tofTools team for providing tools for mass spectrometry analysis.

Glasius M., Goldstein A. H., (2016). *Env. Sci. & Tech.*, 50:2754.

Hallquist M., Wenger J. C., Baltensperger U., Rudich Y., Simpson D., Claeys, et al., *Atmos. Chem. Phys.* (2009). 9:5155-5236.

Kang E., Root M. J., Toohey D. W., Brune W. H., *Atmos. Chem. Phys.* (2007) 7:5727-5744.

Lambe A. T., Ahern A. T., Williams L. R., Slowik J. G., Wong J. P. S., Abbatt J. P. D., et al., *Atmos. Meas. Tech.* (2011). 4:445-461.

Lopez-Hilfiker F. D., Mohr C., Ehn M., Rubach F., Kleist E., Wildt J., et al., *Atmos. Meas. Tech.*, (2014). 7:983-1001.

# THE EFFECT OF AUTUMNAL MOTH INDUCED VOLATILE ORGANIC COMPOUND EMISSIONS TO AEROSOL LOAD IN SUBARCTIC REGION

I. YLIVINKKA<sup>1</sup>, M. KULMALA<sup>1</sup>, J. ITÄMIES<sup>2</sup> and D. TAIPALE<sup>1</sup>

<sup>1</sup> Institute for Atmospheric and Earth System Research / Physics, Faculty of Science, University of Helsinki, Finland

<sup>2</sup> Kaitoväylä 25 A 6, 90570 Oulu, Finland

Keywords: new particle formation, atmospheric aerosols, VOC, autumnal moth, subarctic region

Autumnal moth (*Epirrita autumnata*) has mass outbreaks in the Finnish Lapland in about ten years cycles. The larvae of the moth feed on mountain birches (*Betula pubescens* spp. *czerepanovii*) increasing biogenic volatile organic compound (BVOC) emissions from the trees. Previous laboratory studies (Joutsensaari et al., 2015; Yli-Pirilä et al., 2016) showed that the BVOCs emitted from the infested trees enhanced secondary organic aerosol (SOA) formation. In this study, we investigate, whether the effect of the larvae induced BVOCs increase the aerosol load observable in field circumstances.

The impact of biotic stresses on aerosol processes have not been investigated before in the field, but if the results are similar to laboratory experiments, phenomenon is atmospherically important. Research of aerosol particles has raised interest due to their effects on Earth's radiation balance, climate and human health. One of the main processes influencing aerosol properties and composition is tropospheric SOA production (Stocker, 2014).

Used measurement site is SMEAR I (Station for Measuring Ecosystem-Atmosphere Relations) in eastern Lapland in Finland. There is long term measurements of aerosol particles, meteorological variables and autumnal moth density. The time interval extends from 1998 to 2016. The site is in a remote area where usually the aerosol particle number concentration is low. This eases the detection of the possible larvae caused effect.

Aerosol particles are measured with a differential mobility particle sizer (DMPS) (Aalto et al., 2001). Both particle number concentration and derived aerosol variables such as formation and growth rates are used in the study. There is two different larval density measurements. Once a year estimated larval index and daily light trap measurements (Hunter et al., 2014).

The SMEAR I is located 390 m a.s.l. in 60-year-old Scots pine (*Pinus sylvestris*) forest on top of Kotovaara hill. South of the station there is Värriö fell range peaking up to 550 m a.s.l. There is old-growth Scots pine forest on southern slope of the hill. Spruce dominated mixed forest ravine separates hill from the mountain birch covered slope of the first fell. The summits are treeless.

Analysis of 18 years of continuous field observations indicate that autumnal moth infested mountain birches do not enhance new particle formation and

growth of atmospheric aerosol particles in a mixed boreal forest. This could possible be due to the relatively small biomass of mountain birches. In addition, during biotically stress free periods, we did also not observe a clear correlation between enhancement in temperature, and hence basal BVOC emissions, and SOA formation or growth, nor between high sulfuric acid concentrations and aerosol processes, which we would otherwise have expected.

This work was supported by the Academy of Finland Center of Excellence programme (grant no. 307331). Further, we thank the University of Turku for providing the larval index data.

Aalto, P., Hämeri, K., Becker, E., Weber, R., Salm, J., Mäkelä, J. M., Hoell, C., O'dowd, C. D., Hansson, H.-C., Väkevä, M., et al. (2001). Physical characterization of aerosol particles during nucleation events. *Tellus B: Chemical and Physical Meteorology*, 53(4):344–358.

Hunter, M. D., Kozlov, M. V., Itämies, J., Pulliainen, E., Bäck, J., Kyrö, E.-M., and Niemelä, P. (2014). Current temporal trends in moth abundance are counter to predicted effects of climate change in an assemblage of subarctic forest moths. *Global change biology*, 20(6):1723–1737.

Joutsensaari, J., Yli-Pirilä, P., Korhonen, H., Arola, A., Blande, J. D., Heijari, J., Kivimäenpää, M., Mikkonen, S., Hao, L., Miettinen, P., et al. (2015). Biotic stress accelerates formation of climate-relevant aerosols in boreal forests. *Atmospheric Chemistry and Physics*, 15(21):12139–12157.

Stocker, T. (2014). *Climate Change 2013: The Physical Science Basis: Working Group I Contribution to the Fifth Assessment Report of the Intergovernmental Panel on Climate Change*. Cambridge University Press.

Yli-Pirilä, P., Copolovici, L., Kannaste, A., Noe, S., Blande, J. D., Mikkonen, S., Klemola, T., Pulkkinen, J., Virtanen, A., Laaksonen, A., et al. (2016). Herbivory by an outbreaking moth increases emissions of biogenic volatiles and leads to enhanced secondary organic aerosol formation capacity. *Environmental science & technology*, 50(21):11501–11510.

# MUTUAL INFORMATION BETWEEN NEW PARTICLE FORMATION AND ATMOSPHERIC VARIABLES

M.A. ZAIDAN<sup>1</sup>, V. HAAPASILTA<sup>2</sup>, R. RELAN<sup>3</sup>, P. PAASONEN<sup>1</sup>, V.-M. KERMINEN<sup>1</sup>, H. JUNNINEN<sup>4</sup>, M. KULMALA<sup>1</sup> and A.S. FOSTER<sup>2</sup>

<sup>1</sup> Institute for Atmospheric and Earth System Research, Faculty of Science, University of Helsinki, Finland

<sup>2</sup> Dept. of Applied Physics, Aalto University, Espoo, Finland

<sup>3</sup> Dept. of Applied Mathematics and Computer Science, Technical University of Denmark, Copenhagen, Denmark

<sup>4</sup> Laboratory of Environmental Physics, University of Tartu, Estonia

Keywords: new-particle formation, atmospheric variables, correlation, mutual information

New-Particle Formation (NPF) is very non-linear process, involving atmospheric chemistry of precursors and clustering physics as well as subsequent growth before NPF can be observed. In order to understand this process in depth, scientists have gathered a tremendous amount of atmospheric data, obtained through continuous measurements directly from the atmosphere. This fact also makes the data analysis more challenging, but on the other hand enables to apply modern data science methods. One of the most interesting research area is to understand the relationship between NPF and atmospheric variables. Previously, Hyvönen et al. (2005) carried out a comprehensive study using data mining methods applied on atmospheric data from Hyytiälä, Finland. Their results support some earlier conclusions, such as described in Boy and Kulmala (2002). However, their methods might not be very effective in dealing with large and complex data sets. The first reason concerns the used features, such as mean and standard deviations. This practice compresses the measurement data into a single quantity for each day, that may potentially result in information loss in the data. The second issue relates to the implementation procedure that is computationally demanding. This requires the exploration of all possible models and variable combination to find the best pairs. The models also need to be run multiple times to ensure their stability.

In order to overcome these drawbacks, we propose here an alternative method - based on information theory - named mutual information (MI). MI is a method for measuring the degree of relatedness between data sets, applicable for both detecting linear and non-linear correlation (Cover and Thomas, 2006). In this work, the MI method is applied on observed NPF events (measured at Hyytiälä, Finland) and a wide variety of simultaneously monitored ambient variables, such as trace gases, meteorology, radiation and a few derived quantities. Figure 1 presents the MI correlation level between NPF and gas concentration as well as aerosol. In this group, the top three highest correlation variables to NPF include water ( $H_2O$ ), condensation sink (CS) and sulfuric acid ( $H_2SO_4$ ). These variables are known to have impact in the NPF process as described in some previous research, such as Boy and Kulmala (2002); Kulmala et al. (2005); Nieminen et al. (2014)

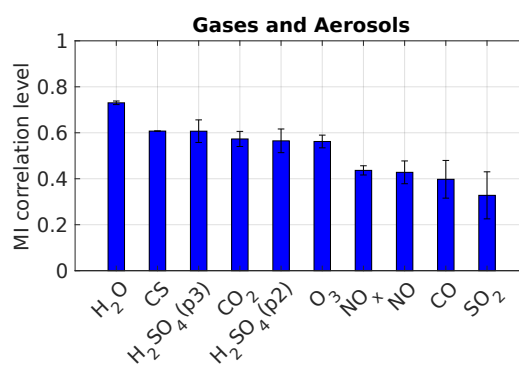


Figure 1: The correlation level between NPF and gas concentration as well as aerosol obtained via mutual information method.

In addition to the group of gases and aerosol, the MI also finds that the formation events correlate strongly with relative humidity, temperature, global and ultraviolet radiation. Previously, these quantities have been well-established to be important players in the NPF phenomenon via dedicated field, laboratory and theoretical research. The novelty of this work is to demonstrate that the same results are now obtained by a data analysis method which operates without supervision and physical insight. This suggests that the method is suitable to be implemented widely in the atmospheric field to discover other interesting phenomena and its relevant variables

Hyvönen, et al. (2005). *Atmos. Chem. Phys.*, 5:3345–3356.

Boy, M. and Kulmala, M. (2002). *Atmos. Chem. Phys.*, 2:1–16.

Kulmala et al. (2005). *Atmos. Chem. Phys.*, 5:409–416.

Nieminen, et al. (2014). *Boreal Environ. Res.*, 19:191–214.

Cover, T. M. and Thomas, J. A. (2006). *Elements of Information Theory*. John Wiley & Sons, 2nd edition.

# NOVEL FACTOR ANALYTICAL TECHNIQUES APPLIED TO HIGHLY OXYGENATED MOLECULES (HOMS)

Y. ZHANG<sup>1</sup>, O. PERÄKYLÄ<sup>1</sup>, C. YAN<sup>1</sup>, L. HEIKKINEN<sup>1</sup>, M. ÄIJÄLÄ<sup>1</sup>, M. RIVA<sup>1</sup>, Q. ZHA<sup>1</sup>, L. QUÉLÉVER<sup>1</sup>, K. DAELLENBACH<sup>1</sup>, P. PAATERO<sup>1</sup>, M. KULMALA<sup>1</sup>, W. DOUGLAS<sup>1,2</sup>, M. EHN<sup>1</sup>

<sup>1</sup> Institute for Atmospheric and Earth System Research / Physics, Faculty of Science, University of Helsinki, Helsinki, 00140, Finland

<sup>2</sup> Aerodyne Research, Inc., Billerica, MA 01821, USA

Keywords: highly oxygenated molecules (HOM), positive matrix factorization (PMF), high resolution, chemical ionization mass spectrometer (CIMS)

Highly Oxygenated Molecules, or HOMs, play an important role in atmospheric physical and chemical processes, contributing significantly to new particle formation and secondary organic aerosols. Chemical ionization high-resolution mass spectra, containing large amounts of information, have increased our capability of investigating the composition and evolution of HOMs (Ehn et al., 2014). However, as the mass-to-charge ratio ( $m/z$ ) increases, the number of possible ions also increases rapidly for one single peak (Stark et al., 2015). The overlapping peaks will sometimes lead to ambiguous peak fitting and ion resolving, resulting in unreliable separation of signals. Very limited research has been conducted to address the problem and improve identification and separate quantification in high-resolution mass spectra (Corbin et al., 2015; Cubison et al., 2015; Stark et al., 2015).

In this study, we present a novel method, semi-high-resolution positive matrix factorization (SHR-PMF), to separate the key components for different HOMs formation pathways. Instead of fitting peaks to the high-resolution mass spectra, as is routinely done in typical analyses, the mass spectra are here divided into smaller  $m/z$  bins with a bin width of 0.02 Th. This method is applied to HOMs measured in the boreal forest in Hyytiälä, southern Finland by a nitrate-ion-based chemical ionization atmospheric pressure-interface time-of-flight mass spectrometer (CI-APi-TOF). With the new SHR-PMF method, we successfully reveal seven plausible factors, consisting of 1 nighttime factor, 5 daytime factors and a clear contamination factor, even with only a small  $m/z$  range (300-350 Th). The contamination factor is related to instrument blank zeroing every three hours and the diurnal trend for this factor accurately retrieves the 3-hour sawtooth pattern of the zero measurements.

As a comparison, the result of SHR-PMF is compared to that of PMF with unit mass resolution (UMR), the method of which has been already applied in Hyytiälä (Yan et al., 2016). With the same mass

range (300-350 Th), the SHR-PMF shows clear superiority in providing more information out of the dataset and separation of the contamination factor, while with such small mass range, the UMR PMF fails to extract the contamination information even though stretched to 20 factors. This novel SHR-PMF method will improve our understanding of HOMs formation pathways, while saving much effort in high-resolution peak fitting and lowering the uncertainty of quantitative separation of overlapping peaks. In the next step, we will apply SHR-PMF to aerosol mass spectrometer data in order to test the improvement achievable with this new technique.

Corbin, J., et al. (2015). "Peak-fitting and integration imprecision in the Aerodyne aerosol mass spectrometer: effects of mass accuracy on location-constrained fits." *Atmos. Meas. Tech.* 8(11): 4615-4636.

Cubison, M. J. and J. L. Jimenez (2015). "Statistical precision of the intensities retrieved from constrained fitting of overlapping peaks in high-resolution mass spectra." *Atmos. Meas. Tech.* 8(6): 2333-2345.

Ehn, M., et al. (2014). "A large source of low-volatility secondary organic aerosol." *Nature* 506(7489): 476-479.

Stark, H., et al. (2015). "Methods to extract molecular and bulk chemical information from series of complex mass spectra with limited mass resolution." *International Journal of Mass Spectrometry* 389: 26-38.

Yan, C., et al. (2016). "Source characterization of highly oxidized multifunctional compounds in a boreal forest environment using positive matrix factorization." *Atmospheric Chemistry and Physics* 16(19): 12715-12731.

# Boreal forest BVOC exchange: emissions versus in-canopy sinks

P. ZHOU<sup>1</sup>, L. GANZVELD<sup>2</sup>, D. TAIPALE<sup>3,4</sup>, ÜLLAR RANNIK<sup>1</sup>, PEKKA RANTALA<sup>1</sup>, M. P. RISSANEN<sup>1</sup>, D. CHEN<sup>1</sup> and M. BOY<sup>1</sup>

<sup>1</sup> Institute for Atmospheric and Earth System Research / Physics, Faculty of Science, University of Helsinki, Finland

<sup>2</sup> Meteorology and Air Quality (MAQ), Department of Environmental Sciences, Wageningen University and Research Centre, Wageningen, the Netherlands

<sup>3</sup> Institute for Atmospheric and Earth System Research / Forest Sciences, Faculty of Agriculture and Forestry, University of Helsinki, Finland

<sup>4</sup> Estonian University of Life Sciences, Department of Plant Physiology, Kreutzwaldi 1, 51014, Estonia

Keywords: BVOC, dry deposition model, boreal canopy, emissions

## Introduction

A multi-layer dry deposition model for biogenic volatile organic compounds (BVOCs) was implemented into a chemical transport column model SOSAA (model to Simulate the concentrations of Organic vapours, Sulphuric Acid and Aerosols; Boy et al., 2011) to investigate the sources and sinks of BVOCs within the canopy. This newly implemented dry deposition model has provided a new insight on the BVOCs exchange of boreal forest. The new parametrization method can also be applied in large-scale models in future.

## Method

The gas dry deposition model was based on the ozone dry deposition model described in Zhou et al. (2017) and extended from Wesely (1989) and Nguyen et al. (2015). The BVOC emissions were calculated using MEGAN (Model of Emissions of Gases and Aerosols from Nature) with the standard emission potentials (SEPs) derived from the measurement data in previous studies. We selected twelve representative compounds to analyse their sources and sinks within the canopy. Monoterpenes, isoprene+MBO, methanol, acetaldehyde, acetone and formaldehyde were chosen to verify the model by comparing their modelled and measured fluxes above the canopy. Acetol was selected as a typical carbonyl compound, together with acetaldehyde, acetone and formaldehyde. Four highly oxidised organic compounds, including pinic acid oxidized from alpha-pinene, BCSOZH oxidized from beta-caryophyllene, ISOP34NO<sub>3</sub> and ISOP34OOH oxidized from isoprene, were selected due to their extremely low volatility and thus prone to deposit onto surfaces and condense onto aerosol particles. The model was applied to investigate the BVOCs exchange over a boreal forest canopy at SMEAR II (Station to Measure Ecosystem-Atmosphere Relations II) in Hyytiälä, Finland, in July 2010.

## Conclusion

The model provided a possibility to analyse individual sources and sinks within the canopy instead of only net fluxes at the canopy top for different compounds. The relative contributions of emission (Qemis), net chemical production and loss (Qchem), turbulent transport into the canopy (Qturb) and deposition onto

vegetation and soil surfaces (Qdepo) are shown in Fig. 1. Here Qturb represents the in-canopy concentration change of BVOCs due to turbulent transport, which can be positive (downward) as a source term or negative (upward) as a sink term. For those compounds emitted from vegetation, e.g. isoprene and monoterpenes, Qemis is the dominant source. The chemical process is significant for highly reactive compounds, it can act as a net source for isoprene oxidation products ISOP34OOH and ISOP34NO<sub>3</sub>, and as net removal mechanism for sesquiterpenes. Deposition is the main sink for most compounds except monoterpenes, sesquiterpenes, isoprene+MBO. The emitted monoterpenes, isoprene+MBO inside the canopy are mainly lost via turbulent transport to the air above the canopy. The bidirectional flux above the canopy for methanol result from the competition between emission and deposition.

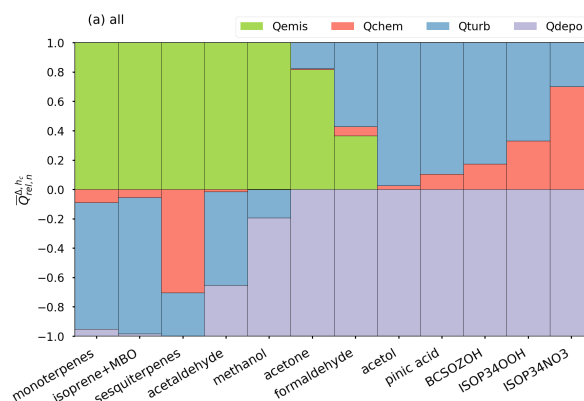


Figure 1: Modelled relative contributions of sources and sinks for different compounds within the canopy.

Boy, M., et al. (2011). *Atmos. Phys. Chem.*, **11**:43-51.

Wesely, M. L. (1989). *Atmos. Env.*, **23**:1293-1304.

Nguyen, T. B., et al. (2015). *PNAS*, **112**:E392-E401.

Zhou, P., et al. (2017). *Atmos. Phys. Chem.*, **17**:1361-1379.

# LINKING RECENT FINDINGS FROM THE STOCKHOLM SEA SPRAY CHAMBER TO GLOBAL CLIMATE MODELS

P. ZIEGER<sup>1,2</sup>, M.E. SALTER<sup>1,2</sup>, B. ROSATI<sup>3</sup>, E.D. NILSSON<sup>1,2</sup>

<sup>1</sup>Department of Environmental Science and Analytical Chemistry, Stockholm University, Sweden

<sup>2</sup>Bolin Centre for Climate Research, Sweden

<sup>3</sup>Department of Chemistry, Aarhus University, Denmark

Keywords: sea spray, hygroscopicity, sea spray source function, global climate models

Sea spray is one of the largest natural aerosol sources and plays an important role in the Earth's radiative budget. These particles are inherently hygroscopic, that is, they take-up moisture from the air, which affects the extent to which they interact with solar radiation. Here, we will describe the most recent in a series of laboratory systems built at Stockholm University to simulate the process of sea spray aerosol formation – the Stockholm sea spray aerosol simulation chamber (Salter et al., 2014).

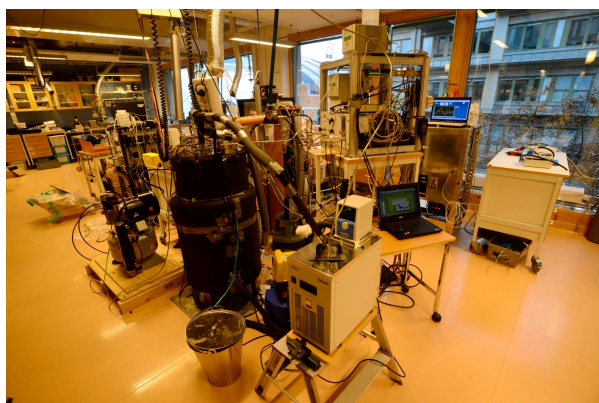


Figure 1: Image of the sea spray simulation chamber at ACES, Stockholm University.

We will present results from a series of experiments that we have conducted in recent years with the aim of improving our understanding of the physical drivers of sea spray aerosol production and the physical and chemical properties of nascent sea spray aerosol. We will show our results linking seawater temperature, bubbles at the seawater surface and the size and number of aerosols produced. Further, we will discuss our approach to parameterizing our laboratory results for use in global climate models (Salter et al., 2015). We will also present our recent findings on the chemical composition of nascent sea spray aerosol – the significant enrichment of calcium in submicrometer nascent sea spray aerosols as well as a tendency for increasing calcium enrichment with decreasing particle size (Salter et al., 2016). Finally, we will describe our recent work determining the hygroscopicity of inorganic sea spray aerosol along with the implications of our results within global climate models (Zieger et al., 2017).

Salter, M. E., Nilsson, E. D., Butcher, A. and Bilde, M. (2014). *On the seawater temperature dependence*

*of the sea spray aerosol generated by a continuous plunging jet.* J. Geophys. Res. 119, 9052–9072.

Salter, M. E., Zieger, P., Acosta Navarro, J. C., Grythe, H., Kirkevåg, A., Rosati, B., Riipinen, I. and Nilsson, E. D. (2015). *An empirically derived inorganic sea spray source function incorporating sea surface temperature* Atmos. Chem. Phys., 15, 11047–11066.

Salter, M. E., Hamacher-Barth, E., Leck, C., Werner, J., Johnson, C. M., Riipinen, I., Nilsson, E. D. and Zieger, P. (2016). Calcium enrichment in sea spray aerosol particles Geophys. Res. Lett., 43, 8277–8285.

Zieger, P., Väisänen, O., Corbin, J., Partridge, D. G., Bastelberger, S., Mousavi-Fard, M., Rosati, B., Gysel, M., Krieger, U., Leck, C., Nenes, A., Riipinen, I., Virtanen, A. and Salter, M. (2017). *Revising the hygroscopicity of inorganic sea salt particles*, Nature Comm., 8.